On the cover from left to right: top: The root of a seedling expressing Ca^{2+} sensor R-GECO1, immunolocalization of PIN2, immunolocalization of PIN1, bottom: 2xFYVE marker localization upon treatment with W-7, transmission electron microscopy image of a root epidermal cell treated with Bepridil, kymograph of DRP1c dynamics in root epidermal cell under control conditions.

GHENT UNIVERSITY – FACULTY OF SCIENCES
DEPARTMENT OF PLANT BIOTECHNOLOGY AND BIOINFORMATICS
VIB CENTER FOR PLANT SYSTEMS BIOLOGY

The role of calcium in auxin-regulated PIN endomembrane trafficking

Ellie Himschoot

Academic Year 2017-2018

Promoters: Prof. Dr. Tom Beeckman and Prof. Dr. Ir. Steffen Vanneste

Thesis submitted as partial fulfillment of the requirements for obtaining the degree of Doctor of Philosophy in Science: Biochemistry and Biotechnology

UGent Special Research Fund

EXAMINATION BOARD

Promoters

Prof. Dr. Tom Beeckman	Ghent University, VIB Center for Plant Systems Biology, Belgium
Prof. Dr. Ir. Steffen Vanneste	Ghent University, VIB Center for Plant Systems Biology, Belgium

Voting Members

Prof. Dr. Geert De Jaeger (Chair)	Ghent University, VIB Center for Plant Systems Biology, Belgium
Prof. Dr. Lieven De Veylder (Secretary)	Ghent University, VIB Center for Plant Systems Biology, Belgium
Prof. Dr. Jiří Friml	Institute of Science and Technology, Austria
Prof. Dr. Alex Costa	University of Milan, Italy
Dr. Simon Stael	Ghent University, VIB Center for Plant Systems Biology, Belgium

Table of Contents

ABBREVIATIONS

2,4-D	2,4-dichlorophenoxy acetic acid
4-Cl-IAA	4-chloroindole-3-acetic acid
ABA	abscisic acid
ABCB	ATP-binding cassette transporters type B
ABCB/PGP	P-glycoproteins of the ABCB transporter family
ABP1	AUXIN BINDING PROTEIN1
ACA	AUTO-INHIBITED Ca^{2+}-ATPASE
ANN	ANNEXIN
AP	ADAPTOR PROTEIN
ARF	ADP-RIBOSYLATION FACTOR or AUXIN RESPONSE FACTOR
ATP	adenosine triphosphate
Aux/IAA	Auxin/INDOLE ACETIC ACID
AUX/LAX	AUXIN1/LIKE-AUX1
AuxRE	Auxin RESPONSE ELEMENT
AX	AUXILIN
BEN	BFA-VISUALIZED ENDOCYTIC TRAFFICKING DEFECTIVE
BEX5	BFA-VISUALIZED EXOCYTIC TRAFFICKING DEFECTIVE5
BFA	brefeldin A
BIG	BFA-INHIBITED GEF
BRET	bioluminescence resonance energy transfer
BRI1	BRASSINOSTEROID INSENSITIVE1
C(D)PK	Ca^{2+}-DEPENDENT PROTEIN KINASE
CA	constitutively active
CalfluxVTN	CALcium FLUX composed of Venus, Troponin and NanoLuc
CaM	CALMODULIN
CaMIN	medium without Ca^{2+}

cAMP	cyclic adenosine monophosphate
CaPLUS	medium with Ca^{2+}
CAX	CATION EXCHANGER
CBL	CALCINEURIN B-LIKE
CCV	clathrin-coated vesicles
CFP	cyan fluorescent protein
cGMP	cyclic guanosine monophosphate
CHC	CLATHRIN HEAVY CHAIN
CIE	clathrin-independent endocytosis
CIPK	CBL-INTERACTING PROTEIN KINASE
CLC	CLATHRIN LIGHT CHAIN
CLSM	confocal laser scanning microscope
CME	clathrin-mediated endocytosis
CML	CALMODULIN-LIKE
CNGC	CYCLIC NUCLEOTIDE-GATED Ca^{2+} CHANNEL
CRK5	Ca^{2+}/CaM-DEPENDENT KINASE-RELATED KINASE5
D6PK	D6 PROTEIN KINASE
DACC	DEPOLARIZATION-ACTIVATED Ca^{2+} CHANNEL
DAO1	DIOXYGENASE FOR AUXIN OXIDATION1
DMSO	dimethylsulfoxide
DRP	DYNAMIN-RELATED PROTEIN
ECA	ER-TYPE Ca^{2+}-ATPASEs
EE	early endosome
ER	endoplasmic reticulum
ESCRT	Endosomal Sorting Complex Required for Transport
estra	estradiol
Fei-Mao	FM
FDM	fused deposition modelling
Flot1	Flotillin1

FLS2	FLAGELLIN SENSING2
FRET	Förster resonance energy transfer
G5A	GFP-aequorin
GAP	GTPase-ACTIVATING PROTEINs
GDI	GUANINE NUCLEOTIDE DISSOCIATION INHIBITOR
GDP	guanosine diphosphate
GECI	genetically encoded Ca^{2+} indicators
GEF	GUANINE NUCLEOTIDE EXCHANGE FACTOR
GFP	green fluorescent protein
GLR	GLUTAMATE RECEPTOR-LIKE
GN	GNOM
GNL1	GNOM-LIKE1
GPI	glycosyl phosphatidyl inositol
GTP	guanosine-5'-triphosphate
HACC	HYPERPOLARIZATION-ACTIVATED Ca^{2+} CHANNELs
HTAM	hydroxytamoxifen
IAA	indole-5-acetic acid
IBA	indole-3-butyric acid
IPA	indole-3-pyruvate
KAT	K^+ TRANSPORTERS OF ARABIDOPSIS THALIANA
K_d	dissociation constant
LE	late endosome
MDP25	MICROTUBULE-DESTABILIZING PROTEIN25
MIN7	HOPM INTERACTOR7
MT	microtubule
MVB	multivesicular body
MβCD	methyl-β-cyclodextrin
Na	Numerical Aperture
NAA	naphthaleneacetic acid (referring to **1**-naphthaleneacetic acid)

NPA	1-*N*-naphthylphthalamic acid
OSCA	REDUCED HYPEROSMOLALITY-INDUCED [$Ca^{(2+)}$]i INCREASE
PA	phosphatidic acid
PAA	phenylacetic acid
PAT	polar auxin transport
PBP1	PID-BINDING PROTEIN1
PEO-IAA	α-(phenyl ethyl-2-one)-indole-3-acetic acid
PI3P	phosphatidylinositol 3-phosphate
PI4P	phosphatidylinositol 4-phosphate
$PI(4,5)P_2$	phosphatidylinositol 4,5-bisphosphate
PID	PINOID
PILS	PIN-LIKES
PIN	PIN-FORMED
PP	PROTEIN PHOSPHATASE
PVC	prevacuolar compartment
RAB	RAS GENES FROM RAT BRAIN
RBOH	RESPIRATORY BURST OXIDASE HOMOLOGUE
RGLG	RING-DOMAIN LIGASE
RIC	ROP INTERACTIVE CRIB MOTIF-CONTAINING PROTEINS
ROI	region of interest
ROP	RHO-LIKE GTPASE FOR PLANTS
ROS	reactive oxygen species
SAC	STRETCH-ACTIVATED Ca^{2+} CHANNEL
scn1	*supercentipede1*
SDM	spinning disc microscope
SKP2A	S-PHASE KINASE-ASSOCIATED PROTEIN 2A
SNARE	SOLUBLE *N*-ETHYL-MALEIMIDE SENSITIVE FUSION FACTOR ATTACHMENT PROTEIN RECEPTOR
SNX1	SORTING NEXIN1
SYP	SYNTAXIN OF PLANT

SYT	SYNAPTOTAGMIN
TAA	TRYPTOPHAN AMINOTRANSFERASE OF ARABIDOPSIS
TAM	tryptamine
TCH3	TOUCH3
TGN	*trans*-Golgi network
TIR1/AFB	TRANSPORT INHIBITOR RESPONSE1/AUXIN SIGNALING F-BOX PROTEINS
TMK	TRANSMEMBRANE KINASE
TPC	T-PLATE complex
TPL	TOPLESS
Troponin C	Tn C
Trp	tryptophan
TWD1	TWISTED DWARF1
VAN3	VASCULAR NETWORK3
VAN4	VASCULAR NETWORK DEFECTIVE4
VHA	V-TYPE PROTON ATPASE
VPS	VACUOLAR PROTEIN SORTING
VSR	VACUOLAR SORTING RECEPTOR
WAG	WAVY ROOT GROWTH
WM	Widefield Microscope
Wm	Wortmannin
YC	Yellow Cameleon
YFP	yellow fluorescent protein
YUC	YUCCA

SUMMARY

Plants have the amazing ability to rapidly adapt their growth and development in order to cope with continuously changing environments. Their plasticity can be to a large extent attributed to the action of phytohormones. Auxin is a prominent phytohormone regulating a wide range of developmental processes and tropisms, and mediating resistance to (a)biotic stresses (**Section I - Chapter 1**). Each of these auxin-regulated processes is characterized by a specific auxin distribution pattern. One of the determinants for establishment of these distribution patterns is directional intercellular auxin transport, also referred to as polar auxin transport. Key players in polar auxin transport are the auxin efflux carriers PINs. The PINs show a polar localization in the apical, basal, or lateral plasma membrane domain thereby mediating auxin efflux from the cell upward, downward, or sideward respectively. PIN proteins are highly dynamic proteins that can be rapidly relocalized to a distinct plasma membrane domain via the endosomal trafficking pathway to modulate auxin flow according to developmental or environmental cues. Alternatively, the direction of auxin flow can also be reinforced by a feedback mechanism by which auxin itself inhibits PIN internalization and consequently also PIN relocalization. This is for example important for forming the leaf pavement cells into puzzle piece-shaped cells. Identifying the underlying mechanism has been a topic of interest for many research groups. Auxin and Ca^{2+} signaling previously have been interconnected in regulation of root gravitropism. Furthermore, Ca^{2+} is also known for its involvement in regulation of cell polarity (**Section I - Chapter 2**), and for its contribution to proper protein sorting throughout the endomembrane system (**Section I - Chapter 3**). Here, we have also identified a role for Ca^{2+} as a second messenger in auxin-inhibited PIN internalization (**Section II – Chapter 2**). Not only is Ca^{2+} required for inhibition of PIN endocytosis by auxin, Ca^{2+} is also sufficient to block PIN internalization. The role of Ca^{2+} most likely relies on early endocytic trafficking steps and might also regulate PIN levels by affecting late endosomal trafficking events towards the vacuole. Furthermore, we have indications that auxin-inhibited PIN endocytosis could be initiated by auxin-induced cytosolic Ca^{2+} dynamics that occur rapidly upon auxin treatment (**Section II - Chapter 1**). However, genetic evidence for the involved Ca^{2+} signaling components still remains to be found.

SAMENVATTING

Planten hebben het indrukwekkende vermogen om hun groei en ontwikkeling snel aan te passen aan hun continu veranderende omgeving. Hun plasticiteit is grotendeels te wijten aan de werking van fytohormonen. Auxine is een belangrijk fytohormoon dat een brede waaier aan ontwikkelingsprocessen en tropismen reguleert, en de planten helpt om weerstand te bieden aan (a)biotische stress (**Sectie I – Hoofdstuk 1**). Elk van deze auxine-gereguleerde processen wordt gekenmerkt door een specifiek auxine verdelingspatroon. Eén van de factoren die bijdraagt aan het tot stand brengen van deze verdelingspatronen is directioneel intercellulair auxine transport, ook wel polair auxine transport genaamd. Essentiële eiwitten voor polair auxine transport zijn de auxine efflux carriers PINs. De PINs hebben een polaire lokalisatie in apicale, basale, of laterale plasmamembraan domeinen waardoor ze auxine respectievelijk opwaarts, neerwaarts, en zijwaarts uit de cel kunnen transporteren. PINs zijn zeer dynamische eiwitten die snel kunnen herlokaliseren naar een ander plasmamembraan domein via de endosomale transport route om de richting van auxine transport aan te passen naargelang ontwikkeling-gerelateerde signalen of signalen vanuit de omgeving. Bovendien beschikt de plant over verschillende mechanismen waarmee auxine de richting van zijn transport zelf kan beïnvloeden zoals het inhiberen van PIN endocytose. Dit is bijvoorbeeld van belang om de epidermale cellen van het blad hun puzzelstuk-achtige vorm te geven. Er werd reeds intensief onderzoek verricht naar het onderliggende mechanisme, maar tot nu toe is onze kennis hieromtrent beperkt.

Het secundaire boodschapper ion Ca^{2+} is een welgekend signaal betrokken in het reguleren van cel polariteit (**Sectie I – Hoofdstuk 2**) en endomembraan transport (**Sectie I – Hoofdstuk 3**). Interessant is dat auxine Ca^{2+} signalen kan induceren (**Sectie II – Hoofdstuk 1**) en dat Ca^{2+} noodzakelijk is voor auxine transport. Dit doet vermoeden dat Ca^{2+} onderdeel zou kunnen uitmaken van de auxine signalisatie cascade via dewelke auxine zijn eigen transport reguleert. Hier tonen we aan dat Ca^{2+} als secundair boodschapper ion zou kunnen optreden in de inhibitie van PIN endocytose door auxine (**Sectie II – Hoofdstuk 2**). Ca^{2+} is niet alleen noodzakelijk voor auxine-gereguleerde inhibitie van PIN endocytose, Ca^{2+} is ook voldoende om PIN internalisatie te blokkeren. Het effect van Ca^{2+} is hoogstwaarschijnlijk afhankelijk van

initiële endosomale transport stappen, en Ca^{2+} zou PIN niveaus mogelijks ook kunnen reguleren door de latere endosmale transport stappen richting vacuole te beïnvloeden. Bovendien hebben we aanwijzingen dat auxine-geïnhibeerde PIN endocytose geïnitieerd zou kunnen worden door de cytosolische auxine-geïnduceerde Ca^{2+} signalen die gevormd worden onmiddellijk na auxine behandeling (**Sectie II – Hoofdstuk 1**). Analyse van een uitgebreide set van mutanten en transgene lijnen doet vermoeden dat auxine een subgroep van Ca^{2+} -afhankelijke kinasen activeert om endocytose te inhiberen. Deze bevindingen moeten echter nog bevestigd worden via analyse van de corresponderende drie- en viervoudige mutanten.

SCOPE OF THE RESEARCH PROJECT

Auxin is a prominent plant hormone that regulates multiple developmental processes and is involved in adjustment of plant growth in response to changing environmental conditions. In many mutants with defects in auxin-regulated processes, their phenotypes can be attributed to distorted directional intercellular auxin transport. Polar auxin transport is established by polarly localized auxin efflux carriers in the plasma membrane, called PINs. These PIN proteins can be relocated via trafficking through the endomembrane system to distinct sides of the cell in order to readjust the direction of auxin flow in response to developmental or environmental signals. Interestingly, auxin itself can feedback regulate the directionality of its own transport by inhibiting clathrin-mediated endocytosis of PIN proteins thereby reinforcing PIN localization at the plasma membrane and sustain auxin efflux in a specific direction.

Over the past years, many research has been conducted to unravel the underlying mechanism by which auxin can inhibit PIN endocytosis. Typically NAA was used for experimental treatments as it is more stable than the natural auxin IAA. Data from roots and leaves have pinpointed a role for intracellular activation of ROP/RIC signaling and downstream modifications of the cytoskeleton. However, more insight on how NAA activates this intracellular signaling cascade is still missing.

In my PhD project we wanted to address what could be the role of the second messenger Ca^{2+}. Ca^{2+} was already shown to operate as a second messenger in auxin-regulated root gravistropism, and many reports had shown that different auxins could induce a cytosolic Ca^{2+} increase in distinct tissues. Most of these reports had focused on the effect of the natural auxin IAA, and to lesser extent on the synthetic auxin NAA. Therefore, our **first** goal was to establish a clear picture of the NAA-induced Ca^{2+} dynamics in *Arabidopsis thaliana* root epidermal cells. It had been shown that auxin-induced Ca^{2+} influx occurred rapidly which made it technically challenging to capture this rapid response. A first step was to obtain an imaging set-up which would allow us to record Ca^{2+} dynamics while applying the NAA treatment. For this purpose, a collaboration with the Schumacher lab (University of Heidelberg, Germany) and the Costa lab (University of Milan, Italy) was initiated. A second step would be to obtain sufficient amount of data using this set-up for image analysis and interpretation. A **second**

goal was to address the impact of pharmacological and genetic manipulation of Ca^{2+} signaling on NAA-regulated PIN endocytosis to verify the importance of Ca^{2+} and possibly identify Ca^{2+} signaling components involved. **Thirdly**, we wanted to more specifically pinpoint at which step in the endosomal (PIN) trafficking pathway Ca^{2+} would be impacting by evaluating NAA-inhibited PIN endocytosis upon Ca^{2+} manipulation in distinct endosomal trafficking mutants. Finally, a **fourth** goal was to link the NAA-induced Ca^{2+} dynamics to NAA its effect on PIN endocytosis by verifying how interfering with the NAA-induced cytosolic Ca^{2+} increase affected inhibition of PIN internalization by NAA.

SECTION I. INTRODUCTION

PREFACE

Section I. Introduction is subdivided in three smaller introductory chapters. In **Chapter 1**, I aim to give a general introduction on auxin, endosomal protein trafficking, and Ca^{2+} signaling in plants; the three main topics that come together in my PhD project. I will address the importance of auxin for plant development, polar auxin transport mediated by the PIN auxin efflux carriers, and the distinct steps of endosomal (PIN) trafficking and their regulation. Furthermore, I will introduce Ca^{2+} signaling in plants and our current knowledge on the involvement of Ca^{2+} as a second messenger in auxin signaling. In Chapters 2 and 3 I will go into more detail on the role of Ca^{2+} in cell polarity and endosomal trafficking respectively. Cell polarity is mainly controlled by activity of small GTPases, balanced exo- and endocytosis controlling membrane tension, and cytoskeletal rearrangements. In **Chapter 2**, the established interconnections between Ca^{2+} and these cell polarity determinants are discusses in more detail. Besides Ca^{2+} signaling, a central topic in my PhD project is PIN-mediated auxin transport and more specifically intracellular endomembrane trafficking of PINs. Therefore, **Chapter 3** is devoted to summarizing our current knowledge on the role of Ca^{2+} in regulation of endomembrane trafficking and membrane integrity in plants.

Together, these chapters will give you a brief introduction to the concepts and experimental data presented in Section II. Results.

Chapter 1:
General introduction to auxin and calcium signaling

Ellie Himschoot[1, 2], Tom Beeckman[1, 2], Steffen Vanneste[1, 2]

[1] Department of Plant Biotechnology and Bio-informatics, Ghent University, B-9052 Ghent, Belgium
[2] Department of Plant Systems Biology, VIB, B-9052 Ghent, Belgium

Author contribution:
E.H. performed the literature study, made the figures, and is the main author of this chapter. T.B. and S.V. revised the chapter and contributed to the writing.

Auxin

Auxin, the phytohormone

In case of animals, the body plan is fully established at birth, and further development into an adult organism mainly consists of further growth of the existing body parts. In plants however, the young seedling formed upon seed germination consist of a single primary root, a hypocotyl and two cotyledons. Many features such as an extensive root system, multiple leaves and other organs such as flowers, remain to be developed. This is orchestrated by phytohormones.

Not only does the seedling still have to continue development, it has to do this in a continuously changing environment being exposed to different environmental stresses such as drought, low nutrient availability, osmotic stress, pathogens,… Whereas animals can migrate away from hostile environments, plants are immobile and had to evolve alternative solutions to cope with harsh environmental conditions. Besides regulating plant development, phytohormones also play vital roles in environmental adaptation of plants. An important phytohormone that is capable of integrating both endogenous and exogenous signals is auxin.

Auxin discovery

Auxin was first discovered as the growth promoting phytohormone regulating phototropism (Darwin, 1881). The phototropic response, allowing plants to grow towards the light, had already been observed long before our time (B.C.). However, then it was still considered that phototropism was caused by the removal of fluids by sun light at the illuminated side, and that there were no activators in the plant itself involved. It was Darwin who discovered that phototropism involved a mobile signal produced in the shoot that was transported to the hypocotyl where it induced bending (Darwin, 1881; Whippo and Hangarter, 2006). The mobile signal was later on identified as the auxin indole-3-acetic acid (IAA) (Kogl, 1931). Cholodny and Went proposed a model in which auxin accumulates asymmetrically, at the non-illuminated side of the hypocotyl, resulting in increased growth on the shaded side and a simultaneous decrease in growth rates on the illuminated side, leading to bending of the shoot towards the light (Went, 1926; Cholodny, 1927; Went, 1928). This model has been challenged by alternative theories. Boysen-Jensen disputed the principle of differential growth rates

between the illuminated and shaded side by stating the growth rate at the shaded side increased while growth rates on the illuminated side were not affected (Boysen-Jensen, 1928). Alternatively, Blaauw and Paal suggested that cell elongation in general decreased with a more pronounced decrease on the illuminated side (Blaauw, 1918; Paal, 1919). Additionally, they hypothesized that phototropic bending can be attributed to light- rather than hormone-regulated growth (photomorphogenesis). Overbeek suggested a combination of the Blaauw and Cholodny-Went models stating that phototropism involves both auxin-regulated growth and photomorphogenesis, and also considered that a differential sensitivity to auxin between both sides contributes to phototropic bending (Overbeek, 1932). Despite these alternative explanations, the Cholodny-Went model has remained the most widely accepted (Whippo and Hangarter, 2006).

Besides IAA, plants synthetize other 'endogenous' auxins, namely phenylacetic acid (PAA), and 4-chloroindole-3-acetic acid (4-Cl-IAA) (Skoog and Miller, 1957). For research purposes the synthetic auxins 2,4-dichlorophenoxy acetic acid (2,4-D) and **1**-naphthaleneacetic acid (NAA) are frequently used. The observation that these auxins perform similar but not necessarily identical functions as IAA, and are structurally diverse, has complicated their structure-function analysis and the search for a possible common mode of action (Ferro et al., 2010). Up till now IAA has been the most extensively described auxin in terms of hormone perception and signaling.

Auxin-regulated developmental processes and environmental adaptation

From early embryogenesis to a full-grown plant, auxin is indispensable during several key developmental steps. Already after the first asymmetric division of the zygote auxin is crucial for establishing the apical-basal axis determining which cell will give rise to the shoot, and which cell will be a precursor for the root (Jürgens, 2001). Later on during root development, auxin mediates the organization of the root apical meristem, primary root growth, lateral root development, and root hair growth contributing to the development of an extensive root network crucial for plant stability and nutrient uptake (Pitts et al., 1998; Rahman et al., 2002; Jiang and Feldman, 2005; Ishida et al., 2008; Péret et al., 2009; Overvoorde et al., 2010). Also

shoot development involving shoot apical meristem patterning and leaf and floral primordia initiation rely on auxin signaling (Vernoux et al., 2010; Gallavotti, 2013).

A textbook example of auxin-regulated environmental adaption is root- and shoot gravitropism allowing plants to reorient their growth direction parallel to the gravity vector (Su et al.; Masson et al., 2002; Sato et al., 2015). Another auxin-regulated tropism, already mentioned in the previous section, is phototropism (Fankhauser and Christie, 2015). This feature is crucial for plants during seed germination or when growing in dense populations to grow towards the light and optimize light exposure to facilitate photosynthesis. Auxin signaling is also crucial during (a)biotic stress such as drought, cold, salt stress, and pathogen attack (Kazan and Manners, 2009; Fu and Wang, 2011; Kazan, 2013; Rahman, 2013).

The extent and diversity of auxin-regulated processes clearly demonstrates the prominent role of this phytohormone for plant development and adaptive plant growth.

Auxin distribution patterns

The different auxin-regulated processes described above rely on distinct auxin distribution patterns. Some auxin responses are triggered by high auxin accumulation in a group of cells (morphogenetic trigger), while others require a graded auxin distribution (morphogen). During embryogenesis, the apical-basal polarity after the first division of the zygote is established by an auxin maximum in the basal cell defining the future root apical meristem (Fig. 1, A-C) (Friml et al., 2003). In developed root apices, auxin accumulates in the quiescent center with a more graded distribution in the columella cells (Fig. 1, E), and across the primary root meristem (Sabatini et al., 1999; Friml et al., 2002; Petersson et al., 2009). Upon root gravistimulation, the steady-state auxin distribution is perturbed, and auxin is redistributed to the new lower side of the root tip. This asymmetric auxin distribution results in differential growth and thus bending of the root (Fig. 1, F) (Friml and Palme, 2002). In the shoot, auxin accumulation at leaf initiation sites triggers the development of leaf primordia which in turn form an auxin sink (Reinhardt et al., 2003). The graded depletion of auxin in the near vicinity of the primordium prevents formation of a novel primordium within a certain distance and is crucial for proper spacing of the leaf primordia in the shoot apical meristem (Heisler et al.,

2010). Also initiation of floral primordia relies on local auxin accumulation (Fig. 1, D) (Benková et al., 2003).

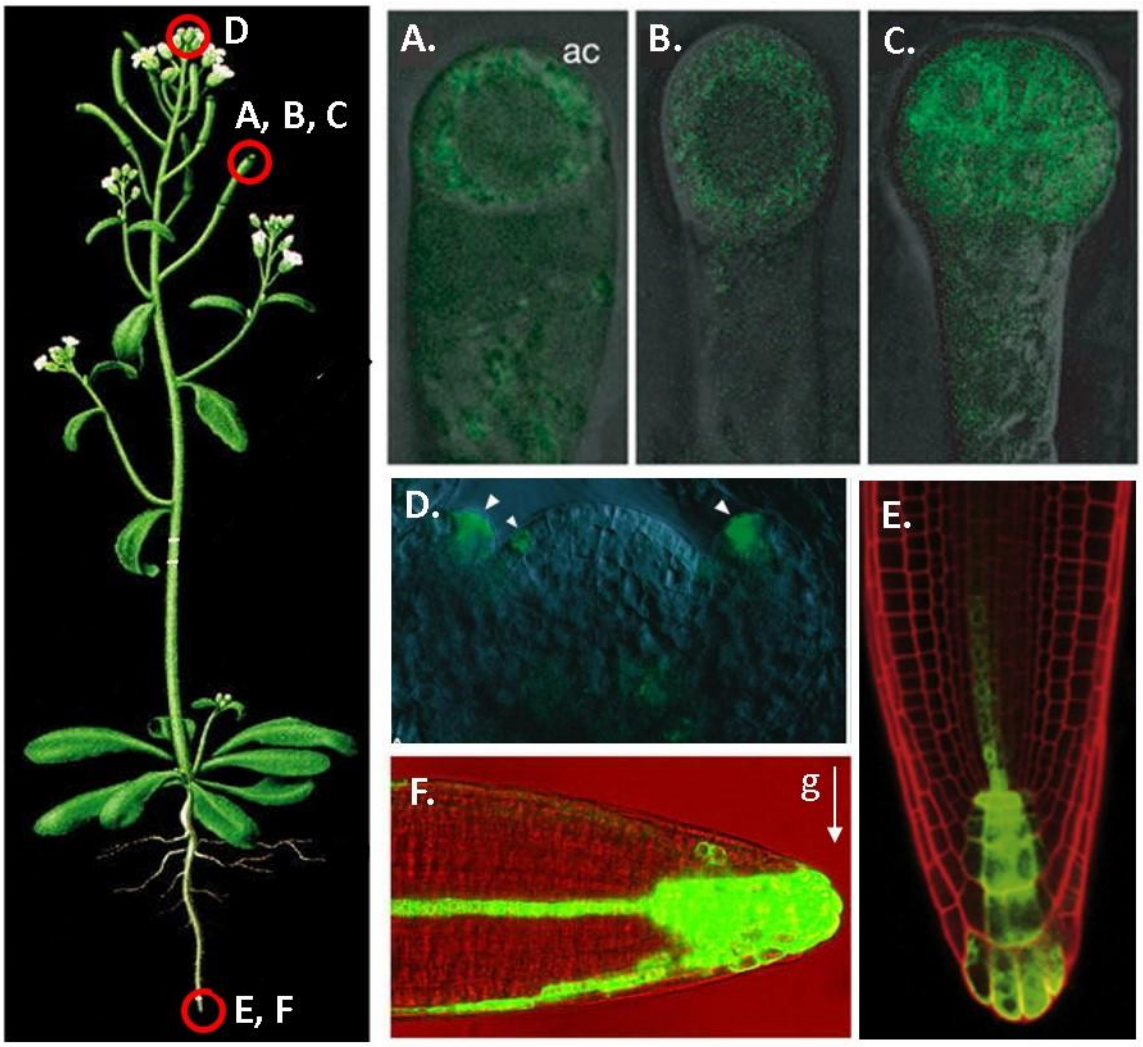

Figure 1: Auxin distribution patterns during plant development and environmental adaptation. Auxin distribution is visualized by means of the auxin reporter DR5rev::GFP. (A-C) An auxin maximum in the apical cell (ac) lineage of a developing embryo after division of the zygote (A), and during the single-cell (B) and eight-cell (C) stage. (D) Auxin accumulation at emerging floral primordia. (E) An auxin maximum in the quiescent center and a more graded auxin distribution in the columella cells of the root meristem. (F) Asymmetric auxin distribution in gravistimulated roots. The arrow represents the direction of the gravity vector. Images were modified from (Friml et al., 2003) (A-C), (Benková et al., 2003) (D), (Moubayidin et al., 2013) (E), (Michniewicz et al., 2007a) (F, *Arabidopsis* drawing).

These characteristic auxin distribution patterns are the outcome of local auxin biosynthesis, regulated auxin conjugation and degradation, and directional auxin transport (Ljung, 2013). IAA biosynthesis pathways are classically subdivided in tryptophan (Trp)-dependent and –independent pathways (Woodward and Bartel, 2005; Korasick et al., 2013; Brumos et al.,

2014; Tivendale et al., 2014). Thus far, only the indole-3-pyruvate (IPA) Trp-dependent pathway has been resolved completely (Zhao, 2014). IPA refers to the intermediate that is formed during a two-step biosynthesis process. First, Trp is transaminated by TRYPTOPHAN AMINOTRANSFERASEs OF ARABIDOPSIS (TAAs) into IPA, which forms the substrate for subsequent oxidative decarboxylation by YUCCAs (YUCs) into IAA (Won et al., 2011). Mutant analysis of *yuc* and *taa* has demonstrated the importance of this IAA biosynthesis pathway during embryogenesis, vascularization, flower development, seedling response to ethylene and NPA, and shade avoidance (Cheng et al., 2006, 2007; Won et al., 2011). Recently, it was shown that the biosynthesis pathway of the endogenous auxin PAA is similar to that of IAA. Even though PAA is synthetized based on phenylalanine instead of Trp, and a phenylpyruvate intermediate is formed, the conversion is also catalyzed by YUC and TAA (Sugawara et al., 2015; Cook et al., 2016). There is also evidence that the YUCs are involved in the Trp-dependent tryptamine (TAM) pathway (Zhao et al., 2001), however, current knowledge on the biochemical mechanisms of alternative IAA synthesis pathways is still fragmented. IAA is considered to be a free active molecule, though, it can also occur in inactive state in the form of indole-3-butyric acid (IBA) or conjugates. Besides *de novo* biosynthesis, IAA can be generated by conversion of the precursor IBA in peroxisomes (Zolman et al., 2000; Zolman et al., 2007). Common IAA conjugates consist of ester-linked simple and complex carbohydrate conjugates, amide-linked amino acid conjugates, and amide-linked peptide and protein conjugates, and the occurrence and amounts can differ among plant species (Ludwig-Müller, 2011; Korasick et al., 2013). Conjugation is reversible and IAA can be released by hydrolysis e.g. during seed germination (Davies et al., 1999; Rampey et al., 2004). Alternatively, auxin degradation can affect local IAA levels. For example, previous work has shown that IAA overproduction triggered IAA catabolism by irreversible IAA oxidation catalyzed by DIOXYGENASE FOR AUXIN OXIDATION1 (DAO1) to 2-oxindole-3-acetic acid in roots (Pěnčík et al., 2013; Porco et al., 2016). Fourthly, auxin distribution is in part also regulated by directional intercellular auxin transport. Since polar auxin transport forms an important subject in my PhD project, this will be discussed in more detail in the paragraph below.

Auxin transport

Generally, two distinct auxin transport pathways are distinguished. One transport route accounts for rapid, long distance, non-polar transport of auxin away from the main auxin source (the shoot) via the phloem (Morris and Thomas, 1978). Upon unloading of the phloem at the level of the sinks (the root), a second slower transport pathway mediates further short distance, directional intercellular transport (Goldsmith, 1977). This polar auxin transport results from the asymmetric distribution of auxin efflux carriers as postulated by the chemiosmotic model (Rubery and Sheldrake, 1974; Raven, 1975). In this model, the weak acid IAA occurs in its protonated lipophilic form when localized in the slightly acidic apoplast (pH 5.5) and can diffuse freely across the plasma membrane into the cytosol where the more alkaline environment (pH 7) results in deprotonation of IAA. Later experiments showed that IAA can also enter the cell via proton-driven influx carriers of the AUXIN1/LIKE-AUX1 (AUX/LAX) family (Bennett et al., 1996; Swarup et al., 2008). In order to facilitate efflux of the lipophobic IAA^- anion from the cytosol, active plasma membrane-localized efflux carriers are required. The chemiosmotic model proposes the asymmetric distribution of auxin efflux carriers mediating directional transport of auxin out of the cell thereby establishing polar cell-to-cell auxin transport. This model mainly applies to IAA, as the endogenous auxin PAA was suggested to not be actively transported in a polar fashion (Sugawara et al., 2015).

The best known auxin efflux carriers are the PIN-formed (PIN) proteins. PINs are transmembrane proteins with multiple hydrophobic membrane-spanning domains at their amino- and carboxy-terminus, and a central hydrophilic loop facing the cytosol (Křeček et al., 2009; Nodzyński et al., 2016). In *Arabidopsis*, the PIN family counts 8 members, which are typically subdivided in two groups, the “long” and “short” PINs, based on the length of the central hydrophilic loop (Křeček et al., 2009; Ganguly et al., 2012). Additionally, the “long” and “short” PINs differ in their subcellular localization. The “long” PINS PIN1, PIN2, PIN3, PIN4, and PIN7 are found in the plasma membrane restricted to specific polar domains, whereas the “short” PINs PIN5, PIN6 and PIN8 localize to the membrane of the endoplasmic reticulum (ER) (Vieten et al., 2007; Zažímalová et al., 2007; Mravec et al., 2009; Zažímalová et al., 2010; Bosco et al., 2012; Ding et al., 2012; Simon et al., 2016b). Given their localization, the “long” PINs account for the directional cell-to-cell transportation of auxin, also referred to as polar auxin transport (PAT), while it is speculated that the “short” PINs are involved in regulating auxin

homeostasis and metabolism by mediating ER-cytosol auxin transport. The “short” PIN6 is more atypical given its dual localization at both the plasma membrane and ER (Simon et al., 2016b). Since plasma membrane-localized PIN6 shows a polar distribution, it can contribute to directional intercellular auxin transport besides regulation of intracellular auxin homeostasis. Besides the “short” PINs, the putative auxin carriers PIN-LIKES (PILS) localize to the ER where they mediate auxin compartmentalization and conjugation thereby reducing free auxin and nuclear auxin signaling (Barbez et al., 2012; Feraru et al., 2012; Béziat et al., 2017). Genetic interference with PINs results in defective auxin-regulated processes, and similar phenotypes can be observed by treatment with auxin efflux inhibitors (Okada et al., 1991). The *pin1* mutant forms a pin-shaped inflorescence (to which the PINs owe their name), has abnormal cotyledon positioning in the seedling stage, and shows defects in vein branching resulting in fused leaves (Gälweiler et al., 1998). Other *pin* mutants have abnormal photo- and gravitropic responses, defective embryo development, and aberrant organogenesis (Luschnig et al., 1998; Benková et al., 2003; Friml et al., 2003; Reinhardt et al., 2003). Together, these observations illustrate the importance of PAT by PINs for different environmental and developmental processes.

Alternatively, auxin efflux from the cell can be mediated by P-glycoproteins of the ABCB transporter family (ABCB/PGP). Several ABCBs are targeted by the auxin efflux inhibitor 1-*N*-naphthylphthalamic acid (NPA) which prevents association with the ABCB-positive regulator TWISTED DWARF 1 (TWD1) (Bailly et al., 2008). In contrast to the PINs, these efflux carriers show no polar localization and therefor do not contribute to PAT. Mutant analyses showed the involvement of ABCBs in multiple developmental processes (Noh et al., 2001), however, since mutant phenotypes mostly differ from those observed in *pin* mutants it could be that they have additional roles in processes not related to auxin transport. Interestingly, some ABCB proteins can switch between mediating auxin efflux or influx depending on the cytoplasmic auxin concentration (Kamimoto et al., 2012; Kubeš et al., 2012).

The PIN- and PGP-dependent auxin efflux mechanisms have been shown to operate both synergistically and antagonistically in specific developmental processes like embryogenesis and lateral root development, but overall both pathways contribute to the establishment and maintenance of proper auxin distribution patterns (Mravec et al., 2008).

PAT via PIN

The polarity of PIN localization is primarily determined by the PIN phosphorylation status. PINOID (PID), a member of the plant specific family of AGCVIII protein kinases, was shown to directly phosphorylate PINs (Michniewicz et al., 2007b). Loss of PID function resulted in plants with *pin1*-like phenotypes while PID overexpression generated plants with agravitropic hypocotyl and root growth, and defective primary root meristems (Bennett et al., 1995; Christensen et al., 2000; Benjamins et al., 2001). Knock-out mutants for the PROTEIN PHOSPHATASE 2A (PP2A) showed similar phenotypes as the PID overexpression plants (Garbers et al., 1996; Rashotte et al., 2001). These observations demonstrated the importance of PID and PP2A function for PIN-dependent PAT. Further research revealed that kinases WAVY ROOT GROWTH1 (WAG1) and WAG2 redundantly regulate PIN phosphorylation together with PID (Dhonukshe et al., 2010), and that PP2A is part of a heterotrimeric phosphatase complex PP6 mediating PIN dephosphorylation (Dai et al., 2012). Interestingly, at the subcellular level, a shift in PIN polarity from the apical side of the cell to the basal side was observed in *pid* mutants (Friml et al., 2004). Conversely, both PID overexpression and PP2A knock-out induced a basal-to-apical shift. This lead to the development of a model in which PIN polarity depends on its phosphorylation status; PID/WAG1/WAG2-dependent PIN phosphorylation recruits PINs in the trafficking pathway to the apical side of the cell, while PP6-dephosphorylated PIN is trafficked to the basal plasma membrane domain (Fig. 2) (Michniewicz et al., 2007b; Kleine-Vehn et al., 2009; Dai et al., 2012).

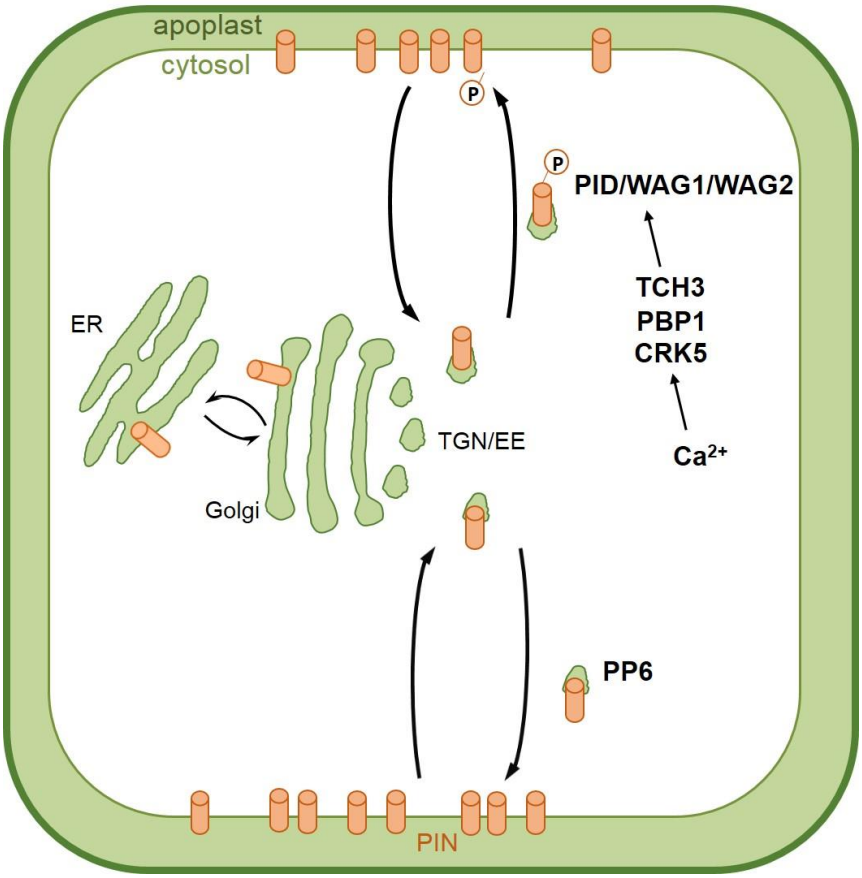

Figure 2: Schematic representation of polar auxin transport (PAT) via PINs. Newly synthetised or endocytosed PINs are targeted to the plasma membrane in a polar fashion depending on the PIN phosphorylation status. Phosphorylated PINs are trafficked to the apical side of the cell, while non-phosphorylated PINs are transported to the basal side. PINs are phosphorylated and dephosphorylated by PINOID(PID)/WAVY ROOT GROWTH1 (WAG1)/WAG2 and the PROTEIN PHOSPHATASE 6 (PP6) complex respectively. PIN phosporylation can also be indirectly regulated by Ca^{2+} via Ca^{2+} binding proteins TOUCH3 (TCH3) and PID BINDING PROTEIN1 (PBP1) and the Ca^{2+}/ CALMODULIN-DEPENDENT KINASE-RELATED KINASES 5 (CRK5). No organelles besides the endoplasmic reticulum (ER), Golgi Apparatus, and *trans*-Golgi network (TGN)/early endosome (EE) are depicted for simplification.

PIN phosphorylation not only affects PIN polarity, it is also important to activate PIN-mediated auxin transport. The D6 PROTEIN KINASE (D6PK) can phosphorylate PINs *in vitro* and *in vivo*, and *d6pk* mutants showed reduced PIN phosphorylation and auxin transport without affecting PIN polarity (Zourelidou et al., 2009; Willige et al., 2013; Barbosa et al., 2014). These observations demonstrate the importance of D6PK-mediated PIN phosphorylation for regulating auxin transport but not PIN polarity. Although both PID and D6PK can phosphorylate the same phosphosites in PIN1, their differential effects can only partially be explained by distinct phosphosite preferences suggesting a more complex mechanism determining PIN polarity (Zourelidou et al., 2014; Weller et al., 2017).

PIN phosphorylation status, and therefor also PIN polarity, can also be regulated more indirectly by modulation of PID activity by second messengers such as Ca^{2+} (Fig. 2) (Benjamins et al., 2003; Zhang et al., 2011). The Ca^{2+} binding proteins TOUCH3 (TCH3) and PID-BINDING PROTEIN1 (PBP1) were found to function upstream of PID enhancing PID activity in a Ca^{2+}-dependent manner (Benjamins et al., 2003). Furthermore, loss-of-function of the Ca^{2+}/ CALMODULIN-DEPENDENT KINASE-RELATED KINASES 5 (CRK5) resulted in defects in apical, PID-dependent, targeting of PIN2 (Rigó et al., 2013) providing additional evidence for the importance of Ca^{2+} for regulation of PIN polarity.

Given the reversible character of PIN phosphorylation, PIN polarity can easily be adjusted to redirect auxin flow depending on developmental or environmental stimuli. For example, during lateral root development PIN1 relocation will take place as the lateral root emerges to redirect the auxin flow towards the future lateral root tip (Benková et al., 2003). Upon unidirectional photostimulation of dark grown hypocotyls, apolarly distributed PIN3 in endodermis cells becomes restricted to the inner later domain of cells localized at the illuminated side of the hypocotyl (Ding et al., 2011). This results in redirection of the auxin flow towards the non-illuminated side where auxin will stimulate cell elongation resulting in hypocotyl bending towards the light. Importantly, the differential removal of PIN3 from the outer lateral domain was dependent on PID/WAG1/WAG2 activity, consistent with a model in which PIN polarity is determined by its phosphorylation status that is under control of environmental and developmental cues.

The endomembrane system and PIN trafficking

Before going into more detail on PIN trafficking I would shortly like to introduce the structure of the endomembrane system and trafficking between the different endomembrane compartments. A plant cell, as well as any other eukaryotic cell, contains a network of intracellular membranes to facilitate protein transport. The so-called endomembrane system consists of the plasma membrane, the ER, *trans*-Golgi network/early endosomes (TGN/EEs), the Golgi Apparatus, the multivesicular body/prevacuolar compartment/late endosomes (MVB/PVC/LEs), and the lytic and storage vacuole (Fig. 3). Trafficking between the different compartments is mediated by membrane-derived vesicles, generally called endosomes, which

bud off from the source compartment and fuse with the membrane of the target compartment to release its cargoes. The proteins that are transported can be either luminal cargoes or transmembrane proteins, e.g. PINs. Inter-compartment transport has a directional character (Fig. 3). For example, plasma membrane localized proteins, can be endocytosed (internalized) and transported to the TGN/EE, and conversely, can be recycled back to the plasma membrane. Newly synthetized proteins can be transported back and forth between the site of synthesis, the ER, and the Golgi. In case of protein degradation, the internalized proteins are targeted from the TGN/EE to MVBs/LEs and are from there onward trafficked unidirectionally to the lytic vacuole (Murphy et al., 2005; Jürgens and Geldner, 2007; Schellmann and Pimpl, 2009; Žárský and Potocký, 2010; Reyes et al., 2011; Robinson and Pimpl, 2014). Key regulators of endosome trafficking between distinct endomembrane compartments are small GTPases and their regulators GEFs and GAPs (Žárský and Potocký, 2010; Kania et al., 2014). Small GTPase proteins are often considered as molecular switches as they can cycle between a guanosine-5'-triphosphate (GTP)-bound form, the 'on' state, and a guanosine diphosphate (GDP)-bound form, the 'off' state. Switching between both forms relies on GTP hydrolysis, mediated by negative regulators named GTPase-ACTIVATING PROTEINs (GAPs), and exchange of GDP for GTP mediated by the positive regulators called GUANINE NUCLEOTIDE EXCHANGE FACTORs (GEFs). There are two main groups of small GTPases involved in regulation of distinct steps during endomembrane trafficking; the ADP-RIBOSYLATION FACTORs (ARFs) and RAS GENES FROM RAT BRAIN (RABs). ARFs are involved in recruitment of coat proteins to sites of vesicle budding thereby forming an important regulator of retrograde and anterograde ER-Golgi transport, and are also involved in mediating endocytosis and recycling as will be discussed in more detail later on (Nielsen et al., 2008; Yorimitsu et al., 2014). The RAB GTPases also operate at distinct steps of endomembrane trafficking coordinating ER-Golgi transport, endocytosis, recycling of cell wall components. Furthermore, they are important for cell polarization and regulation of membrane fusion together with SNAREs (Vernoud et al., 2003; Nielsen et al., 2008; Kania et al., 2014). They also have been shown to be crucial for successful cytokinesis (Davis et al., 2016).

In the following paragraphs I will discuss the different steps in the endosomal trafficking pathway in more detail (Fig. 3).

As can already be deduced from the ability of PINs to relocate, PINs are highly dynamic proteins that can swiftly translocate through the endomembrane system. Plasma membrane-localized PINs are continuously internalized by clathrin-mediated endocytosis (Dhonukshe et al., 2007), and recycled back to the plasma membrane via exocytosis (Geldner et al., 2001). Recycling can occur to the original polarity domain, or to a different side of the cell (Kleine-Vehn et al., 2008b).

Clathrin-mediated endocytosis (CME) is a common endocytic mechanism in plants mediating internalization of a wide range of plasma membrane-localized proteins such as PINs (Kitakura et al., 2011), BRASSINOSTEROID INSENSITIVE1 (BRI1) (Di Rubbo et al., 2013), and the flagellin receptor FLAGELLIN SENSING2 (FLS2) (Mbengue et al., 2016). Early stages of CME are hallmarked by the arrival of the plant-specific TPLATE adaptor complex and ADAPTOR PROTEIN complex 2 (AP2) at the plasma membrane (Gadeyne et al., 2014a). These proteins are crucial for subsequent recruitment of clathrin and other components required for formation of clathrin-coated vesicles (CCVs). In a last step, small GTPases DYNAMIN-RELATED PROTEINs (DRPs) will mediate scission of the CCV from the plasma membrane. After the CCVs are released from the plasma membrane, they will lose their clathrin coat by the action of a.o. the clathrin coat disassembly chaperone AUXILIN (AX) (Lam et al., 2001). The importance of CME for proper PIN trafficking, and consequently auxin transport, is illustrated by the wide range of defective auxin-regulated processes upon interference the CME machinery. For example loss-of-function of DRP1 resulted in PIN2 mislocalization and associated agravitropic root growth (Mravec et al., 2011). Also, interference with clathrin coat assembly and function prevented PIN endocytosis, and caused defective (post)embryonic development and agravitropic root growth (Kitakura et al., 2011). Alternatively, plants can mediate endocytosis via clathrin-independent pathways, however, currently little is known about these mechanisms. In animals, clathrin-independent caveolae- and flotillin-dependent pathways have been described (Kurzchalia and Partan, 1999; Otto and Nichols, 2011). Although the former is not found in plants there is evidence for flotillin-mediated endocytosis. Flotillin1 (Flot1) was found to be present in membrane microdomains distinct from CCVs, mediating formation of membrane-derived endocytic vesicles during symbiotic infection and salt stress (Haney and Long, 2010; Baral et al., 2015). However, the molecular mechanism and components involved remain to be resolved.

Upon scission of CCVs from the plasma membrane, the vesicle loses its clathrin coat and enters the endosomal trafficking pathway at the TGN/EE from where proteins can be recycled back to the plasma membrane, or become targeted to the vacuole for degradation. Early endosomal trafficking is mediated by the ARF-GEF BFA-VISUALIZED ENDOCYTIC TRAFFICKING DEFECTIVE1 (BEN1)/BFA-INHIBITED GEF5 (BIG5)/ HOPM INTERACTOR7 (MIN7) and BEN2/VACUOLAR PROTEIN SORTING45 (VPS45) that are both localized at the TGN/EE (Tanaka et al., 2009; Tanaka et al., 2013). A well-known regulator of PIN recycling is the ARF-GEF GNOM (Geldner et al., 2003). GNOM-mediated recycling is sensitive to the fungal toxin brefeldin A (BFA; Geldner et al., 2001). Besides interfering with GNOM function, BFA also inhibits a subset of other large ARF-GEFs in mammals, yeast, and plants (Peyroche et al., 1996). The basis for BFA sensitivity is defined by the presence of a few key amino acids in the ARF-GEF catalytic Sec domain (Peyroche et al., 1999; Sata et al., 1999; Steinmann et al., 1999). Inhibition of ARF-GEF by BFA consequently prevents ARF activation (Peyroche et al., 1999; Robineau et al., 2000). Given that ARF(-GEFs) mediate multiple endomembrane trafficking steps, BFA can affect the endomembrane system at distinct levels. Interestingly, the impact of BFA treatment was shown to be concentration-dependent. Lower BFA concentrations were reported to block anterograde ER-to-Golgi transport, secretion/recycling, and cause formation of so called BFA bodies, a fusion of TGN, Golgi, and ER, accumulating internalized proteins (Donaldson and Jackson, 2000; Geldner et al., 2001; Nebenfuhr et al., 2002). Higher BFA concentrations additionally block vacuolar trafficking (Tse et al., 2007; Kleine-Vehn et al., 2008b). These features have made BFA a valuable tool to study PIN trafficking. Further investigation showed that recycling of PINs to the apical or basal side of the cell involves distinct ARF-GEFs. BFA-sensitive GNOM primarily regulates basal PIN recycling as sustained BFA treatment resulted in transcytosis from basal PINs to the apical domain (Kleine-Vehn et al., 2008b). This also implicates that the apical targeting pathway is GNOM-independent. The closest GNOM homologue in *Arabidopsis* is the ARF-GEF GNOM-LIKE1 (GNL1) that localizes at the Golgi apparatus where it mediates ER-Golgi transport (Richter et al., 2007). Interestingly, GNOM can take over GNL1 function, but not the other way around. Besides GNOM, also the BFA-INHIBITED GEF (BIG) family of ARF-GEFs is characterized by sensitivity to the fungal toxin BFA. As for GNOM, the BIGs have been shown to be important for regulation of recycling, and are additionally involved in protein secretion during cell division (Shin et al., 2004; Richter et al., 2014; Kitakura et al., 2017). Besides GNOM, also the ARF-GAP VASCULAR NETWORK3 (VAN3),

the RABA1b GTPase BFA-VISUALIZED EXOCYTIC TRAFFICKING DEFECTIVE5 (BEX5), and RAB-GEF VASCULAR NETWORK DEFECTIVE4 (VAN4) operate as regulators of PIN recycling (Koizumi et al., 2005; Sieburth et al., 2006; Feraru et al., 2012; Naramoto et al., 2014). Intriguingly, GNOM, GNL1 and VAN3 also turned out to be involved in regulation of PIN endocytosis indicating their functional versatility (Teh and Moore, 2007; Naramoto et al., 2010). Upon targeting of recycling endosomes to the plasma membrane, endosome-plasma membrane fusion is mediated by the vesicle tethering complex exocyst. This octameric complex is evolutionary conserved mediating a similar function in yeast, animals and plants (Hála et al., 2008; Ory and Gasman, 2011; Liu and Guo, 2012). The importance of exocyst for PIN trafficking is illustrated by delayed PIN recycling and aberrant polar auxin transport in a mutant defective in subunit EXO70A1 (Drdová et al., 2013). Even though the recycling endosomes don't have any characteristic coating like the CCVs, the presence of specific proteins in the endosome compartments might be a determinant for proper protein sorting. The retromer complex consists of multiple proteins that can fulfill this function mediating distinct steps of intracellular trafficking in plants. There has been some debate about the localization and function of retromer subunits (Oliviusson et al., 2006; Niemes et al., 2010). Nevertheless, it seems that the retromer complex is involved in both recycling proteins to the plasma membrane as well as in retrieving proteins from the vacuolar degradation pathway. For example, the retromer subunit SORTING NEXIN1 (SNX1) is known to mark PIN2 endosomes destined for recycling to the plasma membrane (Jaillais et al., 2006). Furthermore, VACUOLAR SORTING RECEPTORs (VSRs) localize to the TGN and MVBs where they mediate vacuolar cargo sorting (Sanderfoot et al., 1998). Upon delivery of their cargo, they are recycled by retrograde transport for subsequent rounds of vacuolar sorting (daSilva et al., 2005; Oliviusson et al., 2006; Niemes et al., 2010). Retrieval of VSR1 to the TGN was shown to be mediated by retromer subunit VACUOLAR PROTEIN SORTING 29 (VPS29) (Kang et al., 2012). Besides a role in retrograde trafficking from MVB to TGN, VPS29, together with retromer subunit VPS35a, where shown to be essential for proper MVB morphology (Nodzyński et al., 2013).

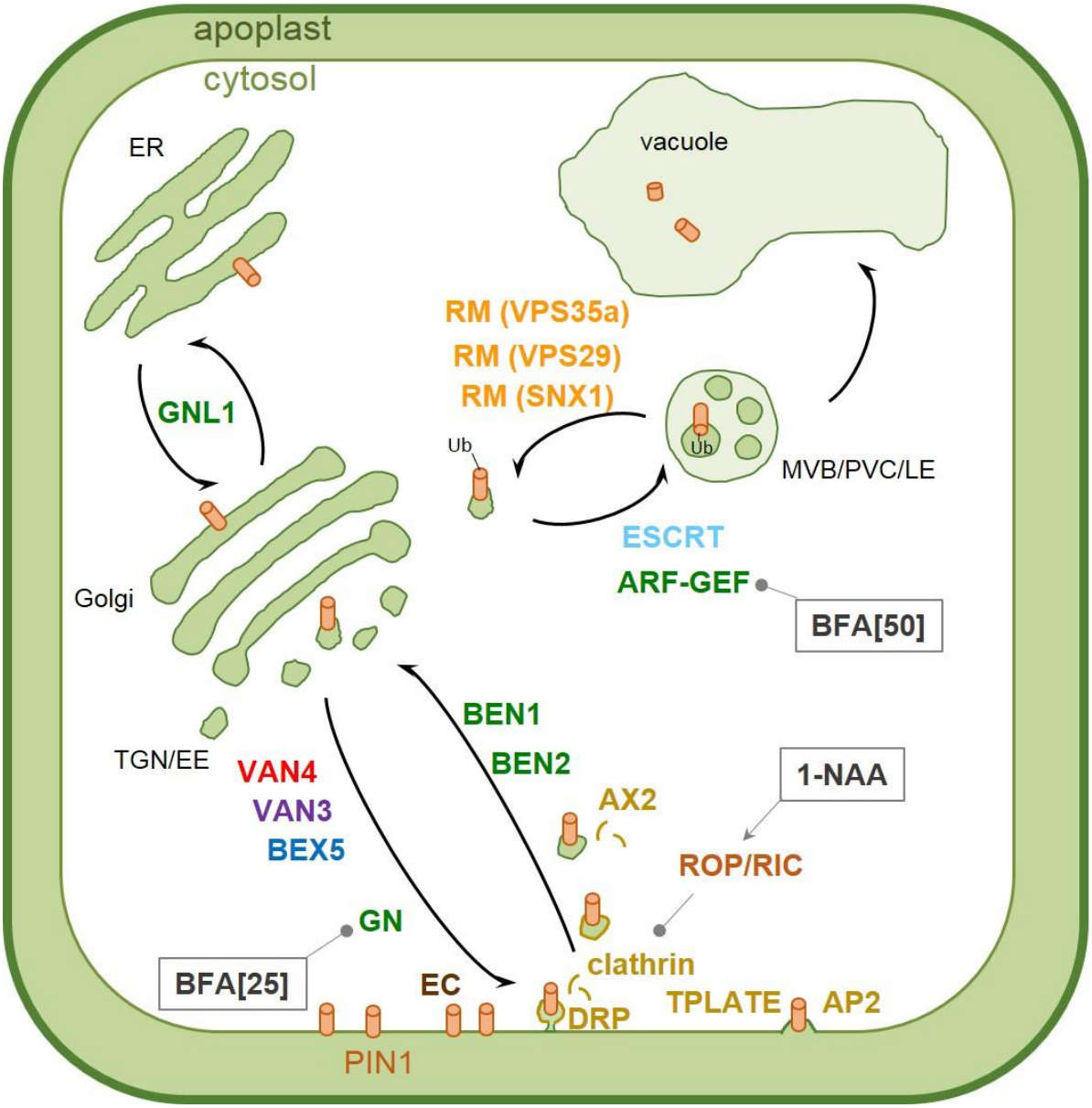

Figure 3: The endomembrane system and endosomal (PIN) trafficking. The endomembrane system consists of the *trans*-Golgi network/early endosomes (TGN/EEs), the Golgi Apparatus, the endoplasmic reticulum (ER), the multivesicular bodies/prevacuolar compartments/late endosomes (MVBs/PVCs/LEs), and the vacuole (lytic and storage). Transport between the different endosomal compartments is mediated by ARF-GEFs (green) and –GAPs (purple), RAB (dark blue), RAB-GEFs (red) and -GAPs, the retromer complex (RM, orange), the exocyst (EC), and Endosomal Sorting Complex Required for Transport (ESCRT). The players that have been identified so far are marked in the figure in the corresponding colors. As an example basally localized PIN1 is shown. Low brefeldin A (BFA) concentrations inhibit protein recycling, while high BFA concentrations additionally block vacuolar trafficking. Vacuolar degradation would involve protein ubiquitylation, however more insight on the players involved is still missing. PIN proteins are internalized via clathrin-mediated endocytosis (CME). Initial stages of CME rely on the TPLATE adaptor complex, and ADAPTOR PROTEIN complex 2 (AP2). DYNAMIN-RELATED PROTEINs (DRPs) are required for pinching off the clathrin-coated vesicles from the plasma membrane. AUXILIN2 (AX2) is involved in clathrin coat disassembly from the vesicles after internalization. The synthetic auxin 1-naphthaleneacetic acid (1-NAA) inhibits CME of PINs via activation of ROP/RIC signaling. BEN1, 2: BFA-VISUALIZED ENDOCYTIC TRAFFICKING DEFECTIVE1, 2; BEX5: BFA-VISUALIZED EXOCYTIC TRAFFICKING DEFECTIVE5; GN: GNOM; GNL1: GNOM-LIKE1; SNX1: SORTING NEXIN1; Ub: ubiquitin; VAN3: VASCULAR NETWORK3; VAN4: VASCULAR NETWORK DEFECTIVE4, VPS29, 35a: VACUOLAR PROTEIN SORTING29, 35a.

As mentioned earlier, the TGN/EE also functions as a sorting point to target internalized proteins to the lytic vacuole for degradation. First, proteins will be integrated in intraluminal vesicles residing in the MVBs, and subsequently the MVBs will release these intraluminal vesicles into the vacuole lumen by MVB – vacuole fusion. Current knowledge on the molecular players involved is still rather fragmented. It has been established that protein ubiquitylation is an important determinant. PIN2 degradation might be mediated by ubiquitylation by RING-DOMAIN LIGASE (RGLG) E3 ubiquitin ligases at the plasma membrane (Yin et al., 2007; Leitner et al., 2012). Ubiquitinylated proteins are recognized by the Endosomal Sorting Complex Required for Transport (ESCRT) mediating the uptake into the intraluminal vesicles of the MVBs (Schellmann and Pimpl, 2009). Furthermore, it has been suggested that PIN2 vacuolar trafficking relies on activity of an ARF-GEF, different from GNOM (Kleine-Vehn et al., 2008b). Interestingly, while low BFA concentrations inhibit PIN recycling, high BFA concentrations additionally interfere with vacuolar trafficking suggesting the ARF-GEF involved is BFA-sensitive (Kleine-Vehn et al., 2008a). More recent work has shown that at least three vacuolar trafficking pathways can be distinguished in plants, each transporting specific cargo (Ebine et al., 2014). A first pathway involves subsequent action of small GTPases RAB5 and RAB7, regulated by the RAB-GEF SAND-CCZ1, and was shown to be a vacuolar transport route for 12S globulin (Cui et al., 2014; Ebine et al., 2014; Singh et al., 2014). Alternatively, vacuolar proteins such as the tonoplast-localized SYNTAXIN OF PLANTS 22 (SYP22) and V-TYPE PROTON ATPASE SUBUNIT a3 (VHA-a3), can be targeted through a RAB5-dependent, RAB7-independent pathway (Ebine et al., 2014; Feng et al., 2017). Thirdly, a RAB5/7- independent ADAPTOR PROTEIN-3 (AP-3)-dependent pathway has been proposed. AP-3 is a tetrameric adaptor complex regulating vacuolar trafficking as shown by the vacuolar defects that can be observed when interfering with AP-3 subunit function (Feraru et al., 2010; Zwiewka et al., 2011). Interestingly, it is suggested that this pathway mediates direct targeting to the vacuole thereby bypassing endosome maturation via the MVBs (Feraru et al., 2010), which corresponds to AP-3-mediated lysosome trafficking in yeast, flies, and animals (Cowles et al., 1997; Stepp et al., 1997; Dell'Angelica et al., 1999; Feng et al., 1999; Kretzschmar et al., 2000). Vacuolar PIN degradation can be stimulated by different triggers that modulate PAT. During root gravistimulation, asymmetric auxin distribution at the root tip is partially established by auxin-induced vacuolar degradation of PIN2 in epidermal cells at the lower side of the root

(Baster et al., 2013). Also dark treatment induces PIN2 targeting to the vacuole for degradation (Laxmi et al., 2008).

Altogether, our knowledge from literature shows us the highly dynamic nature of the PINs and the ability of plants to modify PIN localization, and thereby redirect auxin flow, through a complex tightly regulated endosomal trafficking network.

Auxin-regulated PIN trafficking

The dynamic nature of PINs and their ability to translocate between plasma membrane domains allows for rapid PIN relocation as demonstrated by previous examples. Besides developmental cues and environmental signals, also auxin itself can feedback regulate PIN localization, and thereby the directionality of its own flow (Benjamins and Scheres, 2008). This can be achieved by auxin-regulated PIN transcription and -turnover (Sieberer et al., 2000; Vieten et al., 2005). Alternatively, auxin can regulate its direction of transport by affecting PIN trafficking. It has been documented that auxin inhibits CME of PINs thereby reinforcing PIN localization at the plasma membrane (Paciorek et al., 2005).

The molecular mechanism underlying auxin-inhibited PIN endocytosis has been further unraveled over the years with leaf pavement cells and root epidermal cells as a model. For both models the involvement of intracellular RHO-LIKE GTPASE FOR PLANTS (ROPs) and their ROP INTERACTIVE CRIB MOTIF-CONTAINING PROTEINS (RIC) effectors and downstream modulation of the actin cytoskeleton has been demonstrated (Chen et al., 2012; Lin et al., 2012; Nagawa et al., 2012). Upstream of this pathway, auxin was proposed to be perceived by an AUXIN BINDING PROTEIN1 (ABP1) receptor complex (Xu et al., 2014). However, the finding that *abp1* full knock-out alleles have no obvious phenotypes (see below), suggests that the ABP1 function in this model needs to be reassessed and corrected. Therefore, the main questions which remain to be addressed are which auxin receptor is involved in mediation of this rapid auxin response, and how auxin perception results in intracellular activation of ROP/RIC signaling.

Auxin perception and signaling in brief

Until recently, two main auxin perception and signaling mechanisms have been distinguished: the $SCF^{TIR1/AFB}$-Aux/IAA-dependent mechanism, and the ABP1-dependent pathway.

$SCF^{TIR1/AFB}$-Aux/IAA-dependent auxin perception and -signaling takes place in the nucleus and mediates transcriptionally-regulated auxin responses (Wang and Estelle, 2014; Salehin et al., 2015). The main components of the pathway are TRANSPORT INHIBITOR RESPONSE 1/AUXIN SIGNALING F-BOX PROTEINS (TIR1/AFB), Auxin/INDOLE ACETIC ACID (Aux/IAA) transcriptional repressors, and transcription factors AUXIN RESPONSE FACTORs (ARFs). At low auxin levels, ARF transcription factors bound to Auxin RESPONSE ELEMENTs (AuxREs) (Ulmasov et al., 1995; Ulmasov et al., 1997a; Ulmasov et al., 1997b) in promoters of auxin responsive genes are kept inactive by association with the Aux/IAA transcriptional suppressors and the cosuppressor TOPLESS (TPL) (Szemenyei et al., 2008). Upon high auxin concentrations, auxin perception by the TIR1 auxin receptor (Dharmasiri et al., 2005; Kepinski and Leyser, 2005) results in targeting of the Aux/IAAs to the ubiquitin protein ligase $SCF^{TIR1/AFB}$ mediating proteolysis of these transcriptional repressors (Gray et al., 1999; Gray et al., 2001; Ramos et al., 2001; Tan et al., 2007) allowing the ARFs to activate transcription. In *Arabidopsis*, TIR1/AFBs, Aux/IAAs, and ARFs are represented by small to large gene families counting 6, 29, and 22 members respectively in *Arabidopsis* (Enders et al., 2015; Li et al., 2016). Specific combinations of ARFs and Aux/IAAs account for the wide range of diverse auxin-mediated responses (Weijers et al., 2005), and different combinations of TIR1 and Aux/IAAs show distinct auxin-binding affinity (Calderón Villalobos et al., 2012).

Since this signaling pathway relies on transcriptional regulation, it is mediating rather slow auxin responses such as auxin-induced lateral root formation (Gray et al., 2001), root gravitropism (Baster et al., 2013), and hypocotyl growth (Fendrych et al., 2016). However, some cellular auxin responses occur rapidly. For example, exogenous auxin treatment can trigger a cytosolic Ca^{2+} increase within seconds (Sabatini et al., 1999; Shishova and Lindberg, 2004). Also, inhibition of clathrin-mediated PIN endocytosis by auxin was shown to be TIR1-independent (Paciorek et al., 2005b), suggesting that some (rapid) auxin responses might be regulated by an alternative perception and signaling mechanism, independent of transcriptional regulation. For some time, it was believed that such responses are mediated by the auxin receptor ABP1. It was found that ABP1 can bind auxin with high affinity (Hertel

et al., 1972), and is a regulator of different auxin-regulated processes such as cell expansion (Jones et al., 1998), embryogenesis (Chen et al., 2001), postembryonic shoot development (Braun et al., 2008), root growth (Tromas et al., 2009), hypocotyl elongation (Effendi et al., 2013) and auxin-regulated PIN trafficking in leaves and roots (Robert et al., 2010; Xu et al., 2010; Chen et al., 2012). These observations were largely based on analysis of conditional ABP1 knock-down mutants, immunological inactivation of ABP1 function, and ABP1 lines mutated in the auxin-binding pocket (*abp1-5*) as a T-DNA insertion null mutant was shown to be embryo lethal (Chen et al., 2001). However, the technical advancements in molecular biology had more recently enabled the generation of an *abp1* null mutant by means of the CRISPR/Cas9-technology (Gao et al., 2015). Gao and coworkers also picked up a viable T-DNA insertion null mutant. Surprisingly, analysis of these mutants showed no defects in auxin-dependent developmental processes nor abnormal auxin-regulated gene expression. Later work had shown that the auxin-related phenotypes observed in the conditional knock-down lines and *abp1-5* where caused by off-target effects and background mutations (Enders et al., 2015; Michalko et al., 2016). These recent insights in ABP1 function have brought into question the role of ABP1 as a mediator of auxin signaling, and further research will be indispensable to get a better insight in possible alternative auxin perception mechanisms.

Interestingly, recently, more and more alternative auxin perception mechanisms are being uncovered. Similarly to TIR1, the F-box protein S-PHASE KINASE-ASSOCIATED PROTEIN 2A (SKP2A) was reported to specifically bind to auxin, and interconnect auxin perception with regulation of cell division (Jurado et al., 2010). In addition, the ARF3/ETTIN was found to sense auxin directly to regulate its transcriptional activity (Simonini et al., 2016; Simonini et al., 2017). Therefore, it will be interesting to follow the further developments in identifying auxin sensing proteins and how they control cellular auxin responses.

Ca^{2+} signaling

Ca^{2+} as a second messenger during plant development

It is well-established that Ca^{2+} is indispensable for proper plant growth and development. Even though Ca^{2+} is among the most abundant cations in the soil, Ca^{2+} deficiency can occur on acidic and sandy soils, or locally within the plant due to aberrant Ca^{2+} distribution. Ca^{2+} deprivation

causes severe defects in roots, stems, leaves and fruits depending on the plant species (Bussler, 1962; Hewitt, 1963), stressing the importance of this cation for healthy plant growth. Ca^{2+} is known for its structural function contributing to plant cell rigidity by crosslinking pectates in the cell wall and regulating membrane integrity (Wyn Jones, 1967; Burstrom, 1968; Marschner, 1995).

Besides this structural role, Ca^{2+} also operates as a second messenger in a wide range of signaling pathways related to coping with biotic and abiotic stress, and plant development (Dodd et al., 2010; Kudla et al., 2010). It is well documented that pathogen attack and herbivory trigger a cytosolic Ca^{2+} burst during the early stages of plant immunity and defense (Arimura and Maffei, 2010; Ma et al., 2012; Ma et al., 2013; Keinath et al., 2015). Besides biotic stress, also beneficial biotic interactions such as symbiosis of root hairs with rhizobia is known to require a Nod factor-induced Ca^{2+} influx followed by specific perinuclear Ca^{2+} oscillations (Shaw and Long, 2003). Multiple abiotic stress factors such as drought and cold induce Ca^{2+}-mediated stomata closure which is essential to maintain the water balance in the plant (McAinsh, 1990; Kudla et al., 2010). Mediating nitrate signaling and triggering protection mechanisms to osmotic stress, touch, and oxidative stress is also initiated by stimulus-specific Ca^{2+} signatures (Knight et al., 1991; Rentel and Knight, 2004; Riveras et al., 2015; Huang et al., 2017). In case of pollen tube and root hair development, Ca^{2+} operates as a key mediator of polarized tip growth (Himschoot et al., 2015a) (see also Section I - Chapter 2). These are only a few examples out of a wide range of Ca^{2+}-mediated signaling pathways illustrating the importance of this second messenger for plant development and environmental adaptation.

Ca^{2+} as a second messenger in auxin-regulated processes

Previous work has demonstrated an interconnection between auxin- and Ca^{2+} signaling. Analysis of cytosolic Ca^{2+} concentrations and surface pH of gravistimulated roots showed an increase in cytosolic Ca^{2+} levels of epidermal cells and elevated surface pH at the lower, but not the upper, side of the root (Monshausen et al., 2011). This pattern coincides with the asymmetric auxin distribution at the root tip, with increased auxin levels at the lower side of the root (Ottenschläger et al., 2003; Swarup et al., 2005). Furthermore, exogenous application of auxin was shown to induce a rapid and transient cytosolic Ca^{2+} increase in different tissues

and plant species (Felle, 1988; Gehring et al., 1990; Shishova and Lindberg, 1999, 2004; Shishova et al., 2007). In Chapter 1 of the Results section (Section II - Chapter 1), NAA-induced Ca^{2+} dynamics in *Arabidopsis* roots will be discussed in more detail. Auxin-induced Ca^{2+} dynamics have been shown to occur rapidly within seconds to minutes, which is too rapid to be mediated by TIR1-dependent transcriptional regulation. Indeed, the Ca^{2+} signals and the Ca^{2+}-dependent surface pH dynamics accompanying root gravitropism are not affected in the *tir1* mutant, nor in the *abp1* null mutant (Monshausen et al., 2011; Shih et al., 2015), indicating that the auxin receptor involved in this pathway remains to be identified.

Ca^{2+} signaling in plants

Ca^{2+} uptake takes place at the extensive root system from where it is mainly distributed towards the shoot by xylem-mediated transport (White, 2001). At the cellular level, Ca^{2+} is stored in the apoplast, ER, and vacuole (Stael et al., 2012). A strong Ca^{2+} concentration gradient is kept between the cytosol (100-200 nM) and the Ca^{2+} storages (mM range) allowing rapid Ca^{2+} influx into the cytosol upon stimulation (Fig. 4).

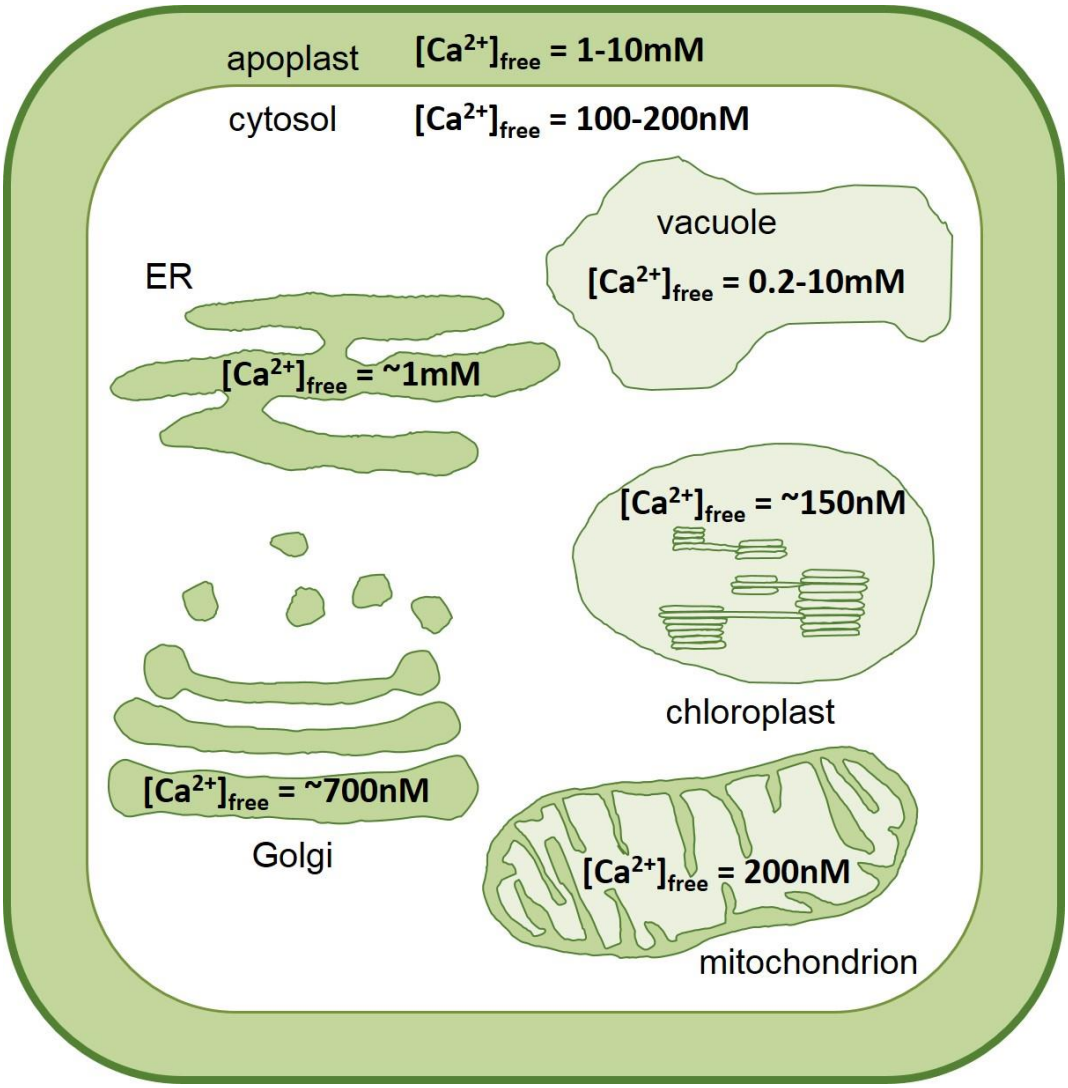

Figure 4: Ca^{2+} distribution in plant cell organelles. The organellar Ca^{2+} concentrations were derived from (Johnson et al., 1995; Nomura et al., 2012; Logan and Knight, 2003; Medvedev, 2005; Ordenes et al., 2012). The ER, vacuole and apoplast operate as Ca^{2+} stores. Note that the depicted Ca^{2+} concentrations are for free Ca^{2+}. Ca^{2+} can also be bound to e.g. Ca^{2+} chelators.

As described above, Ca^{2+} operates in a wide range of signaling pathways, and plants have evolved an extensive toolkit of Ca^{2+} channels, Ca^{2+} pumps, Ca^{2+} sensors, and Ca^{2+}-dependent protein kinases responsible for generating/encoding, amplifying and translating/decoding stimulus-specific Ca^{2+} signatures and mediating recovery to Ca^{2+} resting levels (Fig. 5). Each of these Ca^{2+} signaling components are represented by large gene families making genetics challenging.

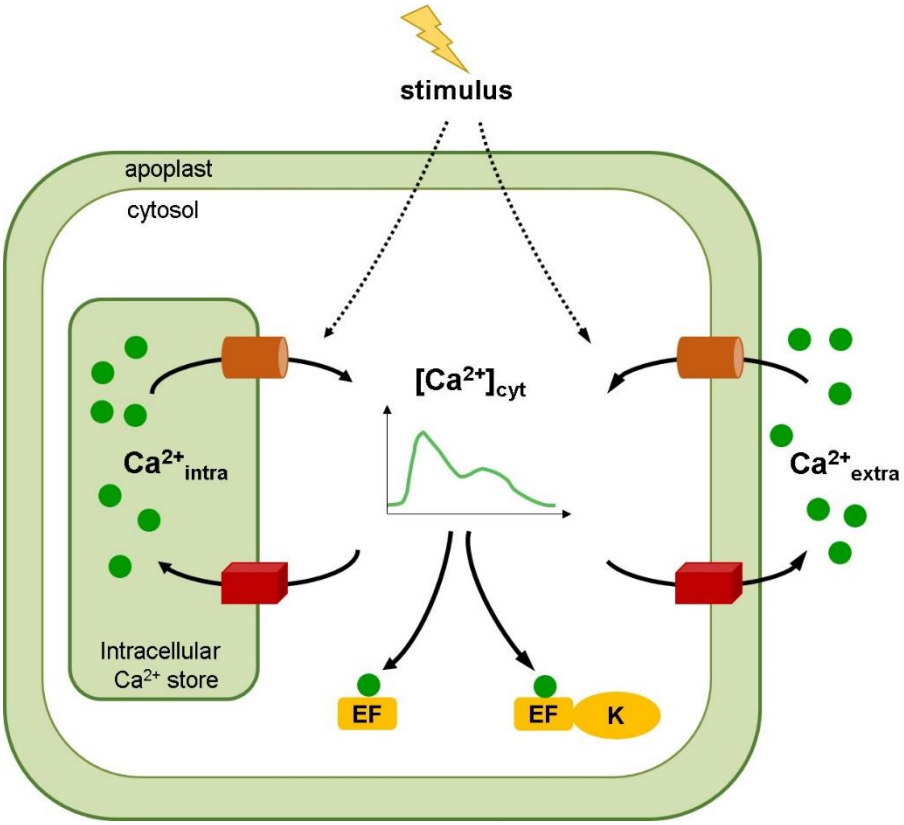

Figure 5: A schematic representation of the different levels of Ca^{2+} signaling in plants. Upon stimulation, the Ca^{2+} influx pathway (brown), consisting of Ca^{2+} channels in the plasma membrane and membranes of intracellular stores, generates a specific cytosolic Ca^{2+} signatures. Sensing this Ca^{2+} signature relies on sensor relays (e.g. CaM) and sensor responders (e.g. Ca^{2+}-dependent protein kinases) (yellow). They in turn can associate with or activate a downstream target to evoke a stimulus-specific response. Finally, the Ca^{2+} efflux pathway (red) mediated by Ca^{2+} pumps and transporters in the plasma membrane and intracellular store membranes, assures the Ca^{2+} resting levels in the cytosol are reestablished.

In plants, Ca^{2+} channels are classified according to their activation mechanism. One can distinguish voltage-activated and voltage-independent Ca^{2+} channels, ligand-gated Ca^{2+} channels, and mechano-stimulated Ca^{2+} channels (Kudla et al., 2010; Swarbreck et al., 2013). The ANNEXINs are more difficult to classify in one of these groups as they can be activated by distinct signals. Since a few years a new class of Ca^{2+} channels can be added to the list. The OSCAs are a family of osmosensing Ca^{2+} channels mediating Ca^{2+} influx in high osmolality environments (Yuan et al., 2014). Note that the term Ca^{2+} channels not necessarily means that these channels exclusively transport Ca^{2+}. Most channels are non-selective cation channels that in many cases have a preference for e.g. K^{+} over Ca^{2+} (Véry and Davies, 2000; Demidchik and Maathuis, 2007). For convenience the term Ca^{2+} channels will be used throughout the ong the voltage-activated Ca^{2+} channels, the HYPERPOLARIZATION-ACTIVATED Ca^{2+} CHANNELs

(HACC) have been most extensively studied and are known for mediating Ca^{2+} influx in guard cells triggered by voltage but also abscisic acid (ABA) (Hamilton et al., 2000), and in root hairs where they coexist with DEPOLARIZATION-ACTIVATED Ca^{2+} CHANNEL (DACC) (Demidchik et al., 2002; Miedema et al., 2008). The ligand-gated Ca^{2+} channels are subdivided in GLUTAMATE RECEPTOR-LIKE Ca^{2+} channels (GLRs) and CYCLIC NUCLEOTIDE-GATED Ca^{2+} CHANNELs (CNGCs). Both groups of Ca^{2+} channels are represented by 20 members in *Arabidopsis* (Mäser et al., 2001; Davenport, 2002). In contrast to what the name suggests, GLR are not exclusively activated by glutamate but can be triggered by broad range of amino acids (Forde and Roberts, 2014). Although the biological role of most of the GLRs remains to be identified, a subset of GLRs is known for their function in the plant defense response. For example, the AtGLR3.3 was shown to be required for induction of defense genes upon infection with the biotrophic pathogens *Pseudomonas syringae* and *Hyaloperonospora arabidopsidis* (Li et al., 2013; Manzoor et al., 2013), and in response to mechanical wounding which reassembles herbivory (Mousavi et al., 2013). Recently, *Physcomitrella* GLRs were shown to be involved in sperm chemotaxis (Ortiz-Ramírez et al., 2017).

CNGCs can be activated by cyclic nucleotides cyclic adenosine monophosphate (cAMP), cyclic guanosine monophosphate (cGMP) and are inhibited by CaM (McAinsh and Pittman, 2009). They have been more extensively studied compared to GLRs, and CNGC-mediated Ca^{2+} influx has been shown to be important in guard cells (Wang et al., 2013), seed germination (Gobert et al., 2006), pollen tube and root hair tip growth (Frietsch et al., 2007; Zhang et al., 2017), pathogen defense (Yoshioka et al., 2006; Ma and Berkowitz, 2011), and auxin responses (Shih et al., 2015).

The mechano-stimulated Ca^{2+} channels, also known as membrane-tension-activated Ca^{2+} channels, respond to mechanical stimuli such as touch, chewing during herbivory, gravity, and membrane tension changes associated with outgrowth of lateral roots, pollen tube growth, and cell wall damage (Nakagawa et al., 2007; Lucas et al., 2013; Monshausen and Haswell, 2013; Toyota and Gilroy, 2013; Appel and Cocroft, 2014). Also a hypo-osmotic challenge can cause membrane stretching and thereby activation of mechanosensitive channels (Qi et al., 2004; Veley et al., 2012).

Another family of Ca^{2+} channels which is activated by changes in osmolarity are the REDUCED HYPEROSMOLALITY-INDUCED [$Ca^{(2+)}$]i INCREASEs (OSCAs) (Yuan et al., 2014). Study of *osca1*

has shown a role for this OSCA in mediating Ca^{2+} signaling in guard and root cells under osmotic stress in order to regulate water transpiration. OSCA4 was identified in a screen for regulators of vacuolar protein sorting (Fuji et al., 2007a).

The ANNEXINs (ANNs), which are represented by 8 members in *Arabidopsis* (Clark et al., 2012), are more atypical Ca^{2+} channels. ANNs are soluble proteins that can associate with membranes in a Ca^{2+}-dependent or –independent manner (Breton et al., 2000; Hofmann et al., 2000; Gorecka et al., 2007; Hu et al., 2008; Laohavisit et al., 2009). They are often classified as voltage-gated channels, however, they can also be activated by different reactive oxygen species (ROS) and adenosine triphosphate (ATP) (Shang et al., 2009; Kudla et al., 2010; Laohavisit et al., 2012; Richards et al., 2014). Furthermore, while conventional Ca^{2+} channels mostly localize to specific membranes, ANNs can occur at multiple sites simultaneously, even extracellularly. AtANN1 for example was reported to be found in the plasma membrane, at the ER, mitochondria, chloroplast, vacuole, and in the cell wall (Laohavisit and Davies, 2009; Obata et al., 2011). Factors that can determine ANN position are salt stress, cold, mechanical stimulation and gravistimulation (Thonat et al., 1997; Breton et al., 2000; Clark et al., 2000; Lee et al., 2004). ANNs have been shown to be important for mediating osmotic stress, salt and drought tolerance, and ABA signaling (Lee et al., 2004; Gorantla et al., 2005; Laohavisit et al., 2013). Besides mediating Ca^{2+} transport, some ANNs also show ATPase and peroxidase activity (McClung et al., 1994; Gorecka et al., 2005). Given their property to associate with membrane phospholipids in a Ca^{2+}-dependent matter, it has also been suggested that ANNs operate as regulators of membrane trafficking (Konopka-Postupolska and Clark, 2017).

In order to transduce diverse stimuli-induced Ca^{2+} signatures, plants have evolved an extensive set of Ca^{2+} sensors. Sensor relays only have a Ca^{2+}-binding domain and need to associate with an interaction partner (e.g. a protein kinase) to transduce the Ca^{2+} signal. Plant sensor relays are CaM and CALCINEURIN B-LIKE (CBL) proteins which bind Ca^{2+} ions through their EF hand domains (Luan et al., 2002). Among CaM targets are protein kinases, metabolic enzymes, and cytoskeleton-associated proteins (Zielinski, 1998; Snedden and Fromm, 2001; Reddy et al., 2002). CBLs associate with CBL-INTERACTING PROTEIN KINASEs (CIPKs) (Shi et al., 1999) and function in salt stress signaling and adaptation, response to wounding, cold, and drought, regulation of ABA sensitivity and biosynthesis, and nutrient sensing (Luan et al., 2002). Sensor responders combine the role of Ca^{2+} binding and signal transduction in one

protein (Sanders et al., 2002). Ca^{2+}-DEPENDENT PROTEIN KINASEs (CDPKs or CPKs) contain 4 EF hand domains for Ca^{2+} binding and a kinase domain for Ca^{2+}-dependent phosphorylation of a downstream target. *Arabidopsis* has 34 CDPKs (Cheng et al., 2002b) operating in a diverse range of signaling pathways related to plant immunity, regulation of the cytoskeleton, ion and water transport, nitrogen and phospholipid metabolism,… (Cheng et al., 2002b; Reddy and Reddy, 2004; Boudsocq et al., 2010).

After the Ca^{2+} signature has been sensed and decoded into a specific response, the Ca^{2+} resting levels in the cytoplasm have to be reestablished. This is achieved by active efflux of Ca^{2+} ions by Ca^{2+}-ATPases and Ca^{2+}-H^+ antiporters, also named CATION EXCHANGERs (CAX). Ca^{2+}-ATPases can be further subdivided in ER-TYPE Ca^{2+}-ATPASEs (ECAs) and AUTO-INHIBITED Ca^{2+}-ATPASEs (ACA) (Geisler et al., 2000a; Sze et al., 2000; Bonza and De Michelis, 2011). These pumps have been reported to localize at membranes of intracellular Ca^{2+} storages such as the ER, the vacuole, the Golgi Apparatus, endosomes, and at the plasma membrane (Liang et al., 1997; Harper et al., 1998; Hong et al., 1999; Bonza et al., 2000; Geisler et al., 2000b; Schiøtt et al., 2004; Lee et al., 2007; George et al., 2008; Li et al., 2008b; Mills et al., 2008; Kudla et al., 2010; Limonta et al., 2014). Initially AtACA1 was identified in the chloroplast envelop (Huang et al., 1993), however, more recent observations have brought the relevance of ACA1 for chloroplast Ca^{2+} import into question (Hochmal et al., 2015). Interestingly, ECAs and ACAs can be selectively inhibited by Cyclopiazonic acid and Eosin Y respectively (Liang and Sze, 1998; Bonza et al., 2004), making these drug interesting tools to study ECA and ACA function. *Arabidopsis* counts 4 ECAs (Sze et al., 2000) of which ECA1 and ECA3 were reported to be important for Mn^{2+} homeostasis (Wu et al., 2002; Mills et al., 2008). Knowledge on the functionality of other ECAs remains to be obtained. The AtACAs are represented by 10 members (Sze et al., 2000) that are activated by osmotic and cold stress (Beffagna et al., 2005; Schiøtt and Palmgren, 2005), are involved in inflorescence architecture (George et al., 2008), and perform a profound role in plant defense during pathogen infection (Boursiac et al., 2010; Frei dit Frey et al., 2012; Yang et al., 2017). While Ca^{2+}-ATPases obtain energy from ATP hydrolysis to transport Ca^{2+} against the strong cytosol-intracellular store gradient, Ca^{2+} efflux by CAX is driven by Ca^{2+} -H^+ exchange. CAX are mainly found at the tonoplast, but have also been identified at the plasma membrane (Hirschi, 2000; Cheng et al., 2002a; Cheng et al., 2005; Luo et al., 2005). CAXs are important for proper plant growth and nutrient acquisition

(Cheng et al., 2005), salt stress tolerance (Luo et al., 2005), and virus-induced oxidative stress resistance (Shabala et al., 2011).

Conclusions and perspectives

In this chapter we aimed to give a general introduction on auxin and Ca^{2+} signaling, and illustrate where these two fields come together. We exemplified the importance of regulated endomembrane trafficking and polarity of the PIN auxin efflux carriers for proper directional auxin transport and consequently the successful progression of a wide range of auxin-dependent developmental processes and tropisms. We also described how auxin can feedback regulated the directionality of its own transport by inhibiting clathrin-mediated PIN endocytosis. Currently, it has been established to involve auxin-dependent activation of ROP/RIC signaling, but the auxin receptor involved remains to be identified. In this respect we have discussed the controversy on the role of ABP1 as an auxin receptor. In the second part of the introduction we focused on sketching our current understanding on the physiological importance and genetics of Ca^{2+} signaling in plants. As we aim to bring together auxin and Ca^{2+} in this PhD project, we highlighted our current knowledge on Ca^{2+}-dependent auxin signaling. The following introductory chapters will elaborate in more depth on Ca^{2+} and its role in cell polarity (Section I – Chapter 2) and endomembrane trafficking (Section 1 – Chapter 3).

References

Appel, H.M., and Cocroft, R.B. (2014). Plants respond to leaf vibrations caused by insect herbivore chewing. Oecologia **175,** 1257-1266.

Arimura, G.-i., and Maffei, M.E. (2010). Calcium and secondary CPK signaling in plants in response to herbivore attack. Biochemical and Biophysical Research Communications **400,** 455-460.

Bailly, A., Sovero, V., Vincenzetti, V., Santelia, D., Bartnik, D., Koenig, B.W., Mancuso, S., Martinoia, E., and Geisler, M. (2008). Modulation of P-glycoproteins by Auxin Transport Inhibitors Is Mediated by Interaction with Immunophilins. Journal of Biological Chemistry **283,** 21817-21826.

Baral, A., Irani, N.G., Fujimoto, M., Nakano, A., Mayor, S., and Mathew, M.K. (2015). Salt-Induced Remodeling of Spatially Restricted Clathrin-Independent Endocytic Pathways in Arabidopsis Root. The Plant Cell **27,** 1297-1315.

Barbez, E., Kubes, M., Rolcik, J., Beziat, C., Pencik, A., Wang, B., Rosquete, M.R., Zhu, J., Dobrev, P.I., Lee, Y., Zazimalova, E., Petrasek, J., Geisler, M., Friml, J., and Kleine-Vehn, J. (2012). A novel putative auxin carrier family regulates intracellular auxin homeostasis in plants. Nature **485,** 119-122.

Barbosa, Inês C.R., Zourelidou, M., Willige, Björn C., Weller, B., and Schwechheimer, C. (2014). D6 PROTEIN KINASE Activates Auxin Transport-Dependent Growth and PIN-FORMED Phosphorylation at the Plasma Membrane. Developmental Cell **29,** 674-685.

Baster, P., Robert, S., Kleine-Vehn, J., Vanneste, S., Kania, U., Grunewald, W., De Rybel, B., Beeckman, T., and Friml, J. (2013). SCF(TIR1/AFB)-auxin signalling regulates PIN vacuolar trafficking and auxin fluxes during root gravitropism. The EMBO Journal **32,** 260-274.

Beffagna, N., Buffoli, B., and Busi, C. (2005). Modulation of Reactive Oxygen Species Production During Osmotic Stress in Arabidopsis thaliana Cultured Cells: Involvement of the Plasma Membrane Ca2+-ATPase and H+-ATPase. Plant and Cell Physiology **46,** 1326-1339.

Benjamins, R., and Scheres, B. (2008). Auxin: The Looping Star in Plant Development. Annual Review of Plant Biology **59,** 443-465.

Benjamins, R., Ampudia, C.S.G., Hooykaas, P.J.J., and Offringa, R. (2003). PINOID-Mediated Signaling Involves Calcium-Binding Proteins. Plant Physiology **132,** 1623-1630.

Benjamins, R., Quint, A., Weijers, D., Hooykaas, P., and Offringa, R. (2001). The PINOID protein kinase regulates organ development in Arabidopsis by enhancing polar auxin transport. Development **128,** 4057-4067.

Benková, E., Michniewicz, M., Sauer, M., Teichmann, T., Seifertová, D., Jürgens, G., and Friml, J. (2003). Local, Efflux-Dependent Auxin Gradients as a Common Module for Plant Organ Formation. Cell **115,** 591-602.

Bennett, M.J., Marchant, A., Green, H.G., May, S.T., Ward, S.P., Millner, P.A., Walker, A.R., Schulz, B., and Feldmann, K.A. (1996). Arabidopsis AUX1 Gene: A Permease-Like Regulator of Root Gravitropism. Science **273,** 948-950.

Bennett, S.R.M., Alvarez, J., Bossinger, G., and Smyth, D.R. (1995). Morphogenesis in pinoid mutants of Arabidopsis thaliana. The Plant Journal **8,** 505-520.

Béziat, C., Barbez, E., Feraru, M.I., Lucyshyn, D., and Kleine-Vehn, J. (2017). Light triggers PILS-dependent reduction in nuclear auxin signalling for growth transition **3,** 17105.

Blaauw, A. H. (1918). Mededel. Landbouwhoogeschool Wageningen, 15, 91.

Bonza, M.C., and De Michelis, M.I. (2011). The plant Ca2+-ATPase repertoire: biochemical features and physiological functions. Plant Biology **13,** 421-430.

Bonza, M.C., Luoni, L., and De Michelis, M.I. (2004). Functional expression in yeast of an N-deleted form of At-ACA8, a plasma membrane Ca2+-ATPase of Arabidopsis thaliana, and characterization of a hyperactive mutant. Planta **218,** 814-823.

Bonza, M.C., Morandini, P., Luoni, L., Geisler, M., Palmgren, M.G., and De Michelis, M.I. (2000). At-ACA8 Encodes a Plasma Membrane-Localized Calcium-ATPase of Arabidopsis with a Calmodulin-Binding Domain at the N Terminus. Plant Physiology **123,** 1495-1506.

Bosco, C.D., Dovzhenko, A., Liu, X., Woerner, N., Rensch, T., Eismann, M., Eimer, S., Hegermann, J., Paponov, I.A., Ruperti, B., Heberle-Bors, E., Touraev, A., Cohen, J.D., and Palme, K. (2012). The endoplasmic reticulum localized PIN8 is a pollen-specific auxin carrier involved in intracellular auxin homeostasis. The Plant Journal **71,** 860-870.

Boudsocq, M., Willmann, M.R., McCormack, M., Lee, H., Shan, L., He, P., Bush, J., Cheng, S.-H., and Sheen, J. (2010). Differential innate immune signalling via Ca2+ sensor protein kinases. Nature **464,** 418-422.

Boursiac, Y., Lee, S.M., Romanowsky, S., Blank, R., Sladek, C., Chung, W.S., and Harper, J.F. (2010). Disruption of the Vacuolar Calcium-ATPases in Arabidopsis Results in the Activation of a Salicylic Acid-Dependent Programmed Cell Death Pathway. Plant Physiology **154,** 1158-1171.

Boysen-Jensen, P.(1928). Planta 6, 464-477.

Braun, N., Wyrzykowska, J., Muller, P., David, K., Couch, D., Perrot-Rechenmann, C., and Fleming, A.J. (2008). Conditional Repression of AUXIN BINDING PROTEIN1 Reveals That It Coordinates Cell Division and Cell Expansion during Postembryonic Shoot Development in Arabidopsis and Tobacco. The Plant Cell **20,** 2746-2762.

Breton, G., Vazquez-Tello, A., Danyluk, J., and Sarhan, F. (2000). Two novel intrinsic annexins accumulate in wheat membranes in response to low temperature. Plant and Cell Physiology **41,** 177-184.

Brumos, J., Alonso, J.M., and Stepanova, A.N. (2014). Genetic aspects of auxin biosynthesis and its regulation. Physiologia Plantarum **151,** 3-12.

Burstrom, H.G. (1968). Calcium and plant growth. Biol. Rev. (Camb.) **43** 287–316.

Bussler, W. (1962). Ca-Mangelsymptome bei Sonnenblumen. Zeitschrift für Pflanzenernährung, Düngung, Bodenkunde **99,** 207-215.

Calderón Villalobos, L.I.A., Lee, S., De Oliveira, C., Ivetac, A., Brandt, W., Armitage, L., Sheard, L.B., Tan, X., Parry, G., Mao, H., Zheng, N., Napier, R., Kepinski, S., and Estelle, M. (2012). A combinatorial TIR1/AFB–Aux/IAA co-receptor system for differential sensing of auxin. Nat Chem Biol **8,** 477-485.

Chen, J.-G., Ullah, H., Young, J.C., Sussman, M.R., and Jones, A.M. (2001). ABP1 is required for organized cell elongation and division in Arabidopsis embryogenesis. Genes & Development **15,** 902-911.

Chen, X., Naramoto, S., Robert, S., Tejos, R., Löfke, C., Lin, D., Yang, Z., and Friml, J. (2012). ABP1 and ROP6 GTPase Signaling Regulate Clathrin-Mediated Endocytosis in Arabidopsis Roots. Current Biology **22,** 1326-1332.

Cheng, N.-h., Pittman, J.K., Shigaki, T., and Hirschi, K.D. (2002a). Characterization of CAX4, an Arabidopsis H⁺/Cation Antiporter. Plant Physiology **128,** 1245-1254.

Cheng, N.-H., Pittman, J.K., Shigaki, T., Lachmansingh, J., LeClere, S., Lahner, B., Salt, D.E., and Hirschi, K.D. (2005). Functional Association of Arabidopsis CAX1 and CAX3 Is Required for Normal Growth and Ion Homeostasis. Plant Physiology **138,** 2048-2060.

Cheng, S., Willmann, M.R., Chen, H., and Sheen, J. (2002b). Calcium Signaling through Protein Kinases. The Arabidopsis Calcium-Dependent Protein Kinase Gene Family. Plant Physiology **129,** 469-485.

Cheng, Y., Dai, X., and Zhao, Y. (2006). Auxin biosynthesis by the YUCCA flavin monooxygenases controls the formation of floral organs and vascular tissues in Arabidopsis. Genes & Development **20,** 1790-1799.

Cheng, Y., Dai, X., and Zhao, Y. (2007). Auxin Synthesized by the YUCCA Flavin Monooxygenases Is Essential for Embryogenesis and Leaf Formation in Arabidopsis. The Plant Cell **19,** 2430-2439.

Cholodny, N. (1927). Wuchshormone und tropismem bei den planzen. Biol. Zentralbl. **47,** 604-626.

Christensen, S.K., Dagenais, N., Chory, J., and Weigel, D. (2000). Regulation of Auxin Response by the Protein Kinase PINOID. Cell **100,** 469-478.

Clark, G.B., Morgan, R.O., Fernandez, M.-P., and Roux, S.J. (2012). Evolutionary adaptation of plant annexins has diversified their molecular structures, interactions and functional roles. New Phytologist **196,** 695-712.

Clark, G.B., Rafati, D.S., Bolton, R.J., Dauwalder, M., and Roux, S.J. (2000). Redistribution of annexin in gravistimulated pea plumules. Plant Physiology and Biochemistry **38,** 937-947.

Cook, S.D., Nichols, D.S., Smith, J., Chourey, P.S., McAdam, E.L., Quittenden, L.J., and Ross, J.J. (2016). Auxin biosynthesis: Are the indole-3-acetic acid and phenylacetic acid biosynthesis pathways mirror images? Plant Physiology.

Cowles, C.R., Odorizzi, G., Payne, G.S., and Emr, S.D. (1997). The AP-3 Adaptor Complex Is Essential for Cargo-Selective Transport to the Yeast Vacuole. Cell **91,** 109-118.

Cui, Y., Zhao, Q., Gao, C., Ding, Y., Zeng, Y., Ueda, T., Nakano, A., and Jiang, L. (2014). Activation of the Rab7 GTPase by the MON1-CCZ1 Complex Is Essential for PVC-to-Vacuole Trafficking and Plant Growth in Arabidopsis. The Plant Cell Online.

Dai, M., Zhang, C., Kania, U., Chen, F., Xue, Q., McCray, T., Li, G., Qin, G., Wakeley, M., Terzaghi, W., Wan, J., Zhao, Y., Xu, J., Friml, J., Deng, X.W., and Wang, H. (2012). A PP6-Type Phosphatase Holoenzyme Directly Regulates PIN Phosphorylation and Auxin Efflux in Arabidopsis. The Plant Cell **24,** 2497-2514.

Darwin, C., Darwin F. (1881). The power of movement in plants. Appleton and Co., New York, NY, USA.

daSilva, L.L.P., Taylor, J.P., Hadlington, J.L., Hanton, S.L., Snowden, C.J., Fox, S.J., Foresti, O., Brandizzi, F., and Denecke, J. (2005). Receptor Salvage from the Prevacuolar Compartment Is Essential for Efficient Vacuolar Protein Targeting. The Plant Cell **17,** 132-148.

Davenport, R. (2002). Glutamate Receptors in Plants. Annals of Botany **90,** 549-557.

Davies, R.T., Goetz, D.H., Lasswell, J., Anderson, M.N., and Bartel, B. (1999). IAR3 encodes an auxin conjugate hydrolase from Arabidopsis. The Plant Cell **11,** 365-376.

Davis, D.J., McDowell, S.C., Park, E., Hicks, G., Wilkop, T.E., and Drakakaki, G. (2016). The RAB GTPase RABA1e localizes to the cell plate and shows distinct subcellular behavior from RABA2a under Endosidin 7 treatment. Plant Signaling & Behavior **11,** e984520.

Dell'Angelica, E.C., Shotelersuk, V., Aguilar, R.C., Gahl, W.A., and Bonifacino, J.S. (1999). Altered Trafficking of Lysosomal Proteins in Hermansky-Pudlak Syndrome Due to Mutations in the β3A Subunit of the AP-3 Adaptor. Molecular Cell **3,** 11-21.

Demidchik, V., and Maathuis, F.J.M. (2007). Physiological roles of nonselective cation channels in plants: from salt stress to signalling and development. New Phytologist **175,** 387-404.

Demidchik, V., Bowen, H.C., Maathuis, F.J.M., Shabala, S.N., Tester, M.A., White, P.J., and Davies, J.M. (2002). Arabidopsis thaliana root non-selective cation channels mediate calcium uptake and are involved in growth. The Plant Journal **32,** 799-808.

Dharmasiri, N., Dharmasiri, S., and Estelle, M. (2005). The F-box protein TIR1 is an auxin receptor. Nature **435,** 441-445.

Dhonukshe, P., Aniento, F., Hwang, I., Robinson, D.G., Mravec, J., Stierhof, Y.-D., and Friml, J. (2007). Clathrin-Mediated Constitutive Endocytosis of PIN Auxin Efflux Carriers in Arabidopsis. Current Biology **17,** 520-527.

Dhonukshe, P., Huang, F., Galvan-Ampudia, C.S., Mähönen, A.P., Kleine-Vehn, J., Xu, J., Quint, A., Prasad, K., Friml, J., Scheres, B., and Offringa, R. (2010). Plasma membrane-bound AGC3 kinases phosphorylate PIN auxin carriers at TPRXS(N/S) motifs to direct apical PIN recycling. Development **137,** 3245-3255.

Di Rubbo, S., Irani, N.G., Kim, S.Y., Xu, Z.-Y., Gadeyne, A., Dejonghe, W., Vanhoutte, I., Persiau, G., Eeckhout, D., Simon, S., Song, K., Kleine-Vehn, J., Friml, J., De Jaeger, G., Van Damme, D., Hwang, I., and Russinova, E. (2013). The Clathrin Adaptor Complex AP-2 Mediates Endocytosis of BRASSINOSTEROID INSENSITIVE1 in Arabidopsis. The Plant Cell **25,** 2986-2997.

Ding, Z., Galvan-Ampudia, C.S., Demarsy, E., Langowski, L., Kleine-Vehn, J., Fan, Y., Morita, M.T., Tasaka, M., Fankhauser, C., Offringa, R., and Friml, J. (2011). Light-mediated polarization of the PIN3 auxin transporter for the phototropic response in Arabidopsis. Nat Cell Biol **13,** 447-452.

Ding, Z., Wang, B., Moreno, I., Dupláková, N., Simon, S., Carraro, N., Reemmer, J., Pěnčík, A., Chen, X., Tejos, R., Skůpa, P., Pollmann, S., Mravec, J., Petrášek, J., Zažímalová, E., Honys, D., Rolčík, J., Murphy, A., Orellana, A., Geisler, M., and Friml, J. (2012). ER-localized auxin transporter PIN8 regulates auxin homeostasis and male gametophyte development in Arabidopsis **3,** 941.

Dodd, A.N., Kudla, J., and Sanders, D. (2010). The Language of Calcium Signaling. Annual Review of Plant Biology **61,** 593-620.

Donaldson, J.G., and Jackson, C.L. (2000). Regulators and effectors of the ARF GTPases. Current Opinion in Cell Biology **12,** 475-482.

Drdová, E.J., Synek, L., Pečenková, T., Hála, M., Kulich, I., Fowler, J.E., Murphy, A.S., and Žárský, V. (2013). The exocyst complex contributes to PIN auxin efflux carrier recycling and polar auxin transport in Arabidopsis. The Plant Journal **73,** 709-719.

Ebine, K., Inoue, T., Ito, J., Ito, E., Uemura, T., Goh, T., Abe, H., Sato, K., Nakano, A., and Ueda, T. (2014). Plant Vacuolar Trafficking Occurs through Distinctly Regulated Pathways. Current Biology **24,** 1375-1382.

Effendi, Y., Jones, A.M., and Scherer, G.F.E. (2013). AUXIN-BINDING-PROTEIN1 (ABP1) in phytochrome-B-controlled responses. Journal of Experimental Botany **64,** 5065-5074.

Enders, T.A., Oh, S., Yang, Z., Montgomery, B.L., and Strader, L.C. (2015). Genome Sequencing of Arabidopsis abp1-5 Reveals Second-Site Mutations That May Affect Phenotypes. The Plant Cell **27,** 1820-1826.

Ettinger, W.F., Clear, A.M., Fanning, K.J., and Peck, M.L. (1999). Identification of a Ca(2+)/H(+) Antiport in the Plant Chloroplast Thylakoid Membrane. Plant Physiology **119,** 1379-1386.

Fankhauser, C., and Christie, John M. (2015). Plant Phototropic Growth. Current Biology **25,** R384-R389.

Felle, H. (1988). Auxin causes oscillations of cytosolic free calcium and pH inZea mays coleoptiles. Planta **174,** 495-499.

Fendrych, M., Leung, J., and Friml, J. (2016). TIR1/AFB-Aux/IAA auxin perception mediates rapid cell wall acidification and growth of Arabidopsis hypocotyls. eLife **5,** e19048.

Feng, L., Seymour, A.B., Jiang, S., To, A., Peden, A.A., Novak, E.K., Zhen, L., Rusiniak, M.E., Eicher, E.M., Robinson, M.S., Gorin, M.B., and Swank, R.T. (1999). The β3A Subunit Gene (Ap3B1) of the Ap-3 Adaptor Complex Is Altered in the Mouse Hypopigmentation Mutant Pearl, a Model for Hermansky-Pudlak Syndrome and Night Blindness. Human Molecular Genetics **8,** 323-330.

Feng, Q.-N., Zhang, Y., and Li, S. (2017). Tonoplast targeting of VHA-a3 relies on a Rab5-mediated but Rab7-independent vacuolar trafficking route. Journal of Integrative Plant Biology **59,** 230-233.

Feraru, E., Paciorek, T., Feraru, M.I., Zwiewka, M., De Groodt, R., De Rycke, R., Kleine-Vehn, J., and Friml, J. (2010). The AP-3 β Adaptin Mediates the Biogenesis and Function of Lytic Vacuoles in Arabidopsis. The Plant Cell **22,** 2812-2824.

Feraru, E., Feraru, M.I., Asaoka, R., Paciorek, T., De Rycke, R., Tanaka, H., Nakano, A., and Friml, J. (2012). BEX5/RabA1b Regulates trans-Golgi Network-to-Plasma Membrane Protein Trafficking in Arabidopsis. The Plant Cell **24,** 3074-3086.

Ferro, N., Bredow, T., Jacobsen, H.-J., and Reinard, T. (2010). Route to Novel Auxin: Auxin Chemical Space toward Biological Correlation Carriers. Chemical Reviews **110,** 4690-4708.

Forde, B.G., and Roberts, M.R. (2014). Glutamate receptor-like channels in plants: a role as amino acid sensors in plant defence? F1000Prime Reports **6,** 37.

Frei dit Frey, N., Mbengue, M., Kwaaitaal, M., Nitsch, L., Altenbach, D., Häweker, H., Lozano-Duran, R., Njo, M.F., Beeckman, T., Huettel, B., Borst, J.W., Panstruga, R., and Robatzek, S. (2012). Plasma Membrane Calcium ATPases Are Important Components of Receptor-Mediated Signaling in Plant Immune Responses and Development. Plant Physiology **159,** 798-809.

Frietsch, S., Wang, Y.-F., Sladek, C., Poulsen, L.R., Romanowsky, S.M., Schroeder, J.I., and Harper, J.F. (2007). A cyclic nucleotide-gated channel is essential for polarized tip growth of pollen. Proceedings of the National Academy of Sciences **104,** 14531-14536.

Friml, J., and Palme, K. (2002). Polar auxin transport – old questions and new concepts? Plant Molecular Biology **49,** 273-284.

Friml, J., Vieten, A., Sauer, M., Weijers, D., Schwarz, H., Hamann, T., Offringa, R., and Jurgens, G. (2003). Efflux-dependent auxin gradients establish the apical-basal axis of Arabidopsis. Nature **426,** 147-153.

Friml, J., Benková, E., Blilou, I., Wisniewska, J., Hamann, T., Ljung, K., Woody, S., Sandberg, G., Scheres, B., Jürgens, G., and Palme, K. (2002). AtPIN4 Mediates Sink-Driven Auxin Gradients and Root Patterning in Arabidopsis. Cell **108,** 661-673.

Friml, J., Yang, X., Michniewicz, M., Weijers, D., Quint, A., Tietz, O., Benjamins, R., Ouwerkerk, P.B.F., Ljung, K., Sandberg, G., Hooykaas, P.J.J., Palme, K., and Offringa, R. (2004). A PINOID-Dependent Binary Switch in Apical-Basal PIN Polar Targeting Directs Auxin Efflux. Science **306,** 862-865.

Fu, J., and Wang, S. (2011). Insights into Auxin Signaling in Plant–Pathogen Interactions. Frontiers in plant science **2,** 74.

Fuji, K., Shimada, T., Takahashi, H., Tamura, K., Koumoto, Y., Utsumi, S., Nishizawa, K., Maruyama, N., and Hara-Nishimura, I. (2007). Arabidopsis Vacuolar Sorting Mutants (green fluorescent seed) Can Be Identified Efficiently by Secretion of Vacuole-Targeted Green Fluorescent Protein in Their Seeds. The Plant Cell **19,** 597-609.

Gadeyne, A., Sánchez-Rodríguez, C., Vanneste, S., Di Rubbo, S., Zauber, H., Vanneste, K., Van Leene, J., De Winne, N., Eeckhout, D., Persiau, G., Van De Slijke, E., Cannoot, B., Vercruysse, L., Mayers, Jonathan R., Adamowski, M., Kania, U., Ehrlich, M., Schweighofer, A., Ketelaar, T., Maere, S., Bednarek, Sebastian Y., Friml, J., Gevaert, K., Witters, E., Russinova, E., Persson, S., De Jaeger, G., and Van Damme, D. (2014). The TPLATE Adaptor Complex Drives Clathrin-Mediated Endocytosis in Plants. Cell **156,** 691-704.

Gallavotti, A. (2013). The role of auxin in shaping shoot architecture. Journal of Experimental Botany **64,** 2593-2608.

Gälweiler, L., Guan, C., Müller, A., Wisman, E., Mendgen, K., Yephremov, A., and Palme, K. (1998). Regulation of Polar Auxin Transport by AtPIN1 in Arabidopsis Vascular Tissue. Science **282,** 2226-2230.

Ganguly, A., Sasayama, D., and Cho, H.-T. (2012). Regulation of the Polarity of Protein Trafficking by Phosphorylation. Molecules and Cells **33,** 423-430.

Gao, Y., Zhang, Y., Zhang, D., Dai, X., Estelle, M., and Zhao, Y. (2015). Auxin binding protein 1 (ABP1) is not required for either auxin signaling or Arabidopsis development. Proceedings of the National Academy of Sciences **112,** 2275-2280.

Garbers, C., DeLong, A., Deruére, J., Bernasconi, P., and Söll, D. (1996). A mutation in protein phosphatase 2A regulatory subunit A affects auxin transport in Arabidopsis. The EMBO Journal **15,** 2115-2124.

Gehring, C.A., Irving, H.R., and Parish, R.W. (1990). Effects of auxin and abscisic acid on cytosolic calcium and pH in plant cells. Proceedings of the National Academy of Sciences of the United States of America **87,** 9645-9649.

Geisler, M., Axelsen, K.B., Harper, J.F., and Palmgren, M.G. (2000a). Molecular aspects of higher plant P-type Ca2+-ATPases. Biochimica et Biophysica Acta (BBA) - Biomembranes **1465,** 52-78.

Geisler, M., Frangne, N., Gomès, E., Martinoia, E., and Palmgren, M.G. (2000b). The ACA4 Gene of Arabidopsis Encodes a Vacuolar Membrane Calcium Pump That Improves Salt Tolerance in Yeast. Plant Physiology **124,** 1814-1827.

Geldner, N., Friml, J., Stierhof, Y.-D., Jurgens, G., and Palme, K. (2001). Auxin transport inhibitors block PIN1 cycling and vesicle trafficking. Nature **413,** 425-428.

Geldner, N., Anders, N., Wolters, H., Keicher, J., Kornberger, W., Muller, P., Delbarre, A., Ueda, T., Nakano, A., and Jürgens, G. (2003). The Arabidopsis GNOM ARF-GEF Mediates Endosomal Recycling, Auxin Transport, and Auxin-Dependent Plant Growth. Cell **112,** 219-230.

George, L., Romanowsky, S.M., Harper, J.F., and Sharrock, R.A. (2008). The ACA10 Ca2+-ATPase Regulates Adult Vegetative Development and Inflorescence Architecture in Arabidopsis. Plant Physiology **146,** 716-728.

Gobert, A., Park, G., Amtmann, A., Sanders, D., and Maathuis, F.J.M. (2006). Arabidopsis thaliana Cyclic Nucleotide Gated Channel 3 forms a non-selective ion transporter involved in germination and cation transport. Journal of Experimental Botany **57,** 791-800.

Goldsmith, M.H.M. (1977). Polar Transport of Auxin. Annual Review of Plant Physiology and Plant Molecular Biology **28,** 439-478.

Gorantla, M., Babu, P.R., Lachagari, V.B.R., Feltus, F.A., Paterson, A.H., and Reddy, A.R. (2005). Functional genomics of drought stress response in rice: Transcript mapping of annotated unigenes of an indica rice (Oryza sativa L. cv. Nagina 22). Current Science **89,** 496-514.

Gorecka, K.M., Thouverey, C., Buchet, R., and Pikula, S. (2007). Potential Role of Annexin AnnAt1 from Arabidopsis thaliana in pH-Mediated Cellular Response to Environmental Stimuli. Plant and Cell Physiology **48,** 792-803.

Gorecka, K.M., Konopka-Postupolska, D., Hennig, J., Buchet, R., and Pikula, S. (2005). Peroxidase activity of annexin 1 from Arabidopsis thaliana. Biochemical and Biophysical Research Communications **336,** 868-875.

Gray, W.M., Kepinski, S., Rouse, D., Leyser, O., and Estelle, M. (2001). Auxin regulates SCFTIR1-dependent degradation of AUX/IAA proteins. Nature **414,** 271-276.

Gray, W.M., del Pozo, J.C., Walker, L., Hobbie, L., Risseeuw, E., Banks, T., Crosby, W.L., Yang, M., Ma, H., and Estelle, M. (1999). Identification of an SCF ubiquitin–ligase complex required for auxin response in Arabidopsis thaliana. Genes & Development **13,** 1678-1691.

Hála, M., Cole, R., Synek, L., Drdová, E., Pečenková, T., Nordheim, A., Lamkemeyer, T., Madlung, J., Hochholdinger, F., Fowler, J.E., and Žárský, V. (2008). An Exocyst Complex Functions in Plant Cell Growth in Arabidopsis and Tobacco. The Plant Cell **20,** 1330-1345.

Hamilton, D.W.A., Hills, A., Köhler, B., and Blatt, M.R. (2000). Ca2+ channels at the plasma membrane of stomatal guard cells are activated by hyperpolarization and abscisic acid. Proceedings of the National Academy of Sciences **97,** 4967-4972.

Haney, C.H., and Long, S.R. (2010). Plant flotillins are required for infection by nitrogen-fixing bacteria. Proceedings of the National Academy of Sciences **107,** 478-483.

Harper, J.F., Hong, B., Hwang, I., Guo, H.Q., Stoddard, R., Huang, J.F., Palmgren, M.G., and Sze, H. (1998). A Novel Calmodulin-regulated Ca2+-ATPase (ACA2) from Arabidopsis with an N-terminal Autoinhibitory Domain. Journal of Biological Chemistry **273,** 1099-1106.

Heisler, M.G., Hamant, O., Krupinski, P., Uyttewaal, M., Ohno, C., Jönsson, H., Traas, J., and Meyerowitz, E.M. (2010). Alignment between PIN1 Polarity and Microtubule Orientation in the Shoot Apical Meristem Reveals a Tight Coupling between Morphogenesis and Auxin Transport. PLOS Biology **8,** e1000516.

Hertel, R., Thomson, K.-S., and Russo, V.E.A. (1972). In-vitro auxin binding to particulate cell fractions from corn coleoptiles. Planta **107,** 325-340.

Sze, H., Liang, F., Hwang, I., and, A.C.C., and Harper, J.F. (2000). DIVERSITY AND REGULATION OF PLANT Ca2+ PUMPS: Insights from Expression in Yeast. Annual Review of Plant Physiology and Plant Molecular Biology **51,** 433-462.

Hewitt, E.J. (1963). CHAPTER TWO - The Essential Nutrient Elements: Requirements and Interactions in Plants A2 - STEWARD, F.C. In Inorganic Nutrition of Plants (Academic Press), pp. 137-360.

Himschoot, E., Beeckman, T., Friml, J., and Vanneste, S. (2015). Calcium is an organizer of cell polarity in plants. Biochimica et Biophysica Acta (BBA) - Molecular Cell Research **1853,** 2168-2172.

Hirschi, K. (2000). Vacuolar H- Ca2 transport: who's directing the traffic? Trends in Plant Science **6,** 100-104.

Hochmal, A.K., Schulze, S., Trompelt, K., and Hippler, M. (2015). Calcium-dependent regulation of photosynthesis. Biochimica et Biophysica Acta (BBA) - Bioenergetics **1847,** 993-1003.

Hofmann, A., Proust, J., Dorowski, A., Schantz, R., and Huber, R. (2000). Annexin 24 from Capsicum annuum : X-RAY STRUCTURE AND BIOCHEMICAL CHARACTERIZATION. Journal of Biological Chemistry **275,** 8072-8082.

Hong, B., Ichida, A., Wang, Y., Scott Gens, J., Pickard, B.G., and Harper, J.F. (1999). Identification of a Calmodulin-Regulated Ca(2+)-ATPase in the Endoplasmic Reticulum. Plant Physiology **119,** 1165-1176.

Hu, N.-J., Yusof, A.M., Winter, A., Osman, A., Reeve, A.K., and Hofmann, A. (2008). The Crystal Structure of Calcium-bound Annexin Gh1 from Gossypium hirsutum and Its Implications for Membrane Binding Mechanisms of Plant Annexins. Journal of Biological Chemistry **283,** 18314-18322.

Huang, L., Berkelman, T., Franklin, A.E., and Hoffman, N.E. (1993). Characterization of a gene encoding a Ca(2+)-ATPase-like protein in the plastid envelope. Proceedings of the National Academy of Sciences of the United States of America **90,** 10066-10070.

Huang, F., Luo, J., Ning, T., Cao, W., Jin, X., Zhao, H., Wang, Y., and Han, S. (2017). Cytosolic and Nucleosolic Calcium Signaling in Response to Osmotic and Salt Stresses Are Independent of Each Other in Roots of Arabidopsis Seedlings. Frontiers in Plant Science **8**.

Ishida, T., Kurata, T., Okada, K., and Wada, T. (2008). A Genetic Regulatory Network in the Development of Trichomes and Root Hairs. Annual Review of Plant Biology **59,** 365-386.

Jaillais, Y., Fobis-Loisy, I., Miege, C., Rollin, C., and Gaude, T. (2006). AtSNX1 defines an endosome for auxin-carrier trafficking in Arabidopsis. Nature **443,** 106-109.

Jiang, K., and Feldman, L.J. (2005). REGULATION OF ROOT APICAL MERISTEM DEVELOPMENT. Annual Review of Cell and Developmental Biology **21,** 485-509.

Johnson, C., Knight, M., Kondo, T., Masson, P., Sedbrook, J., Haley, A., and Trewavas, A. (1995). Circadian oscillations of cytosolic and chloroplastic free calcium in plants. Science **269,** 1863-1865.

Jones, A.M., Im, K.-H., Savka, M.A., Wu, M.-J., DeWitt, N.G., Shillito, R., and Binns, A.N. (1998). Auxin-Dependent Cell Expansion Mediated by Overexpressed Auxin-Binding Protein 1. Science **282,** 1114-1117.

Jurado, S., Abraham, Z., Manzano, C., López-Torrejón, G., Pacios, L.F., and Del Pozo, J.C. (2010). The Arabidopsis Cell Cycle F-Box Protein SKP2A Binds to Auxin. The Plant Cell **22,** 3891-3904.

Jürgens, G. (2001). NEW EMBO MEMBER'S REVIEW: Apical–basal pattern formation in Arabidopsis embryogenesis. The EMBO Journal **20,** 3609-3616.

Jürgens, G., and Geldner, N. (2007). The High Road and the Low Road: Trafficking Choices in Plants. Cell **130,** 977-979.

Kamimoto, Y., Terasaka, K., Hamamoto, M., Takanashi, K., Fukuda, S., Shitan, N., Sugiyama, A., Suzuki, H., Shibata, D., Wang, B., Pollmann, S., Geisler, M., and Yazaki, K. (2012). Arabidopsis ABCB21 is a Facultative Auxin Importer/Exporter Regulated by Cytoplasmic Auxin Concentration. Plant and Cell Physiology **53,** 2090-2100.

Kang, H., Kim, S.Y., Song, K., Sohn, E.J., Lee, Y., Lee, D.W., Hara-Nishimura, I., and Hwang, I. (2012). Trafficking of Vacuolar Proteins: The Crucial Role of Arabidopsis Vacuolar Protein Sorting 29 in Recycling Vacuolar Sorting Receptor. The Plant Cell **24,** 5058-5073.

Kania, U., Fendrych, M., and Friml, J. (2014). Polar delivery in plants; commonalities and differences to animal epithelial cells. Open Biology **4**.

Kazan, K. (2013). Auxin and the integration of environmental signals into plant root development. Annals of Botany **112,** 1655-1665.

Kazan, K., and Manners, J.M. (2009). Linking development to defense: auxin in plant–pathogen interactions. Trends in Plant Science **14,** 373-382.

Keinath, N.F., Waadt, R., Brugman, R., Schroeder, Julian I., Grossmann, G., Schumacher, K., and Krebs, M. (2015). Live Cell Imaging with R-GECO1 Sheds Light on flg22- and Chitin-Induced Transient [Ca²⁺]_{cyt} Patterns in Arabidopsis. Molecular Plant **8,** 1188-1200.

Kepinski, S., and Leyser, O. (2005). The Arabidopsis F-box protein TIR1 is an auxin receptor. Nature **435,** 446-451.

Kitakura, S., Vanneste, S., Robert, S., Löfke, C., Teichmann, T., Tanaka, H., and Friml, J. (2011). Clathrin Mediates Endocytosis and Polar Distribution of PIN Auxin Transporters in Arabidopsis. The Plant Cell **23,** 1920-1931.

Kitakura, S., Adamowski, M., Matsuura, Y., Santuari, L., Kouno, H., Arima, K., Hardtke, C.S., Friml, J., Kakimoto, T., and Tanaka, H. (2017). BEN3/BIG2 ARF GEF is Involved in Brefeldin A-Sensitive Trafficking at the trans-Golgi Network/Early Endosome in Arabidopsis thaliana. Plant and Cell Physiology**,** pcx118-pcx118.

Kleine-Vehn, J., Leitner, J., Zwiewka, M., Sauer, M., Abas, L., Luschnig, C., and Friml, J. (2008a). Differential degradation of PIN2 auxin efflux carrier by retromer-dependent vacuolar targeting. Proceedings of the National Academy of Sciences **105,** 17812-17817.

Kleine-Vehn, J., Huang, F., Naramoto, S., Zhang, J., Michniewicz, M., Offringa, R., and Friml, J. (2009). PIN Auxin Efflux Carrier Polarity Is Regulated by PINOID Kinase-Mediated Recruitment into GNOM-Independent Trafficking in Arabidopsis. The Plant Cell **21,** 3839-3849.

Kleine-Vehn, J., Dhonukshe, P., Sauer, M., Brewer, P.B., Wiśniewska, J., Paciorek, T., Benková, E., and Friml, J. (2008b). ARF GEF-Dependent Transcytosis and Polar Delivery of PIN Auxin Carriers in Arabidopsis. Current Biology **18,** 526-531.

Knight, M.R., Campbell, A.K., Smith, S.M., and Trewavas, A.J. (1991). Transgenic plant aequorin reports the effects of touch and cold-shock and elicitors on cytoplasmic calcium. Nature **352,** 524-526.

Kogl, F.a.H.-S., A.J. (1931). Uber die Chemie des Wuchsstoffs K. Akad. Wetenschap. Amsterdam. Proc. Sect. Sci. **34,** 1411-1416.

Koizumi, K., Naramoto, S., Sawa, S., Yahara, N., Ueda, T., Nakano, A., Sugiyama, M., and Fukuda, H. (2005). VAN3 ARF–GAP-mediated vesicle transport is involved in leaf vascular network formation. Development **132,** 1699-1711.

Konopka-Postupolska, D., and Clark, G. (2017). Annexins as Overlooked Regulators of Membrane Trafficking in Plant Cells. International Journal of Molecular Sciences **18,** 863.

Korasick, D.A., Enders, T.A., and Strader, L.C. (2013). Auxin biosynthesis and storage forms. Journal of Experimental Botany **64,** 2541-2555.

Křeček, P., Skůpa, P., Libus, J., Naramoto, S., Tejos, R., Friml, J., and Zažímalová, E. (2009). The PIN-FORMED (PIN) protein family of auxin transporters. Genome Biology **10,** 249-249.

Kretzschmar, D., Poeck, B., Roth, H., Ernst, R., Keller, A., Porsch, M., Strauss, R., and Pflugfelder, G.O. (2000). Defective pigment granule biogenesis and aberrant behavior caused by mutations in the Drosophila AP-3beta adaptin gene ruby. Genetics **155,** 213-223.

Kubeš, M., Yang, H., Richter, G.L., Cheng, Y., Młodzińska, E., Wang, X., Blakeslee, J.J., Carraro, N., Petrášek, J., Zažímalová, E., Hoyerová, K., Peer, W.A., and Murphy, A.S. (2012). The Arabidopsis concentration-dependent influx/efflux transporter ABCB4 regulates cellular auxin levels in the root epidermis. The Plant Journal **69,** 640-654.

Kudla, J., Batistič, O., and Hashimoto, K. (2010). Calcium Signals: The Lead Currency of Plant Information Processing. The Plant Cell **22,** 541-563.

Kurzchalia, T.V., and Partan, R.G. (1999). Membrane microdomains and caveolae. Current Opinion in Cell Biology **11,** 424-431.

Lam, B.C.H., Sage, T.L., Bianchi, F., and Blumwald, E. (2001). Role of SH3 Domain–Containing Proteins in Clathrin-Mediated Vesicle Trafficking in Arabidopsis. The Plant Cell **13,** 2499-2512.

Laohavisit, A., and Davies, J.M. (2009). Multifunctional annexins. Plant Science **177,** 532-539.

Laohavisit, A., Richards, S.L., Shabala, L., Chen, C., Colaço, R.D.D.R., Swarbreck, S.M., Shaw, E., Dark, A., Shabala, S., Shang, Z., and Davies, J.M. (2013). Salinity-Induced Calcium Signaling and Root Adaptation in Arabidopsis Require the Calcium Regulatory Protein Annexin1. Plant Physiology **163,** 253-262.

Laohavisit, A., Mortimer, J.C., Demidchik, V., Coxon, K.M., Stancombe, M.A., Macpherson, N., Brownlee, C., Hofmann, A., Webb, A.A.R., Miedema, H., Battey, N.H., and Davies, J.M. (2009). Zea mays Annexins Modulate Cytosolic Free Ca(2+) and Generate a Ca(2+)-Permeable Conductance. The Plant Cell **21,** 479-493.

Laohavisit, A., Shang, Z., Rubio, L., Cuin, T.A., Véry, A.-A., Wang, A., Mortimer, J.C., Macpherson, N., Coxon, K.M., Battey, N.H., Brownlee, C., Park, O.K., Sentenac, H., Shabala, S., Webb, A.A.R., and Davies, J.M. (2012). Arabidopsis Annexin1 Mediates the Radical-Activated Plasma Membrane Ca(2+)- and K(+)-Permeable Conductance in Root Cells. The Plant Cell **24,** 1522-1533.

Laxmi, A., Pan, J., Morsy, M., and Chen, R. (2008). Light Plays an Essential Role in Intracellular Distribution of Auxin Efflux Carrier PIN2 in Arabidopsis thaliana. PLoS ONE **3,** e1510.

Lee, S., Lee, E.J., Yang, E.J., Lee, J.E., Park, A.R., Song, W.H., and Park, O.K. (2004). Proteomic Identification of Annexins, Calcium-Dependent Membrane Binding Proteins That Mediate Osmotic Stress and Abscisic Acid Signal Transduction in Arabidopsis. The Plant Cell **16,** 1378-1391.

Lee, S.M., Kim, H.S., Han, H.J., Moon, B.C., Kim, C.Y., Harper, J.F., and Chung, W.S. (2007). Identification of a calmodulin-regulated autoinhibited Ca2+-ATPase (ACA11) that is localized to vacuole membranes in Arabidopsis. FEBS Letters **581,** 3943-3949.

Leitner, J., Petrášek, J., Tomanov, K., Retzer, K., Pařezová, M., Korbei, B., Bachmair, A., Zažímalová, E., and Luschnig, C. (2012). Lysine63-linked ubiquitylation of PIN2 auxin carrier protein governs hormonally controlled adaptation of Arabidopsis root growth. Proceedings of the National Academy of Sciences **109,** 8322-8327.

Li, F., Wang, J., Ma, C., Zhao, Y., Wang, Y., Hasi, A., and Qi, Z. (2013). Glutamate Receptor-Like Channel3.3 Is Involved in Mediating Glutathione-Triggered Cytosolic Calcium Transients, Transcriptional Changes, and Innate Immunity Responses in Arabidopsis. Plant Physiology **162,** 1497-1509.

Li, S.-B., Xie, Z.-Z., Hu, C.-G., and Zhang, J.-Z. (2016). A Review of Auxin Response Factors (ARFs) in Plants. Frontiers in Plant Science **7,** 47.

Li, X., Chanroj, S., Wu, Z., Romanowsky, S.M., Harper, J.F., and Sze, H. (2008). A Distinct Endosomal Ca2+Mn2+ Pump Affects Root Growth through the Secretory Process. Plant Physiology **147,** 1675-1689.

Liang, F., and Sze, H. (1998). A High-Affinity Ca(2+) Pump, ECA1, from the Endoplasmic Reticulum Is Inhibited by Cyclopiazonic Acid but Not by Thapsigargin. Plant Physiology **118,** 817-825.

Liang, F., Cunningham, K.W., Harper, J.F., and Sze, H. (1997). ECA1 complements yeast mutants defective in Ca2+ pumps and encodes an endoplasmic reticulum-type Ca2+-ATPase in Arabidopsis thaliana. Proceedings of the National Academy of Sciences **94,** 8579-8584.

Limonta, M., Romanowsky, S., Olivari, C., Bonza, M.C., Luoni, L., Rosenberg, A., Harper, J.F., and De Michelis, M.I. (2014). ACA12 Is a Deregulated Isoform of Plasma Membrane Ca(2+)-ATPase of Arabidopsis thaliana. Plant molecular biology **84,** 387-397.

Lin, D., Nagawa, S., Chen, J., Cao, L., Chen, X., Xu, T., Li, H., Dhonukshe, P., Yamamuro, C., Friml, J., Scheres, B., Fu, Y., and Yang, Z. (2012). A ROP GTPase-Dependent Auxin Signaling Pathway Regulates the Subcellular Distribution of PIN2 in Arabidopsis Roots. Current Biology **22,** 1319-1325.

Liu, J., and Guo, W. (2012). The exocyst complex in exocytosis and cell migration. Protoplasma **249,** 587-597.

Ljung, K. (2013). Auxin metabolism and homeostasis during plant development. Development **140,** 943-950.

Logan, D.C., and Knight, M.R. (2003). Mitochondrial and Cytosolic Calcium Dynamics Are Differentially Regulated in Plants. Plant Physiology **133,** 21-24.

Luan, S., Kudla, J., Rodriguez-Concepcion, M., Yalovsky, S., and Gruissem, W. (2002). Calmodulins and Calcineurin B–like Proteins: Calcium Sensors for Specific Signal Response Coupling in Plants. The Plant Cell **14,** s389-s400.

Lucas, M., Kenobi, K., von Wangenheim, D., Voβ, U., Swarup, K., De Smet, I., Van Damme, D., Lawrence, T., Péret, B., Moscardi, E., Barbeau, D., Godin, C., Salt, D., Guyomarc'h, S., Stelzer, E.H.K., Maizel, A., Laplaze, L., and Bennett, M.J. (2013). Lateral root morphogenesis is dependent on the mechanical properties of the overlaying tissues. Proceedings of the National Academy of Sciences of the United States of America **110,** 5229-5234.

Ludwig-Müller, J. (2011). Auxin conjugates: their role for plant development and in the evolution of land plants. Journal of Experimental Botany **62,** 1757-1773.

Luo, G.-Z., Wang, H.-W., Huang, J., Tian, A.-G., Wang, Y.-J., Zhang, J.-S., and Chen, S.-Y. (2005). A Putative Plasma Membrane Cation/proton Antiporter from Soybean Confers Salt Tolerance in Arabidopsis. Plant Molecular Biology **59,** 809-820.

Luschnig, C., Gaxiola, R.A., Grisafi, P., and Fink, G.R. (1998). EIR1, a root-specific protein involved in auxin transport, is required for gravitropism in Arabidopsis thaliana. Genes & Development **12,** 2175-2187.

Ma, W., and Berkowitz, G.A. (2011). Ca2+ conduction by plant cyclic nucleotide gated channels and associated signaling components in pathogen defense signal transduction cascades. New Phytologist **190,** 566-572.

Ma, Y., Walker, R.K., Zhao, Y., and Berkowitz, G.A. (2012). Linking ligand perception by PEPR pattern recognition receptors to cytosolic Ca2+ elevation and downstream immune signaling in plants. Proceedings of the National Academy of Sciences **109,** 19852-19857.

Ma, Y., Zhao, Y., Walker, R.K., and Berkowitz, G.A. (2013). Molecular Steps in the Immune Signaling Pathway Evoked by Plant Elicitor Peptides: Ca(2+)-Dependent Protein Kinases, Nitric Oxide, and Reactive Oxygen Species Are Downstream from the Early Ca(2+) Signal. Plant Physiology **163,** 1459-1471.

Manzoor, H., Kelloniemi, J., Chiltz, A., Wendehenne, D., Pugin, A., Poinssot, B., and Garcia-Brugger, A. (2013). Involvement of the glutamate receptor AtGLR3.3 in plant defense signaling and resistance to Hyaloperonospora arabidopsidis. The Plant Journal **76,** 466-480.

Marschner, H. (1995). Mineral Nutrition of Plants. Academic Press, Boston **Ed. 2**.

Mäser, P., Thomine, S., Schroeder, J.I., Ward, J.M., Hirschi, K., Sze, H., Talke, I.N., Amtmann, A., Maathuis, F.J.M., Sanders, D., Harper, J.F., Tchieu, J., Gribskov, M., Persans, M.W., Salt, D.E., Kim, S.A., and Guerinot, M.L. (2001). Phylogenetic Relationships within Cation Transporter Families of Arabidopsis. Plant Physiology **126,** 1646-1667.

Masson, P.H., Tasaka, M., Morita, M.T., Guan, C., Chen, R., and Boonsirichai, K. (2002). Arabidopsis thaliana: A Model for the Study of Root and Shoot Gravitropism. The Arabidopsis Book / American Society of Plant Biologists **1,** e0043.

Mbengue, M., Bourdais, G., Gervasi, F., Beck, M., Zhou, J., Spallek, T., Bartels, S., Boller, T., Ueda, T., Kuhn, H., and Robatzek, S. (2016). Clathrin-dependent endocytosis is required for immunity mediated by pattern recognition receptor kinases. Proceedings of the National Academy of Sciences **113,** 11034-11039.

McAinsh, B.H.M.R.C.A.M. (1990). Abscisic acid-induced elevation of guard cell cytosolic Ca2+ precedes stomatal closure. Nature **343,** 186-188.

McAinsh, M.R., and Pittman, J.K. (2009). Shaping the calcium signature. New Phytologist **181,** 275-294.

McClung, A.D., Carroll, A.D., and Battey, N.H. (1994). Identification and characterization of ATPase activity associated with maize (Zea mays) annexins. Biochemical Journal **303,** 709-712.

Medvedev, S.S. (2005). Calcium signaling system in plants. Russian Journal of Plant Physiology **52,** 249-270.

Michalko, J., Glanc, M., Perrot-Rechenmann, C., and Friml, J. (2016). Strong morphological defects in conditional Arabidopsis abp1 knock-down mutants generated in absence of functional ABP1 protein. F1000Research **5,** 86.

Michniewicz, M., Brewer, P.B., and Friml, J. (2007a). Polar Auxin Transport and Asymmetric Auxin Distribution. The Arabidopsis Book / American Society of Plant Biologists **5,** e0108.

Michniewicz, M., Zago, M.K., Abas, L., Weijers, D., Schweighofer, A., Meskiene, I., Heisler, M.G., Ohno, C., Zhang, J., Huang, F., Schwab, R., Weigel, D., Meyerowitz, E.M., Luschnig, C., Offringa, R., and Friml, J. (2007b). Antagonistic Regulation of PIN Phosphorylation by PP2A and PINOID Directs Auxin Flux. Cell **130,** 1044-1056.

Miedema, H., Demidchik, V., Véry, A.-A., Bothwell, J.H.F., Brownlee, C., and Davies, J.M. (2008). Two voltage-dependent calcium channels co-exist in the apical plasma membrane of Arabidopsis thaliana root hairs. New Phytologist **179,** 378-385.

Mills, R.F., Doherty, M.L., López-Marqués, R.L., Weimar, T., Dupree, P., Palmgren, M.G., Pittman, J.K., and Williams, L.E. (2008). ECA3, a Golgi-Localized P_{2A}-Type ATPase, Plays a Crucial Role in Manganese Nutrition in Arabidopsis. Plant Physiology **146,** 116-128.

Monshausen, G.B., and Haswell, E.S. (2013). A force of nature: molecular mechanisms of mechanoperception in plants. Journal of Experimental Botany **64,** 4663-4680.

Monshausen, G.B., Miller, N.D., Murphy, A.S., and Gilroy, S. (2011). Dynamics of auxin-dependent Ca2+ and pH signaling in root growth revealed by integrating high-resolution imaging with automated computer vision-based analysis. The Plant Journal **65,** 309-318.

Morris, D.A., and Thomas, A.G. (1978). A Microautoradiographic Study of Auxin Transport in the Stem of Intact Pea Seedlings (Pisum sativum L.). Journal of Experimental Botany **29,** 147-157.

Moubayidin, L., Di Mambro, R., Sozzani, R., Pacifici, E., Salvi, E., Terpstra, I., Bao, D., van Dijken, A., Ioio, R.D., Perilli, S., Ljung, K., Benfey, P.N., Heidstra, R., Costantino, P., and Sabatini, S. (2013). Spatial coordination between stem cell activity and cell differentiation in the root meristem. Developmental cell **26,** 405-415.

Mousavi, S., Chauvin, A., Pascaud, F., Kellenberger, S., and Farmer, E. (2013). GLUTAMATE RECEPTOR-LIKE genes mediate leaf-to-leaf wound signalling. Nature **500,** 422-426.

Mravec, J., Kubeš, M., Bielach, A., Gaykova, V., Petrášek, J., Skůpa, P., Chand, S., Benková, E., Zažímalová, E., and Friml, J. (2008). Interaction of PIN and PGP transport mechanisms in auxin distribution-dependent development. Development **135,** 3345-3354.

Mravec, J., Petrášek, J., Li, N., Boeren, S., Karlova, R., Kitakura, S., Pařezová, M., Naramoto, S., Nodzyński, T., Dhonukshe, P., Bednarek, Sebastian Y., Zažímalová, E., de Vries, S., and Friml, J. (2011). Cell Plate Restricted Association of DRP1A and PIN Proteins Is Required for Cell Polarity Establishment in Arabidopsis. Current Biology **21,** 1055-1060.

Mravec, J., Skupa, P., Bailly, A., Hoyerova, K., Krecek, P., Bielach, A., Petrasek, J., Zhang, J., Gaykova, V., Stierhof, Y.-D., Dobrev, P.I., Schwarzerova, K., Rolcik, J., Seifertova, D., Luschnig, C., Benkova, E., Zazimalova, E., Geisler, M., and Friml, J. (2009). Subcellular homeostasis of phytohormone auxin is mediated by the ER-localized PIN5 transporter. Nature **459,** 1136-1140.

Murphy, A.S., Bandyopadhyay, A., Holstein, S.E., and Peer, W.A. (2005). ENDOCYTOTIC CYCLING OF PM PROTEINS. Annual Review of Plant Biology **56,** 221-251.

Nagawa, S., Xu, T., Lin, D., Dhonukshe, P., Zhang, X., Friml, J., Scheres, B., Fu, Y., and Yang, Z. (2012). ROP GTPase-Dependent Actin Microfilaments Promote PIN1 Polarization by Localized Inhibition of Clathrin-Dependent Endocytosis. PLOS Biology **10,** e1001299.

Nakagawa, Y., Katagiri, T., Shinozaki, K., Qi, Z., Tatsumi, H., Furuichi, T., Kishigami, A., Sokabe, M., Kojima, I., Sato, S., Kato, T., Tabata, S., Iida, K., Terashima, A., Nakano, M., Ikeda, M., Yamanaka, T., and Iida, H. (2007). Arabidopsis plasma membrane protein crucial for Ca(2+) influx and touch sensing in roots. Proceedings of the National Academy of Sciences of the United States of America **104,** 3639-3644.

Naramoto, S., Nodzyński, T., Dainobu, T., Takatsuka, H., Okada, T., Friml, J., and Fukuda, H. (2014). VAN4 Encodes a Putative TRS120 That is Required for Normal Cell Growth and Vein Development in Arabidopsis. Plant and Cell Physiology **55,** 750-763.

Naramoto, S., Kleine-Vehn, J., Robert, S., Fujimoto, M., Dainobu, T., Paciorek, T., Ueda, T., Nakano, A., Van Montagu, M.C.E., Fukuda, H., and Friml, J. (2010). ADP-ribosylation factor machinery mediates endocytosis in plant cells. Proceedings of the National Academy of Sciences of the United States of America **107,** 21890-21895.

Nebenfuhr, A., Ritzenthaler, C., and Robinson, D.G. (2002). Brefeldin A: Deciphering an Enigmatic Inhibitor of Secretion. Plant Physiology **130,** 1102-1108.

Nielsen, E., Cheung, A.Y., and Ueda, T. (2008). The Regulatory RAB and ARF GTPases for Vesicular Trafficking. Plant Physiology **147,** 1516-1526.

Niemes, S., Langhans, M., Viotti, C., Scheuring, D., San Wan Yan, M., Jiang, L., Hillmer, S., Robinson, D.G., and Pimpl, P. (2010). Retromer recycles vacuolar sorting receptors from the trans-Golgi network. The Plant Journal **61,** 107-121.

Nodzyński, T., Vanneste, S., Zwiewka, M., Pernisová, M., Hejátko, J., and Friml, J. (2016). Enquiry into the Topology of Plasma Membrane-Localized PIN Auxin Transport Components. Molecular Plant **9,** 1504-1519.

Nodzyński, T., Feraru, M.I., Hirsch, S., De Rycke, R., Niculaes, C., Boerjan, W., Van Leene, J., De Jaeger, G., Vanneste, S., and Friml, J. (2013). Retromer Subunits VPS35A and VPS29 Mediate Prevacuolar Compartment (PVC) Function in Arabidopsis. Molecular Plant **6,** 1849-1862.

Noh, B., Murphy, A.S., and Spalding, E.P. (2001). Multidrug Resistance–like Genes of Arabidopsis Required for Auxin Transport and Auxin-Mediated Development. The Plant Cell **13,** 2441-2454.

Nomura, H., Komori, T., Uemura, S., Kanda, Y., Shimotani, K., Nakai, K., Furuichi, T., Takebayashi, K., Sugimoto, T., Sano, S., Suwastika, I.N., Fukusaki, E., Yoshioka, H., Nakahira, Y., and Shiina, T. (2012). Chloroplast-mediated activation of plant immune signalling in Arabidopsis. Nature Communications **3,** 926.

Obata, T., Matthes, A., Koszior, S., Lehmann, M., Araújo, W.L., Bock, R., Sweetlove, L.J., and Fernie, A.R. (2011). Alteration of mitochondrial protein complexes in relation to metabolic regulation under short-term oxidative stress in Arabidopsis seedlings. Phytochemistry **72,** 1081-1091.

Okada, K., Ueda, J., Komaki, M.K., Bell, C.J., and Shimura, Y. (1991). Requirement of the Auxin Polar Transport System in Early Stages of Arabidopsis Floral Bud Formation. The Plant Cell **3,** 677-684.

Oliviusson, P., Heinzerling, O., Hillmer, S., Hinz, G., Tse, Y.C., Jiang, L., and Robinson, D.G. (2006). Plant Retromer, Localized to the Prevacuolar Compartment and Microvesicles in Arabidopsis, May Interact with Vacuolar Sorting Receptors. The Plant Cell **18,** 1239-1252.

Ordenes, V.R., Moreno, I., Maturana, D., Norambuena, L., Trewavas, A.J., and Orellana, A. (2012). In vivo analysis of the calcium signature in the plant Golgi apparatus reveals unique dynamics. Cell Calcium **52,** 397-404.

Ortiz-Ramírez, C., Michard, E., Simon, A.A., Damineli, D.S.C., Hernández-Coronado, M., Becker, J.D., and Feijó, J.A. (2017). GLUTAMATE RECEPTOR-LIKE channels are essential for chemotaxis and reproduction in mosses. Nature **549,** 91-95.

Ory, S., and Gasman, S. (2011). Rho GTPases and exocytosis: What are the molecular links? Seminars in Cell & Developmental Biology **22,** 27-32.

Ottenschläger, I., Wolff, P., Wolverton, C., Bhalerao, R.P., Sandberg, G., Ishikawa, H., Evans, M., and Palme, K. (2003). Gravity-regulated differential auxin transport from columella to lateral root cap cells. Proceedings of the National Academy of Sciences of the United States of America **100,** 2987-2991.

Otto, G.P., and Nichols, B.J. (2011). The roles of flotillin microdomains – endocytosis and beyond. Journal of Cell Science **124,** 3933-3940.

Overbeek, J.V. (1932). An analysis of phototropism in dicotyledons. Proc. K. Ned. Akad. Wet. **35,** 1325-1335.

Overvoorde, P., Fukaki, H., and Beeckman, T. (2010). Auxin Control of Root Development. Cold Spring Harbor Perspectives in Biology **2**.

Paal, A. (1919). Jahrb. wiss. Bot., 58, 406-458.

Paciorek, T., Zazimalova, E., Ruthardt, N., Petrasek, J., Stierhof, Y.-D., Kleine-Vehn, J., Morris, D.A., Emans, N., Jurgens, G., Geldner, N., and Friml, J. (2005). Auxin inhibits endocytosis and promotes its own efflux from cells. Nature **435,** 1251-1256.

Peyroche, A., Paris, S., and Jackson, C.L. (1996). Nucleotide exchange on ARF mediated by yeast Geal protein. Nature **384,** 479.

Peyroche, A., Antonny, B., Robineau, S., Acker, J., Cherfils, J., and Jackson, C.L. (1999). Brefeldin A Acts to Stabilize an Abortive ARF–GDP–Sec7 Domain Protein Complex. Molecular Cell **3,** 275-285.

Pěnčík, A., Simonovik, B., Petersson, S.V., Henyková, E., Simon, S., Greenham, K., Zhang, Y., Kowalczyk, M., Estelle, M., Zažímalová, E., Novák, O., Sandberg, G., and Ljung, K. (2013). Regulation of Auxin Homeostasis and Gradients in Arabidopsis Roots through the Formation of the Indole-3-Acetic Acid Catabolite 2-Oxindole-3-Acetic Acid. The Plant Cell **25,** 3858-3870.

Péret, B., De Rybel, B., Casimiro, I., Benková, E., Swarup, R., Laplaze, L., Beeckman, T., and Bennett, M.J. (2009). Arabidopsis lateral root development: an emerging story. Trends in Plant Science **14,** 399-408.

Petersson, S.V., Johansson, A.I., Kowalczyk, M., Makoveychuk, A., Wang, J.Y., Moritz, T., Grebe, M., Benfey, P.N., Sandberg, G., and Ljung, K. (2009). An Auxin Gradient and Maximum in the Arabidopsis Root Apex Shown by High-Resolution Cell-Specific Analysis of IAA Distribution and Synthesis. The Plant Cell **21,** 1659-1668.

Pitts, R.J., Cernac, A., and Estelle, M. (1998). Auxin and ethylene promote root hair elongation in Arabidopsis. The Plant Journal **16,** 553-560.

Porco, S., Pěnčík, A., Rashed, A., Voß, U., Casanova-Sáez, R., Bishopp, A., Golebiowska, A., Bhosale, R., Swarup, R., Swarup, K., Peňáková, P., Novák, O., Staswick, P., Hedden, P., Phillips, A.L., Vissenberg, K., Bennett, M.J., and Ljung, K. (2016). Dioxygenase-encoding AtDAO1 gene controls IAA oxidation and homeostasis in Arabidopsis. Proceedings of the National Academy of Sciences **113,** 11016-11021.

Qi, Z., Kishigami, A., Nakagawa, Y., Iida, H., and Sokabe, M. (2004). A Mechanosensitive Anion Channel in Arabidopsis thaliana Mesophyll Cells. Plant and Cell Physiology **45,** 1704-1708.

Rahman, A. (2013). Auxin: a regulator of cold stress response. Physiologia Plantarum **147,** 28-35.

Rahman, A., Hosokawa, S., Oono, Y., Amakawa, T., Goto, N., and Tsurumi, S. (2002). Auxin and Ethylene Response Interactions during Arabidopsis Root Hair Development Dissected by Auxin Influx Modulators. Plant Physiology **130,** 1908-1917.

Ramos, J.A., Zenser, N., Leyser, O., and Callis, J. (2001). Rapid Degradation of Auxin/Indoleacetic Acid Proteins Requires Conserved Amino Acids of Domain II and Is Proteasome Dependent. The Plant Cell **13,** 2349-2360.

Rampey, R.A., LeClere, S., Kowalczyk, M., Ljung, K., Sandberg, G., and Bartel, B. (2004). A Family of Auxin-Conjugate Hydrolases That Contributes to Free Indole-3-Acetic Acid Levels during Arabidopsis Germination. Plant Physiology **135,** 978-988.

Rashotte, A.M., DeLong, A., and Muday, G.K. (2001). Genetic and Chemical Reductions in Protein Phosphatase Activity Alter Auxin Transport, Gravity Response, and Lateral Root Growth. The Plant Cell **13,** 1683-1697.

Raven, J.A. (1975). Transport of Indoleacetic-Acid in Plant-Cells in Relation to Ph and Electrical Potential Gradients, and Its Significance for Polar Iaa Transport. New Phytologist **74,** 163-172.

Reddy, V.S., and Reddy, A.S.N. (2004). Proteomics of calcium-signaling components in plants. Phytochemistry **65,** 1745-1776.

Reddy, V.S., Ali, G.S., and Reddy, A.S.N. (2002). Genes Encoding Calmodulin-binding Proteins in the Arabidopsis Genome. Journal of Biological Chemistry **277,** 9840-9852.

Reinhardt, D., Pesce, E.-R., Stieger, P., Mandel, T., Baltensperger, K., Bennett, M., Traas, J., Friml, J., and Kuhlemeier, C. (2003). Regulation of phyllotaxis by polar auxin transport. Nature **426,** 255-260.

Rentel, M.C., and Knight, M.R. (2004). Oxidative Stress-Induced Calcium Signaling in Arabidopsis. Plant Physiology **135,** 1471-1479.

Reyes, F.C., Buono, R., and Otegui, M.S. (2011). Plant endosomal trafficking pathways. Current Opinion in Plant Biology **14,** 666-673.

Richards, S.L., Laohavisit, A., Mortimer, J.C., Shabala, L., Swarbreck, S.M., Shabala, S., and Davies, J.M. (2014). Annexin 1 regulates the H2O2-induced calcium signature in Arabidopsis thaliana roots. The Plant Journal **77,** 136-145.

Richter, S., Geldner, N., Schrader, J., Wolters, H., Stierhof, Y.-D., Rios, G., Koncz, C., Robinson, D.G., and Jurgens, G. (2007). Functional diversification of closely related ARF-GEFs in protein secretion and recycling. Nature **448,** 488-492.

Richter, S., Kientz, M., Brumm, S., Nielsen, M.E., Park, M., Gavidia, R., Krause, C., Voss, U., Beckmann, H., Mayer, U., Stierhof, Y.-D., and Jürgens, G. (2014). Delivery of endocytosed proteins to the cell–division plane requires change of pathway from recycling to secretion. eLife **3,** e02131.

Rigó, G., Ayaydin, F., Tietz, O., Zsigmond, L., Kovács, H., Páy, A., Salchert, K., Darula, Z., Medzihradszky, K.F., Szabados, L., Palme, K., Koncz, C., and Cséplő, Á. (2013). Inactivation of Plasma Membrane–Localized CDPK-RELATED KINASE5 Decelerates PIN2 Exocytosis and Root Gravitropic Response in Arabidopsis. The Plant Cell **25,** 1592-1608.

Riveras, E., Alvarez, J.M., Vidal, E.A., Oses, C., Vega, A., and Gutiérrez, R.A. (2015). The Calcium Ion Is a Second Messenger in the Nitrate Signaling Pathway of Arabidopsis. Plant Physiology **169,** 1397-1404.

Robert, S., Kleine-Vehn, J., Barbez, E., Sauer, M., Paciorek, T., Baster, P., Vanneste, S., Zhang, J., Simon, S., Čovanová, M., Hayashi, K., Dhonukshe, P., Yang, Z., Bednarek, S.Y., Jones, A.M., Luschnig, C., Aniento, F., Zažímalová, E., and Friml, J. (2010). ABP1 Mediates Auxin Inhibition of Clathrin-Dependent Endocytosis in Arabidopsis. Cell **143,** 111-121.

Robineau, S., Chabre, M., and Antonny, B. (2000). Binding site of brefeldin A at the interface between the small G protein ADP-ribosylation factor 1 (ARF1) and the nucleotide-exchange factor Sec7 domain. Proceedings of the National Academy of Sciences of the United States of America **97,** 9913-9918.

Robinson, D.G., and Pimpl, P. (2014). Clathrin and post-Golgi trafficking: a very complicated issue. Trends in Plant Science **19,** 134-139.

Rubery, P.H., and Sheldrake, A.R. (1974). Carrier-Mediated Auxin Transport. Planta **118,** 101-121.

Sabatini, S., Beis, D., Wolkenfelt, H., Murfett, J., Guilfoyle, T., Malamy, J., Benfey, P., Leyser, O., Bechtold, N., Weisbeek, P., and Scheres, B. (1999). An auxin-dependent distal organizer of pattern and polarity in the Arabidopsis root. Cell **99,** 463-472.

Sata, M., Moss, J., and Vaughan, M. (1999). Structural basis for the inhibitory effect of brefeldin A on guanine nucleotide-exchange proteins for ADP-ribosylation factors. Proceedings of the National Academy of Sciences of the United States of America **96,** 2752-2757.

Salehin, M., Bagchi, R., and Estelle, M. (2015). SCF(TIR1/AFB)-Based Auxin Perception: Mechanism and Role in Plant Growth and Development. The Plant Cell **27,** 9-19.

Sanderfoot, A.A., Ahmed, S.U., Marty-Mazars, D., Rapoport, I., Kirchhausen, T., Marty, F., and Raikhel, N.V. (1998). A putative vacuolar cargo receptor partially colocalizes with AtPEP12p on a prevacuolar compartment in Arabidopsis roots. Proceedings of the National Academy of Sciences of the United States of America **95,** 9920-9925.

Sanders, D., Pelloux, J., Brownlee, C., and Harper, J.F. (2002). Calcium at the crossroads of signaling. Plant Cell **14,** S401-S417.

Sato, E.M., Hijazi, H., Bennett, M.J., Vissenberg, K., and Swarup, R. (2015). New insights into root gravitropic signalling. Journal of Experimental Botany **66,** 2155-2165.

Schellmann, S., and Pimpl, P. (2009). Coats of endosomal protein sorting: retromer and ESCRT. Current Opinion in Plant Biology **12,** 670-676.

Schindelin, J., Arganda-Carreras, I., Frise, E., Kaynig, V., Longair, M., Pietzsch, T., Preibisch, S., Rueden, C., Saalfeld, S., Schmid, B., Tinevez, J.-Y., White, D.J., Hartenstein, V., Eliceiri, K., Tomancak, P., and Cardona, A. (2012). Fiji - an Open Source platform for biological image analysis. Nature methods **9,** 10.1038/nmeth.2019.

Schiøtt, M., and Palmgren, M.G. (2005). Two plant Ca2+ pumps expressed in stomatal guard cells show opposite expression patterns during cold stress. Physiologia Plantarum **124,** 278-283.

Schiøtt, M., Romanowsky, S.M., Bækgaard, L., Jakobsen, M.K., Palmgren, M.G., and Harper, J.F. (2004). A plant plasma membrane Ca2+ pump is required for normal pollen tube growth and fertilization. Proceedings of the National Academy of Sciences of the United States of America **101,** 9502-9507.

Shabala, S., BÆKgaard, L., Shabala, L., Fuglsang, A., Babourina, O., Palmgren, M.G., Cuin, T.A., Rengel, Z.E.D., and Nemchinov, L.G. (2011). Plasma membrane Ca2+ transporters mediate virus-induced acquired resistance to oxidative stress. Plant, Cell & Environment **34,** 406-417.

Shang, Z., Laohavisit, A., and Davies, J.M. (2009). Extracellular ATP activates an Arabidopsis plasma membrane Ca(2+)-permeable conductance. Plant Signaling & Behavior **4,** 989-991.

Shaw, S.L., and Long, S.R. (2003). Nod Factor Elicits Two Separable Calcium Responses in Medicago truncatula Root Hair Cells. Plant Physiology **131,** 976-984.

Shi, J., Kim, K.N., Ritz, O., Albrecht, V., Gupta, R., Harter, K., Luan, S., and Kudla, J. (1999). Novel protein kinases associated with calcineurin B-like calcium sensors in Arabidopsis. The Plant Cell **11,** 2393-2405.

Shih, H.-W., DePew, Cody L., Miller, Nathan D., and Monshausen, Gabriele B. (2015). The Cyclic Nucleotide-Gated Channel CNGC14 Regulates Root Gravitropism in Arabidopsis thaliana. Current Biology **25,** 3119-3125.

Shin, H.-W., Morinaga, N., Noda, M., and Nakayama, K. (2004). BIG2, A Guanine Nucleotide Exchange Factor for ADP-Ribosylation Factors: Its Localization to Recycling Endosomes and Implication in the Endosome Integrity. Molecular Biology of the Cell **15,** 5283-5294.

Shishova, M., and Lindberg, S. (1999). Auxin-induced Cytosol Acidification in Wheat Leaf Protoplasts Depends on External Concentration of Ca2+. Journal of Plant Physiology **155,** 190-196.

Shishova, M., and Lindberg, S. (2004). Auxin induces an increase of Ca2+ concentration in the cytosol of wheat leaf protoplasts. Journal of Plant Physiology **161,** 937-945.

Shishova, M., Yemelyanov, V., Rudashevskaya, E., and Lindberg, S. (2007). A shift in sensitivity to auxin within development of maize seedlings. Journal of Plant Physiology **164,** 1323-1330.

Sieberer, T., Seifert, G.J., Hauser, M.-T., Grisafi, P., Fink, G.R., and Luschnig, C. (2000). Post-transcriptional control of the Arabidopsis auxin efflux carrier EIR1 requires AXR1. Current Biology **10,** 1595-1598.

Sieburth, L.E., Muday, G.K., King, E.J., Benton, G., Kim, S., Metcalf, K.E., Meyers, L., Seamen, E., and Van Norman, J.M. (2006). tSCARFACE Encodes an ARF-GAP That Is Required for Normal Auxin Efflux and Vein Patterning in Arabidopsis. The Plant Cell **18,** 1396-1411.

Simon, S., Skůpa, P., Viaene, T., Zwiewka, M., Tejos, R., Klíma, P., Čarná, M., Rolčík, J., De Rycke, R., Moreno, I., Dobrev, P.I., Orellana, A., Zažímalová, E., and Friml, J. (2016). PIN6 auxin transporter at endoplasmic reticulum and plasma membrane mediates auxin homeostasis and organogenesis in Arabidopsis. New Phytologist **211,** 65-74.

Simonini, S., Bencivenga, S., Trick, M., and Ostergaard, L. (2017). Auxin-Induced Modulation of ETTIN Activity Orchestrates Gene Expression in Arabidopsis. The Plant Cell.

Simonini, S., Deb, J., Moubayidin, L., Stephenson, P., Valluru, M., Freire-Rios, A., Sorefan, K., Weijers, D., Friml, J., and Østergaard, L. (2016). A noncanonical auxin-sensing mechanism is required for organ morphogenesis in Arabidopsis. Genes & Development **30,** 2286-2296.

Singh, Manoj K., Krüger, F., Beckmann, H., Brumm, S., Vermeer, Joop E.M., Munnik, T., Mayer, U., Stierhof, Y.-D., Grefen, C., Schumacher, K., and Jürgens, G. (2014). Protein Delivery to Vacuole Requires SAND Protein-Dependent Rab GTPase Conversion for MVB-Vacuole Fusion. Current Biology **24,** 1383-1389.

Skoog, F., and Miller, C.O. (1957). Chemical regulation of growth and organ formation in plant tissues cultured in vitro. Symposia of the Society for Experimental Biology **11,** 118-130.

Snedden, W.A., and Fromm, H. (2001). Calmodulin as a versatile calcium signal transducer in plants. New Phytologist **151,** 35-66.

Stael, S., Wurzinger, B., Mair, A., Mehlmer, N., Vothknecht, U.C., and Teige, M. (2012). Plant organellar calcium signalling: an emerging field. Journal of experimental botany **63,** 1525-1542.

Steinmann, T., Geldner, N., Grebe, M., Mangold, S., Jackson, C.L., Paris, S., Gälweiler, L., Palme, K., and Jürgens, G. (1999). Coordinated Polar Localization of Auxin Efflux Carrier PIN1 by GNOM ARF GEF. Science **286,** 316-318.

Stepp, J.D., Huang, K., and Lemmon, S.K. (1997). The Yeast Adaptor Protein Complex, AP-3, Is Essential for the Efficient Delivery of Alkaline Phosphatase by the Alternate Pathway to the Vacuole. The Journal of Cell Biology **139,** 1761-1774.

Su, S.-H., Gibbs, N.M., Jancewicz, A.L., and Masson, P.H. Molecular Mechanisms of Root Gravitropism. Current Biology **27,** R964-R972.

Sugawara, S., Mashiguchi, K., Tanaka, K., Hishiyama, S., Sakai, T., Hanada, K., Kinoshita-Tsujimura, K., Yu, H., Dai, X., Takebayashi, Y., Takeda-Kamiya, N., Kakimoto, T., Kawaide, H., Natsume, M., Estelle, M., Zhao, Y., Hayashi, K.-i., Kamiya, Y., and Kasahara, H. (2015). Distinct Characteristics of Indole-3-Acetic Acid and Phenylacetic Acid, Two Common Auxins in Plants. Plant and Cell Physiology **56,** 1641-1654.

Swarbreck, S.M., Colaço, R., and Davies, J.M. (2013). Plant Calcium-Permeable Channels. Plant Physiology **163,** 514-522.

Swarup, K., Benkova, E., Swarup, R., Casimiro, I., Peret, B., Yang, Y., Parry, G., Nielsen, E., De Smet, I., Vanneste, S., Levesque, M.P., Carrier, D., James, N., Calvo, V., Ljung, K., Kramer, E., Roberts, R., Graham, N., Marillonnet, S., Patel, K., Jones, J.D.G., Taylor, C.G., Schachtman, D.P., May, S., Sandberg, G., Benfey, P., Friml, J., Kerr, I., Beeckman, T., Laplaze, L., and Bennett, M.J. (2008). The auxin influx carrier LAX3 promotes lateral root emergence. Nat Cell Biol **10,** 946-954.

Swarup, R., Kramer, E.M., Perry, P., Knox, K., Leyser, H.M.O., Haseloff, J., Beemster, G.T.S., Bhalerao, R., and Bennett, M.J. (2005). Root gravitropism requires lateral root cap and epidermal cells for transport and response to a mobile auxin signal. Nat Cell Biol **7,** 1057-1065.

Szemenyei, H., Hannon, M., and Long, J.A. (2008). TOPLESS Mediates Auxin-Dependent Transcriptional Repression During Arabidopsis Embryogenesis. Science **319,** 1384-1386.

Tan, X., Calderon-Villalobos, L.I.A., Sharon, M., Zheng, C., Robinson, C.V., Estelle, M., and Zheng, N. (2007). Mechanism of auxin perception by the TIR1 ubiquitin ligase. Nature **446,** 640-645.

Tanaka, H., Kitakura, S., De Rycke, R., De Groodt, R., and Friml, J. (2009). Fluorescence Imaging-Based Screen Identifies ARF GEF Component of Early Endosomal Trafficking. Current Biology **19,** 391-397.

Tanaka, H., Kitakura, S., Rakusová, H., Uemura, T., Feraru, M.I., De Rycke, R., Robert, S., Kakimoto, T., and Friml, J. (2013). Cell Polarity and Patterning by PIN Trafficking through Early Endosomal Compartments in Arabidopsis thaliana. PLOS Genetics **9,** e1003540.

Teh, O.-k., and Moore, I. (2007). An ARF-GEF acting at the Golgi and in selective endocytosis in polarized plant cells. Nature **448,** 493-496.

Thonat, C., Mathieu, C., Crevecoeur, M., Penel, C., Gaspar, T., and Boyer, N. (1997). Effects of a Mechanical Stimulation on Localization of Annexin-Like Proteins in Bryonia dioica Internodes. Plant Physiology **114,** 981-988.

Tivendale, N.D., Ross, J.J., and Cohen, J.D. (2014). The shifting paradigms of auxin biosynthesis. Trends in Plant Science **19,** 44-51.

Toyota, M., and Gilroy, S. (2013). Gravitropism and mechanical signaling in plants. American Journal of Botany **100,** 111-125.

Tromas, A., Braun, N., Muller, P., Khodus, T., Paponov, I.A., Palme, K., Ljung, K., Lee, J.-Y., Benfey, P., Murray, J.A.H., Scheres, B., and Perrot-Rechenmann, C. (2009). The AUXIN BINDING PROTEIN 1 Is Required for Differential Auxin Responses Mediating Root Growth. PLOS ONE **4,** e6648.

Tse, Y.C., Lam, S.K., and Jiang, L. (2007). Enigmatic Brefeldin A. Plant Signaling & Behavior **2,** 199-202.

Ulmasov, T., Hagen, G., and Guilfoyle, T.J. (1997a). ARF1, a Transcription Factor That Binds to Auxin Response Elements. Science **276,** 1865-1868.

Ulmasov, T., Liu, Z.B., Hagen, G., and Guilfoyle, T.J. (1995). Composite structure of auxin response elements. The Plant Cell **7,** 1611-1623.

Ulmasov, T., Murfett, J., Hagen, G., and Guilfoyle, T.J. (1997b). Aux/IAA proteins repress expression of reporter genes containing natural and highly active synthetic auxin response elements. The Plant Cell **9,** 1963-1971.

Veley, Kira M., Marshburn, S., Clure, Cara E., and Haswell, Elizabeth S. (2012). Mechanosensitive Channels Protect Plastids from Hypoosmotic Stress During Normal Plant Growth. Current Biology **22,** 408-413.

Vernoud, V., Horton, A.C., Yang, Z., and Nielsen, E. (2003). Analysis of the Small GTPase Gene Superfamily of Arabidopsis. Plant Physiology **131,** 1191-1208.

Vernoux, T., Besnard, F., and Traas, J. (2010). Auxin at the Shoot Apical Meristem. Cold Spring Harbor Perspectives in Biology **2,** a001487.

Véry, A.-A., and Davies, J.M. (2000). Hyperpolarization-activated calcium channels at the tip of Arabidopsis root hairs. Proceedings of the National Academy of Sciences **97,** 9801-9806.

Vieten, A., Sauer, M., Brewer, P.B., and Friml, J. (2007). Molecular and cellular aspects of auxin-transport-mediated development. Trends in Plant Science **12,** 160-168.

Vieten, A., Vanneste, S., Wiśniewska, J., Benková, E., Benjamins, R., Beeckman, T., Luschnig, C., and Friml, J. (2005). Functional redundancy of PIN proteins is accompanied by auxin-dependent cross-regulation of PIN expression. Development **132,** 4521-4531.

Wang, R., and Estelle, M. (2014). Diversity and specificity: auxin perception and signaling through the TIR1/AFB pathway. Current opinion in plant biology **0,** 51-58.

Wang, Y.-F., Munemasa, S., Nishimura, N., Ren, H.-M., Robert, N., Han, M., Puzõrjova, I., Kollist, H., Lee, S., Mori, I., and Schroeder, J.I. (2013). Identification of Cyclic GMP-Activated Nonselective Ca(2+)-Permeable Cation Channels and Associated CNGC5 and CNGC6 Genes in Arabidopsis Guard Cells. Plant Physiology **163,** 578-590.

Weijers, D., Benkova, E., Jäger, K.E., Schlereth, A., Hamann, T., Kientz, M., Wilmoth, J.C., Reed, J.W., and Jürgens, G. (2005). Developmental specificity of auxin response by pairs of ARF and Aux/IAA transcriptional regulators. The EMBO Journal **24,** 1874-1885.

Weller, B., Zourelidou, M., Frank, L., Barbosa, I.C.R., Fastner, A., Richter, S., Jürgens, G., Hammes, U.Z., and Schwechheimer, C. (2017). Dynamic PIN-FORMED auxin efflux carrier phosphorylation at the plasma membrane controls auxin efflux-dependent growth. Proceedings of the National Academy of Sciences **114,** E887-E896.

Went, F.W. (1926). On growth accelerating substances in the coleoptile of Avena sativa. Proc. K. Akad. Wet. **30,** 10-19.

Went, F.W. (1928). Wuchsstoff und Wachstum. Recl. Trav. Bot. Neerland. **25,** 1-116.

Whippo, C.W., and Hangarter, R.P. (2006). Phototropism: Bending towards Enlightenment. The Plant Cell **18,** 1110-1119.

White, P.J. (2001). The pathways of calcium movement to the xylem. Journal of Experimental Botany **52,** 891-899.

Willige, B.C., Ahlers, S., Zourelidou, M., Barbosa, I.C.R., Demarsy, E., Trevisan, M., Davis, P.A., Roelfsema, M.R.G., Hangarter, R., Fankhauser, C., and Schwechheimer, C. (2013). D6PK AGCVIII Kinases Are Required for Auxin Transport and Phototropic Hypocotyl Bending in Arabidopsis. The Plant Cell **25,** 1674-1688.

Won, C., Shen, X., Mashiguchi, K., Zheng, Z., Dai, X., Cheng, Y., Kasahara, H., Kamiya, Y., Chory, J., and Zhao, Y. (2011). Conversion of tryptophan to indole-3-acetic acid by TRYPTOPHAN AMINOTRANSFERASES OF ARABIDOPSIS and YUCCAs in Arabidopsis. Proceedings of the National Academy of Sciences of the United States of America **108,** 18518-18523.

Woodward, A.W., and Bartel, B. (2005). Auxin: Regulation, Action, and Interaction. Annals of Botany **95,** 707-735.

Wu, Z., Liang, F., Hong, B., Young, J.C., Sussman, M.R., Harper, J.F., and Sze, H. (2002). An Endoplasmic Reticulum-Bound Ca(2+)/Mn(2+) Pump, ECA1, Supports Plant Growth and Confers Tolerance to Mn(2+) Stress. Plant Physiology **130,** 128-137.

Wyn Jones, R.G., and Lunt, O.R. (1967). The function of calcium in plants. Bot. Rev. **33** 407–426.

Xu, T., Wen, M., Nagawa, S., Fu, Y., Chen, J.-G., Wu, M.-J., Perrot-Rechenmann, C., Friml, J., Jones, A.M., and Yang, Z. (2010). Cell surface- and Rho GTPase-based auxin signaling controls cellular interdigitation in Arabidopsis. Cell **143,** 99-110.

Xu, T., Dai, N., Chen, J., Nagawa, S., Cao, M., Li, H., Zhou, Z., Chen, X., De Rycke, R., Rakusová, H., Wang, W., Jones, A.M., Friml, J., Patterson, S.E., Bleecker, A.B., and Yang, Z. (2014). Cell Surface ABP1-TMK Auxin-Sensing Complex Activates ROP GTPase Signaling. Science (New York, N.Y.) **343,** 1025-1028.

Yang, D.-L., Shi, Z., bao, Y., Yan, J., Yang, Z., Yu, H., Li, Y., Gou, M., wang, s., zou, b., Xu, D., ma, z., Kim, J., and Hua, J. (2017). Calcium pumps and interacting BON1 protein modulate calcium signature, stomatal closure, and plant immunity. Plant Physiology.

Yin, X.-J., Volk, S., Ljung, K., Mehlmer, N., Dolezal, K., Ditengou, F., Hanano, S., Davis, S.J., Schmelzer, E., Sandberg, G., Teige, M., Palme, K., Pickart, C., and Bachmair, A. (2007). Ubiquitin Lysine 63 Chain–Forming Ligases Regulate Apical Dominance in Arabidopsis. The Plant Cell **19,** 1898-1911.

Yorimitsu, T., Sato, K., and Takeuchi, M. (2014). Molecular mechanisms of Sar/Arf GTPases in vesicular trafficking in yeast and plants. Frontiers in Plant Science **5**.

Yoshioka, K., Moeder, W., Kang, H.-G., Kachroo, P., Masmoudi, K., Berkowitz, G., and Klessig, D.F. (2006). The Chimeric Arabidopsis CYCLIC NUCLEOTIDE-GATED ION CHANNEL11/12 Activates Multiple Pathogen Resistance Responses. The Plant Cell **18,** 747-763.

Yuan, F., Yang, H., Xue, Y., Kong, D., Ye, R., Li, C., Zhang, J., Theprungsirikul, L., Shrift, T., Krichilsky, B., Johnson, D.M., Swift, G.B., He, Y., Siedow, J.N., and Pei, Z.-M. (2014). OSCA1 mediates osmotic-stress-evoked Ca2+ increases vital for osmosensing in Arabidopsis. Nature **514,** 367-371.

Žárský, V., and Potocký, M. (2010). Recycling domains in plant cell morphogenesis: small GTPase effectors, plasma membrane signalling and the exocyst. Biochemical Society Transactions **38,** 723-728.

Zažímalová, E., Křeček, P., Skůpa, P., Hoyerová, K., and Petrášek, J. (2007). Polar transport of the plant hormone auxin – the role of PIN-FORMED (PIN) proteins. Cellular and Molecular Life Sciences **64,** 1621-1637.

Zažímalová, E., Murphy, A.S., Yang, H., Hoyerová, K., and Hošek, P. (2010). Auxin Transporters—Why So Many? Cold Spring Harbor Perspectives in Biology **2,** a001552.

Zhang, J., Vanneste, S., Brewer, Philip B., Michniewicz, M., Grones, P., Kleine-Vehn, J., Löfke, C., Teichmann, T., Bielach, A., Cannoot, B., Hoyerová, K., Chen, X., Xue, H.-W., Benková, E., Zažímalová, E., and Friml, J. (2011). Inositol Trisphosphate-Induced Ca2+ Signaling Modulates Auxin Transport and PIN Polarity. Developmental Cell **20,** 855-866.

Zhang, S., Pan, Y., Tian, W., Dong, M., Zhu, H., Luan, S., and Li, L. (2017). Arabidopsis CNGC14 Mediates Calcium Influx Required for Tip Growth in Root Hairs. Molecular Plant **10,** 1004-1006.

Zhao, Y. (2014). Auxin Biosynthesis. The Arabidopsis Book / American Society of Plant Biologists **12,** e0173.

Zhao, Y., Christensen, S.K., Fankhauser, C., Cashman, J.R., Cohen, J.D., Weigel, D., and Chory, J. (2001). A Role for Flavin Monooxygenase-Like Enzymes in Auxin Biosynthesis. Science **291,** 306-309.

Zielinski, R.E. (1998). CALMODULIN AND CALMODULIN-BINDING PROTEINS IN PLANTS. Annual Review of Plant Physiology and Plant Molecular Biology **49,** 697-725.

Zolman, B.K., Yoder, A., and Bartel, B. (2000). Genetic analysis of indole-3-butyric acid responses in Arabidopsis thaliana reveals four mutant classes. Genetics **156,** 1323-1337.

Zolman, B.K., Nyberg, M., and Bartel, B. (2007). IBR3, a novel peroxisomal acyl-CoA dehydrogenase-like protein required for indole-3-butyric acid response. Plant Molecular Biology **64,** 59-72.

Zourelidou, M., Müller, I., Willige, B.C., Nill, C., Jikumaru, Y., Li, H., and Schwechheimer, C. (2009). The polarly localized D6 PROTEIN KINASE is required for efficient auxin transport in Arabidopsis thaliana. Development **136,** 627-636.

Zourelidou, M., Absmanner, B., Weller, B., Barbosa, I.C.R., Willige, B.C., Fastner, A., Streit, V., Port, S.A., Colcombet, J., de la Fuente van Bentem, S., Hirt, H., Kuster, B., Schulze, W.X., Hammes, U.Z., and Schwechheimer, C. (2014). Auxin efflux by PIN-FORMED proteins is activated by two different protein kinases, D6 PROTEIN KINASE and PINOID. eLife **3,** e02860.

Zwiewka, M., Feraru, E., Möller, B., Hwang, I., Feraru, M.I., Kleine-Vehn, J., Weijers, D., and Friml, J. (2011). The AP-3 adaptor complex is required for vacuolar function in Arabidopsis. Cell Research **21,** 1711-1722.

Chapter 2:
Calcium is an organizer of cell polarity in plants

Ellie Himschoot[1, 2], Tom Beeckman[1, 2], Jiří Friml[3], Steffen Vanneste[1, 2]

[1] Department of Plant Biotechnology and Bio-informatics, Ghent University, B-9052 Ghent, Belgium
[2] Department of Plant Systems Biology, VIB, B-9052 Ghent, Belgium
[3] Institute of Science and Technology Austria (IST Austria), 3400 Klosterneuburg, Austria

Adapted from:
Ellie Himschoot[1, 2], Tom Beeckman[1, 2], Jiří Friml[3], Steffen Vanneste[1, 2]. *Calcium is an organizer of cell polarity in plants.* Biochimica et Biophysica Acta - Molecular Cell Research 2015, 1853(9): 2168-2172.

Author contribution:
E.H. performed the literature study and is the main author of this chapter. T.B, J.F., and S.V. contributed to the writing and revision of the manuscript.

Abstract

Cell polarity is a fundamental property of pro- and eukaryotic cells. It is necessary for coordination of cell division, cell morphogenesis and signaling processes. How polarity is generated and maintained is a complex issue governed by interconnected feed-back regulations between small GTPase signaling and membrane tension-based signaling that controls membrane trafficking, and cytoskeleton organization and dynamics. Here, we will review the potential role for calcium as a crucial signal that connects and coordinates the respective processes during polarization processes in plants. This article is part of a Special Issue entitled: 13th European Symposium on Calcium.

Introduction to polarity and plant development

At its simplest level, polarity can be defined as an asymmetric distribution of components along one or more axes, thereby breaking symmetry (Bloch and Yalovsky, 2013). The most basic type of polarity involves establishing a single polar domain and can be found in a wide range of biological processes in unicellular as well as in multicellular organisms, ranging from asymmetric cell divisions, polarized axon growth, directional movement of motile cells, pollen tube and root hair formation in plants, zygote polarization in algae, etc. In each of these examples, the polarity is defined by the local accumulation of cellular components to one side of the cell.

In multicellular organisms, cells are often embedded in a three-dimensional tissue context, requiring additional dimensions of polarity. Hitherto, molecular markers exist defining apical and basal polarity (reflecting position along the embryonic axis), as well as inner- and outer-lateral polar domains (radial polarity) that can coexist within a single plant cell (Dettmer and Friml, 2011). In addition to these four polar domains, specialized cell types have the capacity to develop additional polar features, superimposed on or across other polar domains, such as in the endodermis that develops casparian strips that encircle the cells (Alassimone et al., 2012) and root hairs that develop at a discrete positions in the outer-lateral domains of root epidermal cells (Grebe, 2012). Another complex manifestation of polarity in plants is seen during the morphogenesis of leaf epidermal cells in dicotyledons that is characterized by

interdigitation of adjacent cells via the coordinated formation of lobes and indentations (Yang and Lavagi, 2012).

How plants can generate such complex polarity patterns remains poorly understood. Yet, several of the mechanisms underlying generation and maintenance of polarity become identified step by step. Two important cellular processes control polarity: 1) anisotropic membrane trafficking by local delivery or removal of specific membrane proteins and lipids, and 2) the polar organization and dynamics of the cytoskeleton. These cellular processes are believed to be controlled by signals derived from the local activity of small GTPases and from cellular mechanosensing mechanisms. These different aspects of polarity are tightly interconnected, making it difficult to assess their individual contribution to polarity and how they are coordinated to generate and maintain polarity.

In this review, we will focus on the mechanisms by which the second messenger Ca^{2+} is connected to each of the aforementioned polarity processes and signaling cascades and we elaborate on how Ca^{2+} could serve as a general coordinative and integrative signal for plant polarity, a principle that we propose not to be restricted to tip-growing cells (Fig. 1).

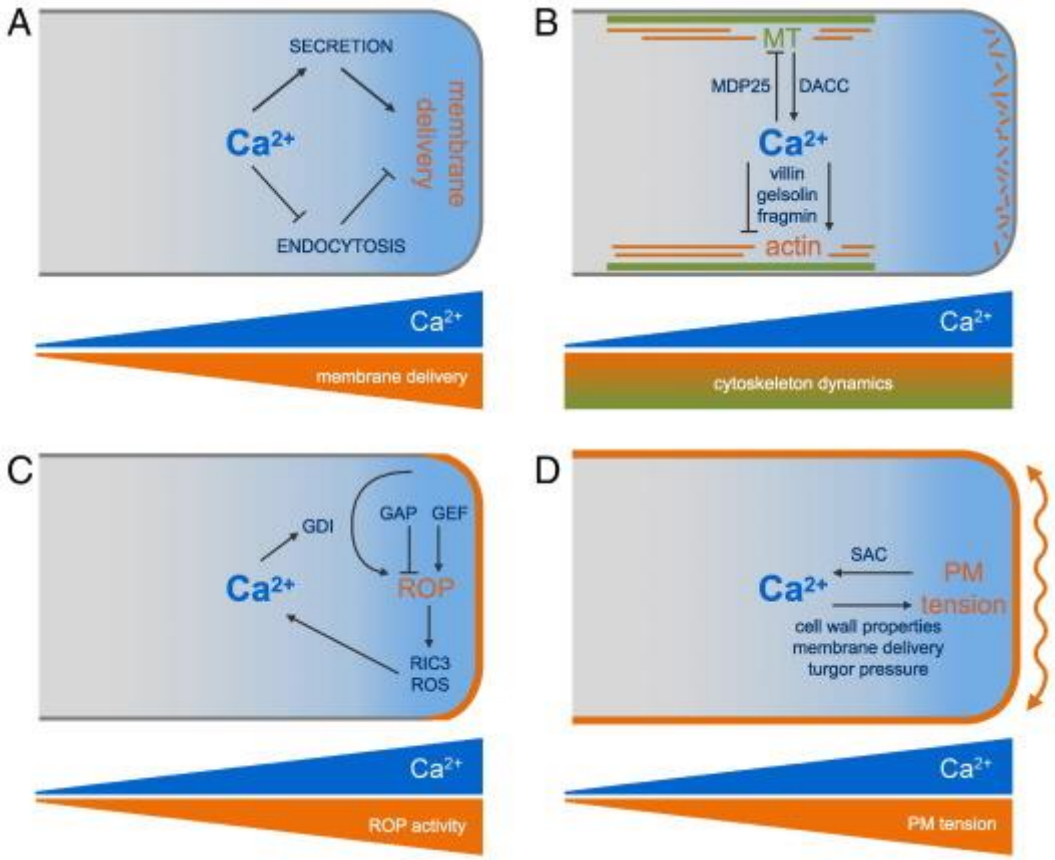

Fig. 1. Interconnection between Ca^{2+} and polarity components. A. A Ca^{2+} gradient spatially coordinates membrane trafficking. High Ca^{2+} concentrations to one side of a cell locally stimulate secretion while reducing (clathrin-mediated) endocytosis thereby locally promoting membrane delivery. The blue and orange color represent the gradients in Ca^{2+} and membrane delivery respectively. B. A Ca^{2+} gradient differentially controls cytoskeleton dynamics. Ca^{2+} controls F-actin dynamics and organization through Ca^{2+}-dependent actin regulating proteins of the villin/gelsolin/fragmin superfamily, regulating actin organization and dynamics. Via MICROTUBULE-DESTABILIZING PROTEIN25 (MDP25) Ca^{2+} can destabilize cortical microtubules (MT). In turn, MTs can stabilize Ca^{2+} signaling via controlling DEPOLARIZATION-ACTIVATED Ca^{2+} CHANNELS (DACC). The blue color represents the Ca^{2+} gradient and the orange/green color the actin/MT dynamics respectively. C. Interaction between Ca^{2+} and ROP signaling to generate and maintain cell polarity. Polarized ROPs (orange gradient) locally stimulate Ca^{2+} entry through the ROP effector RIC3 and ROP-induced reactive oxygen species (ROS) production. ROP activity is positively or negatively regulated by GEFs or GAPs respectively. Polar localization of ROPs to the apex is maintained by GDI which in turn can be controlled by Ca^{2+}. The blue and orange color represent the gradients in Ca^{2+} and ROP activity respectively. D. Interplay between Ca^{2+} and PM tension. The plant cell wall and local differences in plasma membrane (PM) tension both contribute to cell polarization. Upon cellular growth, increased PM tension results in opening of STRETCH-ACTIVATED Ca^{2+} CHANNELS (SACs) resulting in local Ca^{2+} influx. Ca^{2+} itself can control cell wall rigidity and membrane delivery and turgor pressure to regulate PM tension. The blue and orange color represent the Ca^{2+} gradient and locally high PM tension respectively.

Calcium hallmarks polarity

Calcium is an elusive second messenger because it can be triggered by a wide range of signals and is transient in nature (Kudla et al., 2010). Therefore, it is commonly described in terms of Ca^{2+} signatures that can be very local and short-lived, making it often difficult to detect

reliably. Under these limitations, a sharp Ca^{2+} gradient can be detected in the tip of growing pollen tubes and root hairs, that is essential for polar growth (Cole and Fowler, 2006; Steinhorst and Kudla, 2013). In addition, local Ca^{2+} signaling is also central to polarity establishment in fucoid algal zygotes (Hable and Hart, 2010). Importantly, manipulations that refocus Ca^{2+} signals are sufficient to reorient polarity of tip growth, not only in pollen tubes (Malho and Trewavas, 1996), but also in root hairs (Bibikova et al., 1997) demonstrating the potential of Ca^{2+} gradients as instructive signals for polarity. The role of Ca^{2+} as a regulator of polarity is mainly derived from studies on tip growth in pollen tubes, a cell type that is easily accessible, and expresses only a relatively small subset of the Ca^{2+} toolkit (Berridge et al., 2000). However, it must be noted that Ca^{2+} levels were also found to impact on apical–basal polarity in root cells (Zhang et al., 2011), suggesting that the role of Ca^{2+} in plant polarity is not restricted to tip growth.

At least four distinct Ca^{2+} channels contribute to the Ca^{2+} gradient that exists at the pollen tube tip. The first, and most important Ca^{2+} channels for the tip-focused Ca^{2+} gradient, are STRETCH-ACTIVATED Ca^{2+} CHANNELS (SAC) that open in response to plasma membrane strain, such as the strain associated with rapid growth (Dutta and Robinson, 2004). However, the underlying molecular nature of these channels remains completely unknown. Secondly, members of the GLUTAMATE RECEPTOR-LIKE (GLR) family, AtGLR1.2 and AtGLR3.7 have been demonstrated to form Ca^{2+} channels in pollen tubes in response to D-Serine derived from the pistil to guide pollen tube growth (Michard et al., 2011). Thirdly, several CYCLIC NUCLEOTIDE GATED CATION CHANNEL (CNGC) genes have been implicated in pollen tube growth (Steinhorst and Kudla, 2013). Among them, CNGC18 displays a clear apical localization, with its strongest localization just behind the apex, a position that would allow to refocus the Ca^{2+} maximum in response to directional cues (Frietsch et al., 2007). A fourth family of Ca^{2+} channeling proteins that could contribute to tip-focused Ca^{2+} gradients are the ANNEXINs, that can generate Ca^{2+}-permeable channels in response to hydroxyl radicals (Laohavisit et al., 2010). Whereas these Ca^{2+} channels reflect mechanisms by which Ca^{2+} enters the cell through the plasma membrane, Ca^{2+}-ATPases are continuously active to move Ca^{2+} from the cytosol into adjacent cellular compartments or the apoplast. These mechanisms can contribute to shaping the Ca^{2+} signal (Steinhorst and Kudla, 2013). Several of these Ca^{2+}-ATPases, such as

ACA9, do not show polar localization (Schiøtt et al., 2004), but are instead activated by local high Ca^{2+} concentrations, acting to dissipate Ca^{2+} signals.

Given that Ca^{2+} carries no structural information, the information embedded in Ca^{2+} gradients and temporal signatures needs to be decoded and translated into a cellular response. This can be achieved by a complex set of Ca^{2+}-binding proteins (> 250 in Arabidopsis) (Hashimoto and Kudla, 2011a) that represent Ca^{2+} sensors with enzymatic activity (Ca^{2+} sensor responders; Ca^{2+}-DEPENDENT PROTEIN KINASE (CDPK/CPK)) or without enzymatic activity (Ca^{2+} sensor relays; CALMODULIN (CaM), CALMODULIN-LIKE (CML), CALCINEURIN B-LIKE (CBL)). Strong polarity defects in pollen tubes have thus far only been reported for overexpression of CDPKs (Zhou et al., 2009), supporting the importance of local CDPK activity in directing pollen tube polarity (Moutinho et al., 1998). Many known targets of CDPKs are ion channels, allowing to regulate osmotic pressure and membrane potential in the context of Ca^{2+} signals (Kudla et al., 2010). Moreover, it was recently found that CPK32 directly contributes to the tip-focused Ca^{2+} gradient by activating the Ca^{2+} permeability of CNGC18 (Zhou et al., 2014). Moreover, CNGC activity can be further modulated by interaction with active CaM (Fischer et al., 2013), revealing a complex Ca^{2+}-dependent regulation of the Ca^{2+} channeling activities of CNGCs.

The complexity of Ca^{2+} signaling that is already needed for generating polarity within a simple pollen tube, suggests that the additional dimensions of polarity that exist in cells embedded in a tissue context will involve even more complex Ca^{2+} signaling. In the following paragraphs we will highlight the connections that exist between Ca^{2+} signaling and the cellular processes and signaling cascades that impact on polarity throughout the plant body.

Calcium coordinates the balance of exo- and endocytosis

The semi-fluid nature of the plasma membrane allows diffusion of membrane proteins and lipids, implying that maintenance of polarity requires spatially regulated membrane trafficking. Consistently, membrane trafficking is a crucial process to maintain tip growth in pollen (Moscatelli and Idilli, 2009; Zhao et al., 2010), root hairs (Synek et al., 2006), as well as in apical–basal polarity in the plant body (Men et al., 2008; Kitakura et al., 2011; Fan et al., 2013). During tip growth, exocytosis (secretion and recycling) occurs predominantly in the tip, whereas endocytosis occurs subapically. Similarly, in apical polar domains of root cells, exo-

and endocytosis are also spatially separated; exocytosis occurs in a super-apical domain, while endocytosis occurs mainly at the flanks of the respective polar domains (Kleine-Vehn et al., 2011).

In plants, the exocytosis-stimulating effect of Ca^{2+} could be mediated by ANNEXINs (ANNs). These are Ca^{2+}-dependent phospholipid binding proteins that regulate secretion in animals (Gerke and Moss, 2002), and possibly also in plants (Clark et al., 2012). Consistently, overexpression of AtANN5 rendered *Arabidopsis* pollen partially resistant to Brefeldin A (BFA) (Zhu et al., 2014) (a fungal toxin which targets BARF GTPase guanine-nucleotide exchange factors, thereby inhibiting endosomal recycling (Geldner et al., 2003) and late secretory and vacuolar trafficking (Richter et al., 2014)), and root hair growth is reduced in AtANN1 mutants (Laohavisit et al., 2012). However, the function of ANNs in regulating Ca^{2+}-dependent secretion in plants remains to be demonstrated unequivocally. Importantly, it should be noted that the tip-focused Ca^{2+} gradient and the maximal growth phase of the pollen tube oscillate partially out of phase with each other (Messerli et al., 2000; Holdaway-Clarke et al., 2003), making a direct link between Ca^{2+} and secretion not very intuitive.

Clathrin-mediated endocytosis (CME) occurs mainly subapically in growing pollen tubes (Moscatelli and Idilli, 2009), as if excluded from the high Ca^{2+} concentrations found in the tip. Consistently, several components of the core CME machinery displayed a subapical localization in growing pollen (Zhao et al., 2010; Gadeyne et al., 2014). Moreover, several subunits of a recently identified endocytic adaptor complex (TPLATE complex; TPC) contain predicted Ca^{2+} binding EF-hand motifs (Gadeyne et al., 2014a), suggestive of a Ca^{2+} sensitive activity. Consistently, a treatment with the presumed intracellular Ca^{2+} store leak inducer, caffeine (Cessna et al., 1998), could dislodge the TPC subunit, TPLATE and CLATHRIN LIGHT CHAIN2 from the cell plate during cytokinesis (Van Damme et al., 2011b). This is consistent with a model in which high Ca^{2+} concentrations act to inactivate CME. Calcium can also have an indirect effect on CME via phosphatidylinositides, at least in pollen tubes, where Ca^{2+} signals control the subapical localization of the phosphatidylinositol 4,5-bisphosphate ($PI(4,5)P_2$)-hydrolyzing enzyme NtPLC3 (Helling et al., 2006). Interestingly, $PI(4,5)P_2$ is required for CME and polarity in pollen tubes (Zhao et al., 2010) as well as root cells (Ischebeck et al., 2013a; Tejos et al., 2014). However the role of Ca^{2+} in regulating $PI(4,5)P_2$ homeostasis in root cells remains to be demonstrated.

Together, these findings suggest that Ca^{2+} could control polarity in different plant cell types through coordination of exo- and endocytosis (Fig. 1, A).

Reciprocal interaction between calcium signaling and the cytoskeleton

The actin filaments (F-actin) are critical elements in cell morphogenesis and directional growth. These dynamic structures control membrane trafficking, including correct delivery of secretory vesicles and regulation of vesicle docking and fusion (Gu et al., 2003), as well as actin regulation of endocytosis (Dhonukshe et al., 2008; Nagawa et al., 2012). Interestingly, the actin filaments in pollen tubes occur in a polarized gradient overlapping with the tip-focused Ca^{2+} gradient (Fan et al., 2004) (Fig. 1, B), an observation that can be mechanistically explained via the Ca^{2+}-dependence of actin organizing proteins (nucleation, bundling, and severing) such as members of the villin/gelsolin/fragmin superfamily (Huang et al., 2015), which also control directional elongation in other cell types (van der Honing et al., 2012).

Polarity can also be regulated via microtubules (MT) by providing structural rigidity and stiffness to the cell, imposing restrictions on cell expansion (Sedbrook and Kaloriti, 2008). In addition, MTs were recently found to be part of a symmetry breaking system for secondary wall patterning in metaxylem cells (Oda and Fukuda, 2012). Interestingly, Ca^{2+} can destabilize cortical MTs via MICROTUBULE-DESTABILIZING PROTEIN25 (MDP25) during directional elongation of hypocotyl cells (Li et al., 2011a). Conversely, the MTs seem to contribute to the stability of Ca^{2+} signaling via control over the activity of depolarization-activated Ca^{2+} channels (Fig. 1, B).

This demonstrates that the intimate link between Ca^{2+} signaling and cytoskeleton dynamics is involved in sustaining and/or generating polarity in plants.

Calcium interdependence of ROP-based polarity signaling

Small GTPases of the RHO superfamily, such as Rac and Cdc42, play major roles in generating and stabilizing asymmetry (Hable and Hart, 2010; Mogilner et al., 2012; Freisinger et al., 2013). Land plants have no Rac or Cdc42 in their genomes. Instead, they have a plant-specific subfamily dubbed ‘RHO-LIKE GTPASE FOR PLANT’ or ROPs, that are closely associated with

polarity in higher land plants (Yang and Lavagi, 2012), and recently also in the lower land plant *Physcomitrella patens* (Ito et al., 2014). The polarization of RHO GTPase family members tightly interconnects via several effectors to other polarity-associated processes, including exo- and endocytosis and cytoskeleton organization (Chen and Friml, 2014).

ROP GTPases are active when bound to GTP and return to an inactive, GDP-bound state by hydrolysis of GTP to GDP. The exchange of GDP by GTP can be promoted by GEFs (GUANINE-NUCLEOTIDE EXCHANGE FACTORs), whereas inactivation is stimulated by GAPs (GTPASE ACTIVATING PROTEINs) (Fig. 1, C). Mechanisms that control GEFs and GAPs can thus be used for local regulation of ROP activity (Kost, 2008). In addition, RHO-GDIs (GUANINE NUCLEOTIDE DISSOCIATION INHIBITOR) seem to act as conserved polarity facilitators of RHO GTPases via stimulation of RHO GTPase recycling (Fig. 1, C). In yeast, the polarization of Cdc42 was proposed to be regulated by GDI-dependent Cdc42 removal from the plasma membrane, and subsequent rapid polar recycling (Freisinger et al., 2013). A similar mechanism could also be active for ROP polarization, as a mutant in AtRHO-GDI1 (*supercentipede1*/*scn1*) shows ectopic ROP2 accumulation associated with multiple root hair initiation sites along a single trichoblast (Carol et al., 2005), and knock-down of AtRHO-GDI2a showed strong pollen depolarization (Hwang et al., 2010). Two lines of evidence suggest that this GDI-mediated mechanism is under control of Ca^{2+}. Firstly, the strength of pollen tube depolarization in AtRHO-GDI2a knock-downs was found to be dependent on the Ca^{2+} concentration in the germination medium (Hwang et al., 2010). Secondly, it was shown that the phosphorylation status of conserved CPK3 phosphorylation sites in AtRHO-GDI1, impacts on ROP-regulated polarization processes during pavement cell morphogenesis (Wu et al., 2013). Although the direct involvement of Ca^{2+} in this process remains to be demonstrated unequivocally, it represents an interesting hypothesis on how Ca^{2+} can feed into ROP polarity.

While these data suggest that ROP polarity can be Ca^{2+}-regulated, ROPs can in turn control Ca^{2+} signaling in pollen tubes, via ROP-INTERACTIVE CRIB-CONTAINING PROTEIN3 (RIC3)-regulated Ca^{2+} influx at the apex of pollen tubes (Gu et al., 2005) (Fig. 1, C). Moreover, ROPs can also directly activate reactive oxygen species (ROS) production via RESPIRATORY BURST OXIDASE HOMOLOGUEs (RBOHs) (Wong et al., 2007), to activate Ca^{2+} channels that contribute to the tip-focused Ca^{2+} gradient in root hairs (Foreman et al., 2003). Interestingly, whereas the

fungus *Piriformospora indica* can activate ROP-dependent actin remodeling, ROP signaling is not required for Ca^{2+} signals that are induced during infection (Venus and Oelmüller, 2013).

In biological systems, polarization mechanisms involve coupled feed-back mechanisms that are optimized for robust symmetry breaking (Freisinger et al., 2013). The reciprocal regulation between Ca^{2+} and ROP signaling could thus represent such a feedback mechanism that underlies symmetry breaking in plants.

Mechano-sensitive polarity signaling involves calcium

Until recently, the cell wall was mostly regarded as a passive capsule that protects the cell against the high turgor pressure. However, it is becoming more and more clear that the interaction between the cell and its encapsulating cell wall has important implications for polarity (Fig. 1, D).

On the one hand, the cell wall contributes directly to the maintenance of polarity by restricting lateral diffusion rates of plasma membrane proteins (Feraru et al., 2011; Martinière et al., 2012). On the other hand, local differences in the strength or elasticity of the cell wall in conjunction with the turgor pressure, as well as the anchorage of the plasma membrane to the cell wall can generate local differences in membrane tension, thereby directly impacting on polarity (Asnacios and Hamant, 2012). Although the underlying mechanism is not well understood, local differences in plasma membrane tension can be directly translated in polarity instructing Ca^{2+} signals via stretch-activated Ca^{2+} channels in the plasma membrane. This mechanism is believed to be relevant for tip growth processes where the fast growth generates a significant strain on the plasma membrane (Steinhorst and Kudla, 2013).

In addition, Ca^{2+} seems to contribute to several determinants of plasma membrane strain. At the level of the cell wall, Ca^{2+} can change the mechanical properties of de-esterified pectin, via cross-linking (Harholt et al., 2010). On the other hand, Ca^{2+} signaling could modify the cell wall via control over secretion of e.g. cell wall modifying enzymes (Guan et al., 2013), as indicated by the tremendous anisotropy in cell wall composition observed in root hairs and pollen tubes (Gu and Nielsen, 2013). In addition Ca^{2+} itself can reduce the plasma membrane tension via modulation of membrane trafficking (cf. above) and via regulation of ion channel

activities that modify the turgor pressure (Kudla et al., 2010). Thus, Ca^{2+} provides an interesting signal through which such mechanical signals can be translated in changes in polarity.

Conclusions and perspectives

Polarity in plants is a complex issue involving complex membrane trafficking and dynamic cytoskeleton reorganization in the context of an interconnected signaling network of small GTPases and physical cues. Although most of our knowledge derives from studies in pollen tubes and root hairs, which are examples of extremely polarized cells, it is slowly becoming more and more clear that cellular processes and signaling networks that govern polarity in tip growth are probably also at work in generating and maintaining polarity in other polarized cells and tissues.

The second messenger Ca^{2+} is commonly accepted as a core regulator of polarity in tip growth. Here, we illustrated the potential of Ca^{2+} as a general regulator of polarity, through highlighting the intimate connections between Ca^{2+} and polarity-driving processes and signaling cascades that are active throughout plant development. The lack of reports demonstrating Ca^{2+} gradients coinciding with other polarity-hallmarking events, argues against our generalization of Ca^{2+} as ubiquitous polarity-instructing signal. Yet, we believe that the reports thus far lack the necessary spatio-temporal resolution and sensitivity to visualize such Ca^{2+} signals in plant cells within a complex tissue context. Consistent with this notion is that the use of an ultra-sensitive genetically-encoded Ca^{2+} indicator (GECI), Yellow Cameleon (YCnano), has only recently allowed to visualize a wave of Ca^{2+} signals moving from the root to the shoot upon application of salt stress through the cortical cell file (Choi et al., 2014). Similarly, a BRET-based GFP-aequorin (G5A) Ca^{2+} reporter was recently tested in plants, also visualizing a similar salt-induced mobile Ca^{2+} signal with high sensitivity (Xiong et al., 2014). This suggests that implementation of alternative GECIs in plants, could provide the plant community with an unprecedented sensitivity and resolution to revisit this question.

Other difficulties associated with assessing the role of Ca^{2+} signaling in polarity are directly related to the Ca^{2+} signaling toolkit of plants. On the one hand, gene function can be masked by extensive functional redundancy among Ca^{2+} channels and decoders, as they are often

encoded in large multi-gene families (Verret et al., 2010; Hashimoto and Kudla, 2011a). On the other hand, through divergence in evolution, plants lack well-characterized Ca^{2+} channels present in animals, such as L-type voltage-dependent Ca^{2+} channels, transient receptor potential channels, inositol triphosphate receptors and ryanodine receptors (Verret et al., 2010). This implies that we cannot simply use Ca^{2+} channel blockers or agonists that were developed to target specific animal Ca^{2+} channels, to dissect the involvement of related Ca^{2+} channels in plants. While several important types of Ca^{2+} channels can be characterized electrophysiologically in plant cells, the molecular nature of the channels is often not known. Prominently among them are the SACs that contribute to the Ca^{2+} gradient in pollen tubes. This fundamental gap in plant Ca^{2+} signaling, precludes the thorough evaluation of Ca^{2+} signaling in plant polarity. Recently, a completely new family of Ca^{2+} channels involved in osmosensing has been identified in plants (Yuan et al., 2014), opening up new avenues for Ca^{2+} research and polarity.

References

Alassimone, J., Roppolo, D., Geldner, N., and Vermeer, J.E.M. (2012). The endodermis—development and differentiation of the plant's inner skin. Protoplasma **249:** 433-443.

Asnacios, A., and Hamant, O. (2012). The mechanics behind cell polarity. Trends in Cell Biology **22:** 584-591.

Berridge, M.J., Lipp, P., and Bootman, M.D. (2000). The versatility and universality of calcium signalling. Nat Rev Mol Cell Biol **1:** 11-21.

Bibikova, T.N., Zhigilei, A., and Gilroy, S. (1997). Root hair growth in Arabidopsis thaliana is directed by calcium and an endogenous polarity. Planta **203:** 495-505.

Bloch, D., and Yalovsky, S. (2013). Cell polarity signaling. Current Opinion in Plant Biology **16:** 734-742.

Carol, R.J., Takeda, S., Linstead, P., Durrant, M.C., Kakesova, H., Derbyshire, P., Drea, S., Zarsky, V., and Dolan, L. (2005). A RhoGDP dissociation inhibitor spatially regulates growth in root hair cells. Nature **438:** 1013-1016.

Cessna, S.G., Chandra, S., and Low, P.S. (1998). Hypo-osmotic Shock of Tobacco Cells Stimulates Ca2+Fluxes Deriving First from External and then Internal Ca2+Stores. Journal of Biological Chemistry **273:** 27286-27291.

Chen, X., and Friml, J. (2014). Rho-GTPase-regulated vesicle trafficking in plant cell polarity. Biochemical Society Transactions **42:** 212-218.

Choi, W.-G., Toyota, M., Kim, S.-H., Hilleary, R., and Gilroy, S. (2014). Salt stress-induced Ca2+ waves are associated with rapid, long-distance root-to-shoot signaling in plants. Proceedings of the National Academy of Sciences **111:** 6497-6502.

Clark, G.B., Morgan, R.O., Fernandez, M.-P., and Roux, S.J. (2012). Evolutionary adaptation of plant annexins has diversified their molecular structures, interactions and functional roles. New Phytologist **196:** 695-712.

Cole, R.A., and Fowler, J.E. (2006). Polarized growth: maintaining focus on the tip. Current Opinion in Plant Biology **9:** 579-588.

Dettmer, J., and Friml, J. (2011). Cell polarity in plants: when two do the same, it is not the same. Current Opinion in Cell Biology **23:** 686-696.

Dhonukshe, P., et al. (2008). Auxin transport inhibitors impair vesicle motility and actin cytoskeleton dynamics in diverse eukaryotes. Proceedings of the National Academy of Sciences **105:** 4489-4494.

Dutta, R., and Robinson, K.R. (2004). Identification and Characterization of Stretch-Activated Ion Channels in Pollen Protoplasts. Plant Physiology **135:** 1398-1406.

Fan, L., Hao, H., Xue, Y., Zhang, L., Song, K., Ding, Z., Botella, M.A., Wang, H., and Lin, J. (2013). Dynamic analysis of Arabidopsis AP2 σ subunit reveals a key role in clathrin-mediated endocytosis and plant development. Development **140:** 3826-3837.

Fan, X., Hou, J., Chen, X., Chaudhry, F., Staiger, C.J., and Ren, H. (2004). Identification and Characterization of a Ca(2+)-Dependent Actin Filament-Severing Protein from Lily Pollen. Plant Physiology **136:** 3979-3989.

Feraru, E., Feraru, M.I., Kleine-Vehn, J., Martinière, A., Mouille, G., Vanneste, S., Vernhettes, S., Runions, J., and Friml, J. (2011). PIN Polarity Maintenance by the Cell Wall in Arabidopsis. Current Biology **21:** 338-343.

Fischer, C., Kugler, A., Hoth, S., and Dietrich, P. (2013). An IQ Domain Mediates the Interaction with Calmodulin in a Plant Cyclic Nucleotide-Gated Channel. Plant and Cell Physiology **54:** 573-584.

Foreman, J., Demidchik, V., Bothwell, J.H.F., Mylona, P., Miedema, H., Torres, M.A., Linstead, P., Costa, S., Brownlee, C., Jones, J.D.G., Davies, J.M., and Dolan, L. (2003). Reactive oxygen species produced by NADPH oxidase regulate plant cell growth. Nature **422:** 442-446.

Freisinger, T., Klünder, B., Johnson, J., Müller, N., Pichler, G., Beck, G., Costanzo, M., Boone, C., Cerione, R.A., Frey, E., and Wedlich-Söldner, R. (2013). Establishment of a robust single axis of cell polarity by coupling multiple positive feedback loops **4:** 1807.

Frietsch, S., Wang, Y.-F., Sladek, C., Poulsen, L.R., Romanowsky, S.M., Schroeder, J.I., and Harper, J.F. (2007). A cyclic nucleotide-gated channel is essential for polarized tip growth of pollen. Proceedings of the National Academy of Sciences **104:** 14531-14536.

Gadeyne, A., et al. (2014). The TPLATE Adaptor Complex Drives Clathrin-Mediated Endocytosis in Plants. Cell **156:** 691-704.

Geldner, N., Anders, N., Wolters, H., Keicher, J., Kornberger, W., Muller, P., Delbarre, A., Ueda, T., Nakano, A., and Jürgens, G. The Arabidopsis GNOM ARF-GEF Mediates Endosomal Recycling, Auxin Transport, and Auxin-Dependent Plant Growth. Cell **112:** 219-230.

Geldner, N., Anders, N., Wolters, H., Keicher, J., Kornberger, W., Muller, P., Delbarre, A., Ueda, T., Nakano, A., and Jürgens, G. (2003). The Arabidopsis GNOM ARF-GEF Mediates Endosomal Recycling, Auxin Transport, and Auxin-Dependent Plant Growth. Cell **112:** 219-230.

Gerke, V., and Moss, S.E. (2002). Annexins: From Structure to Function. Physiological Reviews **82:** 331-371.

Grebe, M. (2012). The patterning of epidermal hairs in Arabidopsis—updated. Current Opinion in Plant Biology **15:** 31-37.

Gu, F., and Nielsen, E. (2013). Targeting and Regulation of Cell Wall Synthesis During Tip Growth in Plants. Journal of Integrative Plant Biology **55:** 835-846.

Gu, Y., Vernoud, V., Fu, Y., and Yang, Z. (2003). ROP GTPase regulation of pollen tube growth through the dynamics of tip-localized F-actin. Journal of Experimental Botany **54:** 93-101.

Gu, Y., Fu, Y., Dowd, P., Li, S., Vernoud, V., Gilroy, S., and Yang, Z. (2005). A Rho family GTPase controls actin dynamics and tip growth via two counteracting downstream pathways in pollen tubes. The Journal of Cell Biology **169:** 127-138.

Guan, Y., Guo, J., Li, H., and Yang, Z. (2013). Signaling in Pollen Tube Growth: Crosstalk, Feedback, and Missing Links. Molecular Plant **6:** 1053-1064.

Hable, W.E., and Hart, P.E. (2010). Signaling mechanisms in the establishment of plant and fucoid algal polarity. Molecular Reproduction and Development **77:** 751-758.

Harholt, J., Suttangkakul, A., and Vibe Scheller, H. (2010). Biosynthesis of Pectin. Plant Physiology **153:** 384-395.

Hashimoto, K., and Kudla, J. (2011). Calcium decoding mechanisms in plants. Biochimie **93:** 2054-2059.

Helling, D., Possart, A., Cottier, S., Klahre, U., and Kost, B. (2006). Pollen Tube Tip Growth Depends on Plasma Membrane Polarization Mediated by Tobacco PLC3 Activity and Endocytic Membrane Recycling. The Plant Cell **18:** 3519-3534.

Holdaway-Clarke, T.L., Weddle, N.M., Kim, S., Robi, A., Parris, C., Kunkel, J.G., and Hepler, P.K. (2003). Effect of extracellular calcium, pH and borate on growth oscillations in Lilium formosanum pollen tubes. Journal of Experimental Botany **54:** 65-72.

Huang, S., Qu, X., and Zhang, R. (2015). Plant villins: Versatile actin regulatory proteins. Journal of Integrative Plant Biology **57:** 40-49.

Hwang, J.-U., Wu, G., Yan, A., Lee, Y.-J., Grierson, C.S., and Yang, Z. (2010). Pollen-tube tip growth requires a balance of lateral propagation and global inhibition of Rho-family GTPase activity. Journal of Cell Science **123:** 340-350.

Ischebeck, T., et al. (2013). Phosphatidylinositol 4,5-Bisphosphate Influences PIN Polarization by Controlling Clathrin-Mediated Membrane Trafficking in Arabidopsis. The Plant Cell **25:** 4894-4911.

Ito, K., Ren, J., and Fujita, T. (2014). Conserved function of Rho-related Rop/RAC GTPase signaling in regulation of cell polarity in Physcomitrella patens. Gene **544:** 241-247.

Kitakura, S., Vanneste, S., Robert, S., Löfke, C., Teichmann, T., Tanaka, H., and Friml, J. (2011). Clathrin Mediates Endocytosis and Polar Distribution of PIN Auxin Transporters in Arabidopsis. The Plant Cell **23:** 1920-1931.

Kleine-Vehn, J., et al. (2011). Recycling, clustering, and endocytosis jointly maintain PIN auxin carrier polarity at the plasma membrane. Molecular Systems Biology **7:** 540-540.

Kost, B. (2008). Spatial control of Rho (Rac-Rop) signaling in tip-growing plant cells. Trends in Cell Biology **18:** 119-127.

Kudla, J., Batistič, O., and Hashimoto, K. (2010). Calcium Signals: The Lead Currency of Plant Information Processing. The Plant Cell **22:** 541-563.

Laohavisit, A., Brown, A.T., Cicuta, P., and Davies, J.M. (2010). Annexins: Components of the Calcium and Reactive Oxygen Signaling Network. Plant Physiology **152:** 1824-1829.

Laohavisit, A., et al. (2012). Arabidopsis Annexin1 Mediates the Radical-Activated Plasma Membrane Ca(2+)- and K(+)-Permeable Conductance in Root Cells. The Plant Cell **24:** 1522-1533.

Li, J., Wang, X., Qin, T., Zhang, Y., Liu, X., Sun, J., Zhou, Y., Zhu, L., Zhang, Z., Yuan, M., and Mao, T. (2011). MDP25, A Novel Calcium Regulatory Protein, Mediates Hypocotyl Cell Elongation by Destabilizing Cortical Microtubules in Arabidopsis. The Plant Cell **23:** 4411-4427.

Malho, R., and Trewavas, A.J. (1996). Localized Apical Increases of Cytosolic Free Calcium Control Pollen Tube Orientation. The Plant Cell **8:** 1935-1949.

Martinière, A., et al. (2012). Cell wall constrains lateral diffusion of plant plasma-membrane proteins. Proceedings of the National Academy of Sciences **109:** 12805-12810.

Men, S., Boutte, Y., Ikeda, Y., Li, X., Palme, K., Stierhof, Y.-D., Hartmann, M.-A., Moritz, T., and Grebe, M. (2008). Sterol-dependent endocytosis mediates post-cytokinetic acquisition of PIN2 auxin efflux carrier polarity. Nat Cell Biol **10:** 237-244.

Messerli, M.A., Créton, R., Jaffe, L.F., and Robinson, K.R. (2000). Periodic increases in elongation rate precede increases in cytosolic Ca2+ during pollen tube growth. Developmental Biology **222:** 84-98.

Michard, E., Lima, P.T., Borges, F., Silva, A.C., Portes, M.T., Carvalho, J.E., Gilliham, M., Liu, L.-H., Obermeyer, G., and Feijó, J.A. (2011). Glutamate Receptor–Like Genes Form Ca²⁺ Channels in Pollen Tubes and Are Regulated by Pistil d-Serine. Science **332:** 434-437.

Mogilner, A., Allard, J., and Wollman, R. (2012). Cell Polarity: Quantitative Modeling as a Tool in Cell Biology. Science **336:** 175-179.

Moscatelli, A., and Idilli, A.I. (2009). Pollen Tube Growth: a Delicate Equilibrium Between Secretory and Endocytic Pathways. Journal of Integrative Plant Biology **51:** 727-739.

Moutinho, A., Trewavas, A.J., and Malhó, R. (1998). Relocation of a Ca²-Dependent Protein Kinase Activity during Pollen Tube Reorientation. The Plant Cell **10:** 1499-1509.

Nagawa, S., Xu, T., Lin, D., Dhonukshe, P., Zhang, X., Friml, J., Scheres, B., Fu, Y., and Yang, Z. (2012). ROP GTPase-Dependent Actin Microfilaments Promote PIN1 Polarization by Localized Inhibition of Clathrin-Dependent Endocytosis. PLOS Biology **10:** e1001299.

Oda, Y., and Fukuda, H. (2012). Initiation of Cell Wall Pattern by a Rho- and Microtubule-Driven Symmetry Breaking. Science **337:** 1333-1336.

Richter, S., Kientz, M., Brumm, S., Nielsen, M.E., Park, M., Gavidia, R., Krause, C., Voss, U., Beckmann, H., Mayer, U., Stierhof, Y.-D., and Jürgens, G. (2014). Delivery of endocytosed proteins to the cell–division plane requires change of pathway from recycling to secretion. eLife **3:** e02131.

Schiøtt, M., Romanowsky, S.M., Bækgaard, L., Jakobsen, M.K., Palmgren, M.G., and Harper, J.F. (2004). A plant plasma membrane Ca2+ pump is required for normal pollen tube growth and fertilization. Proceedings of the National Academy of Sciences of the United States of America **101:** 9502-9507.

Sedbrook, J.C., and Kaloriti, D. (2008). Microtubules, MAPs and plant directional cell expansion. Trends in Plant Science **13:** 303-310.

Steinhorst, L., and Kudla, J. (2013). Calcium - a central regulator of pollen germination and tube growth. Biochimica et Biophysica Acta (BBA) - Molecular Cell Research **1833:** 1573-1581.

Synek, L., Schlager, N., Eliáš, M., Quentin, M., Hauser, M.-T., and Žárský, V. (2006). AtEXO70A1, a member of a family of putative exocyst subunits specifically expanded in land plants, is important for polar growth and plant development. The Plant Journal **48:** 54-72.

Tejos, R., Sauer, M., Vanneste, S., Palacios-Gomez, M., Li, H., Heilmann, M., van Wijk, R., Vermeer, J.E.M., Heilmann, I., Munnik, T., and Friml, J. (2014). Bipolar Plasma Membrane Distribution of Phosphoinositides and Their Requirement for Auxin-Mediated Cell Polarity and Patterning in Arabidopsis. The Plant Cell **26:** 2114-2128.

Van Damme, D., Gadeyne, A., Vanstraelen, M., Inzé, D., Van Montagu, M.C.E., De Jaeger, G., Russinova, E., and Geelen, D. (2011). Adaptin-like protein TPLATE and clathrin recruitment during plant somatic cytokinesis occurs via two distinct pathways. Proceedings of the National Academy of Sciences of the United States of America **108:** 615-620.

van der Honing, H.S., Kieft, H., Emons, A.M.C., and Ketelaar, T. (2012). Arabidopsis VILLIN2 and VILLIN3 Are Required for the Generation of Thick Actin Filament Bundles and for Directional Organ Growth. Plant Physiology **158:** 1426-1438.

Venus, Y., and Oelmüller, R. (2013). Arabidopsis ROP1 and ROP6 Influence Germination Time, Root Morphology, the Formation of F-Actin Bundles, and Symbiotic Fungal Interactions. Molecular Plant **6:** 872-886.

Verret, F., Wheeler, G., Taylor, A.R., Farnham, G., and Brownlee, C. (2010). Calcium channels in photosynthetic eukaryotes: implications for evolution of calcium-based signalling. New Phytologist **187:** 23-43.

Wong, H.L., Pinontoan, R., Hayashi, K., Tabata, R., Yaeno, T., Hasegawa, K., Kojima, C., Yoshioka, H., Iba, K., Kawasaki, T., and Shimamoto, K. (2007). Regulation of Rice NADPH Oxidase by Binding of Rac GTPase to Its N-Terminal Extension. The Plant Cell **19:** 4022-4034.

Wu, Y., Zhao, S., Tian, H., He, Y., Xiong, W., Guo, L., and Wu, Y. (2013). CPK3-phosphorylated RhoGDI1 is essential in the development of Arabidopsis seedlings and leaf epidermal cells. Journal of Experimental Botany **64:** 3327-3338.

Xiong, T.C., Ronzier, E., Sanchez, F., Corratgé-Faillie, C., Mazars, C., and Thibaud, J.-B. (2014). Imaging long distance propagating calcium signals in intact plant leaves with the BRET-based GFP-aequorin reporter. Frontiers in Plant Science **5:** 43.

Yang, Z., and Lavagi, I. (2012). Spatial control of plasma membrane domains: ROP GTPase-based symmetry breaking. Current Opinion in Plant Biology **15:** 601-607.

Yuan, F., et al. (2014). OSCA1 mediates osmotic-stress-evoked Ca2+ increases vital for osmosensing in Arabidopsis. Nature **514:** 367-371.

Zhang, J., et al. (2011). Inositol Trisphosphate-Induced Ca2+ Signaling Modulates Auxin Transport and PIN Polarity. Developmental Cell **20:** 855-866.

Zhao, Y., Yan, A., Feijó, J.A., Furutani, M., Takenawa, T., Hwang, I., Fu, Y., and Yang, Z. (2010). Phosphoinositides Regulate Clathrin-Dependent Endocytosis at the Tip of Pollen Tubes in Arabidopsis and Tobacco. The Plant Cell **22:** 4031-4044.

Zhou, L., Fu, Y., and Yang, Z. (2009). A Genome-wide Functional Characterization of Arabidopsis Regulatory Calcium Sensors in Pollen Tubes. Journal of Integrative Plant Biology **51:** 751-761.

Zhou, L., Lan, W., Jiang, Y., Fang, W., and Luan, S. (2014). A Calcium-Dependent Protein Kinase Interacts with and Activates A Calcium Channel to Regulate Pollen Tube Growth. Molecular Plant **7:** 369-376.

Zhu, J., Wu, X., Yuan, S., Qian, D., Nan, Q., An, L., and Xiang, Y. (2014). Annexin5 Plays a Vital Role in Arabidopsis Pollen Development via Ca2+-Dependent Membrane Trafficking. PLOS ONE **9:** e102407.

Chapter 3:
The ins and outs of Ca^{2+} in plant endomembrane trafficking

Ellie Himschoot[1,2,*], Roman Pleskot[1,2,3,*], Daniël Van Damme[1,2], Steffen Vanneste[1,2]

[1] Department of Plant Biotechnology and Bio-informatics, Ghent University, B-9052 Ghent, Belgium
[2] Department of Plant Systems Biology, VIB, B-9052 Ghent, Belgium
[3] Institute of Experimental Botany, Czech Academy of Sciences, Rozvojova 263, 16502 Prague, Czech Republic

Adapted from:
Ellie Himschoot[1,2,*], Roman Pleskot[1,2,3,*], Daniël Van Damme[1,2], Steffen Vanneste[1,2]. *The ins and outs of Ca^{2+} in plant endomembrane trafficking.* Current Opinion in Plant Biology 2017, 40C: 131-137.

Author contribution:
E.H. and R.P. contributed equally. Figures were made by R.P.. D.V.D. and S.V. contributed to the writing and revision of the manuscript.

Abstract

Trafficking of proteins and lipids within the plant endomembrane system is essential to support cellular functions and is subject to rigorous regulation. Despite this seemingly strict regulation, endomembrane trafficking needs to be dynamically adjusted to ever-changing internal and environmental stimuli, while maintaining cellular integrity. Although often overlooked, the versatile second messenger Ca^{2+} is intimately connected to several endomembrane-associated processes. Here, we discuss the impact of electrostatic interactions between Ca^{2+} and anionic phospholipids on endomembrane trafficking, and illustrate the direct role of Ca^{2+}-sensing proteins in regulating endomembrane trafficking and membrane integrity preservation. Moreover, we discuss how Ca^{2+} can control protein sorting within the plant endomembrane system. We thus highlight Ca^{2+} signaling as a versatile mechanism by which numerous signals can be integrated into plant endomembrane trafficking dynamics.

Introduction

The alkaline earth metal calcium is one of most abundant elements on earth. Much of the Ca^{2+} as we know it is present as calcium phosphate in bones and teeth, or as calcium carbonate in lime stone, pearls and shells. These prominent forms of Ca^{2+} have been generated by living organisms that employ calcium's chemical propensity to precipitate anions such as phosphates and carbonate as scaffolds and protection for their bodies. Besides such structural functions, Ca^{2+} acts in all living organisms as a second messenger in the context of a wide range of cellular processes and signaling cascades. In plants, the second messenger function of Ca^{2+} is best described in the context of responses to biotic and abiotic stress, symbiosis, tip growth of pollen tubes and root hairs and egg cell fertilization. For a detailed overview of the complexities that underlie Ca^{2+} signal generation and transduction in plants, the reader is referred to a number of recent outstanding reviews on the topic and references therein (Dodd et al., 2010; Hashimoto and Kudla, 2011; Boudsocq and Sheen, 2013; Edel et al., 2017)

Importantly, one of the key aspects of Ca^{2+} signaling, which is often overlooked, is the local nature of Ca^{2+} signals, acting in microdomains within the cell. To avoid toxic effects of high

Ca^{2+} e.g. at the level of phosphate metabolism, cells keep cytoplasmic Ca^{2+} levels very low (typically in the submicromolar range: 100-200nM), via energy consuming Ca^{2+} transport into the apoplast and intracellular organelles, which can have Ca^{2+} concentrations in the millimolar range (reviewed in (Stael et al., 2012), Fig. 1). The resulting steep concentration gradients over the cellular membranes thus allow to rapidly generate a local cytoplasmic Ca^{2+} signal by opening a few Ca^{2+} channels. Moreover, electrostatic interaction with anionic moieties buffer the cytoplasm against rapid Ca^{2+} diffusion, resulting in sharply defined microdomains of high Ca^{2+} (>100µM) in the direct proximity (+/-100nM) of activated Ca^{2+} channels (Berridge, 2006; Demuro and Parker, 2006; Filadi and Pozzan, 2015). Therefore, such discrete Ca^{2+} signals allow for regulation of subcellular processes with sub-micrometer precision.

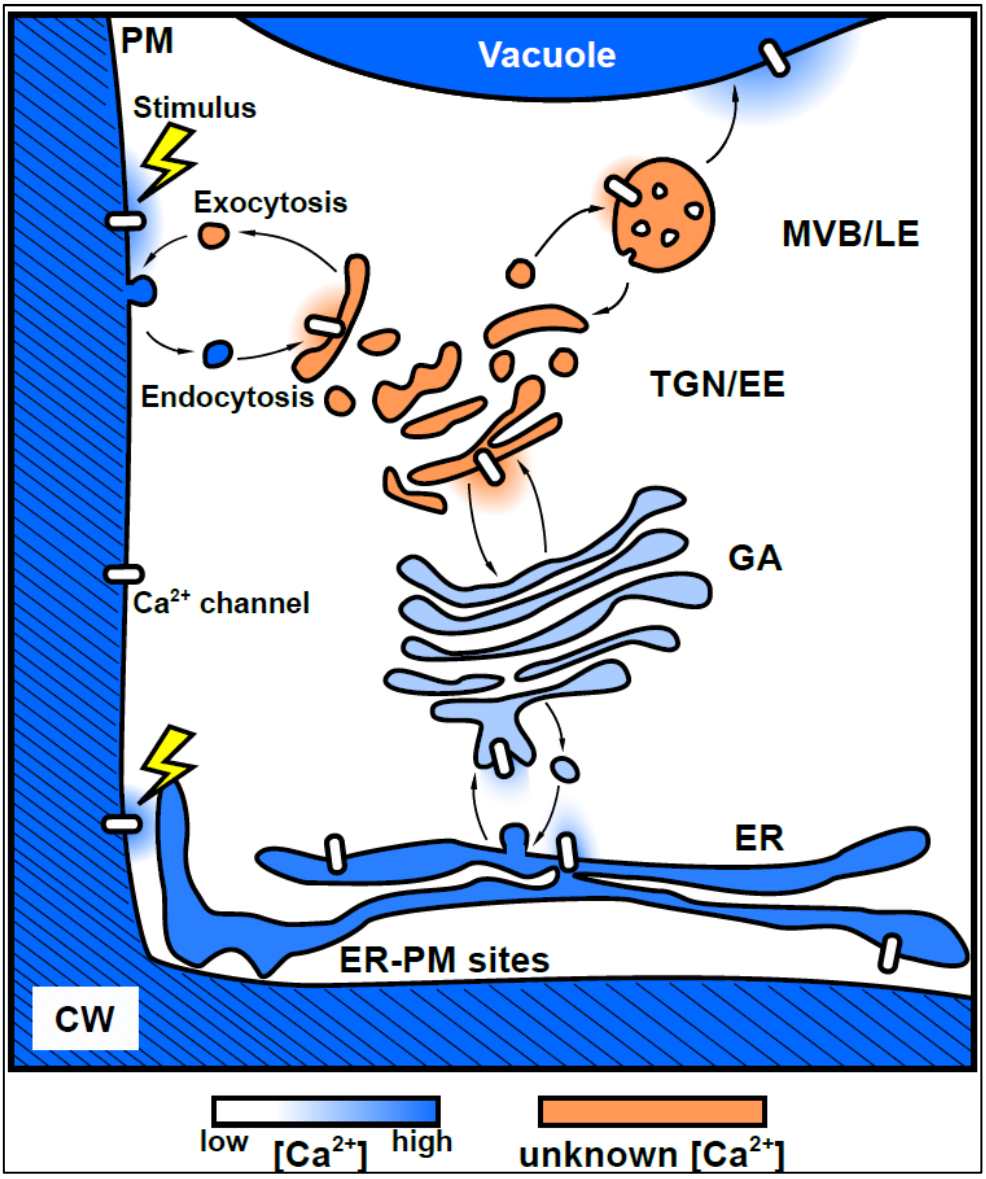

Figure 1: Calcium distribution within the plant endomembrane system. In blue: summary of experimental estimates of Ca^{2+} levels, being high (millimolar range) in the apoplast, the endoplasmic reticulum (ER) and vacuole, intermediately high (700nM) in the Golgi Apparatus (GA) and low in the cytoplasm (submicromolar range). In orange: Unknown Ca^{2+} levels across the endomembrane system. Extrapolations from the animal field and biochemical observations suggest the folowing: 1) Vesicle budding does not allow exclusion of Ca^{2+} from the lumen of budding vesicles and is illustrated as the budding vesicle having the same Ca^{2+} concentration as its donor organelle. 2) Ca^{2+} can be released from the vesicles during trafficking or by fusion to the target organelle. 3) Each endomembrane compartment is postulated to be decorated with Ca^{2+} channels that can generate Ca^{2+} signals for regulation of e.g. membrane fusion events. 4) Stress and other stimuli activate Ca^{2+} channels that generate Ca^{2+} signals that are focused around the mouth of the Ca^{2+} channel. 5) Because VSRs are dissociated from their ligands in the *trans*-Golgi Network/Early Endosomes (TGN/EE), we postulate that this reflects Ca^{2+} levels being lower in the TGN/EE than in the GA. 6) The presence of the Ca^{2+}-ATPase ER-TYPE Ca^{2+}-ATPASE3 (ECA3) in Multi Vesicular Bodies/Late Endosomes (MVB/LE) suggests the Ca^{2+} levels to be at least higher than in the cytoplasm, but are difficult to further resolve relative to those in the TGN/EE.

In animal cells, local Ca^{2+} signaling is well known for its role as a regulator of endomembrane trafficking; the process in which proteins are selectively moved between interconnected subcellular endomembrane compartments via tightly regulated membrane budding, transport and fusion. This paradigm is nicely illustrated in neurotransmission, where local cytoplasmic Ca^{2+} signals in axon termini trigger the exocytosis of neurotransmitter-filled vesicles to activate downstream neurons (Benarroch, 2013). Despite the common evolutionary origin of Ca^{2+} signaling in Eukaryotes, it is often difficult to identify conserved molecular mechanisms of Ca^{2+} signaling between animals and plants, as the large evolutionary distance also allowed for a remarkable Kingdom-specific diversification and specializations within the Ca^{2+} toolset (Edel and Kudla, 2015; Marchadier et al., 2016; Edel et al., 2017).

In this review, we provide an overview of how Ca^{2+} regulates plant endomembrane trafficking and discuss possible underlying molecular mechanisms. In particular, we will discuss the interplay between Ca^{2+} and phospholipids, the direct effect of Ca^{2+} on the endomembrane machinery and how luminal Ca^{2+} levels are connected to protein sorting in the endomembrane system. Despite the well described functions of Ca^{2+} in plant stress responses, limited information is available regarding the cell biological relevance of Ca^{2+} signaling in plants. Therefore, we will at some points resort to reasonable extrapolations from observations in metazoans to bridge some gaps in our knowledge in plants.

Calcium sensing via anionic phospholipids

Although only representing a minor fraction of the total membrane lipids, anionic phosphoinositides and phosphatidic acid are key endomembrane components. Each endomembrane compartment is hallmarked by a specific phosphoinositide signature that determines differential protein recruitment (Simon et al., 2014; Simon et al., 2016), which underlies important connections to processes such as regulation of cytoskeleton dynamics (Pleskot et al., 2013; Pleskot et al., 2014), exocytosis (Yamashita et al., 2010; Bloch et al., 2016) and endocytosis (Cocucci et al., 2012; Ischebeck et al., 2013; Tejos et al., 2014). Recently, a unique electrostatic signature controlled by phosphatidylinositol 4-phosphate (PI4P) was described for the plant plasma membrane and the cell plate of dividing cells (Simon et al., 2016). The membrane surface charge was found to control the plasma membrane recruitment of several peripheral plasma membrane proteins. The net negative charge of anionic phospholipids depends on local pH and could allow for dynamic pH-dependent modulation of proteins interaction at the membrane (see Box 1). This biochemical principle is probably universally valid as a similar pH sensing function has been described in yeast and animals for phosphatidic acid (PA) (Young et al., 2010; Shin and Loewen, 2011) (Fig. 2). Consistently with such an electrostatic regulation at the plasma membrane, the dynamics of clathrin-mediated endocytosis were shown to depend on anionic phospholipids (Ischebeck et al., 2013b), and cytoplasmic pH (Ischebeck et al., 2013b; Dejonghe et al., 2016).

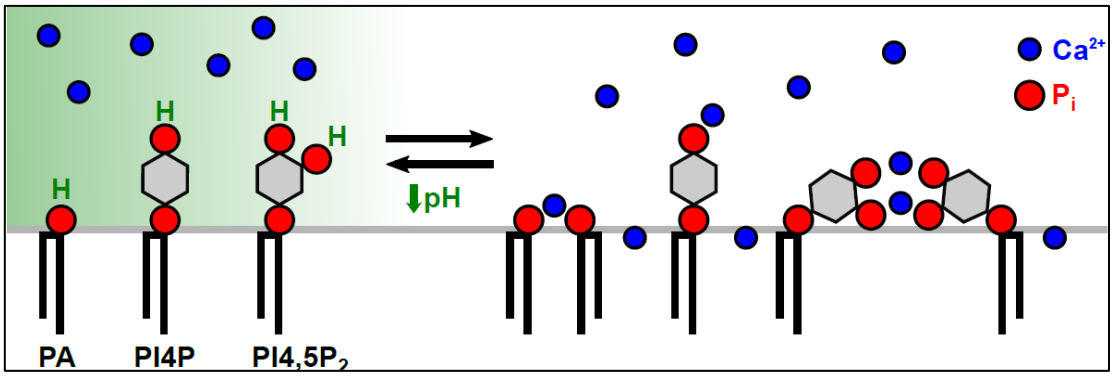

Figure 2: Schematic representation of the pH-dependent interplay between Ca^{2+} and anionic phospholipids. Ca^{2+} interacts electrostatically with the phosphate head groups in phosphatidic acid (PA) and phosphoinositides, such as phosphatidylinositol 4-phosphate, PI4P and phosphatidylinositol 4,5-bisphosphate, $PI(4,5)P_2$ (right). Interaction of Ca^{2+} neutralizes negative charges of the lipids, can induce clustering and lipid head group tilting, which stimulates or interferes with specific protein-lipid interactions. Under conditions of low pH, Ca^{2+}

dissociation from the lipids is stimulated (left), thereby reverting the Ca^{2+} dependent effects on phospholipids and their interaction with proteins.

Box 1: Electrostatic interactions of phospholipids with ions

Non-covalent interactions are key interactions in biological systems; they play essential roles in protein folding, DNA replication or enzyme catalysis. Electrostatic interactions, hydrogen bonds and van der Waals interactions are the three fundamental non-covalent interactions. Electrostatic interactions between two charged molecules or ions could be either repulsive in the case of same charges or attractive in the case of opposite charges. The presence of acidic phospholipids in the cytoplasmic face of the eukaryotic membranes results in a significant negative surface charge (Slochower et al., 2014), which recruits mobile counterions from the cytoplasm that can cause pronounced changes in membrane curvature and surface patterning (Slochower et al., 2014; Graber et al., 2017). Phosphatidic acid, PI4P and $PI(4,5)P_2$ contain phosphate group(s) as a part of their head group region (Figure 2). Protonation state, i.e. the negative charge (-1 or -2) of the phosphate group, changes within a physiological pH range (i.e. 6.9 to 7.9) (Kooijman et al., 2005). Changes in the negative charge of the phosphate group affect interaction with positively charged ions and/or proteins and thus enable anionic phospholipid containing the phosphate group to work as pH sensors (Young et al., 2010; Shin and Loewen, 2011). Moreover, electrostatic interaction allows to concentrate Ca^{2+} in the direct proximity of the membrane, exceeding ten times the bulk concentration in the cytoplasm (Mclaughlin et al., 1981). On the one hand, Ca^{2+} could act as a charge bridge connecting phospholipids and proteins as was recently shown for mammalian syntaxin 1 (Milovanovic et al., 2016). On the other hand, specific binding of Ca^{2+} to $PI(4,5)P_2$ changes the phospholipid head group conformation and inhibits $PI(4,5)P_2$ recognition by pleckstrin homology (PH) domain (Bilkova et al., 2017).

The bivalent cation Ca^{2+} binds to deprotonated anionic phospholipids and has, besides effects on protein interactions, many biophysical consequences for membrane organization (reviewed in (Wang et al., 2014)). Importantly, the positive charge of Ca^{2+} modulates the

effective charge of the cytoplasmic leaflet of the endomembranes, and could thus interfere with electrostatic interactions at these positions. This is relevant during membrane fusion, where Ca^{2+} facilitates contact of two proximal membranes by bridging lipid head groups (Tsai et al., 2013). However, several recent studies have suggested that the interaction of Ca^{2+} with membranes is more complex and is not just limited to Ca^{2+}-regulated vesicle fusion (Melcrova et al., 2016; Bilkova et al., 2017; Magarkar et al., 2017).

Besides modulating the electrostatic properties of the membrane, Ca^{2+} binding to the phosphatidylinositol 4,5-bisphosphate ($PI(4,5)P_2$) head group and carbonyl regions leads to confined lipid head group tilting and conformational rearrangements that modify lipid recognition specificity (Bilkova et al., 2017). Together, these findings imply that Ca^{2+} allows to rapidly modulate the local electrostatic environment and presentation of phospholipids in membranes for differential recruitment and/or activity of phospholipid-binding proteins.

Conversely, the Ca^{2+} buffering capacity of membranes can also modify Ca^{2+} signaling, as lipids can display high lateral diffusion rates within the membrane (Melcrova et al., 2016), and can locally release the Ca^{2+} bound to anionic phospholipids by acidification of the cytoplasm, or by enzymatic removal of the phosphate head group. Together, this intricate electrostatic interplay between Ca^{2+} and phospholipids highlights a fundamental mechanism by which Ca^{2+} signals are integrated in controlling endomembrane trafficking.

Calcium sensing proteins that regulate endomembrane trafficking

Endomembrane trafficking encompasses highly orchestrated membrane budding and fusion and cytoskeleton-based transport in which Ca^{2+} sensing proteins are involved. Calcium sensing is usually conferred by the presence of one or more highly conserved Ca^{2+} binding domains (Marchadier et al., 2016). For example, the Arabidopsis genome encodes for at least 250 proteins, including prominent regulators of endomembrane trafficking, with one or more EF-hands, archetypal Ca^{2+} binding sites (Day et al., 2002). Several endocytic regulators as well as subunits of the T-PLATE adaptor complex (TPC) were reported to contain EF hand motifs (Bar et al., 2008; Gadeyne et al., 2014). Although not experimentally validated, Ca^{2+} binding via the EF hands in the TPC may explain the potent and immediate effect of caffeine treatment on the removal of TPC subunits as well as clathrin from the growing cell plate during cytokinesis

(Van Damme et al., 2011a). In this model, caffeine-induced Ca^{2+} release from intracellular stores is sensed by TPC subunits and blocks their recruitment. The released Ca^{2+} is not efficiently dissipated during cell plate expansion. Following cell plate attachment to the plasma membrane, membrane recruitment of the TPC and other CME machinery rapidly recovers, suggesting restoration of Ca^{2+} dissipation after establishing a continuum between the cell plate lumen and the apoplast. Next to endomembrane trafficking, many regulators of the actin and microtubule cytoskeleton are known to be regulated by Ca^{2+} (Burstenbinder et al., 2013; Hepler, 2016; Burstenbinder et al., 2017). In addition to Ca^{2+}-dependent regulation of somatic cell shape and growth, this is highly relevant for tip growing pollen tubes, where an oscillating tip-focused Ca^{2+} gradient instructs targeted secretion in a positive feedback regulation between Ca^{2+} and ROS production (Boisson-Dernier et al., 2013; Himschoot et al., 2015b).

In animals, Ca^{2+} sensing via CALMODULIN (CaM) fine-tunes core regulatory mechanisms of vesicle tethering and fusion at the level of RAB GTPase and SNARE (SOLUBLE *N*-ETHYL-MALEIMIDE SENSITIVE FUSION FACTOR ATTACHMENT PROTEIN RECEPTOR) activity (Reviewed in (Burgoyne and Clague, 2003)). In plants, canonical CaM has not yet been reported to be enriched in RAB or SNARE enriched endosomal fractions (Fujiwara et al., 2014; Heard et al., 2015). However, Arabidopsis CALMODULIN-LIKE4 (AtCML4) and AtCML5 are CaM domain-containing membrane proteins that reside in endosomal populations that overlap with Golgi and MVB/LE markers (Ruge et al., 2016), suggesting that they could modulate Ca^{2+}-dependent vesicle trafficking at these endosomal compartments.

Two other classes of bona fide Ca^{2+}-sensing proteins seem to be involved in endomembrane trafficking: ANNEXINs and SYNAPTOTAGMINs. ANNEXINs (ANNs) are conserved, multifunctional Ca^{2+}-binding proteins that are involved in membrane trafficking, membrane-cytoskeleton interactions, and can even generate Ca^{2+} channels. Plant ANNs display many similarities to their metazoan counterparts (reviewed in (Laohavisit and Davies, 2011)). As their name suggests, they function to bring together/annex membranes, a process intrinsic to endomembrane trafficking. Consistently, purified maize ANNs (ZmANN33/35) could potentiate Ca^{2+}-regulated exocytosis in root cap protoplasts (Carroll et al., 1998), and overexpression of *Arabidopsis* ANN5 (AtANN5) renders pollen tube growth more resistant to the exocytosis-inhibiting fungal toxin, Brefeldin A (Zhu et al., 2014). In addition, AtANN4 co-

purifies with the Qa-SNAREs SYNTAXIN OF PLANT121 (SYP121), SYP122, SYP123, SYP21 and SYP22 (Fujiwara et al., 2014), suggesting that plant ANNs act in conjunction with the core membrane fusion machinery. However, genetic evidence supporting the role of plant ANNs in membrane trafficking remains scarce. One clear example is that protoplasts expressing a RNAi construct directed against AtANN3 display defective segregation of TGN/EE and MVB/LE markers, connecting this AtANN3 to vacuolar trafficking (Scheuring et al., 2011).

On the other hand, plant SYNAPTOTAGMINs (SYTs), such as SYT1, act as molecular tethers between the ER and the plasma membrane (Perez-Sancho et al., 2015). In their C-terminal domains, they have Ca^{2+}-sensing C2 domains for Ca^{2+}-dependent interaction with phospholipids (Schapire et al., 2008). Interestingly, expression of a truncated SYT1 construct in tobacco inhibits endocytosis as indicated by a reduced uptake of the endocytic tracer dye FM4-64 and aberrant localization of the endosomal marker RabF1/Ara6-GFP (Lewis and Lazarowitz, 2010). Similarly, the structurally related *Xenopus* EXTENDED SYNAPTOTAGMIN2 acts as an early endocytic adaptor for the rapid phase of endocytosis of activated Fibroblast Growth Factor Receptors (Jean et al., 2010), suggesting a conserved functionality for such Ca^{2+} sensing proteins in regulation of endocytosis in animals and in plants.

Together, these examples illustrate how Ca^{2+}-sensing proteins control endomembrane trafficking.

Calcium connects endomembrane trafficking to membrane integrity

One of the most fundamental battles that cells are engaged in, is the continuous fight to preserve their membrane integrity in an ever-changing environmental and developmental context and this involves a strict coordination with endomembrane trafficking. A striking example is the reversible change in guard cell surface, up to 40%, during stomatal movement, that is dependent on concomitant changes in endo- and exocytosis rates due to the limited elasticity of the plasma membrane (Shope et al., 2003; Meckel et al., 2007). Similarly, cell volume changes triggered by changes in turgor pressure during osmotic challenges are followed by changes in endomembrane trafficking. When plants are subjected to acute hyper-osmotic stress, endocytosis (including bulk internalization) increases and exocytosis decreases, while hypo-osmotic conditions have the opposite effect (Baral et al., 2015;

Zwiewka et al., 2015; Pou et al., 2016). The functional connection to membrane integrity systems is illustrated by mutants defective in early endocytic steps being more sensitive to hyperosmotic stress compared to controls (Zwiewka et al., 2015). This is consistent with a model in which stress hijacks endomembrane trafficking processes to lower membrane tension and preserve cellular integrity by changing the balance between endo- and exocytosis. Given that Ca^{2+} signals are readily elicited upon stress perception, it is easy to envision a role for Ca^{2+} sensing regulators of endomembrane trafficking in membrane integrity preservation, which is the case for plant ANNs and SYTs. Indeed, mutants *Atann1* and *Atann4*, but also overexpressors of AtANN8 are tolerant to abiotic stress (Huh et al., 2010; Yadav et al., 2016). Given their presumed conserved role in membrane fusion (see above), plant ANNs could thus be involved in a patch-like membrane repair mechanism in which vesicles are fused as a 'membrane patch' across the plasma membrane breach (Laohavisit and Davies, 2011). On the other hand, *syt1* mutants are hypersensitive to mechanical stress (Perez-Sancho et al., 2015), hyperosmotic stress (Schapire et al., 2008) and freezing (Yamazaki et al., 2008), while overexpression of a truncated SYT1 results in inhibition of endocytosis (Lewis and Lazarowitz, 2010). These examples illustrate the Ca^{2+}-dependent interconnection between controlled endomembrane trafficking and membrane integrity preservation mechanisms.

Calcium and protein sorting

Endomembrane trafficking involves highly regulated sorting of specific cargoes of the secretory and the endocytic pathways for secretion, recycling and/or degradation. VACUOLAR SORTING RECEPTORs (VSRs) divert vacuolar cargoes away from the default secretory pathway into the vacuolar pathway, as mutants defective in VSR function missort vacuolar cargoes to the apoplast (Fuji et al., 2007b; Sanmartin et al., 2007; Sohn et al., 2007). For reasons of cellular economy, the VSRs do not follow their ligands into the vacuole, but become recycled to the TGN/EE via retrograde transport from MVB/LE. Therefore, VSRs have to dissociate from their ligands prior to being released in the intraluminal bodies of the MVB/LE. In mammalian cells, this dissociation is induced by rapid acidification and a loss of Ca^{2+} from the maturing endosome, based on pH- and Ca^{2+}-sensitive ligand binding (Andersen and Moestrup, 2014). Similarly, in plants, Ca^{2+} strongly stabilizes receptor-ligand interactions, albeit independently

of pH (Watanabe et al., 2002; Shimada et al., 2003). The latter is consistent with the absence of a dramatic acidification within the anterograde endosomal pathway (Luo et al., 2015). Interestingly, targeted retention of soluble VSRs in different subcellular compartments demonstrated that the VSR-ligand interaction occurs in the ER and the GA, but not the TGN/EE and MVB/LEs (Kunzl et al., 2016). This raises the possibility that Ca^{2+} release from the endosomal lumen could promote VSR-ligand dissociation. Consistently with this notion, the GA has a relatively low Ca^{2+} concentration (700nM) (Ordenes et al., 2012) compared to the expected Ca^{2+} levels in the ER (Stael et al., 2012). Moreover, one might expect even lower Ca^{2+} levels in the TGN/EE to effect VSR-ligand dissociation. Therefore, it will be of interest to further dissect the Ca^{2+} dynamics along the endomembrane system and the underlying homeostasis mechanisms (Fig. 1). Prime candidates for endosomal Ca^{2+} homeostasis are the Ca^{2+}-ATPase ER-TYPE Ca^{2+}-ATPASE3 (ECA3) which resides in MVB/LE (Li et al., 2008a), and an uncharacterized member of the REDUCED HYPEROSMOLALITY-INDUCED [Ca(2+)]i INCREASE (OSCA)-type Ca^{2+}-permeable cation channels, whose loss of function results in missorting of vacuolar cargoes to the apoplast (Fuji et al., 2007).

Conclusions and perspectives

The flexibility of plant growth and development depends largely on its ability to integrate numerous environmental stimuli and endogenous cues. This involves a tight coupling with endomembrane trafficking as illustrated by the modulation of cellular signal transduction and transport capacities in the plasma membrane through endocytic regulation of receptors and transporters (Paciorek et al., 2005a; Robatzek et al., 2006; Sutter et al., 2007; Kasai et al., 2011; Ortiz-Morea et al., 2016). Ca^{2+} is well known as a second messenger downstream of many cellular stimuli, including those that also modify endomembrane trafficking. From the examples outlined above it is clear that Ca^{2+} is a potent regulator of endomembrane trafficking, making it tempting to speculate that Ca^{2+} connects stimulus perception to modulation of endomembrane trafficking. Thus resolving the molecular mechanisms by which Ca^{2+} controls endomembrane trafficking remains one of the major open questions in plant cell biology.

Acknowledgments

This work was funded by the Special Research Fund of Ghent University; E.H.), the Czech Science foundation (grant no. 17-27477S; R.P.) and the European Research Counsel (grant agreement number 682436 T-Rex; D.V.D)

References

Andersen, C.B., and Moestrup, S.K. (2014). How calcium makes endocytic receptors attractive. Trends Biochem. Sci. **39,** 82-90.

Bar, M., Aharon, M., Benjamin, S., Rotblat, B., Horowitz, M., and Avni, A. (2008). AtEHDs, novel Arabidopsis EH-domain-containing proteins involved in endocytosis. The Plant journal : for cell and molecular biology **55,** 1025-1038.

Baral, A., Irani, N.G., Fujimoto, M., Nakano, A., Mayor, S., and Mathew, M.K. (2015). Salt-induced remodeling of spatially restricted clathrin-independent endocytic pathways in Arabidopsis root. Plant Cell **27,** 1297-1315.

Benarroch, E.E. (2013). Synaptic vesicle exocytosis: molecular mechanisms and clinical implications. Neurology **80,** 1981-1988.

Berridge, M.J. (2006). Calcium microdomains: organization and function. Cell Calcium **40,** 405-412.

Bilkova, E., Pleskot, R., Rissanen, S., Sun, S., Czogalla, A., Cwiklik, L., Rog, T., Vattulainen, I., Cremer, P.S., Jungwirth, P., and Coskun, U. (2017). Calcium Directly Regulates Phosphatidylinositol 4,5-Bisphosphate Headgroup Conformation and Recognition. J. Am. Chem. Soc. **139,** 4019-4024.

Bloch, D., Pleskot, R., Pejchar, P., Potocky, M., Trpkosova, P., Cwiklik, L., Vukasinovic, N., Sternberg, H., Yalovsky, S., and Zarsky, V. (2016). Exocyst SEC3 and Phosphoinositides Define Sites of Exocytosis in Pollen Tube Initiation and Growth. Plant Physiol. **172,** 980-1002.

Boisson-Dernier, A., Lituiev, D.S., Nestorova, A., Franck, C.M., Thirugnanarajah, S., and Grossniklaus, U. (2013). ANXUR receptor-like kinases coordinate cell wall integrity with growth at the pollen tube tip via NADPH oxidases. PLoS Biol. **11,** e1001719.

Boudsocq, M., and Sheen, J. (2013). CDPKs in immune and stress signaling. Trends in plant science **18,** 30-40.

Burgoyne, R.D., and Clague, M.J. (2003). Calcium and calmodulin in membrane fusion. Biochim. Biophys. Acta **1641,** 137-143.

Burstenbinder, K., Moller, B., Plotner, R., Stamm, G., Hause, G., Mitra, D., and Abel, S. (2017). The IQD Family of Calmodulin-Binding Proteins Links Calcium Signaling to Microtubules, Membrane Subdomains, and the Nucleus. Plant Physiol. **173,** 1692-1708.

Burstenbinder, K., Savchenko, T., Muller, J., Adamson, A.W., Stamm, G., Kwong, R., Zipp, B.J., Dinesh, D.C., and Abel, S. (2013). Arabidopsis calmodulin-binding protein IQ67-domain 1 localizes to microtubules and interacts with kinesin light chain-related protein-1. J. Biol. Chem. **288,** 1871-1882.

Carroll, A.D., Moyen, C., Van Kesteren, P., Tooke, F., Battey, N.H., and Brownlee, C. (1998). Ca2+, annexins, and GTP modulate exocytosis from maize root cap protoplasts. The Plant cell **10,** 1267-1276.

Cocucci, E., Aguet, F., Boulant, S., and Kirchhausen, T. (2012). The first five seconds in the life of a clathrin-coated pit. Cell **150,** 495-507.

Day, I.S., Reddy, V.S., Shad Ali, G., and Reddy, A.S. (2002). Analysis of EF-hand-containing proteins in Arabidopsis. Genome Biol. **3,** RESEARCH0056.

Dejonghe, W., Kuenen, S., Mylle, E., Vasileva, M., Keech, O., Viotti, C., Swerts, J., Fendrych, M., Ortiz-Morea, F.A., Mishev, K., Delang, S., Scholl, S., Zarza, X., Heilmann, M., Kourelis, J., Kasprowicz, J., Nguyen le, S.L., Drozdzecki, A., Van Houtte, I., Szatmari, A.M., Majda, M., Baisa, G., Bednarek, S.Y., Robert, S., Audenaert, D., Testerink, C., Munnik, T., Van Damme, D., Heilmann, I., Schumacher, K., Winne, J., Friml, J., Verstreken, P., and Russinova, E. (2016). Mitochondrial uncouplers inhibit clathrin-mediated endocytosis largely through cytoplasmic acidification. Nature communications **7,** 11710.

Demuro, A., and Parker, I. (2006). Imaging single-channel calcium microdomains. Cell Calcium **40,** 413-422.

Dodd, A.N., Kudla, J., and Sanders, D. (2010). The language of calcium signaling. Annu. Rev. Plant Biol. **61,** 593-620.

Edel, K.H., and Kudla, J. (2015). Increasing complexity and versatility: how the calcium signaling toolkit was shaped during plant land colonization. Cell Calcium **57,** 231-246.

Edel, K.H., Marchadier, E., Brownlee, C., Kudla, J., and Hetherington, A.M. (2017). The Evolution of Calcium-Based Signalling in Plants. Curr. Biol. **27,** R667-R679.

Filadi, R., and Pozzan, T. (2015). Generation and functions of second messengers microdomains. Cell Calcium **58,** 405-414.

Fuji, K., Shimada, T., Takahashi, H., Tamura, K., Koumoto, Y., Utsumi, S., Nishizawa, K., Maruyama, N., and Hara-Nishimura, I. (2007). Arabidopsis vacuolar sorting mutants (green fluorescent seed) can be identified efficiently by secretion of vacuole-targeted green fluorescent protein in their seeds. Plant Cell **19,** 597-609.

Fujiwara, M., Uemura, T., Ebine, K., Nishimori, Y., Ueda, T., Nakano, A., Sato, M.H., and Fukao, Y. (2014). Interactomics of Qa-SNARE in Arabidopsis thaliana. Plant Cell Physiol. **55,** 781-789.

Gadeyne, A., Sanchez-Rodriguez, C., Vanneste, S., Di Rubbo, S., Zauber, H., Vanneste, K., Van Leene, J., De Winne, N., Eeckhout, D., Persiau, G., Van De Slijke, E., Cannoot, B., Vercruysse, L., Mayers, J.R., Adamowski, M., Kania, U., Ehrlich, M., Schweighofer, A., Ketelaar, T., Maere, S., Bednarek, S.Y., Friml, J., Gevaert, K., Witters, E., Russinova, E., Persson, S., De Jaeger, G., and Van Damme, D. (2014). The TPLATE adaptor complex drives clathrin-mediated endocytosis in plants. Cell **156,** 691-704.

Graber, Z.T., Shi, Z., and Baumgart, T. (2017). Cations induce shape remodeling of negatively charged phospholipid membranes. Phys. Chem. Chem. Phys. **19,** 15285-15295.

Hashimoto, K., and Kudla, J. (2011). Calcium decoding mechanisms in plants. Biochimie **93,** 2054-2059.

Heard, W., Sklenar, J., Tome, D.F., Robatzek, S., and Jones, A.M. (2015). Identification of Regulatory and Cargo Proteins of Endosomal and Secretory Pathways in Arabidopsis thaliana by Proteomic Dissection. Mol. Cell. Proteomics **14,** 1796-1813.

Hepler, P.K. (2016). The Cytoskeleton and Its Regulation by Calcium and Protons. Plant Physiol. **170,** 3-22.

Himschoot, E., Beeckman, T., Friml, J., and Vanneste, S. (2015). Calcium is an organizer of cell polarity in plants. Bba-Mol Cell Res **1853,** 2168-2172.

Huh, S.M., Noh, E.K., Kim, H.G., Jeon, B.W., Bae, K., Hu, H.C., Kwak, J.M., and Park, O.K. (2010). Arabidopsis annexins AnnAt1 and AnnAt4 interact with each other and regulate drought and salt stress responses. Plant Cell Physiol. **51,** 1499-1514.

Ischebeck, T., Werner, S., Krishnamoorthy, P., Lerche, J., Meijon, M., Stenzel, I., Lofke, C., Wiessner, T., Im, Y.J., Perera, I.Y., Iven, T., Feussner, I., Busch, W., Boss, W.F., Teichmann, T., Hause, B., Persson, S., and Heilmann, I. (2013). Phosphatidylinositol 4,5-bisphosphate influences PIN polarization by controlling clathrin-mediated membrane trafficking in Arabidopsis. The Plant cell **25,** 4894-4911.

Jean, S., Mikryukov, A., Tremblay, M.G., Baril, J., Guillou, F., Bellenfant, S., and Moss, T. (2010). Extended-synaptotagmin-2 mediates FGF receptor endocytosis and ERK activation in vivo. Dev. Cell **19,** 426-439.

Kasai, K., Takano, J., Miwa, K., Toyoda, A., and Fujiwara, T. (2011). High boron-induced ubiquitination regulates vacuolar sorting of the BOR1 borate transporter in Arabidopsis thaliana. J. Biol. Chem. **286,** 6175-6183.

Kooijman, E.E., Carter, K.M., van Laar, E.G., Chupin, V., Burger, K.N.J., and de Kruijff, B. (2005). What makes the bioactive lipids phosphatidic acid and lysophosphatidic acid so special? Biochemistry **44,** 17007-17015.

Kunzl, F., Fruholz, S., Fassler, F., Li, B., and Pimpl, P. (2016). Receptor-mediated sorting of soluble vacuolar proteins ends at the trans-Golgi network/early endosome. Nat Plants **2,** 16017.

Laohavisit, A., and Davies, J.M. (2011). Annexins. New Phytol **189,** 40-53.

Lewis, J.D., and Lazarowitz, S.G. (2010). Arabidopsis synaptotagmin SYTA regulates endocytosis and virus movement protein cell-to-cell transport. Proc. Natl. Acad. Sci. U. S. A. **107,** 2491-2496.

Li, X., Chanroj, S., Wu, Z., Romanowsky, S.M., Harper, J.F., and Sze, H. (2008). A distinct endosomal Ca2+/Mn2+ pump affects root growth through the secretory process. Plant Physiol. **147,** 1675-1689.

Luo, Y., Scholl, S., Doering, A., Zhang, Y., Irani, N.G., Di Rubbo, S., Neumetzler, L., Krishnamoorthy, P., Van Houtte, I., Mylle, E., Bischoff, V., Vernhettes, S., Winne, J., Friml, J., Stierhof, Y.D., Schumacher, K., Persson, S., and Russinova, E. (2015). V-ATPase activity in the TGN/EE is required for exocytosis and recycling in Arabidopsis. Nat Plants **1,** 15094.

Magarkar, A., Jurkiewicz, P., Allolio, C., Hof, M., and Jungwirth, P. (2017). Increased Binding of Calcium Ions at Positively Curved Phospholipid Membranes. J. Phys. Chem. Lett. **8,** 518-523.

Marchadier, E., Oates, M.E., Fang, H., Donoghue, P.C., Hetherington, A.M., and Gough, J. (2016). Evolution of the Calcium-Based Intracellular Signaling System. Genome Biol. Evol. **8,** 2118-2132.

Mclaughlin, S., Mulrine, N., Gresalfi, T., Vaio, G., and Mclaughlin, A. (1981). Adsorption of Divalent-Cations to Bilayer-Membranes Containing Phosphatidylserine. J. Gen. Physiol. **77,** 445-473.

Meckel, T., Gall, L., Semrau, S., Homann, U., and Thiel, G. (2007). Guard cells elongate: relationship of volume and surface area during stomatal movement. Biophys. J. **92,** 1072-1080.

Melcrova, A., Pokorna, S., Pullanchery, S., Kohagen, M., Jurkiewicz, P., Hof, M., Jungwirth, P., Cremer, P.S., and Cwiklik, L. (2016). The complex nature of calcium cation interactions with phospholipid bilayers. Sci. Rep. **6,** 38035.

Milovanovic, D., Platen, M., Junius, M., Diederichsen, U., Schaap, I.A.T., Honigmann, A., Jahn, R., and van den Bogaart, G. (2016). Calcium Promotes the Formation of Syntaxin 1 Mesoscale Domains through Phosphatidylinositol 4,5-Bisphosphate. J. Biol. Chem. **291,** 7868-7876.

Ordenes, V.R., Moreno, I., Maturana, D., Norambuena, L., Trewavas, A.J., and Orellana, A. (2012). In vivo analysis of the calcium signature in the plant Golgi apparatus reveals unique dynamics. Cell Calcium **52,** 397-404.

Ortiz-Morea, F.A., Savatin, D.V., Dejonghe, W., Kumar, R., Luo, Y., Adamowski, M., Van den Begin, J., Dressano, K., Pereira de Oliveira, G., Zhao, X., Lu, Q., Madder, A., Friml, J., Scherer de Moura, D., and Russinova, E. (2016). Danger-associated peptide signaling in Arabidopsis requires clathrin. Proc. Natl. Acad. Sci. U. S. A. **113,** 11028-11033.

Paciorek, T., Zazimalova, E., Ruthardt, N., Petrasek, J., Stierhof, Y.D., Kleine-Vehn, J., Morris, D.A., Emans, N., Jurgens, G., Geldner, N., and Friml, J. (2005). Auxin inhibits endocytosis and promotes its own efflux from cells. Nature **435,** 1251-1256.

Perez-Sancho, J., Vanneste, S., Lee, E., McFarlane, H.E., Esteban Del Valle, A., Valpuesta, V., Friml, J., Botella, M.A., and Rosado, A. (2015). The Arabidopsis synaptotagmin1 is enriched in endoplasmic reticulum-plasma membrane contact sites and confers cellular resistance to mechanical stresses. Plant Physiol. **168,** 132-143.

Pleskot, R., Pejchar, P., Staiger, C.J., and Potocky, M. (2014). When fat is not bad: the regulation of actin dynamics by phospholipid signaling molecules. Front Plant Sci **5,** 5.

Pleskot, R., Li, J., Zarsky, V., Potocky, M., and Staiger, C.J. (2013). Regulation of cytoskeletal dynamics by phospholipase D and phosphatidic acid. Trends in plant science **18,** 496-504.

Pou, A., Jeanguenin, L., Milhiet, T., Batoko, H., Chaumont, F., and Hachez, C. (2016). Salinity-mediated transcriptional and post-translational regulation of the Arabidopsis aquaporin PIP2;7. Plant Mol. Biol. **92,** 731-744.

Robatzek, S., Chinchilla, D., and Boller, T. (2006). Ligand-induced endocytosis of the pattern recognition receptor FLS2 in Arabidopsis. Genes Dev. **20,** 537-542.

Ruge, H., Flosdorff, S., Ebersberger, I., Chigri, F., and Vothknecht, U.C. (2016). The calmodulin-like proteins AtCML4 and AtCML5 are single-pass membrane proteins targeted to the endomembrane system by an N-terminal signal anchor sequence. Journal of experimental botany **67,** 3985-3996.

Sanmartin, M., Ordonez, A., Sohn, E.J., Robert, S., Sanchez-Serrano, J.J., Surpin, M.A., Raikhel, N.V., and Rojo, E. (2007). Divergent functions of VTI12 and VTI11 in trafficking to storage and lytic vacuoles in Arabidopsis. Proc. Natl. Acad. Sci. U. S. A. **104,** 3645-3650.

Schapire, A.L., Voigt, B., Jasik, J., Rosado, A., Lopez-Cobollo, R., Menzel, D., Salinas, J., Mancuso, S., Valpuesta, V., Baluska, F., and Botella, M.A. (2008). Arabidopsis synaptotagmin 1 is required for the maintenance of plasma membrane integrity and cell viability. Plant Cell **20,** 3374-3388.

Scheuring, D., Viotti, C., Kruger, F., Kunzl, F., Sturm, S., Bubeck, J., Hillmer, S., Frigerio, L., Robinson, D.G., Pimpl, P., and Schumacher, K. (2011). Multivesicular bodies mature from the trans-Golgi network/early endosome in Arabidopsis. Plant Cell **23,** 3463-3481.

Shimada, T., Fuji, K., Tamura, K., Kondo, M., Nishimura, M., and Hara-Nishimura, I. (2003). Vacuolar sorting receptor for seed storage proteins in Arabidopsis thaliana. Proc. Natl. Acad. Sci. U. S. A. **100,** 16095-16100.

Shin, J.J., and Loewen, C.J. (2011). Putting the pH into phosphatidic acid signaling. BMC Biol. **9,** 85.

Shope, J.C., DeWald, D.B., and Mott, K.A. (2003). Changes in surface area of intact guard cells are correlated with membrane internalization. Plant Physiol. **133,** 1314-1321.

Simon, M.L., Platre, M.P., Marques-Bueno, M.M., Armengot, L., Stanislas, T., Bayle, V., Caillaud, M.C., and Jaillais, Y. (2016). A PtdIns(4)P-driven electrostatic field controls cell membrane identity and signalling in plants. Nat Plants **2,** 16089.

Simon, M.L., Platre, M.P., Assil, S., van Wijk, R., Chen, W.Y., Chory, J., Dreux, M., Munnik, T., and Jaillais, Y. (2014). A multi-colour/multi-affinity marker set to visualize phosphoinositide dynamics in Arabidopsis. Plant J. **77,** 322-337.

Slochower, D.R., Wang, Y.H., Tourdot, R.W., Radhakrishnan, R., and Janmey, P.A. (2014). Counterion-mediated pattern formation in membranes containing anionic lipids. Adv. Colloid Interface Sci. **208,** 177-188.

Sohn, E.J., Rojas-Pierce, M., Pan, S., Carter, C., Serrano-Mislata, A., Madueno, F., Rojo, E., Surpin, M., and Raikhel, N.V. (2007). The shoot meristem identity gene TFL1 is involved in flower development and trafficking to the protein storage vacuole. Proc. Natl. Acad. Sci. U. S. A. **104,** 18801-18806.

Stael, S., Wurzinger, B., Mair, A., Mehlmer, N., Vothknecht, U.C., and Teige, M. (2012). Plant organellar calcium signalling: an emerging field. Journal of experimental botany **63,** 1525-1542.

Sutter, J.U., Sieben, C., Hartel, A., Eisenach, C., Thiel, G., and Blatt, M.R. (2007). Abscisic acid triggers the endocytosis of the arabidopsis KAT1 K+ channel and its recycling to the plasma membrane. Curr. Biol. **17,** 1396-1402.

Tejos, R., Sauer, M., Vanneste, S., Palacios-Gomez, M., Li, H., Heilmann, M., van Wijk, R., Vermeer, J.E., Heilmann, I., Munnik, T., and Friml, J. (2014). Bipolar Plasma Membrane Distribution of Phosphoinositides and Their Requirement for Auxin-Mediated Cell Polarity and Patterning in Arabidopsis. The Plant cell **26,** 2114-2128.

Tsai, H.H., Juang, W.F., Chang, C.M., Hou, T.Y., and Lee, J.B. (2013). Molecular mechanism of Ca(2+)-catalyzed fusion of phospholipid micelles. Biochim. Biophys. Acta **1828,** 2729-2738.

Van Damme, D., Gadeyne, A., Vanstraelen, M., Inze, D., Van Montagu, M.C., De Jaeger, G., Russinova, E., and Geelen, D. (2011). Adaptin-like protein TPLATE and clathrin recruitment during plant somatic cytokinesis occurs via two distinct pathways. Proc. Natl. Acad. Sci. U. S. A. **108,** 615-620.

Wang, Y.H., Slochower, D.R., and Janmey, P.A. (2014). Counterion-mediated cluster formation by polyphosphoinositides. Chem. Phys. Lipids **182,** 38-51.

Watanabe, E., Shimada, T., Kuroyanagi, M., Nishimura, M., and Hara-Nishimura, I. (2002). Calcium-mediated association of a putative vacuolar sorting receptor PV72 with a propeptide of 2S albumin. J. Biol. Chem. **277,** 8708-8715.

Yadav, D., Ahmed, I., Shukla, P., Boyidi, P., and Kirti, P.B. (2016). Overexpression of Arabidopsis AnnAt8 Alleviates Abiotic Stress in Transgenic Arabidopsis and Tobacco. Plants (Basel) **5**.

Yamashita, M., Kurokawa, K., Sato, Y., Yamagata, A., Mimura, H., Yoshikawa, A., Sato, K., Nakano, A., and Fukai, S. (2010). Structural basis for the Rho- and phosphoinositide-dependent localization of the exocyst subunit Sec3. Nat. Struct. Mol. Biol. **17,** 180-186.

Yamazaki, T., Kawamura, Y., Minami, A., and Uemura, M. (2008). Calcium-dependent freezing tolerance in Arabidopsis involves membrane resealing via synaptotagmin SYT1. The Plant cell **20,** 3389-3404.

Young, B.P., Shin, J.J., Orij, R., Chao, J.T., Li, S.C., Guan, X.L., Khong, A., Jan, E., Wenk, M.R., Prinz, W.A., Smits, G.J., and Loewen, C.J. (2010). Phosphatidic acid is a pH biosensor that links membrane biogenesis to metabolism. Science **329,** 1085-1088.

Zhu, J., Wu, X., Yuan, S., Qian, D., Nan, Q., An, L., and Xiang, Y. (2014). Annexin5 plays a vital role in Arabidopsis pollen development via Ca2+-dependent membrane trafficking. PLoS One **9,** e102407.

Zwiewka, M., Nodzynski, T., Robert, S., Vanneste, S., and Friml, J. (2015). Osmotic Stress Modulates the Balance between Exocytosis and Clathrin-Mediated Endocytosis in Arabidopsis thaliana. Mol Plant **8,** 1175-1187.

SECTION II. RESULTS

Chapter 1:
Calcium ion dynamics in roots: imaging and analysis

Ellie Himschoot[1,2], Melanie Krebs[3], Alex Costa[4], Tom Beeckman[1,2], Steffen Vanneste[1,2]

[1] Ghent University, Department of Plant Biotechnology and Bioinformatics, 9052 Ghent, Belgium
[2] VIB Center for Plant Systems Biology, 9052 Ghent, Belgium
[3] Centre for Organismal Studies, Plant Developmental Biology, University of Heidelberg, 69120 Heidelberg, Germany
[4] Department of Biosciences, University of Milan, 20133 Milan, Italy

Adapted from:
Ellie Himschoot[1,2], Melanie Krebs[3], Alex Costa[4], Tom Beeckman[1,2], Steffen Vanneste[1,2]. *Calcium ion dynamics in roots: imaging and analysis.* Methods in Molecular Biology 2017

Author contribution:
E.H. is the main author of this chapter. E.H. performed the experiments described in the chapter, and made the designs for the imaging chamber and the MATLAB script for image analysis. A.C. and M.K. provided guidance for execution of the experiments. A.C, M.K., T.B and S.V. contributed to the writing and revision of the manuscript.

Abstract

Calcium sensors are indispensable tools to study the role of Ca^{2+} and visualize Ca^{2+} dynamics during biological processes. Over the past years, the field of Ca^{2+} imaging has strongly expanded by the development of a wide palette of sensors and optimization of sample handling. Here, we provide guidelines for imaging of the Ca^{2+} sensor R-GECO1 in *Arabidopsis thaliana* roots which can be interpolated to other intensiometric Ca^{2+} sensors. Furthermore, we demonstrate a procedure for image analysis of the acquired time-lapse recordings. Finally, the protocol was used to determine the dose-response of Ca^{2+} signals amplitude of roots treated with different concentrations of the synthetic auxin NAA. Moreover, we demonstrate the impact of reduced extracellular Ca^{2+} availability on the overall amplitude of the NAA-induced Ca^{2+} signal. The resulting data are in turn important in the context of Chapter 2 (Section II – Chapter 2), where we address the functional relevance of auxin-induced Ca^{2+} for regulation of clathrin-mediated endocytosis.

1. Introduction

Calcium is an important second messenger regulating a wide range of developmental processes and environmental responses in plants and animals (Rudd and Franklin-Tong, 1999; Sanders et al., 1999; Knight and Knight, 2001; Sanders et al., 2002a; Scrase-Field and Knight, 2003; Clapham, 2007). Typically, the resting Ca^{2+} concentration in the cytoplasm is kept low, around 100-200nM, while the Ca^{2+} concentration in the organelles and extracellular space is several orders of magnitude higher (reviewed in Himschoot et al., 2017). This steep concentration gradient allows to generate rapid cytoplasmic Ca^{2+} signals by opening only a few Ca^{2+} channels. After a stimulus-induced cytosolic Ca^{2+} increase, the cytoplasmic Ca^{2+} levels are rapidly restored to the resting status. Based on the amplitude and duration of the Ca^{2+} signals, specific Ca^{2+} signatures can be defined for distinct cellular processes. Therefore, to investigate the role of Ca^{2+} in biological processes, it is critical to be able to capture accurately and with high resolution the distinct Ca^{2+} signatures. Given that Ca^{2+} is a bivalent ion, rather than a protein, its dynamics cannot be visualized using standard molecular biology approaches such as translational reporters. Instead, the visualization of Ca^{2+} is commonly done indirectly, based on the change in physical properties of dyes or genetically encoded Ca^{2+} indicators

(GECIs) upon binding of Ca^{2+}. The rapid loading, sensitivity and broad dynamic range makes fluorescent dyes highly attractive to study Ca^{2+} dynamics. This explains why, to date, multiple Ca^{2+}-sensitive dyes, such as Fura-2, are still commonly used to capture dynamic Ca^{2+} signatures in animal cells (Homma et al., 2009; Kettunen, 2012; Dolenšek et al., 2015). However, such dyes have never been commonly used in plants, mainly due to technical difficulties to load the dyes uniformly into the plant tissues and the requirement of specimen manipulations which can introduce artefacts. In contrast, the plant field has benefited a lot from a wide range of GECI which have the key advantage that they can be expressed both in specific tissues and in the entire plant. Moreover, they can be targeted to distinct subcellular compartments to dissect the mechanisms of Ca^{2+} signaling at the organelle level (Krebs et al., 2012; Mehlmer et al., 2012; Bonza et al., 2013; Loro and Costa, 2013).

The GECIs can be subdivided in the chemiluminescence- and fluorescence-based indicators. A frequently used chemiluminescent Ca^{2+} indicator is based on aequorin. This Ca^{2+} binding photoprotein naturally occurs in the jellyfish *Aequorea victoria* and consists of the enzyme apoaequorin and the luminophore coelenterazine (Knight, 1991; Shimomura et al., 1993; Shimomura, 1995). Oxidation of coelenterazine by apoaequorin upon Ca^{2+} binding results in emission of light. For Ca^{2+} imaging, the recombinant apoaequorin is expressed in the seedlings and the substrate coelenterazine is loaded into the cells to visualize Ca^{2+} dynamics. One of the downfalls of chemiluminescent Ca^{2+} indicators is their limited spatial resolution and rather low light emission levels (quantum yield) (Creton et al., 1999). Recent advances in probe optimization have led to the development of the luciferases Nano-latern(Ca^{2+}) (Saito et al., 2012; Takai et al., 2014) and NanoLuc (Hall et al., 2012) having respectively a 20- and 100 to 150-fold increase in brightness resulting in a higher signal-to-noise ratio and improved spatial resolution. Most of the chemiluminescent probes are not ratiometric and do not allow correcting for sample drift and differences in expression levels of the probe. Therefore, ratiometric bioluminescence resonance energy transfer (BRET)-based chemiluminescent sensors such as CALcium FLUX composed of Venus, Troponin and NanoLuc (CalfluxVTN) have been developed (Yang et al., 2016). This probe combines the bright NanoLuc luciferase with a truncated Venus fluorophore, interconnected by linkers and the Ca^{2+} binding protein Troponin C (Tn C). As a substrate, NanoLuc uses furimazine which is less autoluminescent than the typical coelenterazine thereby further improving the signal-to-noise ratio (Hall et al., 2012).

Upon addition of the substrate and in the presence of Ca^{2+}, Ca^{2+} binding to Tn C results in a conformational change bringing NanoLuc and Venus in closer proximity. Consequently, the light released upon NanoLuc-mediated oxidation of furimazine results in BRET-based excitation of Venus, and the ratio of Venus emission over NanoLuc emission reflects the Ca^{2+} dynamics. Unfortunately, these optimized probes have not yet been used in plants, and the need for coelenterazine loading into the cells and tissues, the low light emission and limited cellular resolution of aequorin have prompted the development of fluorescence-based sensors.

Among the fluorescence-based Ca^{2+} sensors, ratiometric and intensiometric sensors can be distinguished. The ratiometric sensors are usually based on Ca^{2+}-dependent Förster resonance energy transfer (FRET), in which a donor and acceptor fluorophore (e.g. CFP-YFP) are interconnected by a Ca^{2+}-controlled interaction module (e.g. CALMODULIN (CaM) and CaM-binding peptide M13). Upon Ca^{2+} sensing, the interaction module induces a conformational change thereby bringing both fluorophores in closer proximity allowing FRET. This FRET causes a simultaneous increase in acceptor fluorescence and decreased donor fluorescence resulting in an increased ratio of acceptor emission/donor emission which can be imaged using confocal microscopy. A great advantage of the ratiometric character of such sensor is that it allows to assess Ca^{2+} dynamics independently of the expression levels and correct for changes of focus. However, ratiometric sensors have a limited dynamic range. Intensiometric sensors are based on enhancement or decrement in fluorescence of a single fluorophore depending on the Ca^{2+}-controlled interaction module. In this case, Ca^{2+} binding leads to a (de)stabilization of the fluorophore, and thus correspondingly an increase or decrease of brightness. These sensors generally have a relatively high dynamic range, and have fast on-off kinetics, but do not allow to correct for differences in expression levels. Multiple intensiometric probes such as the green fluorescent GCaMP series (Allen et al., 1999; Denninger et al., 2014) and GECOs with different spectral properties and sensitivities (Zhao et al., 2011; Zhao et al., 2014; Podor et al., 2015) have been developed over the past years, and are continuously being improved. Recently the red fluorescent R-GECO1 (Fig. 1) (*in planta* dissociation constant (K_d) = 158nM, (Waadt et al., 2017)) and the green fluorescent GCaMP6s (*in vitro* K_d = 144nM, (Chen et al., 2013)), and derivatives thereof have been described as very sensitive probes for monitoring Ca^{2+} dynamics in *A. thaliana* (Keinath et al., 2015; Liu et al., 2017; Waadt et al., 2017).

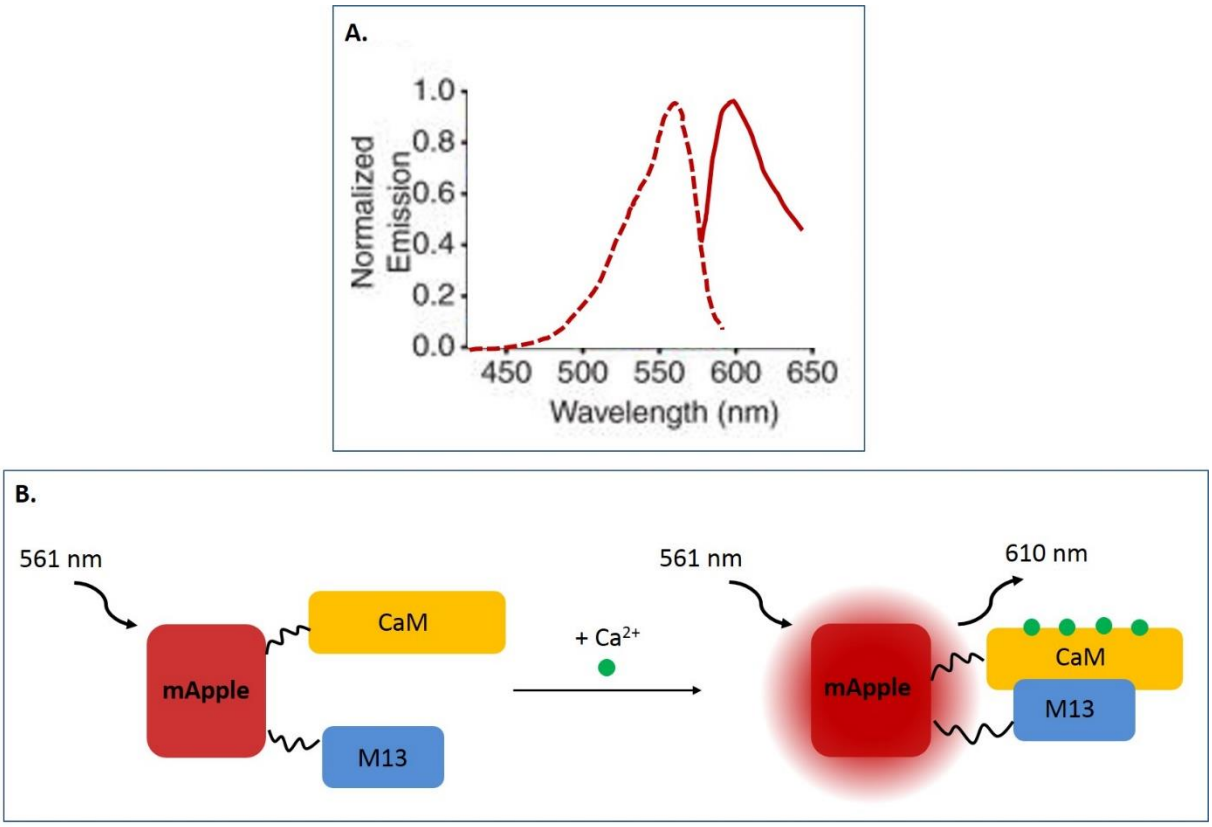

Figure 1: R-GECO1 spectral properties and mode of action. (A) Spectral properties of R-GECO1 with the excitation (dotted line) and emission (full line) spectrum (modified from Zhao et al., 2011). (B) Simplified schematic representation of the mode of action of the intensiometric R-GECO1 Ca2+ sensor. R-GECO1 consists of the mApple red fluorescent protein, the Ca2+ binding protein calmodulin (CaM), and the CaM binding M13 peptide. Binding of Ca2+ ions to CaM induces an intramolecular conformational change resulting in increased fluorescence intensity of mApple upon R-GECO1 excitation with 561 nm light.

Our main interest is to study Ca^{2+} dynamics upon treatment with the plant hormone auxin. Many publications have already demonstrated a rapid and transient increase in cytosolic Ca^{2+} concentrations upon treatment with the natural auxin indole-5-acetic acid (IAA) and synthetic auxin **1**-naphthaleneacetic acid (NAA) in different species and tissues (Gehring et al., 1990; Irving et al., 1992; Ayling et al., 1994; Shishova and Lindberg, 2004, 2010; Monshausen et al., 2011; Waadt et al., 2017). However, we are interested in the impact of the synthetic auxin NAA, which is frequently used in experimental set-ups, as it is more stable than IAA, on Ca^{2+} dynamics in roots of Arabidopsis seedlings. The auxin-induced cytosolic Ca^{2+} increase takes place in a matter of seconds (Shishova and Lindberg, 2004), which makes it experimentally challenging to capture this event. Therefore, we made a customized imaging chamber based on a design developed in the Schumacher lab (Krebs and Schumacher, 2013) which facilitates image acquisition for real-time recording of Ca^{2+} dynamics during treatment while minimizing

sample drift. Here, we provide guidelines for image acquisition of the intensiometric R-GECO1 sensor, which also apply to other intensiometric Ca^{2+} sensors. In addition, we provide a 2D- and 3D design for the imaging chamber and present a method for image analysis using Fiji (manual) and MATLAB (script). Finally, I have included data on auxin-induced Ca^{2+} dynamics in Arabidopsis roots using this set-up to illustrate some expected outcomes, when using this set-up.

2. Materials

1. Seed sterilization

- Eppendorf tubes (2 mL)
- Desiccator in fume hood
- Sterilization solution: 5mL concentrated HCl (37%), 100mL NaClO (13%)

2. Growth medium (0.5x MS)

- For preparation of 1 L growth medium weigh 10 g sucrose, 2.3 g MS salts, 0.5 g MES
- Dissolve in +/-950 mL MilliQ
- Adjust pH to 5.7 using KOH
- Add MilliQ up to 1 L
- Add 8 g of agar and mix well before autoclaving

3. Plant growth and sample preparation

- Growth medium (see 2.)
- Square sterile plates (e.g. Greiner Bio-One, 12/12/17mm, item No. 688161)
- Sterile tooth picks
- Epifluorescence binocular with a suitable filter (e.g. an RFP filter for R-GECO1)

4. Imaging medium (minimal medium)

- For preparation of 1 L growth medium weigh 2,132 g MES, 0,372 g KCl, 1,11 g $CaCl_2$
- Dissolve in +/-950 mL MilliQ
- Adjust pH to 5.7 using KOH
- Add MilliQ up to 1L

5. Imaging chamber

We use a customized imaging chamber (based on the imaging incubation chamber shown in (Krebs and Schumacher, 2013)) suited for imaging on an inverted microscope. The design of the chamber allows to apply treatments during imaging while minimizing sample drift. Here we provide a 2D- and 3D design for fabrication of the chamber by milling/cutting or 3D printing depending on the available equipment (see Notes 1.). The designs are made available through the following link: https://www.psb.ugent.be/docs/himschoot-et-al-2017-calcium-ion-dynamics-in-roots-chamber-designs-and-matlab-script. The required components for assembly of the chamber are listed below.

- Customized imaging chamber with lid (see 2D, 3D design)
- Petri dish (e.g. Greiner Bio-One, 35/10mm, item No. 627161)
- Low viscous silicon paste (e.g. GE Bayer Baysilone from VWR, catalog No. 291-1210) and swab
- Round cover glasses diameter 24 mm, thickness 1 (e.g. from neoLab, item No. 1-6290)
- Chemically pure glass wool (e.g. from Roth, item No. 7377.2)
- 2 M3 x 5mm screws + 2 washers with outer diameter 15mm and inner diameter 4mm (e.g. from Farnell, order code 1420120 and 2426053 respectively)

6. A Widefield Microscope (WM), Confocal Laser Scanning Microscope (CLSM) or Spinning Disk Microscope (SDM)

The procedures described can be applied to any inverted WM, CLSM or SDM.

7. Fiji

Fiji (Fiji Is Just ImageJ) is an open-source image processing package based on ImageJ (Schindelin et al., 2012). The described procedures for image analysis with Fiji can be implemented using any version of Fiji. It is freely available from https://imagej.net/Fiji/Downloads.

8. MATLAB

MATLAB (matrix laboratory) is a multi-paradigm numerical computing environment which is popular among scientists for image processing. A script for image analysis *intensiometric_Ca_imaging.m* is provided under the following link: https://www.psb.ugent.be/docs/himschoot-et-al-2017-calcium-ion-dynamics-in-roots-chamber-designs-and-matlab-script. It was developed in MATLAB 2013a and is compatible with this and more recent MATLAB releases. In contrast to Fiji, it is not available for free and a license is required. In case no MATLAB license is available, a free product trial can be requested on www.mathworks.com.

3. Methods

3.1 Seed sterilization using chlorine gas

1. Put the desired seeds into 2 mL Eppendorf tubes (the recommended amount of seeds is approx. 50 µL) and place the seeds into the desiccator in the fume hood.

2. Add 5 mL of concentrated HCl (37%) and 100 mL 13% NaClO into the desiccator, close the desiccator immediately and incubate the seeds with developed chloral gas for at least 3hrs or overnight.

3. Let the majority of the toxic chloral gas escape from the desiccator in the fume hood. Close the tubes and transfer them to the laminar flow to air out the remnant chloral gas for 15 min.

3.2 Plant growth

1. Square sterile plates for *in vitro* growth are filled with 50 mL growth medium (0.5x MS) with agar.

2. Place the seeds using a sterile tooth pick on the solidified medium. Ensure that the seeds are not too close to one another (+/- 0.5 cm). This will facilitate screening for seedlings with good expression levels later on.

3. After sowing, the plates are transferred to the cold room (4°C, dark) for 1 day vernalization.

4. Transfer the plates to the growth chamber (21°C, continuous light) for 4-5 days.

3.3 Imaging chamber assembly and sample preparation (Fig. 2)

1. Before preparing the samples it is advised to check the seedlings for good expression levels of the sensor. This can be done using an epifluorescence binocular with a suitable filter.

2. Apply a small amount of silicon paste on the rim of the base of the chamber using a swab and mount a round cover glass. The silicon paste will seal the chamber and prevent leakage.

3. Put a seedling in a small Petri dish filled with liquid minimal medium for a few seconds to hydrate the seedling and prevent it from drying out. Transfer the seedling to the center of the cover glass and cover it with a thin layer of glass wool. The glass wool will reduce seedling drift during treatment. Add 200 µL minimal medium to the chamber. It is crucial to perform these operations quickly to avoid the seedling would dry out.

4. Mount the top lid, with the opening parallel to the seedling, and mount the M3 screws with washers. The washer will hold down the top lid.

5. Let the mounted seedling recover for about 30 min before initiating the Ca^{2+} imaging. The mechanostimulation of the seedlings during sample preparation may render the seedlings less responsive to subsequent stimuli. See Notes, 2.

6. Prepare the solution for treatment in 100 µL minimal medium. Ensure the compound concentration is three times higher than the desired end-concentration. See Notes, 3.

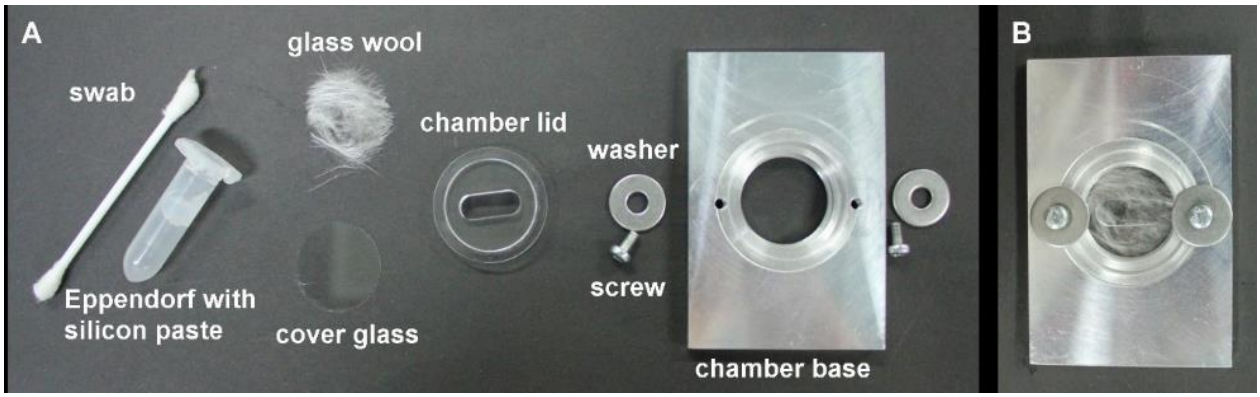

Figure 2: Imaging chamber assembly. A) The imaging chamber components. B) Assembled imaging chamber.

3.3 Ca^{2+} Imaging

The data processing procedure is compatible with widefield microscope (WM), confocal laser scanning microscope (CLSM) and spinning disk microscope (SDM) image acquisition. The main difference between WM and CLSM or SDM is the lack of optical sectioning thereby not only capturing fluorescence from the focal plane, but also out-of-focus light which affects the resolution of the image. A WM typically uses a fluorescent lamp as an excitation source, while a CLSM and SDM are equipped with lasers. The main difference between CLSM and SDM is the method of scanning the sample. In case of CLSM, a point-by-point illumination is used, while in SDM multiple points are illuminated simultaneously, thereby speeding up image acquisition, which can be important to capture very fast Ca^{2+} kinetics. The WM also allows for fast image acquisition. Most steps described below apply to WM, CLSM and SDM set-ups; where differences occur the guidelines will be described for both devices separately.

R-GECO1 is an intensiometric Ca^{2+} sensor, meaning that an increase in fluorescence intensity reflects an increase in Ca^{2+} levels in a single emission channel (Zhao et al., 2011). As it is a red-shifted Ca^{2+} indicator, it can be excited by 561 nm wave-length and emission light can be captured in a range of 620 nm to 650 nm wave-length.

1. Select an objective (see Notes 4.) and set the desired image resolution (e.g. 512 x 512) and bit depth (e.g. 16 bit).

2. Mount the imaging chamber on the stage, position the root tip in the center of the field of view (see Notes 5.), and focus on the root tip.

3. Set the percentage of laser, the pinhole size in case of CLSM, detector gain, and offset to minimize photo bleaching during a time-lapse recording and use the full dynamic range of the detector. The maximal Ca^{2+} signal should not result in pixel saturation, and the background should be close to the detector noise levels for optimal semi-quantitative assessment of Ca^{2+} dynamics in the sample. Therefore, it is advised to perform a test experiment to estimate the extent of fluorescence intensity increase which can be expected, and adjust the settings accordingly.

4. For detection of the signal, microscopes can be equipped with photomultiplier tubes (e.g. CLSM) or (CCD) cameras (e.g. SDM). In case of a camera detector, it is required to set the

exposure time during which the sample is illuminated and fluorescence will be collected by the camera. High laser power combined with long exposure times can cause photobleaching.

5. Set up the time lapse recording (Notes 6.). Time series are recorded by collecting a scan every 3-5 sec. If higher temporal resolution is required, the frame rate can be increased. For very fast data acquisition the SDM is preferred. However, increasing the frame rate will result in more frequent scanning of the sample and possible photobleaching.

6. Start the time lapse recording. Allow the fluorescence level to stabilize (3-5 min) before applying a treatment.

7. Pause the time lapse, write down the frame number, apply the treatment, and resume the recording. Use 100 µL minimal medium supplemented with the 3x concentrated treatment (after addition, the end volume in the imaging chamber will be 300 µl, thereby diluting the treatment to 1x). The frame number will be important for normalization during image analysis of the data (see Notes 7.). In the case of a compound-induced Ca^{2+} increase, the fluorescence levels will increase.

8. Save the time lapse recording. For image analysis the procedures for Fiji and MATLAB are described. It is therefore important that the file format used for saving the time lapse recording is compatible with either program. A wide range of file formats can be opened and processed in Fiji (.lsm, .tiff, .ometiff, …). In case of MATLAB, the number of file formats is more limited (e.g. .lsm cannot be processed by the provided MATLAB script). It is advised to use .tiff or .ometiff files. (see Notes 8.)

3.4 Image analysis:

Here, the fluorescence intensity dynamics will be analyzed for multiple regions of interest. Analysis of these plots will allow to identify the maximal amplitude, duration, onset,… of a Ca^{2+} response upon treatment. The procedure consists of 5 major steps: 1) image registration, 2) measurement of the background levels, 3) measurement of the fluorescence intensity in a selected ROI, 4) background subtraction, and 5) normalization of the background-corrected fluorescence intensities to the initial fluorescence intensity (see Notes 7.). These operations can be performed using different image processing software packages. Here, we provide the

guidelines for manual image analysis in Fiji and a MATLAB script to automate part of the image analysis.

3.4.1 Fiji (Fig. 3)

1. Open the time lapse recording by selecting 'File' > 'Open…'.

2. Perform image registration. In case of movement/drift of the root during the time lapse recording, it is essential to perform an image registration step to align the different frames. This is to avoid that the area of interest would move over time and would no longer be contained within the marked ROI.

To perform intensity-based image registration use the StackReg plugin in Fiji (Thevenaz et al., 1998). Go to 'Plugins' > 'Registration' > 'StackReg'. In case the plugin is not available it can be downloaded here: http://bigwww.epfl.ch/thevenaz/stackreg/. Select a transformation method depending on the type of movement the root makes over time. The transformation methods are Translation, Rigid Body (translation + rotation), Scaled Rotation (translation + rotation + scaling), Affine (more complex movement). In case of root movement due to growth or drift, translation is usually sufficient for proper image alignment.

3. Define a region for background measurement and regions of interest (ROIs). To mark a region use a selection tool of choice (e.g. a polygon) in the toolbar. After drawing the region, it can be saved by going to 'Edit' > 'Selection' > 'Add to Manager'. The region for background measurement should be drawn outside of the root (Fig. 3). Multiple ROIs can be drawn at positions of choice. The number of ROIs is referred to as *n*.

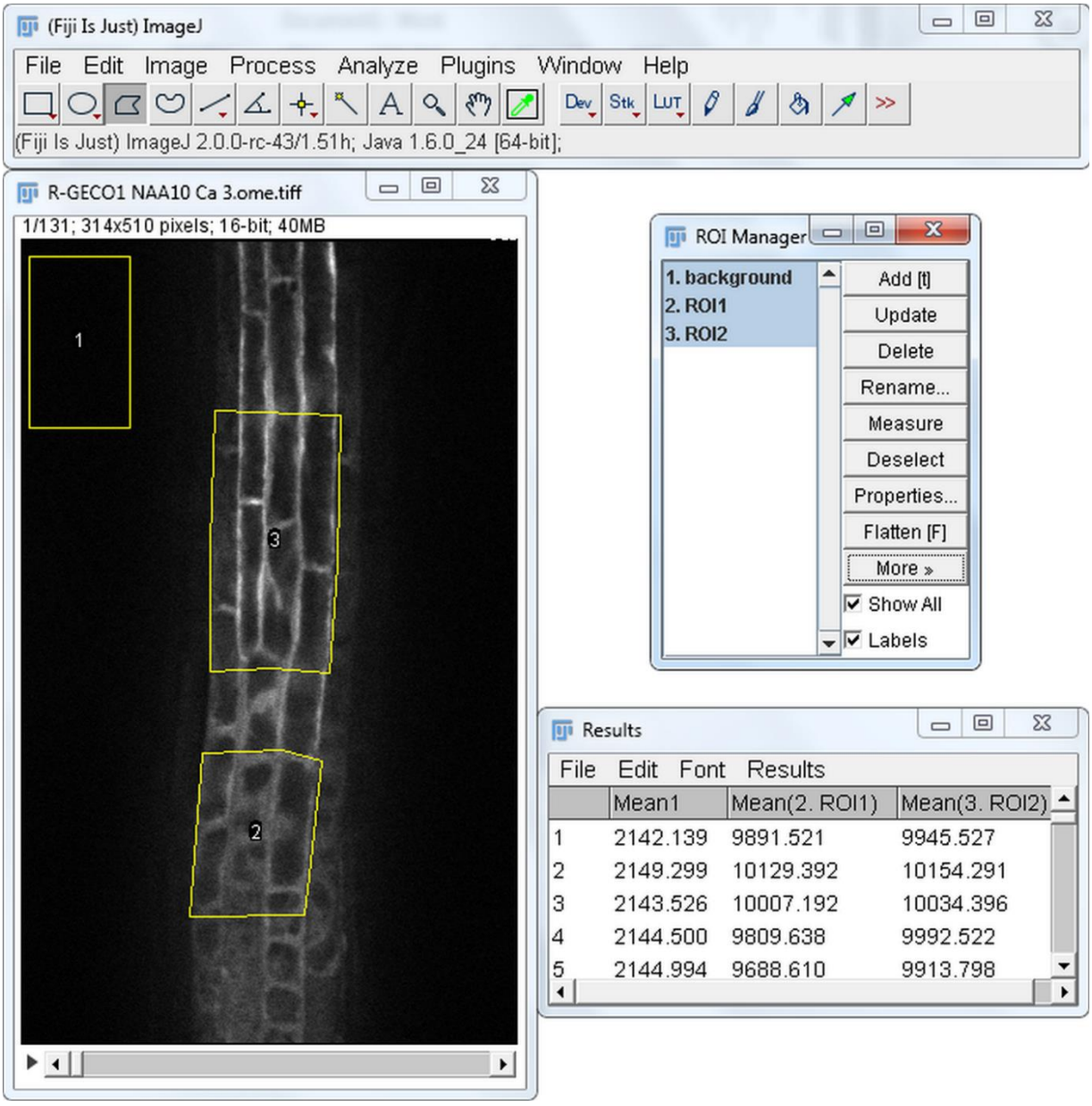

Figure 3: Screen shot of Fiji interface. The ROI Manager window stores the background region and ROIs. The corresponding regions are displayed on the image at the left. The Results window shows the mean gray values for the different regions over time.

4. Measure the mean fluorescence intensity in the background region and *n* ROIs. First, define the parameter that has to be measured. Go to 'Analyze' > 'Set Measurements…' > select 'Mean gray value' > 'OK'. Next, measure the mean gray value in the different regions. In the ROI Manager window, select all regions and click on 'More' > select 'Multi Measure' > enable 'One row per slice…' > 'OK'. The Results window shows the mean fluorescence intensity for the

background region (I_{BG}) and *n* ROI (I_{ROIn}) over time (Fig. 3). The obtained results are further processed in Excel.

5. Perform a background subtraction by calculating (I_{ROIn} - I_{BG}) (*t*). (Fig. 4); Subtract, per frame, the mean background signal I_{BG} from the mean signals in each of the *n* ROI, I_{ROIn}

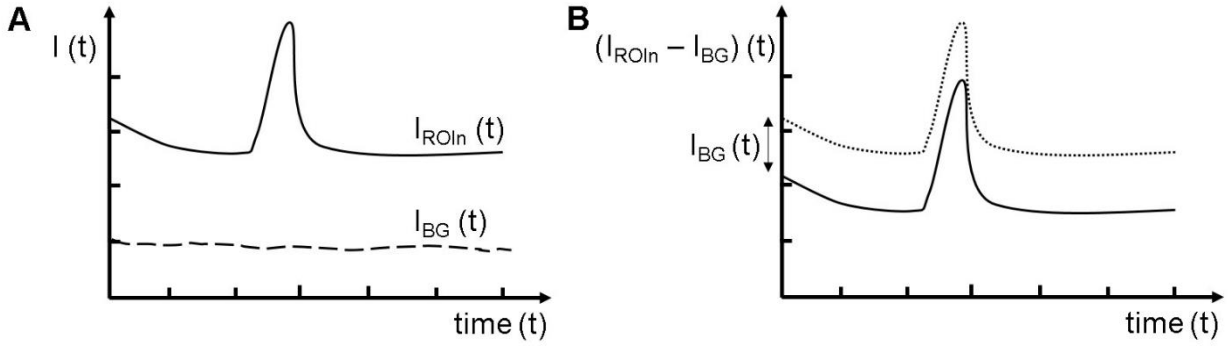

Figure 4: Visualization of background subtraction procedure. (A) The measured mean fluorescence intensity values for ROI *n* (I_{ROIn} (*t*)) and the background region (I_{BG} (*t*)) over time. Note the initial drop in mean fluorescence intensity for ROI *n* due to photobleaching at the start of the time lapse recording. (B) The mean fluorescence intensity values of ROI *n* before (dotted line) and after (full line) background subtraction.

6. Normalize the background-corrected values by calculating [(I_{ROIn} - I_{BG}) (*t*) - (I_{ROIn} - I_{BG}) (t_{ref})] / (I_{ROIn} - I_{BG}) (t_{ref}) (Fig. 5); The background-corrected mean intensities (I_{ROIn} - I_{BG}) for ROI *n* over time *t* are normalized to the background-corrected mean intensity (I_{ROIn} - I_{BG}) at a reference time point t_{ref}. The reference time point is usually a time point prior to the treatment, when fluorescence levels have stabilized (see Notes 7.). For normalization, subtract and subsequently divide the background-corrected mean intensities for a ROI (I_{ROIn} - I_{BG}) (*t*) by the background-corrected mean intensity at the reference time point (I_{ROIn} - I_{BG}) (t_{ref}).

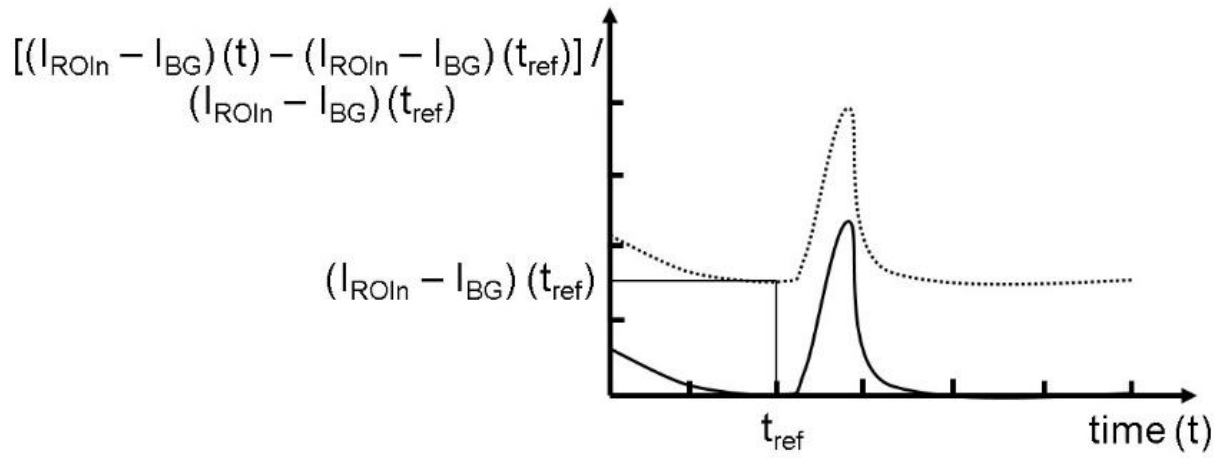

Figure 5: Visualization of normalization procedure. The graph shows the background-corrected mean intensities over time before (dotted line) and after (full line) normalization. The background-corrected mean intensity at timepoint t_{ref} (= (I_{ROIn} – I_{BG}) (t_{ref})) is used for normalization.

7. Plot the data in a line chart. The normalized background-corrected mean intensities [(I_{ROIn} - I_{BG}) (t) - (I_{ROIn} - I_{BG}) (t_{ref})] / (I_{ROIn} - I_{BG}) (t_{ref}) are used for the y-axis values. Recalculate the number of frames to the corresponding time in seconds by taking into account the time interval between subsequent scans (x-axis values).

8. Plot analysis. Different parameters can be extracted from this plot and compared among treatments/genotypes such as the peak amplitude, response time, steepness of the peak, peak duration, …

3.4.2 MATLAB

The workflow of the provided MATLAB script *intensiometric_Ca_imaging.m* is schematically illustrated in Fig. 6 and is described in more detail below. The script does not include an image registration step. Therefore, it should be first performed in Fiji as described above (3.4.1. step 2)).

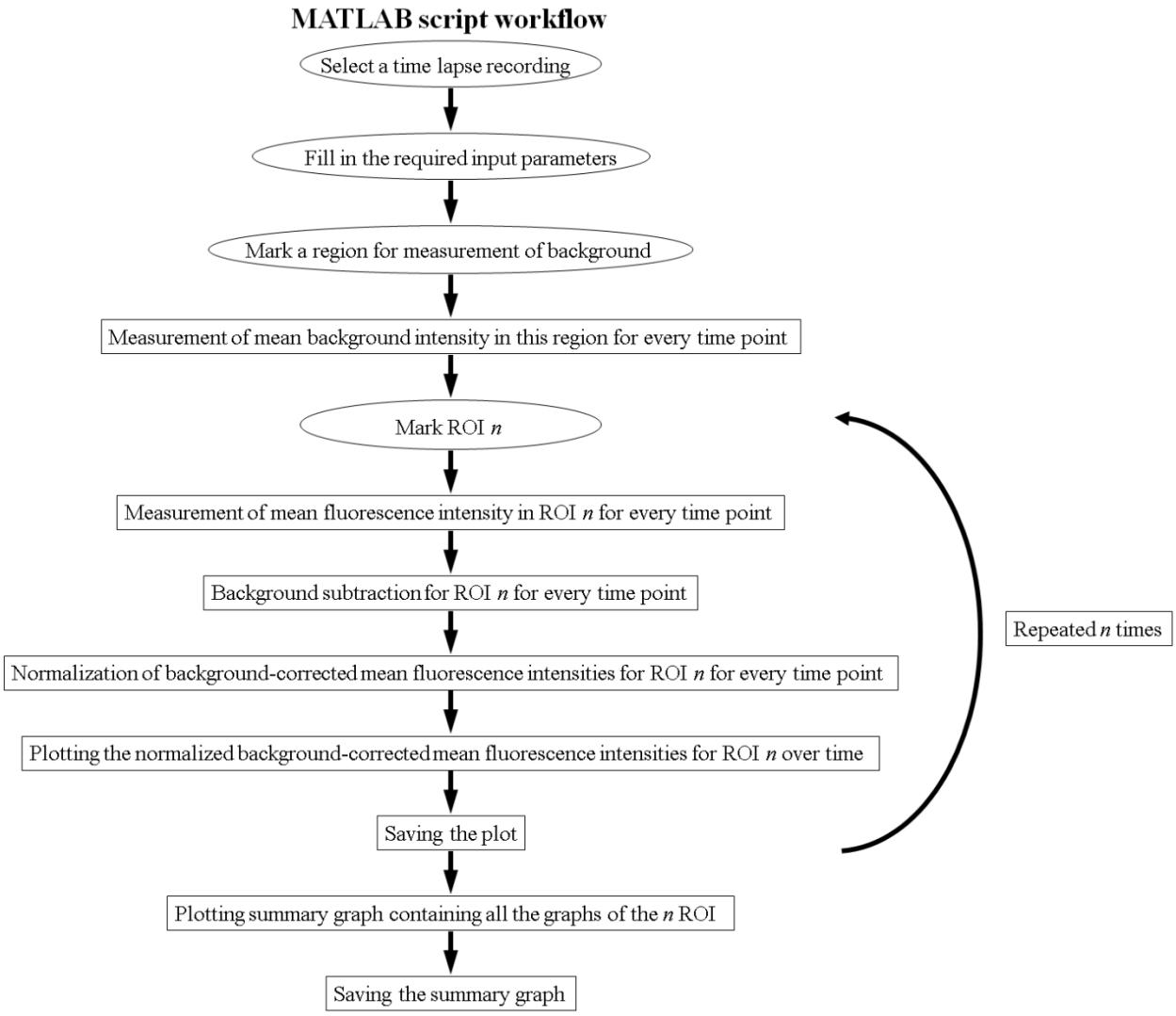

Figure 6: Workflow of MATLAB script *intensiometric_Ca_imaging.m*. The oval shapes indicate steps where user input is required. The rectangular shapes mark the steps which are performed automatically while running the script.

1. Getting started with MATLAB. Copy the provided script *intensiometric_Ca_imaging.m* to the directory used by MATLAB and add it to the path (right click > 'Add to path') (Fig. 7). Ensure that all the movies are in the same directory and added to the path. The plots that will be generated by the script will be saved to this directory. In order to run the script, right-click on *intensiometric_Ca_imaging.m* in the 'Current Folder' panel, and select 'Run'.

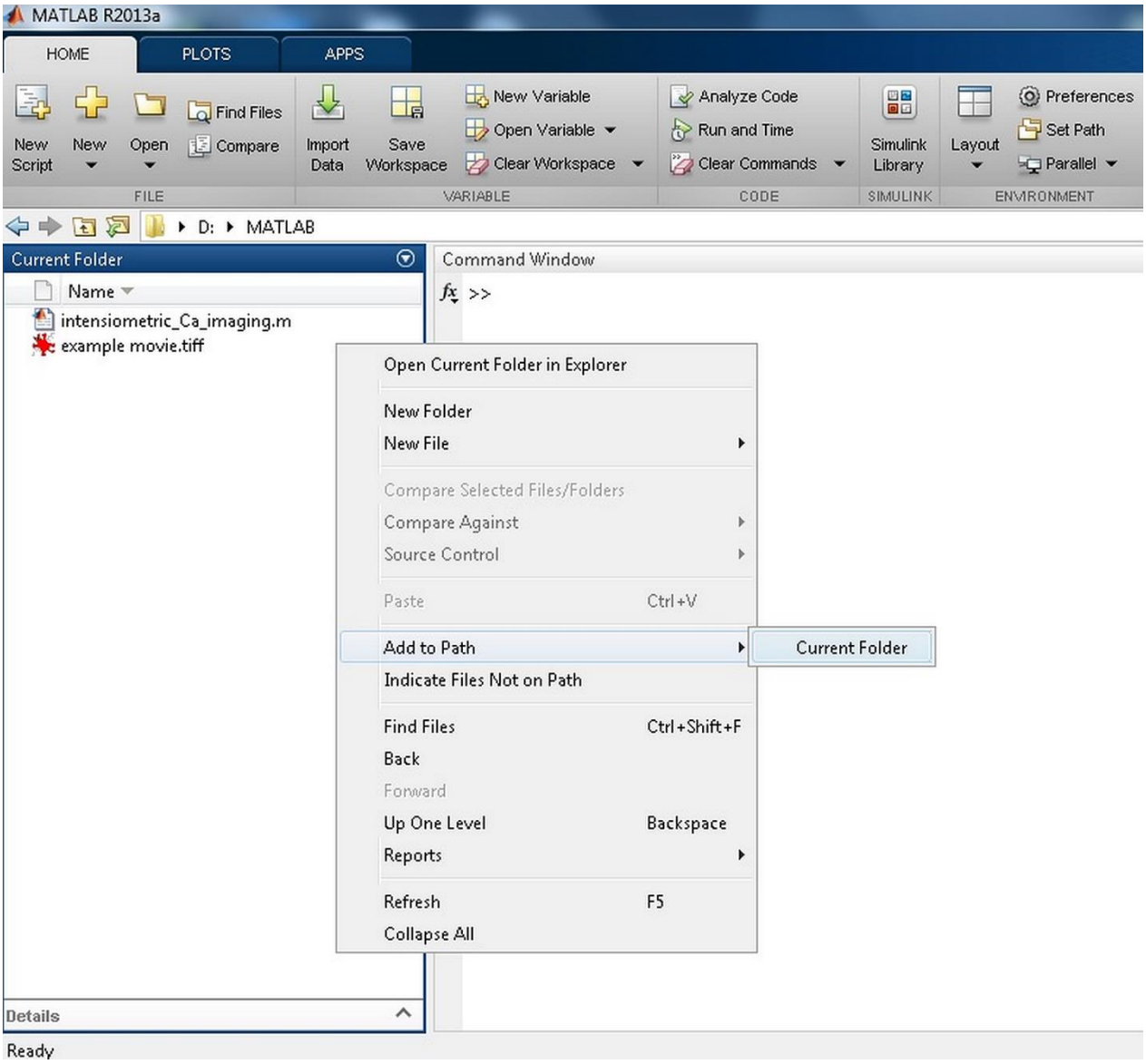

Figure 7: Getting started with MATLAB. The current folder used in this case is D:\MATLAB. Copy the *intensiometric_Ca_imaging.m* script and the movies of interest to this folder and add them to the active path as shown. The plots that will be generated by the script will be saved in this current folder.

2. A 'Select File to Open' window will pop up. Select the time lapse recording of interest and click 'Open'. If the time lapse file is not visible in the opened folder, ensure that 'All Files' is selected and that the time lapse file is stored in this folder.

3. An 'Input' window will be shown. Provide the required input parameters: the number of the frame of which the fluorescence intensity has to be used for normalization (t_{ref}), the time interval between scans in sec (here: 5 sec), and the number of ROI (= n).

4. The first frame of the time lapse recording will appear, together with a window containing the instructions to set a (polygon) region for measurement of background fluorescence. To proceed and start drawing the region, click ‘OK’. Specify the region by selecting vertices of the polygon. To close the polygon, double-click or position the mouse over the first vertex and single-click. The polygon can be moved or resized using the mouse. When the polygon has the desired size and position, create a mask by right-clicking inside the region and selecting ‘Create mask’ from the menu. Once this is done, the script will measure the mean background intensity I_{BG} in the defined region for every frame, and store the values in the I_BG vector.

5. The next step is to mark a first ROI. As in step 4, the first frame of the time lapse recording and a window containing the instructions for drawing the ROI will appear. To start drawing the ROI, click ‘OK’. Draw the ROI as described in step 4. When the polygon is drawn, create a mask by right-clicking inside the region and selecting ‘Create mask’ from the menu.

The following tasks are performed automatically by the commands in the script. The mean fluorescence intensity I_{ROI1} in the defined region is measured for every frame, and the values are stored in the I_ROIn vector. A background subtraction is performed ($I_{ROI1} – I_{BG}$), and the background-corrected mean fluorescence intensities are saved in the I_corr vector. Based on the number of the frame for normalization defined in step 3. (t_{ref}), the background-corrected mean fluorescence intensities for the ROI over time t ($I_{ROI1} – I_{BG}$) (t) are normalized to the background-corrected mean fluorescence intensity of the ROI at t_{ref} by subtracting and subsequently dividing by this value: [(I_{ROI1} - I_{BG}) (t) - (I_{ROI1} - I_{BG}) (t_{ref})] / (I_{ROI1} - I_{BG}) (t_{ref}). The obtained values are stored in the I_corr_norm vector and plotted over time. The graph is saved in the MATLAB directory as JPEG file and is named 'ROI1.jpg' (Fig. 8).

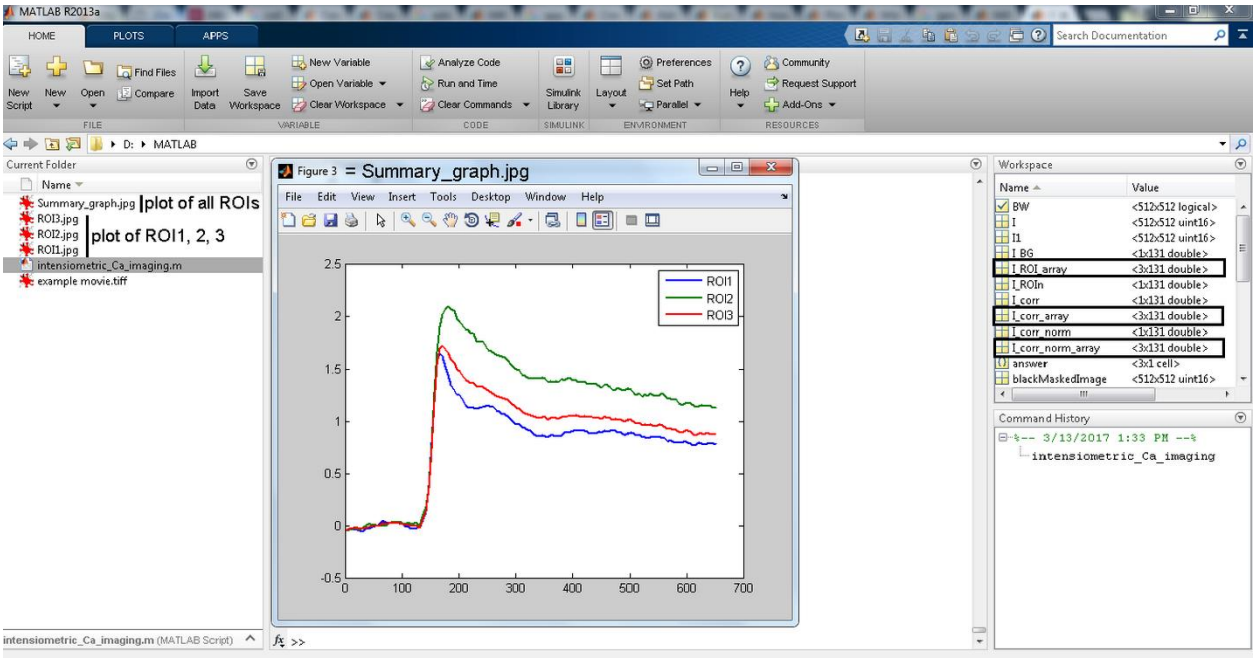

Figure 8: MATLAB output. The script generates a plot for every individual ROI (ROI1.jpg, ROI2.jpg,…) and a summary plot (Summary_graph.jpg) which will be saved to the current folder. The Workspace lists all the vectors containing the fluorescence intensities which have been measured/calculated while running the script. To access the values, see Notes 9.

6. Depending on the number of ROIs (*n*), step 5 is repeated *n* times.

7. In the case of multiple ROIs ($n > 1$) the script generates a single graph containing all the graphs of the *n* ROI (Fig. 8). The graph is saved as a JPEG file named 'Summary_graph.jpg' in the MATLAB directory.

8. Analyze the graphs. Different parameters can be extracted and compared among treatments/genotypes such as the peak amplitude, response time, steepness of the peak, peak duration, … (See Notes 9. and 10.).

9. Before proceeding to analysis of another time lapse recording, ensure to rename the 'Summary_graph' and 'ROIn' plots. Otherwise they will be overwritten during a subsequent run of the script.

4. Notes

1. Two different methods were used for producing the imaging chamber. One set of chambers was made by manually machining the base of the chamber from an aluminum block and the

lid from plexiglass. A second set of chambers was made by 3D printing from PETG plastic. Both methods resulted in functional imaging chambers. The manually machined chambers were made based on the provided 2D drawing. The 3D design is provided as a STL file which is the universal file format for most 3D printers. For 3D printing a fused deposition modelling (FDM) printer was used. Both the base of the chamber and the lid were printed from PETG filament. PETG has a melting temperature of 220°C to 250°C, and it is advised to print it on a heated bed of around 80°C to prevent warping.

2. To increase the time-efficiency during imaging, it is convenient to have several imaging chambers to allow imaging a sample while preparing another sample and let it recover for 30 min.

3. The total volume of the chamber is about 300 µL. Because 200 µL minimal medium is added during sample preparation, only an additional 100 µL can be applied for treatment, resulting in a three-fold dilution of the treatment solution upon mixing it to the sample. Therefore, the concentration of any drug in the treatment solution should be 3x more concentrated than the desired end-concentration.

4. It is recommended to use and objective with high Numerical Aperture (NA). For imaging of root cells it is advised to use a 40X water immersion objective.

5. Keep in mind that root tips might grow out of the field of view during long time lapse recordings. To increase the field of view, tile scanning can be performed at every time point. The frame rate might have to be decreased to have enough time to execute this operation. A SDM might be more suitable for this purpose as it allows for faster data acquisition.

6. Depending on the stimulus, the time of Ca^{2+} response can vary. Set the duration of the time lapse recording according to the purpose of the experiment.

7. By normalization of the fluorescence intensities, the initial fluorescence intensities are brought to a similar level making comparison among different ROIs in a root or among different roots more convenient. Typically, at the start of the time lapse recording, some photobleaching can occur. Therefore, it is advised to wait until the fluorescence levels have stabilized. For normalization, use the fluorescence intensity after fluorescence stabilization, and prior to treatment (t_{ref}).

8. A full overview of the file formats which are supported by Fiji can be found here: http://imagejdocu.tudor.lu/doku.php?id=faq:general:which_file_formats_are_supported_by_imagej. A list of MATLAB- compatible file formats is listed here https://nl.mathworks.com/help/matlab/import_export/supported-file-formats.html.

9. To access the measured fluorescence intensity values and the ones calculated by the MATLAB script, go in the 'Home' tab to 'Open Variable' and select the variable of choice. A 'Variables' window will be opened containing the data which can be selected and copied to e.g. Excel for further analysis. An example for the I_corr_norm_array is shown below. A row corresponds to the normalized background-corrected mean fluorescence intensities of a ROI over time. In the example (Fig. 9) the data for three ROIs are shown.

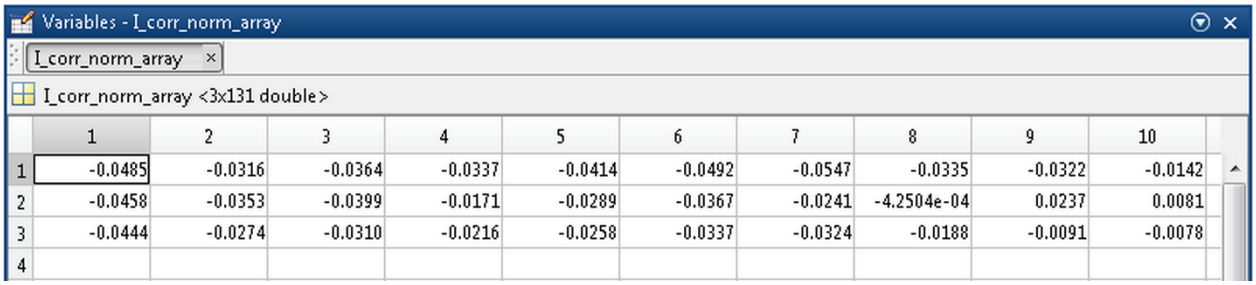
Variables - I_corr_norm_array

I_corr_norm_array

I_corr_norm_array <3x131 double>

	1	2	3	4	5	6	7	8	9	10
1	-0.0485	-0.0316	-0.0364	-0.0337	-0.0414	-0.0492	-0.0547	-0.0335	-0.0322	-0.0142
2	-0.0458	-0.0353	-0.0399	-0.0171	-0.0289	-0.0367	-0.0241	-4.2504e-04	0.0237	0.0081
3	-0.0444	-0.0274	-0.0310	-0.0216	-0.0258	-0.0337	-0.0324	-0.0188	-0.0091	-0.0078
4										

Figure 9: Screen shot of the 'Variables' window containing the data of the desired variable.

10. The absence of changes in fluorescence intensity can be explained by the absence of Ca^{2+} signaling, or by lack of responsiveness of the seedling e.g. when it is damaged. In order to distinguish between both scenarios a positive control treatment can be applied at the end of each time lapse recording (e.g. 0.1 or 1 mM ATP). If the response to the positive control occurs as expected, this suggests the seedling is intact and the test treatment does not elicit a Ca^{2+} increase.

5. Results

Several reports on auxin treatment of different plant species and tissues are available. In the root, most Ca^{2+} dynamics in response to the natural auxin IAA, are well characterized (Monshausen et al., 2011; Waadt et al., 2017). The rapid Ca^{2+} response to IAA was most intense in the region shootwards to the root meristem, corresponding to the elongation zone and differentiation zone. This tissue-specific response could be recorded both with Yellow Cameleon3.6 (YC3.6) and R-GECO1-mTurquoise GECIs. Here, we analyzed Ca^{2+} dynamics upon

treatment with the synthetic auxin NAA in *Arabidopsis* roots. We focused on the root epidermal cells since these cells are at the root surface and therefor easiest to treat, and because R-GECO1 is best expressed in this cell type. Upon treatment with 10µM NAA, a rapid cytosolic Ca^{2+} elevation was observed (Fig. 10). The onset of the Ca^{2+} increase started immediately after NAA application, and the maximal amplitude was reached in about 70 sec. In some seedlings, this primary Ca^{2+} peak was followed by a more subtle secondary Ca^{2+} increase (Fig. 10, B), and a gradual attenuation of the Ca^{2+} signal. These observations suggest the involvement of multiple Ca^{2+} signaling components jointly shaping the NAA-induced Ca^{2+} signature.

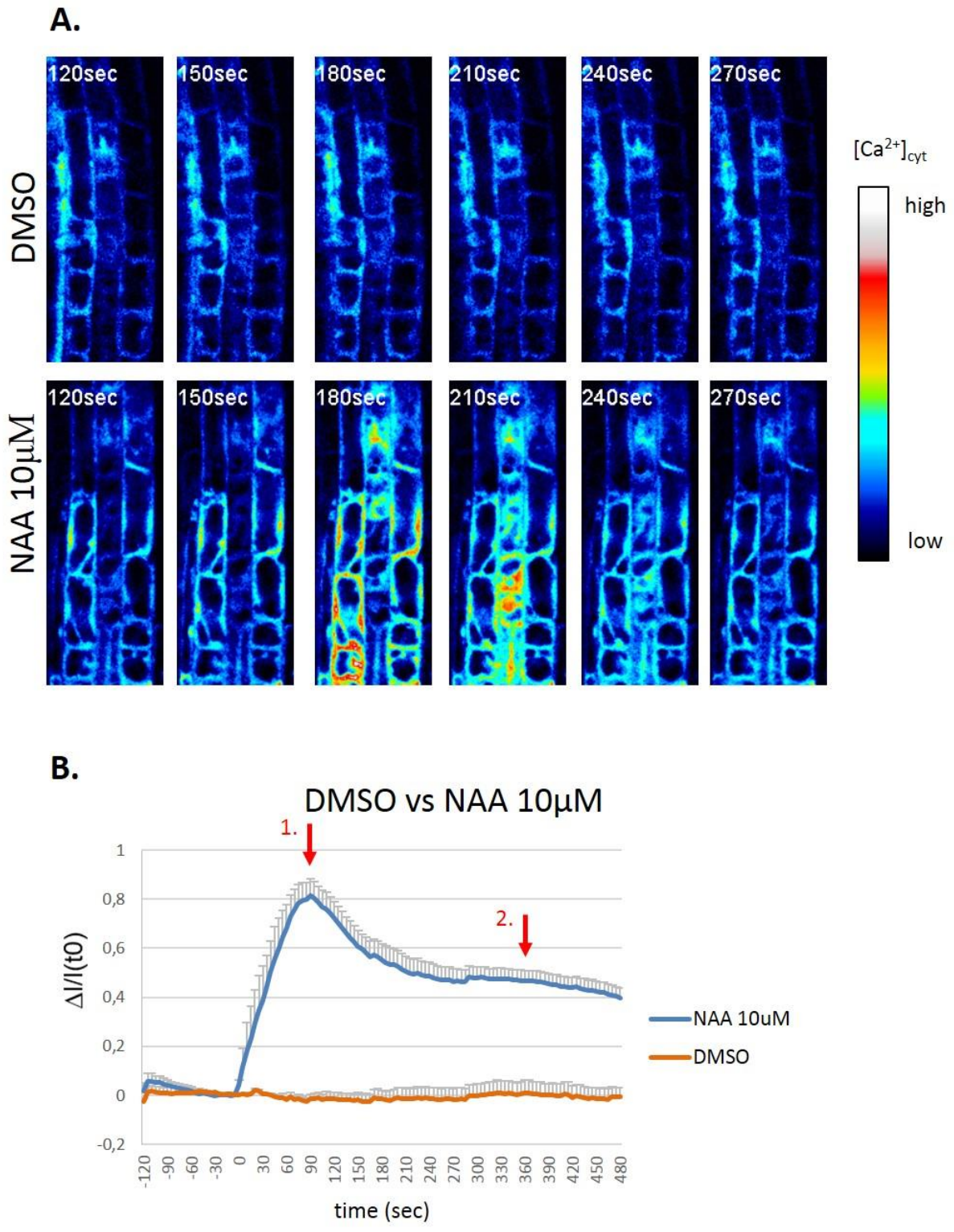

Figure 10: Ca^{2+} dynamics upon NAA treatment in root epidermal cells. (A) Visualization of NAA-induced Ca^{2+} dynamics in the cytosol using the intensiometric Ca^{2+} reporter, R-GECO1. A control treatment with DMSO (top) shows no changes in cytosolic Ca^{2+} concentrations. Treatment with 10µM NAA however induces a rapid cytosolic Ca^{2+} increase. (B) The average normalized fluorescence intensities over time upon DMSO (orange) and 10µM NAA (blue) treatment. 10µM NAA was added at time point 0 sec. The DMSO treatment does not induce a cytosolic Ca^{2+} increase while 10µM NAA rapidly induces a first Ca^{2+} peak (red arrow 1.) followed by a more gentle secondary Ca^{2+} peak (red arrow 2.) in most of the seedlings. Recovery to the initial resting levels occurs gradually. The error bars represent the SE (*n*=10).

Next we evaluated the dose-response of the Ca^{2+} response to different NAA concentrations (Fig. 11). Treatment with 1µM NAA resulted in a cytosolic Ca^{2+} increase, however, the average maximal amplitude was lower than for 10µM NAA treatment. For 100nM NAA, an even lower average maximal amplitude was observed, suggesting that the amplitude of the NAA-induced Ca^{2+} increase is dose-dependent. Note that, as for 10µM NAA, recovery to the initial Ca^{2+} resting levels seemed to occur more slowly.

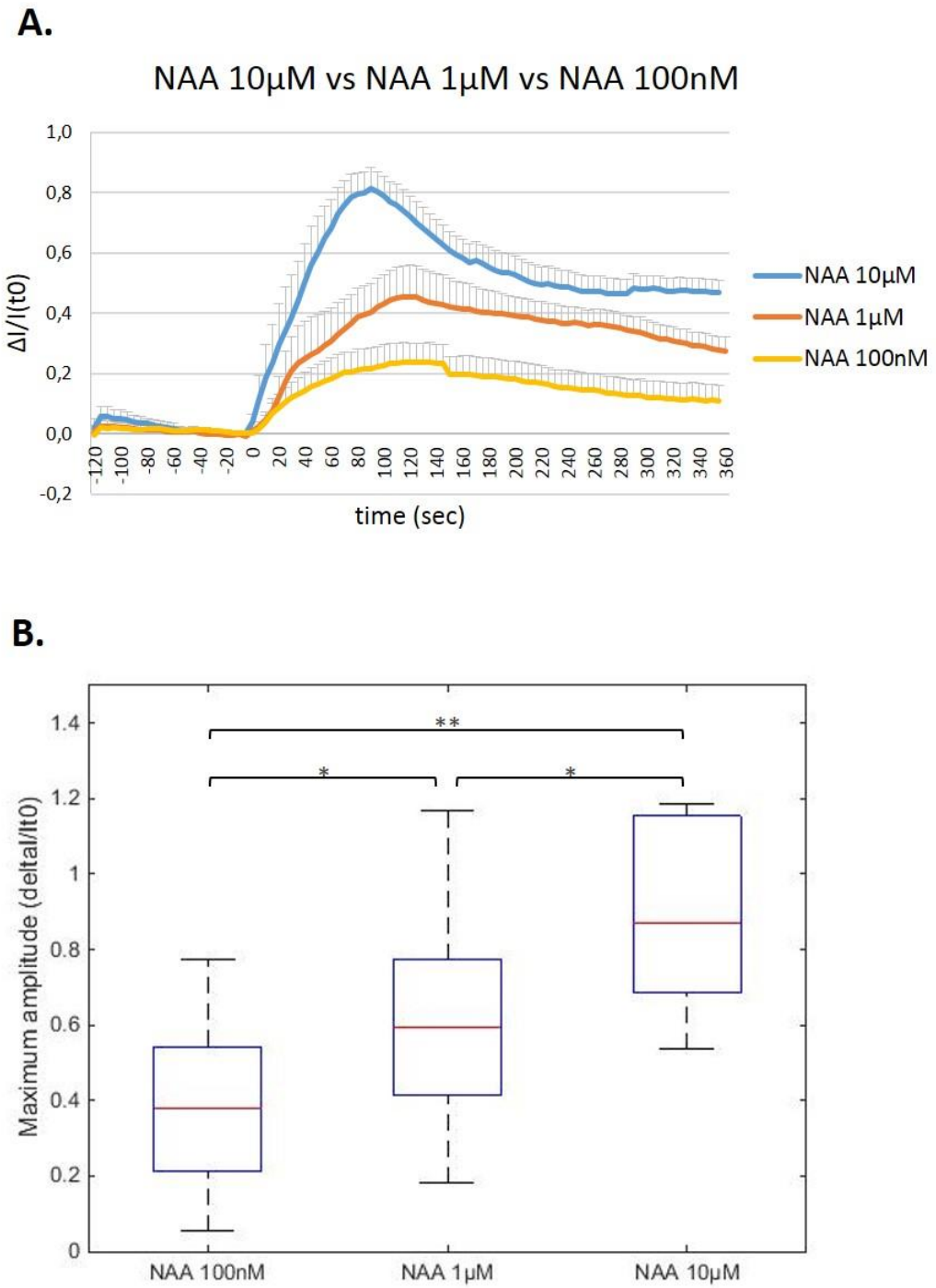

Figure 11: Dose-dependent NAA-induced Ca^{2+} dynamics. (A) The average normalized fluorescence intensities over time upon treatment of R-GECO1 with 100nM, 1µM, 10µM NAA. NAA was added at time point 0 sec. Note that the amplitude of the initial Ca^{2+} peak is higher with increased NAA concentration. The error bars represent the SE. (B) Boxplots of the maximum amplitudes of the initial Ca^{2+} peak induced by treatment with 100nM, 1µM, 10µM NAA. The mean maximum amplitude significantly increases with an increase in NAA concentration. A single and double asterisk represent a p-value <0.05 and <0.01 respectively (t-test; n=10).

Next, we aimed to evaluate the impact of extracellular Ca^{2+} availability on the NAA-induced Ca^{2+} response. Therefore, we prepared 'Ca^{2+}-free medium' (CaMIN), which contains all components present in 0.5x MS medium, but lacks the only Ca^{2+} source $CaCl_2$. By prewashing seedlings for 30 min in CaMIN we aimed to reduce the availability of free Ca^{2+} in the apoplast. Subsequent treatment with 10µM NAA resulted in a considerable reduction of the average amplitude of the Ca^{2+} response, while preserving the secondary Ca^{2+} peak in some of the seedlings, demonstrating the importance of apoplastic Ca^{2+} for NAA-induced Ca^{2+} dynamics (Fig. 12).

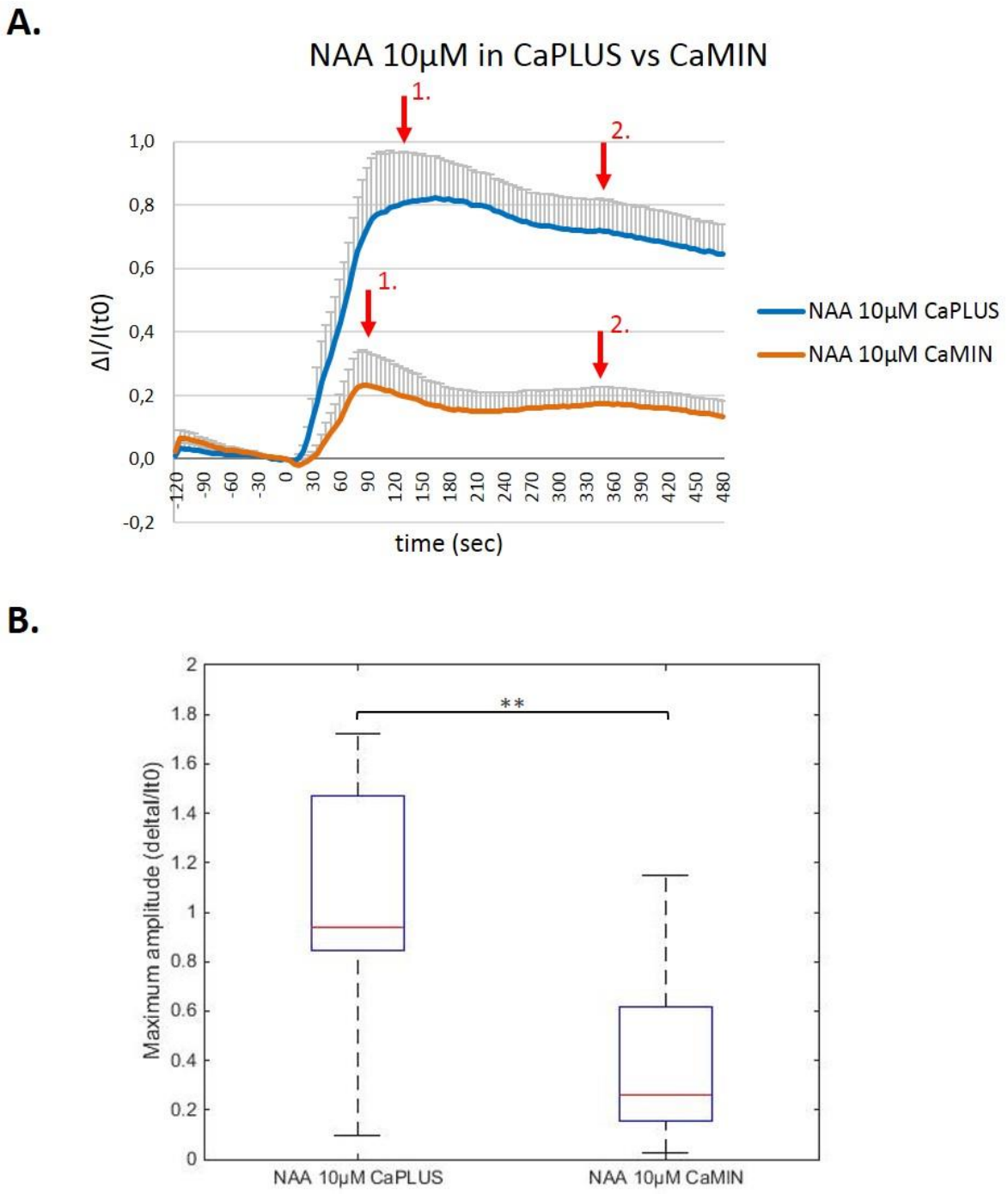

Figure 12: NAA-induced Ca^{2+} dynamics upon extracellular Ca^{2+} reduction. (A) The average normalized fluorescence intensities over time of R-GECO1 upon 10µM NAA treatment after pretreatment with CaPLUS or CaMIN. CaPLUS is 0.5x MS medium, CaMIN is 'Ca^{2+}-free medium' lacking $CaCl_2$. NAA was added at time point 0 sec. NAA treatment upon pretreatment with CaMIN results in a decreased NAA-induced cytosolic Ca^{2+} response compared to pre-incubation with CaPLUS. The red arrows 1. and 2. refer to the first and second Ca^{2+} peak respectively. B) Boxplots of the maximum amplitude of the initial NAA-induced Ca^{2+} peak upon pretreatment with CaPLUS or CaMIN. The average maximum amplitude is significantly lower after CaMIN pre-incubation. The double asterisks represents a p-value <0.01. (t-test; n=11)

Given the promptness of the NAA-induced cytosolic Ca^{2+} increase, this NAA effect could potentially be mediated by the auxin receptor ABP1. Therefore, we aimed to address NAA-induced Ca^{2+} dynamics upon ABP1 inactivation. ABP1 can be found in both the apoplast and ER, but it has been hypothesized that auxin is sensed by the apoplastic ABP1 pool (Tian et al., 1995). The AtSS12S line has been developed in which apoplastic ABP1 can be conditionally inactivated by ethanol (EtOH)-inducible expression of a apoplast-targeted ABP1-specific antibody (Braun et al., 2008). To monitor NAA-induced Ca^{2+} dynamics upon inactivation of apoplastic ABP1, we crossed the AtSS12S line with a Ca^{2+} reporter line. In this case the ratiometric Ca^{2+} sensor Yellow Cameleon 3.6 (YC3.6) was used since R-GECO1 was not available yet in *Arabidopsis* at that time. Unfortunately, induction of ABP1 inactivation resulted in silencing of the reporter expression in the root, except for the root tip (Fig S1, D), for the majority of the seedlings making it problematic to visualize and record the Ca^{2+} dynamics in our region of interest. For the seedlings that did preserve reporter fluorescence upon induction, we obtained very variable results. Some seedlings did not respond to NAA, while other seedlings gave a similar or elevated response compared to wild type. This variability is reflected by the large error bars in the graph (Fig S1, E). Therefore, we could not draw a consistent conclusion on the role of ABP1 in NAA-induced Ca^{2+} dynamics based on these observations.

6. Conclusions and perspectives

Ca^{2+} is an elusive signal that is rapidly generated and in many cases also rapidly dissipated. Therefore, it remains a major challenge to accurately capture the Ca^{2+} signal. In recent years, a revolution in the available GECI is in the process of completely changing our view of Ca^{2+} signaling in plants (Chen et al., 2013; Kanchiswamy et al., 2014; Keinath et al., 2015; Wagner et al., 2015a; Loro et al., 2016; Candeo et al., 2017; Liu et al., 2017; Waadt et al., 2017). Given the increased sensitivity of these new GECI, it is imperative to disturb the sample as little as possible during Ca^{2+} imaging. Here, we reported a detailed protocol for image acquisition of the intensiometric Ca^{2+} sensor R-GECO1 using a customized chamber to facilitate sample treatment during imaging, and provided guidelines for image analysis.

Even though this imaging set-up allows to capture fast Ca^{2+} responses there is room for further optimization. Some experiments might require pulsed treatments or more complex combinations of multiple elicitors/drugs. For those purposes the imaging chamber could be combined with a perfusion system. Another benefit of such system is that it does not require manual application of the compound assuring a more precise, homogenous, and reproducible treatment. A wide range of perfusion solutions have been developed, e.g. a customized chamber combined with a manually controlled peristaltic pump or automated syringe pump, or microfluidic chips. As some of the commercially available systems can be rather costly, open source projects have been initiated to develop and manufacture your own low-cost syringe pump for simple perfusion experiments (Wijnen et al., 2014). Grossmann and coworkers have developed a microfluidic platform, called RootChip, for cultivation of *Arabidopsis* roots and highly controlled perfusion during live-imaging (Grossmann et al., 2011). The main advantages of this set-up are the requirement of small volumes for treatment, and the possibility to image and treat multiple samples in parallel. Nevertheless, this platform requires rather expensive customized production of disposable chips and involves a laborious assembly procedure. For more simplified experimental set-ups, the imaging chamber described here is a much cheaper, less labor intensive and reusable alternative.

In many studies, the synthetic auxin NAA, is preferred over the naturally occurring IAA, in part due to its higher stability under *in vitro* conditions. Although they elicit many similar physiological responses, NAA and IAA have a markedly different chemical structure and physico-chemical properties. This has inevitably dramatic consequences for how they are perceived by the cells. Here, we used our imaging set-up to characterize NAA-induced Ca^{2+} responses in roots. Our findings show that the synthetic auxin NAA induces a rapid, concentration-dependent cytosolic Ca^{2+} increase in root epidermal cells. Furthermore, we observed that Ca^{2+} resting levels are reestablished rather slowly. This might be caused by the sustained presence of NAA, as NAA can be added to the chamber, but not removed. This possibility can be excluded by performing pulsed NAA treatment using e.g. a perfusion system. Alternatively, the gradual recovery could indicate that NAA affects Ca^{2+} pump activity thereby causing a slower Ca^{2+} removal from the cytosol. A third plausible explanation could be that NAA affects Ca^{2+}-ATPase activity via its impact on H^{+}-ATPases. Given that Ca^{2+}-ATPases use H^{+} as a counter ion for Ca^{2+} exchange (Luoni et al., 2000; Zhai et al., 2012), NAA-regulated H^{+}-

ATPase action can indirectly affect Ca^{2+}-ATPase activity and therefore Ca^{2+} removal from the cytosol. In most of the seedlings the NAA-induced Ca^{2+} signature consists of two Ca^{2+} peaks; a rapid first Ca^{2+} peak with high amplitude followed by a slower and smaller second Ca^{2+} peak. Interestingly, Monshausen and coworkers reported that the cytosolic Ca^{2+} increase upon treatment of the YC sensor with 100nM IAA could be prevented by pretreatment with the membrane-impermeable Ca^{2+} channel blocker La^{3+} (Monshausen et al., 2011). This would be in favor of our hypothesis that the first NAA-induced Ca^{2+} peak is derived from the extracellular Ca^{2+} pool in the apoplast (Knight et al., 1997). Indeed, we found that limiting extracellular Ca^{2+} availability reduces the initial NAA-induced cytosolic Ca^{2+} increase. Based on these observations, we hypothesize that NAA induces an extracellular Ca^{2+} influx causing the primary Ca^{2+} peak in the cytosol, and that this primary Ca^{2+} increase in turn triggers Ca^{2+} release from intracellular Ca^{2+} stores causing the subtle secondary Ca^{2+} peak. Analysis of targeted Ca^{2+} sensors (e.g. to the apoplast and ER) yields a higher spatial resolution, and could provide more insight on the postulated intracellular Ca^{2+} source.

Given that the observed NAA-induced Ca^{2+} increase occurs rapidly, we hypothesized that this NAA effect could be mediated by the auxin receptor ABP1. Unfortunately, silencing of the Ca^{2+} reporter upon ABP1 inactivation in the majority of the seedlings and variable responses in the remaining seedlings has made it difficult to draw any robust conclusions from these observations. The recent findings concerning off-target effects in the ABP1 repression lines (Michalko et al., 2016) could explain the variability observed in our data. Therefore, we should address NAA-induced Ca^{2+} dynamics in the more recently developed ABP1 knock-out mutant (Gao et al., 2015). However, given the current debate on the role of ABP1 in auxin signaling, we should keep in mind the possibility that ABP1 might not function as an auxin receptor when analyzing our current and future observations.

Besides NAA, also other plant hormones are known to trigger Ca^{2+} signaling. Abscisic acid (ABA) triggers repetitive Ca^{2+} increases in the cytosol of guard cells thereby regulating stomatal aperture (McAinsh et al., 1997; Allen et al., 1999; Assmann and Shimazaki, 1999), however, in roots ABA does not affect cytosolic Ca^{2+} dynamics (Waadt et al., 2017). A frequently used positive control for induction of a cytosolic Ca^{2+} increase is adenosine triphosphate (ATP). ATP treatment of seedlings expressing the chemiluminescence-based sensor aequorin revealed

that ATP, as NAA, rapidly generates a dual peak Ca^{2+} signature. In contrast, recovery occurred swiftly and Ca^{2+} resting levels where reestablished after about 5min (Tanaka et al., 2010). By pretreatment with Ca^{2+} channel inhibitors Gd^{3+} and La^{3+}, and a Ca^{2+} ionophore, it was demonstrated that the initial Ca^{2+} peak was the outcome of extracellular Ca^{2+} influx, and the second peak mainly resulted from Ca^{2+} release from intracellular stores. It should be noted that these recordings where made from whole seedlings and spatial resolution is lacking, Nevertheless, an ATP-induced cytosolic Ca^{2+} increase also has been reported for roots, albeit only a single Ca^{2+} peak is measured (Costa et al., 2013; Waadt et al., 2017). These observations show that different tissues can have distinct Ca^{2+} responses to the same stimulus, and caution should be taken when comparing Ca^{2+} signatures obtained from distinct tissues and set-ups.

Looking at IAA-induced Ca^{2+} dynamics using R-GECO1, it has been shown that 10µM IAA induces a biphasic cytosolic Ca^{2+} increase with a fast, transient, high amplitude, primary Ca^{2+} peak (about 5min) followed by a smaller prolonged second peak (about 15min; (Waadt et al., 2017). This pattern reassembles the 10µM NAA-induced double peak Ca^{2+} signature that we observed. Furthermore, a dose-dependent effect could be detected. The amplitude of the first peak upon 1µM IAA treatment was lower, yet the second peak could still be observed. Even though, IAA and NAA show some similarities in their Ca^{2+} signature, our observations were made in the meristematic region, while these data where obtained for the root elongation zone. As discussed in the previous paragraph the results obtained from distinct tissues/cell populations should be compared with caution as the observed IAA-induced Ca^{2+} response in the elongation zone might not be visible in the meristematic region. Moreover, the transition between the first and second Ca^{2+} peak is more subtle upon NAA treatment. These subtle differences in IAA- and NAA-induced Ca^{2+} signatures suggest the involvement of distinct Ca^{2+} signaling components mediating the observed Ca^{2+} dynamics. Therefore, an interesting question is which Ca^{2+} channel(s) and/or Ca^{2+} pumps are activated by NAA to establish the NAA-induced cytosolic Ca^{2+} signature. Recently, CYCLIC NUCLEOTIDE-GATED CHANNEL14 (CNGC14) has been identified as a Ca^{2+} channel mediating IAA-induced Ca^{2+} dynamics in roots, and auxin-regulated Ca^{2+} signaling during inhibition of root growth and root gravitropism (Shih et al., 2015). Evaluating Ca^{2+} dynamics upon NAA treatment in the *cngc14* background would allow us to verify to what extent CNGC14 is also relevant for NAA-induced Ca^{2+} signaling.

As a final remark, I would like to point out that, in order to address if the observed Ca^{2+} signature is specific for NAA treatment, additional control experiments with e.g. the weak acid benzoic acid and the auxin-like, yet inactive in the transcriptional auxin response, 2-naphthaleneacetic acid (2-NAA), need to be performed.

7. References

Allen, G.J., Kwak, J.M., Chu, S.P., Llopis, J., Tsien, R.Y., Harper, J.F., and Schroeder, J.I. (1999). Cameleon calcium indicator reports cytoplasmic calcium dynamics in Arabidopsis guard cells. The Plant Journal **19,** 735-747.

Assmann, S.M., and Shimazaki, K. (1999). The Multisensory Guard Cell. Stomatal Responses to Blue Light and Abscisic Acid. Plant Physiology **119,** 809-816.

Ayling, S.M., Brownlee, C., and Clarkson, D.T. (1994). The Cytoplasmic Streaming Response of Tomato Root Hairs to Auxin; Observations of Cytosolic Calcium Levels. Journal of Plant Physiology **143,** 184-188.

Bonza, M.C., Loro, G., Behera, S., Wong, A., Kudla, J., and Costa, A. (2013). Analyses of Ca(2+) Accumulation and Dynamics in the Endoplasmic Reticulum of Arabidopsis Root Cells Using a Genetically Encoded Cameleon Sensor. Plant Physiology **163,** 1230-1241.

Braun, N., Wyrzykowska, J., Muller, P., Karine, D., Couch, D., Perrot-Rechenmann, C., and Fleming, A. (2008). Conditional Repression of AUXIN BINDING PROTEIN1 Reveals That It Coordinates Cell Division and Cell Expansion during Postembryonic Shoot Development in Arabidopsis and Tobacco. The Plant Cell **20**, 2746-2762.

Candeo, A., Doccula, F.G., Valentini, G., Bassi, A., and Costa, A. (2017). Light Sheet Fluorescence Microscopy Quantifies Calcium Oscillations in Root Hairs of Arabidopsis thaliana. Plant and Cell Physiology **58,** 1161-1172.

Chen, T.-W., Wardill, T.J., Sun, Y., Pulver, S.R., Renninger, S.L., Baohan, A., Schreiter, E.R., Kerr, R.A., Orger, M.B., Jayaraman, V., Looger, L.L., Svoboda, K., and Kim, D.S. (2013). Ultrasensitive fluorescent proteins for imaging neuronal activity. Nature **499,** 295-300.

Clapham, D.E. (2007). Calcium Signaling. Cell **131,** 1047-1058.

Costa, A., Candeo, A., Fieramonti, L., Valentini, G., and Bassi, A. (2013). Calcium Dynamics in Root Cells of Arabidopsis thaliana Visualized with Selective Plane Illumination Microscopy. PLOS ONE **8,** e75646.

Creton, R., Kreiling, J.A., and Jaffe, L.F. (1999). Calcium imaging with chemiluminescence. Microsc Res Techniq **46,** 390-397.

Denninger, P., Bleckmann, A., Lausser, A., Vogler, F., Ott, T., Ehrhardt, D.W., Frommer, W.B., Sprunck, S., Dresselhaus, T., and Grossmann, G. (2014). Male–female communication triggers calcium signatures during fertilization in Arabidopsis **5,** 4645.

Dolenšek, J., Špelič, D., Skelin Klemen, M., Žalik, B., Gosak, M., Slak Rupnik, M., and Stožer, A. (2015). Membrane Potential and Calcium Dynamics in Beta Cells from Mouse Pancreas Tissue Slices: Theory, Experimentation, and Analysis. Sensors (Basel, Switzerland) **15,** 27393-27419.

Gao, Y., Zhang, Y., Zhang, D., Dai, X., Estelle, M., and Zhao, Y. (2015). Auxin binding protein 1 (ABP1) is not required for either auxin signaling or Arabidopsis development. Proceedings of the National Academy of Sciences **112,** 2275-2280.

Gehring, C.A., Irving, H.R., and Parish, R.W. (1990). Effects of auxin and abscisic acid on cytosolic calcium and pH in plant cells. Proceedings of the National Academy of Sciences of the United States of America **87,** 9645-9649.

Grossmann, G., Guo, W.-J., Ehrhardt, D.W., Frommer, W.B., Sit, R.V., Quake, S.R., and Meier, M. (2011). The RootChip: An Integrated Microfluidic Chip for Plant Science. The Plant Cell **23,** 4234-4240.

Hall, M.P., Unch, J., Binkowski, B.F., Valley, M.P., Butler, B.L., Wood, M.G., Otto, P., Zimmerman, K., Vidugiris, G., Machleidt, T., Robers, M.B., Benink, H.A., Eggers, C.T., Slater, M.R., Meisenheimer, P.L., Klaubert, D.H., Fan, F., Encell, L.P., and Wood, K.V. (2012). Engineered Luciferase Reporter from a Deep Sea Shrimp Utilizing a Novel Imidazopyrazinone Substrate. ACS Chemical Biology **7,** 1848-1857.

Homma, R., Baker, B.J., Jin, L., Garaschuk, O., Konnerth, A., Cohen, L.B., and Zecevic, D. (2009). Wide-field and two-photon imaging of brain activity with voltage- and calcium-sensitive dyes. Philosophical Transactions of the Royal Society B: Biological Sciences **364,** 2453-2467.

Irving, H.R., Gehring, C.A., and Parish, R.W. (1992). Changes in cytosolic pH and calcium of guard cells precede stomatal movements. Proceedings of the National Academy of Sciences of the United States of America **89,** 1790-1794.

Kanchiswamy, C.N., Malnoy, M., Occhipinti, A., and Maffei, M.E. (2014). Calcium Imaging Perspectives in Plants. International Journal of Molecular Sciences **15,** 3842-3859.

Keinath, N.F., Waadt, R., Brugman, R., Schroeder, Julian I., Grossmann, G., Schumacher, K., and Krebs, M. (2015). Live Cell Imaging with R-GECO1 Sheds Light on flg22- and Chitin-Induced Transient [Ca²⁺]_{cyt} Patterns in Arabidopsis. Molecular Plant **8,** 1188-1200.

Kettunen, P. (2012). Calcium Imaging in the Zebrafish. In Calcium Signaling, M.S. Islam, ed (Dordrecht: Springer Netherlands), pp. 1039-1071.

Knight, M.R., Campbell, A.K., Smith, S.M., Trewavas, A.J. . (1991). Transgenic plant aequorin reports the effects of touch and cold shock and elicitors on cytoplasmic calcium. Nature **352,** 524-526.

Knight, H., and Knight, M.R. (2001). Abiotic stress signalling pathways: specificity and cross-talk. Trends in Plant Science **6,** 262-267.

Knight, H., Trewavas, A.J., and Knight, M.R. (1997). Calcium signalling in Arabidopsis thaliana responding to drought and salinity. The Plant Journal **12,** 1067-1078.

Krebs, M., and Schumacher, K. (2013). Live Cell Imaging of Cytoplasmic and Nuclear Ca2+ Dynamics in Arabidopsis Roots. Cold Spring Harbor Protocols **2013,** pdb.prot073031.

Krebs, M., Held, K., Binder, A., Hashimoto, K., Den Herder, G., Parniske, M., Kudla, J., and Schumacher, K. (2012). FRET-based genetically encoded sensors allow high-resolution live cell imaging of Ca2+ dynamics. The Plant Journal **69,** 181-192.

Liu, K.-h., Niu, Y., Konishi, M., Wu, Y., Du, H., Sun Chung, H., Li, L., Boudsocq, M., McCormack, M., Maekawa, S., Ishida, T., Zhang, C., Shokat, K., Yanagisawa, S., and Sheen, J. (2017). Discovery of nitrate–CPK–NLP signalling in central nutrient–growth networks. Nature **545,** 311-316.

Loro, G., and Costa, A. (2013). Imaging of Mitochondrial and Nuclear Ca2+ Dynamics in Arabidopsis Roots. Cold Spring Harbor Protocols **2013,** pdb.prot073049.

Loro, G., Wagner, S., Doccula, F.G., Behera, S., Weinl, S., Kudla, J., Schwarzländer, M., Costa, A., and Zottini, M. (2016). Chloroplast-Specific in Vivo Ca(2+) Imaging Using Yellow Cameleon Fluorescent Protein Sensors Reveals Organelle-Autonomous Ca(2+) Signatures in the Stroma. Plant Physiology **171,** 2317-2330.

McAinsh, M.R., Brownlee, C., and Hetherington, A.M. (1997). Calcium ions as second messengers in guard cell signal transduction. Physiologia Plantarum **100,** 16-29.

Mehlmer, N., Parvin, N., Hurst, C.H., Knight, M.R., Teige, M., and Vothknecht, U.C. (2012). A toolset of aequorin expression vectors for in planta studies of subcellular calcium concentrations in Arabidopsis thaliana. Journal of experimental botany **63,** 1751-1761.

Michalko, J., Glanc, M., Perrot-Rechenmann, C., and Friml, J. (2016). Strong morphological defects in conditional Arabidopsis abp1 knock-down mutants generated in absence of functional ABP1 protein. F1000Research **5,** 86.

Monshausen, G.B., Miller, N.D., Murphy, A.S., and Gilroy, S. (2011). Dynamics of auxin-dependent Ca2+ and pH signaling in root growth revealed by integrating high-resolution imaging with automated computer vision-based analysis. The Plant Journal **65,** 309-318.

Shimomura, O. (1995). A Short Story of Aequorin. The Biological Bulletin **189,** 1-5.

Shimomura, O., Musicki, B., Kishi, Y., and Inouye, S. (1993). Light-emitting properties of recombinant semisynthetic aequorins and recombinant fluorescein-conjugated aequorin for measuring cellular calcium. Cell Calcium **14,** 373-378.

Podor, B., Hu, Y.-l., Ohkura, M., Nakai, J., Croll, R., and Fine, A. (2015). Comparison of genetically encoded calcium indicators for monitoring action potentials in mammalian brain by two-photon excitation fluorescence microscopy. Neurophotonics **2,** 021014.

Rudd, J.J., and Franklin-Tong, V.E. (1999). Calcium signaling in plants. Cellular and Molecular Life Sciences CMLS **55,** 214-232.

Saito, K., Chang, Y.F., Horikawa, K., Hatsugai, N., Higuchi, Y., Hashida, M., Yoshida, Y., Matsuda, T., Arai, Y., and Nagai, T. (2012). Luminescent proteins for high-speed single-cell and whole-body imaging. Nature Communications **3,** 1262.

Sanders, D., Brownlee, C., and Harper, J.F. (1999). Communicating with Calcium. The Plant Cell **11,** 691-706.

Sanders, D., Pelloux, J., Brownlee, C., and Harper, J.F. (2002). Calcium at the crossroads of signaling. Plant Cell **14**.

Schindelin, J., Arganda-Carreras, I., Frise, E., Kaynig, V., Longair, M., Pietzsch, T., Preibisch, S., Rueden, C., Saalfeld, S., Schmid, B., Tinevez, J.-Y., White, D.J., Hartenstein, V., Eliceiri, K., Tomancak, P., and Cardona, A. (2012). Fiji - an Open Source platform for biological image analysis. Nature methods **9,** 10.1038/nmeth.2019.

Scrase-Field, S.A.M.G., and Knight, M.R. (2003). Calcium: just a chemical switch? Current Opinion in Plant Biology **6,** 500-506.

Shih, H.-W., DePew, Cody L., Miller, Nathan D., and Monshausen, Gabriele B. (2015). The Cyclic Nucleotide-Gated Channel CNGC14 Regulates Root Gravitropism in Arabidopsis thaliana. Current Biology **25,** 3119-3125.

Shishova, M., and Lindberg, S. (2004). Auxin induces an increase of Ca2+ concentration in the cytosol of wheat leaf protoplasts. Journal of Plant Physiology **161,** 937-945.

Shishova, M., and Lindberg, S. (2010). A new perspective on auxin perception. Journal of Plant Physiology **167,** 417-422.

Takai, A., Nakano, M., Saito, K., Haruno, R., Watanabe, T.M., Ohyanagi, T., Jin, T., Okada, Y., and Nagai, T. (2015). Expanded palette of Nano-lanterns for real-time multicolor luminescence imaging. Proceedings of the National Academy of Sciences **112,** 4352-4356.

Tanaka, K., Swanson, S.J., Gilroy, S., and Stacey, G. (2010). Extracellular Nucleotides Elicit Cytosolic Free Calcium Oscillations in Arabidopsis. Plant Physiology **154,** 705-719.

Tian, H., Klämbt, D., and Jones, A.M. (1995). Auxin-binding Protein 1 Does Not Bind Auxin within the Endoplasmic Reticulum Despite This Being the Predominant Subcellular Location for This Hormone Receptor. J. Biol. Chem. **270,** 26962

Thevenaz, P., Ruttimann, U.E., and Unser, M. (1998). A pyramid approach to subpixel registration based on intensity. IEEE Transactions on Image Processing **7,** 27-41.

Waadt, R., Krebs, M., Kudla, J., and Schumacher, K. (2017). Multiparameter imaging of calcium and abscisic acid and high-resolution quantitative calcium measurements using R-GECO1-mTurquoise in Arabidopsis. New Phytologist **216,** 303-320.

Wagner, S., Nietzel, T., Aller, I., Costa, A., Fricker, M.D., Meyer, A.J., and Schwarzländer, M. (2015). Analysis of Plant Mitochondrial Function Using Fluorescent Protein Sensors. In Plant Mitochondria: Methods and Protocols, J. Whelan and M.W. Murcha, eds (New York, NY: Springer New York), pp. 241-252.

Wijnen, B., Hunt, E.J., Anzalone, G.C., and Pearce, J.M. (2014). Open-Source Syringe Pump Library. PLOS ONE **9,** e107216.

Yang, J., Cumberbatch, D., Centanni, S., Shi, S.-q., Winder, D., Webb, D., and Johnson, C.H. (2016). Coupling optogenetic stimulation with NanoLuc-based luminescence (BRET) Ca(++) sensing. Nature Communications **7,** 13268.

Zhao, Y., Abdelfattah, A.S., Zhao, Y., Ruangkittisakul, A., Ballanyi, K., Campbell, R.E., and Harrison, D.J. (2014). Microfluidic cell sorter-aided directed evolution of a protein-based calcium ion indicator with an inverted fluorescent response. Integrative Biology **6,** 714-725.

Zhao, Y., Araki, S., Wu, J., Teramoto, T., Chang, Y.-F., Nakano, M., Abdelfattah, A.S., Fujiwara, M., Ishihara, T., Nagai, T., and Campbell, R.E. (2011). An Expanded Palette of Genetically Encoded Ca(2+) Indicators. Science (New York, N.Y.) **333,** 1888-1891.

Chapter 2:
Calcium orchestrates PIN trafficking through regulation of endocytosis

Ellie Himschoot[1,2], Jian Chen[1,2], Alex Costa[3], Christina Bonza[3], Melanie Krebs[4], Karin Schumacher[4], Riet De Rycke[1,2], Marie Boudsocq[5], Jen Sheen[5], Henning Ruge[6], Ute Vothknecht[6,7], Veronique Storme[1,2], Daniël Van Damme[1,2], Tom Beeckman[1,2], Jiří Friml[8] & Steffen Vanneste[1,2]

[1] Ghent University, Department of Plant Biotechnology and Bioinformatics, 9052 Ghent, Belgium
[2] VIB Center for Plant Systems Biology, 9052 Ghent, Belgium
[3] Department of Biosciences, University of Milan, 20133 Milan, Italy
[4] Centre for Organismal Studies, Plant Developmental Biology, University of Heidelberg, 69120 Heidelberg, Germany
[5] Department of Molecular Biology and Centre for Computational and Integrative Biology, Massachusetts General Hospital, and Department of Genetics, Harvard Medical School, Boston, Massachusetts 02114, USA
[6] Department of Biology I, Faculty of Biology, LMU Munich, D-82152 Planegg, Germany
[7] Center for Integrated Protein Science (Munich) at the Department of Biology I, Faculty of Biology, LMU Munich, D-81377 Munich, Germany
[8] Institute of Science and Technology Austria (IST Austria), 3400 Klosterneuburg, Austria

Manuscript in preparation:
Ellie Himschoot, Jian Chen, Alex Costa, Christina Bonza, Melanie Krebs, Karin Schumacher, Riet De Rycke, Marie Boudsocq, Henning Ruge, Ute Vothknecht, Jen Sheen, Daniël Van Damme, Tom Beeckman, Jiří Friml & Steffen Vanneste. *Calcium controls PIN turnover through regulation of endocytosis and endosome maturation in Arabidopsis.* Aim: Nature Cell Biology, The Plant Cell

Author contribution:
E.H. performed the experiments described in the manuscript. J.C. generated homozygous RxCPK lines, and performed a phenotypic analysis of these lines. E.H. and S.V. wrote the manuscript. R.D.R performed the transmission electron microscopy experiments. V.S. assisted with the statistical analyses. M.B. H.R., U.V. and J.S. kindly provided seeds. K.S., D.V.D., T.B. and J.F. revised the manuscript. A.C, C.B., and M.K. provided technical guidance.

Abstract

The composition of the plasma membrane is a key determinant of cellular behavior, as it defines the cellular potential to perceive signals, transport molecules, and communicate with its environment. The combined action of endomembrane processes like secretion, endocytosis, recycling to the plasma membrane or targeting to the vacuole control plasma membrane composition, and thus cellular functionality. The phytohormone auxin is known to regulate a wide range of developmental processes and mediate adaptation to environmental changes by establishment of specific distribution patterns of the phytohormone. An important element in the establishment of these auxin distribution patterns are the PIN proteins mediating directional auxin efflux by their polar localization in the plasma membrane. Various stimuli and stresses disrupt the balance of endomembrane processes to alter PIN homeostasis and auxin transport. Auxin itself is known to feedback regulate its own distribution by interfering with clathrin-mediated PIN endocytosis. However, the exact mechanisms through which auxin and other stimuli can modify endomembrane trafficking of PINs remain unclear. Here, we reveal a completely novel function for Ca^{2+} in regulating clathrin-mediated endocytosis (CME) of PINs. We found that elevating cytoplasmic Ca^{2+} levels caused a dramatic inhibition of CME at the plasma membrane. Similarly, constitutive activation of the Ca^{2+}-DEPENDENT PROTEIN KINASE30 (CPK30) was sufficient to prevent PIN internalization. Consistent with a model in which auxin-induced Ca^{2+} explains how auxin inhibits endocytosis, reductions in Ca^{2+} availability impaired the inhibitory effect of auxin on endocytosis. Interestingly, we also found that some Ca^{2+} drug could also affect late endosomal PIN trafficking suggesting that Ca^{2+} might be regulating additional steps in the endomembrane trafficking pathway besides endocytosis. Together, these data demonstrate a new function for Ca^{2+} as a second messenger in auxin-regulated PIN trafficking.

Introduction

Auxin is a prominent phytohormone regulating a wide range of developmental processes and is essential for rapid acclimation to environmental challenges. A crucial factor for auxin to be able to exert its function is proper auxin transport resulting in stimulus- or process-specific auxin distribution patterns. The PIN proteins operate as auxin efflux carriers and are essential for polar cell-to-cell auxin transport (Zažímalová et al., 2007). The subcellular polarity of PINs determines the direction of intracellular auxin transport, and is the result of targeted secretion, local endocytosis, degradation and recycling (Kleine-Vehn et al., 2011; Wabnik et al., 2011; Łangowski et al., 2016). PINs are continuously internalized through clathrin-mediated endocytosis (CME) (Dhonukshe et al., 2007) and recycled back to the plasma membrane (Geldner et al., 2001). The dynamic character of these auxin efflux carriers enables rapid PIN redistribution and thereby redirection of auxin flow during plant development. The flexible modulation of directional auxin transport across tissues underlies to a great extent the developmental plasticity observed in plants. Importantly, auxin itself has multiple effects on PIN trafficking and polarization thereby feedback regulating its own distribution by controlling PIN transcription, PIN turnover, and inhibiting CME of the PINs (Sieberer et al., 2000; Paciorek et al., 2005; Vieten et al., 2005; Robert et al., 2010). Our interest goes to investigating the latter feedback mechanism. It has been established that auxin-inhibited PIN endocytosis relies on the auxin receptor ABP1 and involves activation of intracellular ROP/RIC signaling (Robert et al., 2010; Lin et al., 2012; Chen et al., 2012), however, more detailed insight on the molecular players involved is still missing.

A potential mediator of inhibition of PIN endocytosis by auxin is the second messenger Ca^{2+}. Ca^{2+} is known to be involved in different signaling pathways mediating plant development, and responses to (a)biotic stresses (Dodd et al., 2010; Kudla et al., 2010). Many reports have shown that different types of auxin can trigger a rapid cytosolic Ca^{2+} increase in distinct plant species and tissues (Felle, 1988; Gehring et al., 1990; Shishova and Lindberg, 1999, 2004; Shishova et al., 2007). Furthermore, Ca^{2+} has also been identified as a mediator of auxin-regulated root gravitropism (Ma and Berkowitz, 2011; Monshausen et al., 2011; Shih et al., 2015). Given that auxin induces rapid, transient, Ca^{2+} signals in the root, we postulated that auxin controls endocytosis through Ca^{2+}. Due to the diversity of Ca^{2+} signaling components, we initially addressed our question by means of Ca^{2+} pharmacology and treatment with 'Ca^{2+}

-free medium' (CaMIN). These experiments revealed that Ca^{2+} was both required and sufficient for inhibition of PIN internalization. A more in depth analysis showed that the observed effect of CaMIN treatment relies on early endocytic trafficking, while some of the Ca^{2+} drug also seemed to effect post-endocytic trafficking events. Furthermore, we identified a role for the Ca^{2+} -DEPENDENT PROTEIN KINASE30 (CPK30) in regulation of PIN endocytosis. Altogether, these observations confirm our hypothesis that Ca^{2+} is involved in inhibition of PIN endocytosis by auxin.

Materials and methods

Plant material and growth conditions

SYP32/WAVE22- GFP (Geldner et al., 2009), VHAa1-mRFP (Dettmer et al., 2006), SYP42-YFP (Uemura et al., 2012), ARA7-mRFP (Gillooly et al., 2001), VAMP727-YFP (Ueda et al., 2004), 2xFYVE-YFP (Ebine et al., 2008), SYP22-YFP (Robert et al., 2008), CLC2-GFP (Di Rubbo et al., 2013), XVE>>AX2-1 (Ortiz-Morea et al., 2016), INTAM>>HUB1 (Kitakura et al., 2011) and *ben1-2 ben2* (Tanaka et al., 2009) have been described previously. The DRP1c-GFP seeds were kindly provided by Dr. Mates Fendrych. After sowing, plates were transferred to the cold room (4 °C, dark) for 1 day of vernalization, and were subsequently transferred to the growth room (21 °C, continuous light). Three days or 4 days (for inducible lines) after transfer to the growth room, the seedlings were used for immunolocalization experiments. The seedlings for live imaging were kept in the growth room for 4-5 days.

Induction of the mutant lines

For induction of the mutant lines INTAM>>HUB1, amiR-TML, XVE>>AX2-1, and RxCPK13/30, 2 day-old seedlings were transferred to plates with 0,5x MS and 2 µM hydroxytamoxifen, 2 µM β-estradiol, 5 µM β-estradiol, or 10 µM β-estradiol respectively for 2 days. Hydroxytamoxifen and β-estradiol were purchased from Sigma Aldrich and dissolved in DMSO.

Drugs and CaMIN treatments

Three to 4 day-old seedlings were typically pretreated with the Ca^{2+} drugs or CaMIN for 30min followed by a 1h cotreatment with BFA and/or NAA diluted in 0.5x MS medium with (CaPLUS) or without $CaCl_2$ (CaMIN). For analysis of the endomembrane marker lines 5h treatments were performed. The following hormones/drugs were used: NAA (10 µM), BFA (25 µM), Nifedipine (100 µM), Bepridil hydrochloride (50 µM), W-7 (100 µM), Eosin Y (500 nM), Staurosporin (200 nM), and Cantharidin (50 µM). All hormones/drug were dissolved in DMSO, and were obtained from Sigma Aldrich. To prepare 0,5 L liquid CaMIN medium following components were dissolved in MilliQ: 25mL MS basal salt micronutrient solution, 5 g sucrose, 0,05 g myoinositol, 0,25 g MES, 0,413 g NH_4NO_3, 0,045 g $MgSO_4$, 0,475 g KNO_3, 0,043 g H_2KO_4P- and pH was set to 5,7. The liquid CaPLUS medium has the same composition with additionally 0,083 g $CaCl_2$. For solid medium, 4 g of agar was added.

Immunohistochemistry

Immunolocalizations were performed on 3- to 4-d-old seedlings using the Intavis in situ pro robot, as described by Sauer et al. (2006). The primary antibodies used were anti-PIN1 goat and anti-PIN2 rabbit which were both used in 1:800 dilution. For the secondary antibodies, Alexa488 anti-goat and Alexa555 anti-rabbit were used in 1:600 dilution.

Microscopy and image analysis

Ca^{2+} imaging experiments and analysis were performed as described in Himschoot et al., 2017 (see also Section II – Chapter 1). For imaging of immunolocalisation samples and endomembrane markers the confocal laser scanning microscopes Leica SP2 (Leica) and Zeiss 710 (Zeiss) were used. Fluorescence emission of GFP (excitation 488 nm/emission 500-545 nm), Alexa488 (ex 488 nm/em 500-545 nm), Alexa555 (ex 561 nm/em 555-610nm), mRFP (ex 561 nm/em 570-630 nm), and YFP (ex 514 nm/em 520-565 nm) was detected using a 63x water objective (NA 1.2, digital zoom 1,2x). Images were analysed using Fiji (Schindelin et al., 2012). For imaging DRP1c-GFP (ex 488 nm/em 500-540) dynamics an Ultra View Vox spinning disc microscope (Perkin Elmer) was used equipped with a 100x oil immersion objective (NA

1.45) and an electron microscopy charge-coupled device camera (Hamamatsu Phototonics). Time lapses were recorded for 100 sec taking a scan every 0,5 sec. Kymographs were generated in Fiji using the Multi Kymograph plugin.

Transmission electron microscopy

Roottips of 4-days-old seedlings of *Arabidopsis thaliana* treated for 5h with CaPLUS, CaMIN, DMSO, 100 µM Nifedipine, 50 µM Bepridil, and 100 µM W-7 were excised, immersed in

20% (w/v) BSA and frozen immediately in a high-pressure freezer (Leica EM ICE; Leica Microsystems, Vienna, Austria). Freeze substitution was carried out using a Leica EM AFS (Leica Microsystems) in dry acetone containing 1% (w/v) OsO_4 and 0.2% glutaraldehyde over a 4-days period as follows: -90°C for 54 hours, 2°C per hour increase for 15 hours, -60°C for 8 hours, 2°C per hour increase for 15 hours, and -30°C for 8 hours. Samples were then slowly warmed up to 4°C, rinsed 3 times with acetone for 20 min each time and infiltrated stepwise over 3 days at 4°C in Spurr's resin and embedded in capsules. The polymerization was performed at 70 °C for 16 h. Ultrathin sections were made using an ultra-microtome (Leica EM UC6) and post-stained in in a Leica EM AC20 for 40 min in uranyl acetate at 20 °C and for 10 min in lead stain at 20 °C. Sections were collected on formvar-coated copper slot grids.

Grids were viewed with a JEM 1400plus transmission electron microscope (JEOL, Tokyo, Japan) operating at 60 kV.

Growth experiments on CaPLUS and CaMIN

For analysis of the root length, seeds were plated on CaPLUS (0.5x MS) with agar, vernalized in the cold room (4°C, dark) for 1 day, and then transferred to the growth room (21°C, continuous light) for 3 days. Subsequently, seedlings were transferred to plates with CaPLUS or CaMIN with agar for 6,5 days prior to measurement of the root length. For the gravistimulation experiments, 3 day-old seedlings were transferred to CaPLUS or CaMIN with agar for 24hs. To gravistimulate the roots, the plates were rotated over an angle of 90° and gravitropic root bending was analyzed 5hs after onset of gravistimulation.

Statistical analysis

A logistic regression was performed to compare the presence of BFA bodies or CLC2-GFP at the plasma membrane in root cells of untreated roots versus treated roots or wild type versus mutant. A random effect was added to the model for the experiments with multiple repeats to take into account the correlation between measurements done at the same time. An additional random effect was added to the model to account for correlations between roots treated in the same well. The analysis was performed with the glimmix procedure from SAS (Version 9.4 of the SAS System for windows 7 64bit. Copyright 2002-2012 SAS Institute Inc. Cary, NC, USA (www.sas.com). Maximum likelihood estimation was done with the default estimation method. A Wald-type test was performed to estimate the treatment/genotype effect on the presence of BFA bodies in the root cells or localization of CLC2-GFP at the plasma membrane.

Results

Ca^{2+} is required for auxin-regulated PIN endocytosis

In the previous chapter (Section II – Chapter 1), we visualized NAA-induced Ca^{2+} dynamics in root epidermal cells. We found that NAA induces a rapid Ca^{2+} increase in the cytosol, and that this NAA-induced Ca^{2+} signature consists of two distinct Ca^{2+} peaks. Furthermore, we observed a dose-dependent response to NAA as treatment with lower NAA concentrations resulted in a general decrease in amplitude of the Ca^{2+} signature. When reducing the extracellular Ca^{2+} availability by pretreating seedlings with 'Ca^{2+}-free medium' (CaMIN), the maximal amplitude of the initial Ca^{2+} peak was significantly reduced. Together, these data highlight that Ca^{2+} is one of the earliest signals downstream of NAA perception.

A well-known effect of NAA, is that it potently inhibits CME, and thus PIN internalization (Paciorek et al., 2005; Robert et al., 2010). Therefore, we postulated that Ca^{2+} could act in the pathway through which NAA inhibits CME.

To visualize PIN trafficking we used the fungal drug brefeldin A (BFA). BFA inhibits a subgroup of ARF-GEFs amongst others GNOM, an ARF-GEF mediating recycling of PINs to the plasma membrane (Geldner et al., 2003; Peyroche et al., 1996). At a concentration of 25 µM, BFA

interferes with recycling and secretion, and induces the formation of so called BFA bodies that result from fusion of the TGN, Golgi, and ER (Donaldson and Jackson, 2000; Geldner et al., 2001; Nebenfuhr et al., 2002). Consequently, internalized proteins such as PINs cannot be recycled to the plasma membrane and accumulate in the BFA bodies. As a proxy for the rate of CME, we used the amount of PIN-accumulating BFA bodies upon BFA treatment. Roots treated with BFA had substantial amounts of PIN1 in BFA bodies (Fig. 1, A), and this effect was counteracted upon cotreatment with NAA (Fig. 1, B). To address the possible requirement of Ca^{2+}, we pharmacologically interfered with Ca^{2+} influx by cotreatment with Nifedipine and Bepridil hydrochloride (Ketchum and Poole, 1990; Shishova and Lindberg, 2004), two drug that are known to inhibit specific Ca^{2+} channels in animals. When Nifedipine or Bepridil were included in the BFA/NAA co-treatment, PIN1 accumulation in BFA bodies recovered, thus by-passing the inhibitory effect of NAA (Fig. 1, C, D). Similarly, inclusion of the membrane permeable CALMODULIN (CaM) inhibitor W-7 in the BFA/NAA co-treatment resulted in PIN1 accumulation in BFA bodies, again by-passing the inhibitory effect of NAA on PIN1 internalization (Fig. 1, E). These findings suggest that these Ca^{2+} drugs counteract the inhibitory effect of auxin on PIN endocytosis, and/or that they modify BFA-sensitive endocytic trafficking of PINs.

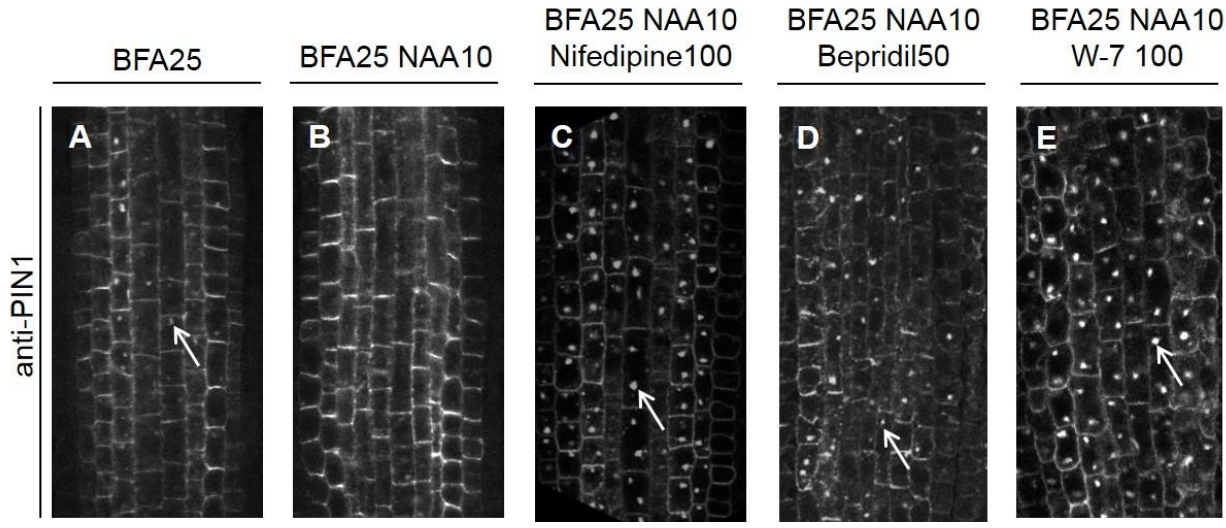

Figure 1: Effect of Ca^{2+} pharmacology on auxin-inhibited PIN1 endocytosis. Analysis of PIN1 internalization through whole-mount immunolocalisation in 3 day-old seedling root meristems. (A) 25µM BFA caused PIN1 accumulation in BFA bodies (white arrow). (B) Co-treatment with 25µM BFA and 10µM NAA interfered with PIN1 internalization, as shown by a lack of BFA bodies. (C-E) Inclusion of Ca^{2+} channel inhibitors Nifedipine (100µM, C) and Bepridil (50µM, D), or the CaM-inhibitor W-7 (100µM, E) restored PIN1 internalization in BFA25/NAA10 co-

treated roots. White arrows highlight PIN1 in BFA bodies. For co-treatments with inhibitors, seedlings were pretreated for 30min.

However, since Nifedipine and Bepridil are animal Ca^{2+} channel blockers and their specificity in plants has not been characterized yet, and off-target effects are to be expected for each inhibitor, we aimed to manipulate Ca^{2+} signaling more specifically by lowering the availability of Ca^{2+} for the cell. Therefore, we prepared 'Ca^{2+}-free 0.5xMS medium', termed CaMIN, lacking $CaCl_2$ which is the only Ca^{2+} source in our medium. As controls we used normal 0.5xMS medium (CaPLUS), CaMIN with 1.5mM $CaCl_2$ and CaMIN with 1.5mM $MgCl_2$. As expected, in CaPLUS medium BFA treatment readily caused PIN1 accumulation in BFA bodies (Fig. 2, C), which was inhibited in the BFA/NAA co-treatment (Fig. 2, E). In contrast, PIN1 accumulated in BFA bodies when the BFA/NAA co-treatment was performed in CaMIN medium (Fig. 2, F), which is consistent with the observations using Ca^{2+} channel or CaM inhibitors. To further confirm the specificity of the treatment to Ca^{2+} availability, we compared PIN1 trafficking in the context of CaMIN supplemented with either 1.5mM $CaCl_2$ or 1.5mM $MgCl_2$. Importantly, only the addition of 1.5mM $CaCl_2$ restored BFA/NAA sensitivity of PIN1 trafficking (Fig. 2, G, H), demonstrating the specific requirement of Ca^{2+} for NAA-inhibited PIN internalization. Together with the observation that the NAA-induced Ca^{2+} signal is strongly reduced in CaMIN, these data are consistent with a model in which auxin-induced Ca^{2+} inhibits PIN internalization.

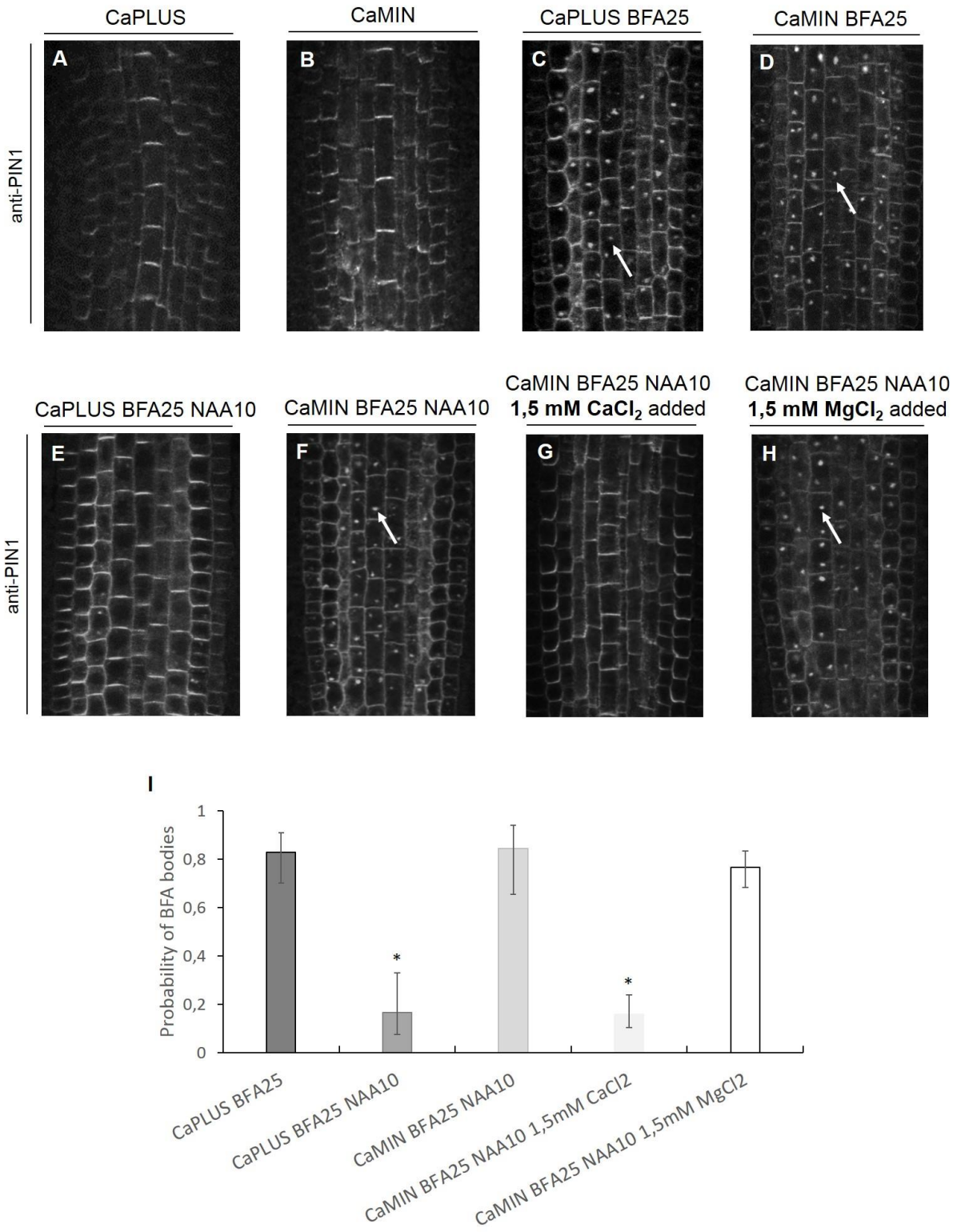

Figure 2: Extracellular Ca^{2+} is required for auxin-inhibited PIN internalization. Analysis of PIN1 internalization through whole-mount immunolocalisation in 3 day-old seedling root meristems. (A, B) Control treatment with CaPLUS (A) and CaMIN (B). (C, D) Treatment with 25µM BFA in CaPLUS (C) and CaMIN (D) results in PIN1 accumulation in BFA bodies (white arrow). (E) Co-treatment with 25µM BFA and 10µM NAA in CaPLUS resulted in the absence of PIN1 accumulation in BFA bodies. (F) In CaMIN (Ca^{2+}-free 0.5xMS medium) NAA could no longer inhibit PIN1 internalization as seen by the presence of PIN1 accumulates in BFA bodies (white arrow). (G) In CaMIN supplemented with 1.5mM $CaCl_2$ no BFA bodies were observed, consistent with a requirement for Ca^{2+} in NAA-inhibited PIN internalization. (H) In CaMIN supplemented with 1.5mM $MgCl_2$ NAA could not prevent PIN1

accumulation in BFA bodies (white arrow), demonstrating the specific requirement of Ca^{2+} for auxin's inhibitory effect. (I) Quantification of the probability that BFA bodies will be present in root cells. The asteriks represents a p-value <0.05. The error bars represent the 95% confidence interval ($n > 5$). Seedlings were pretreated for 30min with either CaPLUS or CaMIN, (supplemented with $CaCl_2$ or $MgCl_2$) as indicated.

As mentioned in the introduction, it has been established that NAA-inhibited PIN endocytosis relies on the putative auxin receptor ABP1 and activation of ROP/RIC signaling (Robert et al., 2010; Lin et al., 2012; Chen et al., 2012). To verify at what level Ca^{2+} could be operating in relation to these molecular players, we performed preliminary experiments in which we evaluated PIN endocytosis upon CaMIN treatment in mutants related to ABP1 and ROP/RIC signaling.

To address if Ca^{2+} would be operating up- or downstream of ABP1, we studied CaMIN-induced PIN internalization in the EtOH-inducible ABP1 antisense mutant (AtABP1AS, Braun et al., 2008) and upon cotreatment with α-(phenyl ethyl-2-one)-indole-3-acetic acid (PEO-IAA), an auxin derivative that specifically activates non-transcriptional auxin signaling (Robert et al., 2010) (Fig. S2). Under control conditions, PIN endocytosis was inhibited in the AtABP1AS mutant and after PEO-IAA treatment reflected by the lack of PIN-accumulating BFA bodies (Fig. S2, B, E). However, in CaMIN medium inhibition of PIN endocytosis was bypassed (Fig. S2, D, F), suggesting that Ca^{2+} operates downstream of ABP1.

ROP/RIC activity is negatively regulated by GUANINE NUCLEOTIDE DISSOCIATION INHIBITORs (GDIs). The mutant *supercentipede1* (*scn1*) is defective in a RHO-GDI resulting in constitutive ROP/RIC activity (Carol et al., 2005). In preliminary experiments we observed that upon BFA treatment of the *scn1* mutant less PIN1-accumulating BFA bodies were formed (Fig. S3, B, E) which fits the model in which ROP/RIC activation is required for inhibition of PIN internalization by NAA. After pretreatment with CaMIN this reduced PIN1 endocytosis was overcome (Fig. S3, D, E) suggesting that Ca^{2+} is also operating downstream of ROP/RIC. Together, these observations suggest that Ca^{2+} functions downstream of ABP1 and ROP/RIC signaling in the inhibition of PIN endocytosis by NAA. However, given the current controversy on the involvement of ABP1 in auxin signaling, it remains unclear what the role of ABP1 is in NAA-regulated PIN endocytosis.

Ca^{2+} drugs impair late endosomal trafficking

BFA targets the activity of several ARF-GEFs in *Arabidopsis*, such as GNOM and BIG2 (Geldner et al., 2003; Kitakura et al., 2017), thereby impairing many processes in the endosomal trafficking pathway. Moreover, altered Ca^{2+} signalling can have dramatic effects on endomembrane trafficking and polarity, which are thus far poorly characterized in plants (Section I – Chapters 1 and 2) (Himschoot et al., 2015; Himschoot et al., 2017). During live imaging of roots, we observed via the transmitted light channel that the Ca^{2+} drugs induced vacuolar rounding and possibly also swelling. Therefore, we tested markers for the Golgi Apparatus (SYNTAXIN OF PLANT32 (SYP32)- GFP/WAVE22) (Geldner et al., 2009), Early Endosomes/*trans*-Golgi Network (EEs/TGN; VHAa1-mRFP, SYP42-YFP) (Dettmer et al., 2006) Uemura et al., 2012), late endosomes (LEs; ARA7-mRFP, VAMP727-YFP, 2xFYVE-YFP) (Gillooly et al., 2001; Ueda et al., 2004; Ebine et al., 2008) and the vacuole (SYP22-YFP) (Robert et al., 2008). No obvious differences could be observed in the shape and size of SYP32-YFP-, VHAa1-mRFP-, SYP42-YFP-, and SYP22-YFP-labelled endosomes after treatment with CaMIN in comparison to CaPLUS. However, clear differences became apparent for LE/MVB markers treated with the Ca^{2+} pharmacology (Fig. 3). ARA7-positive endosomes became enlarged upon W-7 treatment (Fig.3, E), an effect that is reminiscent of Wortmannin (Wm) treatment and mutation in SAND/CCZ1 (Ebine et al., 2008; Singh et al., 2014), suggesting that W-7 affects TGN to MVB maturation. Moreover, Bepridil and W-7 caused a dramatic mislocalisation of the R-SNARE VAMP727 to the tonoplast (Fig. 3, I, J), all features that are consistent with severe defects in vacuolar trafficking by these Ca^{2+} drugs. However, the PI3P marker 2xFYVE-YFP did not become cytoplasmic upon Bepridil treatment (Fig. 3, N), as would be the case after treatment with the PI3P kinase inhibitor Wm (Vermeer et al., 2006), suggesting that it does not interfere with PI3P production. Even though Nifedipine has profound effects on PIN internalization, it did not seem to affect LE morphology like Bepridil and W-7 (Fig. 3, C, H, M) suggesting Nifedipine has a different mode of action.

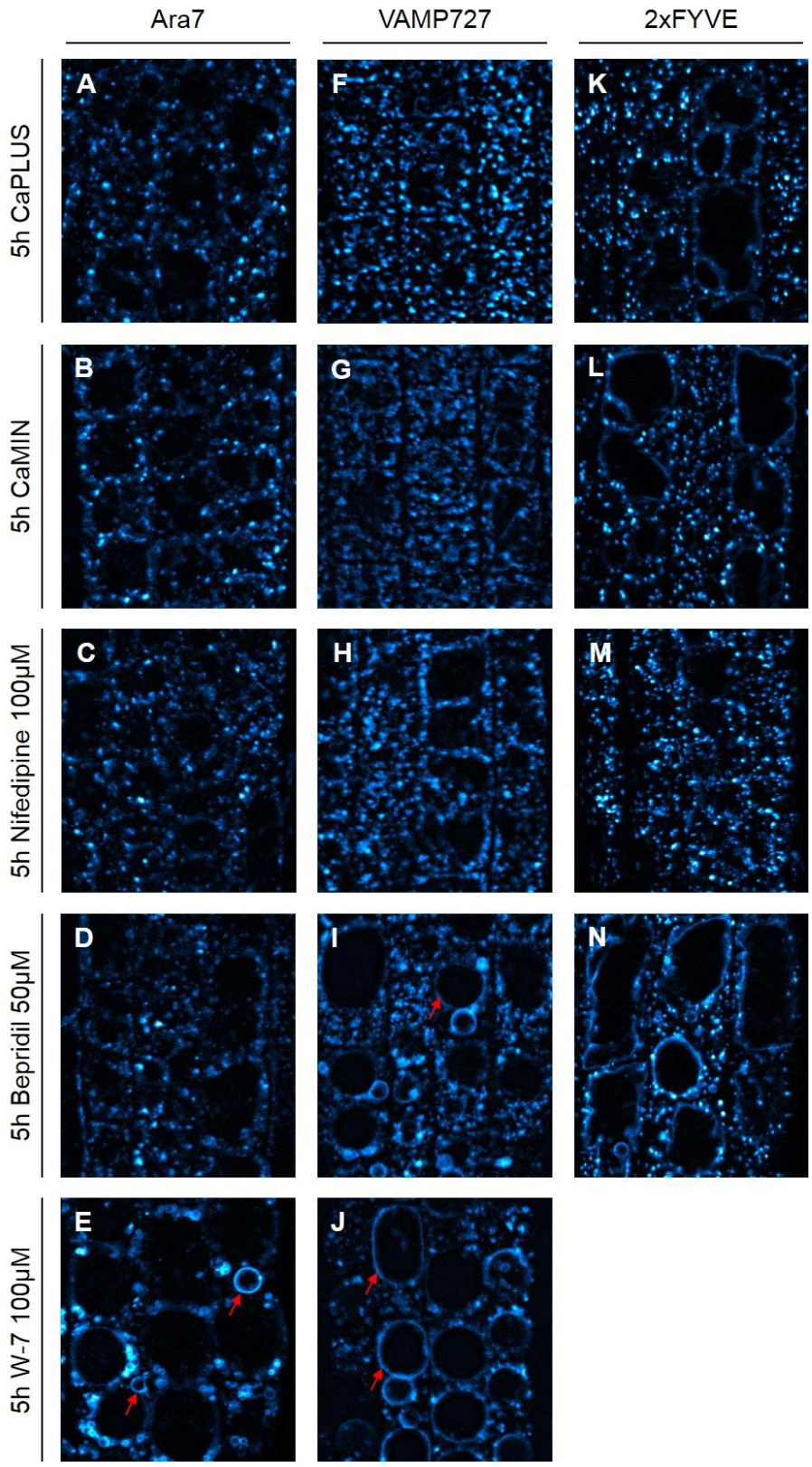

Figure 3: Impact of CaMIN and Ca^{2+} drug treatment on MVB/LE/PVC markers. (A-E) Ara7, (F-J) VAMP727, (K-N) 2xFYVE. Treatments were performed for 5h with concentrations as shown in the figure. (I) 5h treatment with 50µM Bepridil resulted in tonoplast-localized VAMP727 (red arrow). (E, J) 5h treatment with 100µM W-7 results in Ara7 swelling (red arrows) (E), and tonoplast-localized VAMP727 (red arrows) (J).

At the ultrastructural level, prolonged CaMIN treatment did not cause any significant differences in organelle morphology compared to CaPLUS control (Fig. 4, A). Yet, in some cases, root epidermal cells displayed clusters of enlarged TGN/EEs near the *cis*-side of the Golgi Apparatus (GA) (Fig. 4, A-C), and some GAs appeared to have a more cup-shaped appearance (Fig. 4, D). Nifedipine treatment resulted in swelling of the Golgi cisternae that became less electron-dense, reflecting lower protein content, than in the control (Fig. 4, E, F). Bepridil-treated roots in general seemed to have more MVBs/LEs, which often seemed enlarged with a large number of intraluminal vesicles (Fig. 4, G, H), consistent with the defect in vacuolar trafficking as suggested by the mislocalisation of late endosomal markers (Fig. 3). However, more images are required to perform a quantitative analysis of MVB/LE sizes and their intraluminal vesicles. Furthermore, the TGN/EE appeared clustered in some cells (Fig. 4, G, H). As for Bepridil, also W-7 treatment seemed to generate enlarged MVBs/LEs and clustering with TGN in some cases (Fig. 4, I, J).

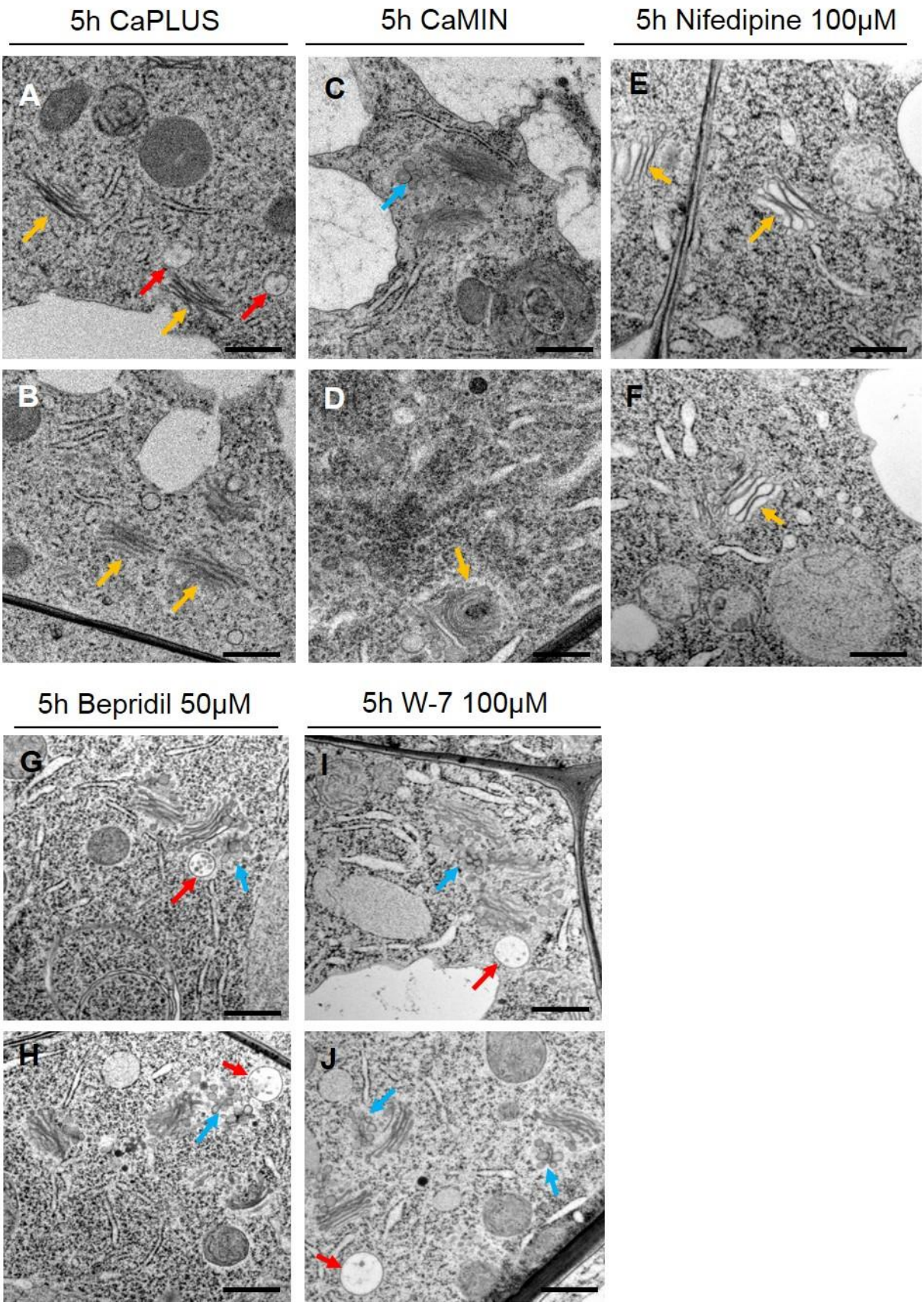

Figure 4: Transmission electron microscopy images of root epidermal cells after CaMIN and Ca^{2+} drug treatment. Root epidermal cell ultrastructure upon 5h treatment with CaPLUS, CaMIN, 100µM Nifedipine, 50µM Bepridil, and 100µM W-7. (A, B) The GA and MVBs indicated by yellow and red arrows respectively reflect the

typical morphology of the Golgi and MVBs/LEs under control conditions. (C, D) In CaMIN-treated roots few TGN clusters (blue arrow) and rounded Golgis (yellow arrow) can be observed. (E, F) Nifedipine treatment results in swollen Golgi cisternae (yellow arrows). (G, H) Generally, MVBs/LEs seem more abundant and enlarged after Bepridil treatment (red arrows), and the TGN appears clustered and swollen (blue arrows). (I, J) As for Bepridil, W-7 also seems to induce MVB/LE swelling (red arrows), and in some cases enlarged and clustered TGN (blue arrows). The scale bar corresponds to 1.0μM.

Together these data demonstrate that Ca^{2+} drugs have profound effects on the endomembrane system in plants. This suggests that the PIN internalization seen during BFA/NAA cotreatment in combination with such Ca^{2+} drugs might be a consequence of a pleiotropic defect in vacuolar trafficking. Therefore, we sought to explore the origin of the internalized PINs in each of the Ca^{2+} manipulations.

Previously, a screen for mutants with reduced BFA-sensitive PIN trafficking resulted in the identification of ARF-GEF BFA-VISUALIZED ENDOCYTIC TRAFFICKING DEFECTIVE1 (BEN1)/BFA-INHIBITED GEF5 (BIG5)/ HOPM INTERACTOR7 (MIN7) (Tanaka et al., 2009), and the Sec1/Munc18 protein BEN2/VACUOLAR PROTEIN SORTING45 (VPS45) (Tanaka et al., 2013), as key regulators of early endocytic trafficking. Consistently with their reported reduced BFA-sensitive PIN trafficking, the *ben1-1 ben2* mutants displayed strong defects in PIN1 accumulation in BFA bodies in CaPLUS (Fig. 5, A, B). Also in CaMIN conditions, PIN1 accumulation in BFA bodies was strongly reduced (Fig. 5, C, D). Similarly, *ben1-1 ben2* double mutants showed reduced PIN1 accumulation in BFA bodies compared to WT, when cotreated with Ca^{2+} channel inhibitors Bepridil and Nifedipine or the CaM inhibitor W-7 (Fig. 5, E-J). Together, these findings suggest that the effect of Ca^{2+} signaling on the BFA sensitivity of PIN trafficking depends on BEN1 and BEN2 function.

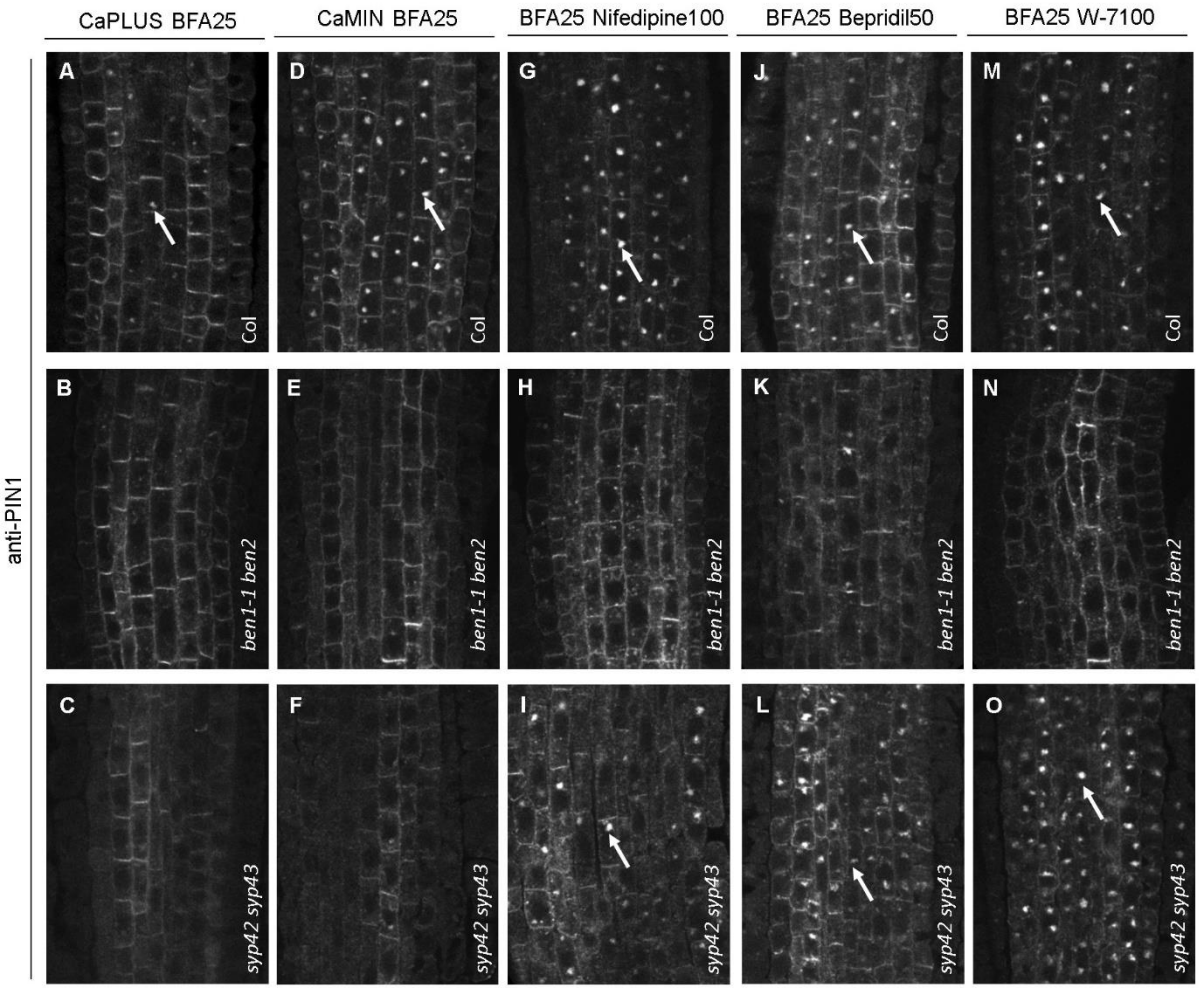

Figure 5: The effect of CaMIN and Ca^{2+} drug on PIN trafficking in *ben1-1 ben2* and *syp42 syp43*. (A, D, G, J, M) Immunolocalisation of PIN1 in wild type upon 25µM BFA cotreatment with (A) CaPLUS, (D) CaMIN, (G) 100µM Nifedipine, (J) 50µM Bepridil, and (M) 100µM W-7. In all cases PIN1-accumulating BFA bodies can be observed (white arrows). (B, E, H, K, N) Immunolocalisation of PIN1 in *ben1-1 ben2* upon 25µM BFA cotreatment with (B) CaPLUS, (E) CaMIN, (H) 100µM Nifedipine, (K) 50µM Bepridil, and (N) 100µM W-7. No PIN internalization can be observed. (C, F, I, L, O) Immunolocalisation of PIN1 in *syp42 syp43* upon 25µM BFA cotreatment with (C) CaPLUS, (F) CaMIN, (I) 100µM Nifedipine, (L) 50µM Bepridil, and (O) 100µM W-7. Note the BFA body formation upon cotreatment with the Ca^{2+} drug, but not CaMIN (white arrows). Seedlings were pretreated with CaPLUS, CaMIN, and the Ca^{2+} drug for 30min prior to 1h co-incubation with BFA.

BEN2/VPS45 controls vacuolar trafficking via the SYP41/SYP61/VTI12 SNARE complex (Zouhar et al., 2009), and the *syp42 syp43* double mutant is defective in secretion and vacuolar trafficking (Uemura et al., 2012). Interestingly, in contrast to *ben1-1 ben2* mutants (Tanaka et al., 2009; Tanaka et al., 2013), *syp42 syp43* does not show defects in uptake of the endocytic tracer dye FM4-64 (Uemura et al., 2012). This suggests that the trafficking defects of *syp42 syp43* are more specific to vacuolar trafficking and secretion, than those in *ben1-1 ben2*. When we analyzed PIN internalisation in the *syp42 syp43* double mutant PIN1 accumulation in BFA

compartments was strongly reduced both in CaPLUS and CaMIN, similarly as for *ben1-1 ben2* (Fig. 5, K, L). However, in contrast to *ben1-1 ben2*, Bepridil, Nifedipine, and W-7 reinstalled the capacity for PIN1 accumulation in BFA bodies in *syp42 syp43* cotreated with BFA (Fig. 5, M-O) and had regained levels that were comparable to those in the WT controls. This suggests that Bepridil, Nifedipine and W-7 have effects on endocytic trafficking in the late endosomal pathway that are not affected by the CaMIN treatment.

Ca^{2+} versus CME

Previously, we demonstrated that NAA interferes with PIN internalization via inhibition of CME (Robert et al., 2010). Therefore, we tested if CaMIN conditions counteract the negative effect of NAA on the plasma membrane residence of clathrin. Consistently with previous reports, we observed that in Ca^{2+}-containing medium (CaPLUS), NAA treatment strongly reduced the number of cells with plasma membrane-localized CLATHRIN LIGHT CHAIN2-GFP (CLC2-GFP) in comparison to the DMSO treated control (Fig. 6, A vs. B). When the NAA treatment was performed in CaMIN (Fig. 6, C), a significant increase in the fraction of cells with CLC2-GFP at their plasma membranes was observed in comparison to NAA-treated roots in CaPLUS (Fig. 6, D,E). This corroborates the notion that Ca^{2+} acts downstream of auxin to inhibit CME.

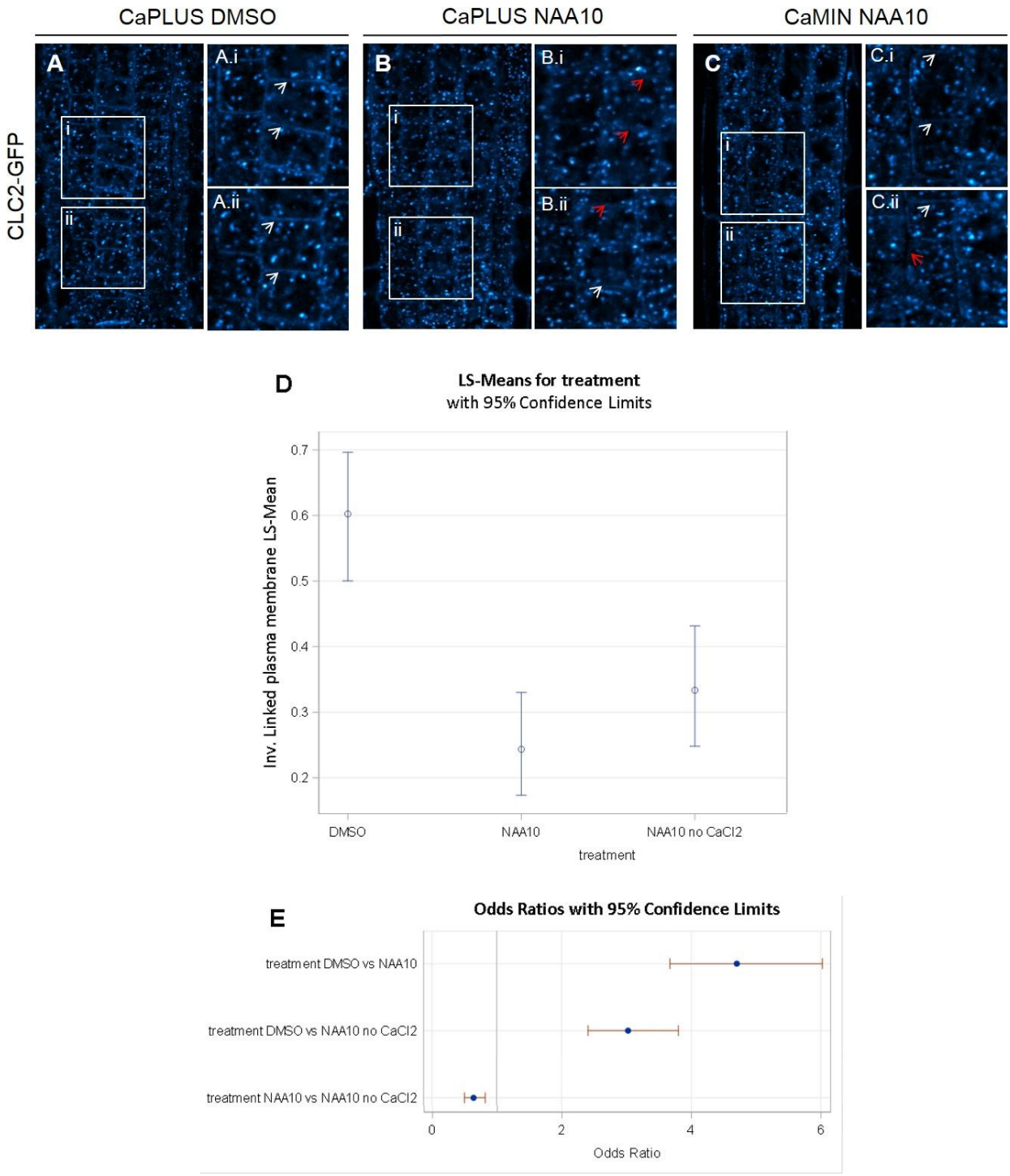

Figure 6: Extracellular Ca^{2+} is involved in auxin-induced displacement of CLATHRIN LIGHT CHAIN 2 (CLC2) from the plasma membrane. CLC2-GFP localization after 1h treatment with (A) DMSO or (B, C) 10µM NAA in CaPLUS (B) and CaMIN (C). Besides the prominent intracellular CLC2-GFP localization, CLC2-GFP is also present a the plasma membrane (i,ii) Details from the respective images. The white and red arrows highlight plasma membranes with and without CLC2-GFP respectively. Seedlings were pretreated for 30min with CaPLUS/CaMIN. (D, E) Quantification and the statistical analysis of the average proportion of cells with plasma membrane-localized CLC2-GFP under the different treatments. (D) The probabilities that CLC2-GFP is localized at the plasma membrane in each of the three treatments as indicated by the Least Square (LS) Means (calculated via linear regression). Error bars indicate the respective lower and upper 95% confidence limits. A high LS Means in DMSO is consistent with a high probability that CLC2-GFP is localized at the plasma membrane. Upon NAA treatment in CaPLUS the probability of finding cells with plasma membrane-localized CLC2-GFP was strongly reduced,

reflecting the inhibitory effect of NAA on CME. When NAA treatment is performed in CaMIN, the probability of finding cells with CLC2-GFP at the plasma membrane was increased, indicating the importance of extracellular Ca^{2+} for CLC2 displacement by NAA. (E) The odds ratios for contrasting the different treatments. The effect of treatment is significant at the 0.05 level when the value 1 (vertical line) is not comprised within the 95% confidence interval as delineate by the error bars.

Next, we questioned if CME would be required for the effects of CaMIN on PIN internalization. Therefore, we used an inducible, dominant-negative fragment of the clathrin coat subunit CHC1 (HTAM>>HUB1) (Kitakura et al., 2011), the inducible silencing of the T-PLATE endocytic adaptor complex subunit TML (amiR-TML) (Gadeyne et al., 2014), and inducible overexpression of the clathrin coat disassembly factor AUXILIN2 (XVE>>AX2-1) (Ortiz-Morea et al., 2016) impairing clathrin-mediated trafficking both at the TGN/EE and PM (HTAM>>HUB1, XVE>>AX2-1) and specifically at the PM (amiR-TML). Consistently with previous reports, induction of these endocytosis-interference constructs resulted in a strong inhibition of PIN accumulation in BFA bodies when the BFA treatment was done in CaPLUS conditions (Fig. 7, A vs B, E vs F, I vs J). Surprisingly, under CaMIN conditions, the complete inhibition of PIN1 accumulation in BFA bodies was by-passed in the HTAM>>HUB1 and amiR-TML line (Fig. 7, D, H), but not in the XVE>>AX2-1 line (Fig. 7, L). Furthermore, the BFA body size in the amiR-TML line seems smaller than in the estradiol-treated control (Fig. 7, H). This implies that the effect of CaMIN on PIN trafficking cannot be solely explained by CME, but could involve an alternative clathrin-independent pathway. However, this does not seem to be in line with the observations for the XVE>>AX2-1 line. The fact that we cannot observe a similar phenotype in the XVE>>AX2-1 line might be explained by the fact that inhibition of CME by the XVE>>AX2-1 construct is much stronger than for the HTAM>>HUB1 and amiR-TML construct. Induced XVE>>AX2-1 seedlings show an occasional accumulation of excess of membranous material around the cell (Ortiz-Morea et al., 2016) which results from a strong inhibition of CME while secretion proceeds normally. This could possibly also explain the loss of PIN polarity in the XVE>>AX2-1 seedlings in the immunolocalization experiments (Fig. 7, J, I). Similar phenotypes have not been reported for the HTAM>>HUB1 and amiR-TML lines. Furthermore, in contrast to the HTAM>>HUB1 and amiR-TML, induction of AX2-1 overexpression results in inhibition of root growth. Altogether, these observations suggest a stronger CME inhibition by AX2-1 overexpression which could explain the distinct phenotypes for the XVE>>AX2-1 versus HTAM>>HUB1 and amiR-TML line. Furthermore, not much is

known about the impact of this AX2-1 overexpression on other endomembrane trafficking steps and the endomembrane system itself which could complicate the interpretation of our observations.

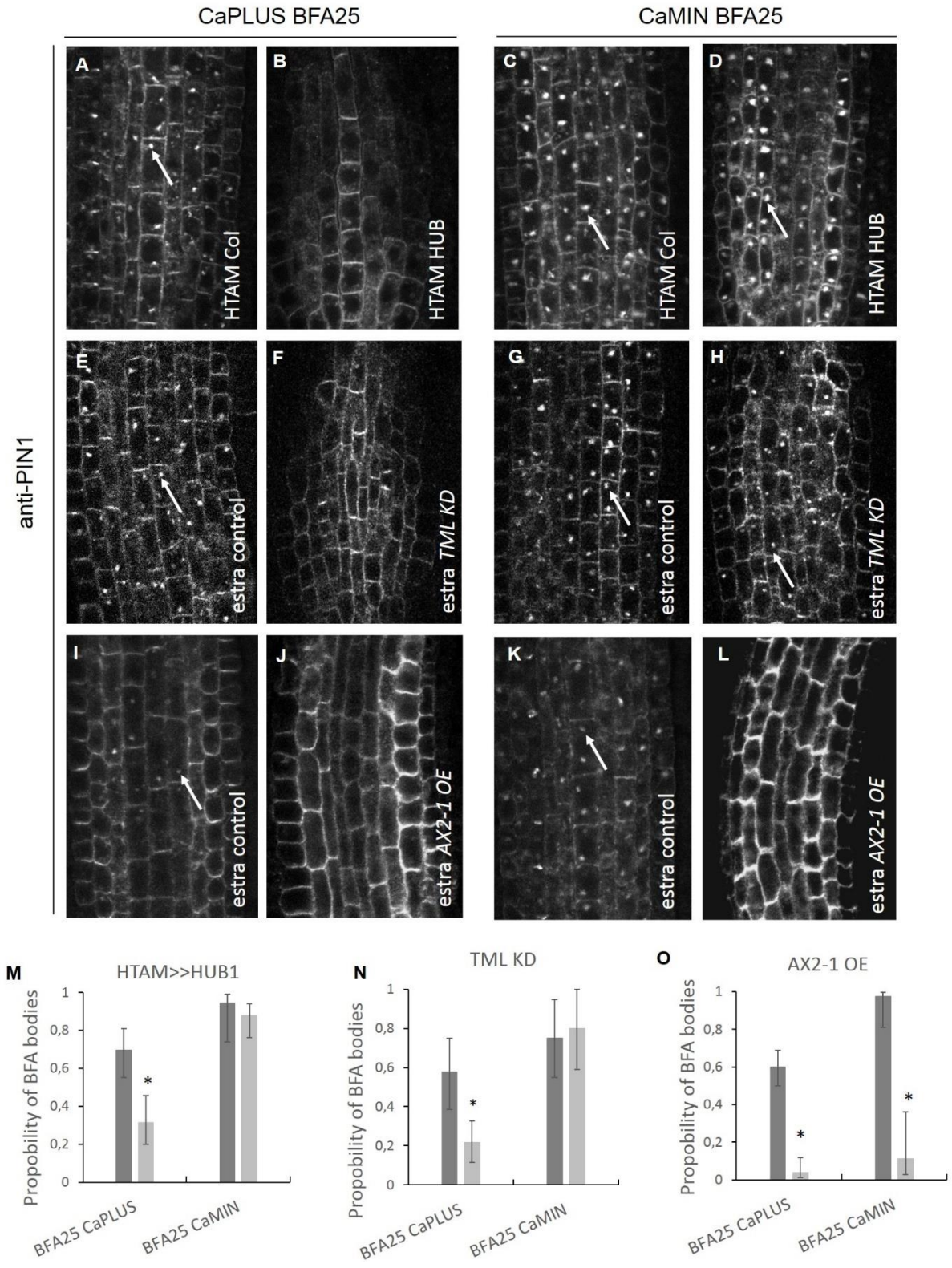

Figure 7: CaMIN treatment enhances PIN1 internalization partially via CME. Immunolocalization of PIN1 in 4 day-old roots treated for 1h with 25µM BFA. (A,B) Under CaPLUS conditions, hydroxytamoxifen (HTAM)-treated wild type seedlings formed PIN1-accumulating BFA bodies (A), while HTAM-treated inducible dominant negative CLATHRIN HEAVY CHAIN1 (CHC1) seedlings (HTAM>>HUB1) did not (B). (C,D) Under CaMIN conditions, both HTAM-treated wild type (C) and HTAM>>HUB1 (D) seedlings formed BFA bodies. (E,F) Under CaPLUS conditions, estradiol (estra)-treated controls formed BFA bodies (E). Estradion-induced TML knock-down (KD) lines did not (F). (G,H) Under CaMIN conditions, both estradiol-treated controls (G) and induced TML knock-down lines (H) formed BFA bodies. (I,J) The estradiol-treated control showed BFA body formation upon CaPLUS treatment (I), while PIN1 internalization was inhibited in the induced XVE>>AX2-1 overexpression (OE) line (J). Under CaMIN conditions, estradiol-treated controls formed BFA bodies (K), however, in contrast to the other lines, the AX2-1 OE line did not (L). (M-O) Quantification of the probability of BFA bodies in the cell for (M) wild type (dark grey) versus HTAM>>HUB1 (light grey), (N) wild type (dark grey) versus TML knock-down (light grey), and (O) wild type (dark grey) versus AX2-1 OE (light grey). The asteriks represents a p-value <0.05. The error bars represent the 95% confidence interval ($n > 5$). Seedlings were pretreated for 30min with CaPLUS/CaMIN. White arrows indicate PIN1-accumulating BFA bodies.

To better understand these observations, we performed preliminary experiments to assess the contribution of clathrin-independent endocytosis to PIN internalization in CaMIN. Therefore, we used methyl-β-cyclodextrin (MβCD) to interfere with lipid-raft-dependent, clathrin-independent endocytosis. This sterol depleting agent efficiently disrupts the sterol-rich detergent-resistant membranes (DRMs; Valitova et al., 2014), also called lipid rafts. When BFA and MβCD cotreatment was performed in CaMIN, no PIN1-accumulating BFA bodies could be observed (Fig. S4, D) suggesting that PIN internalization in CaMIN in the absence of MβCD is mediated by lipid raft-dependent endocytosis. However, similar observations were made in the control medium (Fig. S4, B), opposing the well-established notion that under control conditions PIN internalization relies on clathrin-mediated endocytosis which should not be affected by MβCD treatment. This suggests that MβCD might have secondary effects, thereby directly or indirectly also impairing CME, making it difficult to interpret the outcome of these experiments. Therefore, alternative approaches will have to be explored to address the contribution of clathrin-independent endocytosis.

Cytoplasmic Ca^{2+} is sufficient to inhibit CME

Based on the observation that Ca^{2+} acts downstream of auxin to inhibit CME, we hypothesized that Ca^{2+} signaling negatively regulates endocytosis. Therefore, we targeted Ca^{2+}-ATPase activities as a means to increase cytoplasmic Ca^{2+} levels artificially with the fluorescein derivative, Eosin Y, which efficiently inhibits AUTO-INHIBITED Ca^{2+}-ATPASEs (ACAs) (Bonza et

al., 2013). Consistently with our hypothesis, Eosin Y pretreatment followed by a co-treatment with BFA plus Eosin Y, strongly interfered with PIN1 internalization in BFA bodies (Fig. 8, A, B), suggesting that PIN internalization was inhibited by increased cytoplasmic Ca^{2+} signaling. To confirm that the observed effects of Eosin Y on PIN internalization could indeed be attributed to interference with Ca^{2+}-ATPases, we analyzed the BFA sensitivity of PIN trafficking in amiRNA lines designed to target 9 out of 13 auto-inhibited Ca^{2+}-ATPases in the *Arabidopsis* genome (Zhang et al., 2011). In 2 independent lines (lines 2#1 and 6#4), a reduction of PIN1 accumulation in BFA bodies was observed (Fig. 8, C-E). This observation further corroborates the notion that cytoplasmic Ca^{2+} signaling interferes with PIN internalization.

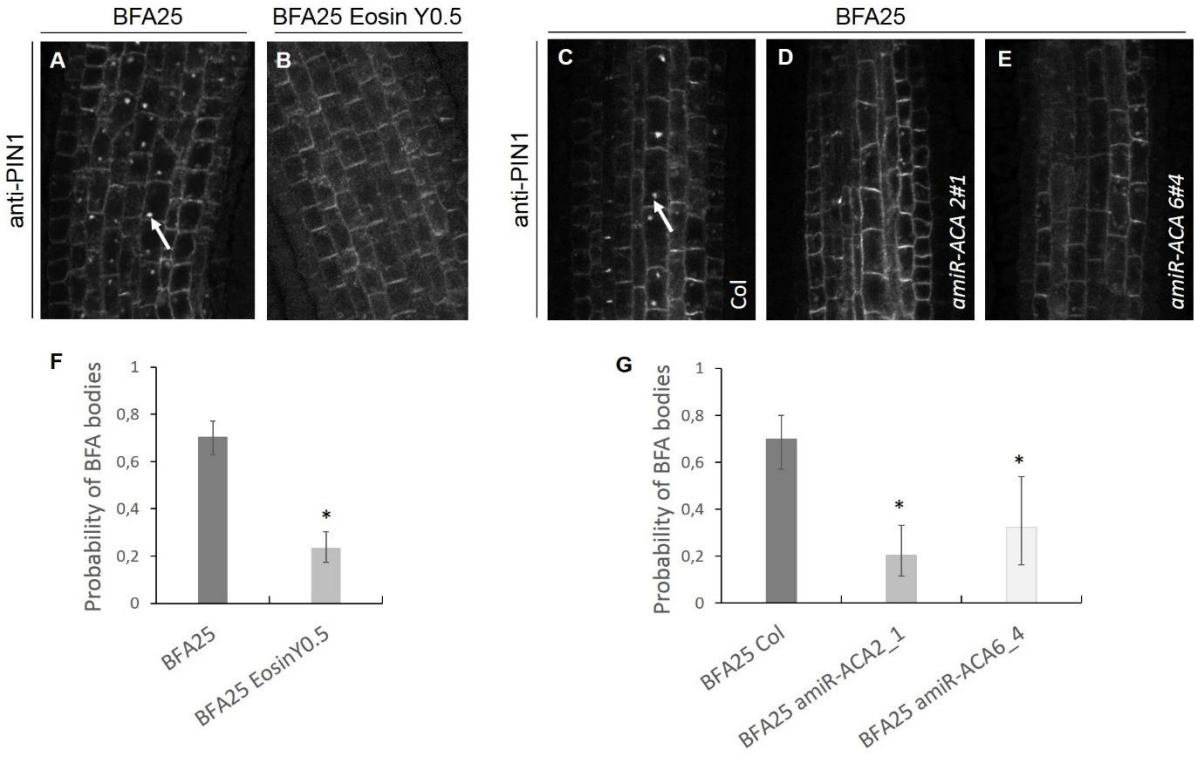

Figure 8: PIN1 localization upon pharmacological and genetic interference with Ca^{2+}-ATPase activity. Immunolocalization of PIN1 in 3 day-old seedling roots. (A, B) Pharmacological interference with ACA function using the Ca^{2+}-ATPase inhibitor Eosin Y. (A) 1 h treatment with 25µM BFA resulted in PIN1 accumulation in BFA bodies (white arrow). (B) Co-treatment with 500nM Eosin Y and 25µM BFA strongly reduced PIN1 accumulation in BFA bodies. (C-E) Genetic interference with ACA function in knock-down lines. 1h treatment with 25µM BFA resulted in BFA body formation in wild type seedlings (C, white arrow), but not in 2 independent knock-down lines, 2#1 (D) and 6#4 (E), expressing amiRNA constructs targeting 9 out of 13 ACAs. (F, G) Quantification of the probability of BFA bodies in the cells upon BFA Eosin Y cotreatment (F) and upon BFA treatment of the ACA knock-down lines (G). The asteriks represents p-values <0.05. The error bars represent the 95% confidence interval (*n* > 8). For Eosin Y treatment seedlings were pretreated for 30min.

Given that CME is the predominant pathway for PIN internalization, we analyzed the effect of Eosin Y on CME dynamics. The progression of CME involves the sequential recruitment of different adaptor complexes that organize all the cargoes in budding endocytic vesicles. The final step of this process requires the activity of DYNAMIN-RELATED PROTEINS (DRPs), which are involved in membrane scission of the budding vesicle. The dynamics of DRPs at the plasma membrane thus reflect the progression through endocytosis. Under control conditions (DMSO), the dwell time of DYNAMIN-RELATED PROTEIN1c-GFP (DRP1c-GFP) at the plasma membrane ranges between 10 and 50 seconds (Fig. 9, A, C). However, in Eosin Y-treated roots, DRP1c-GFP dwell times were dramatically prolonged (Fig. 9, B, D), suggesting an arrest in CME progression. Together, these data demonstrate that cytoplasmic Ca^{2+} is a potent negative regulator of CME.

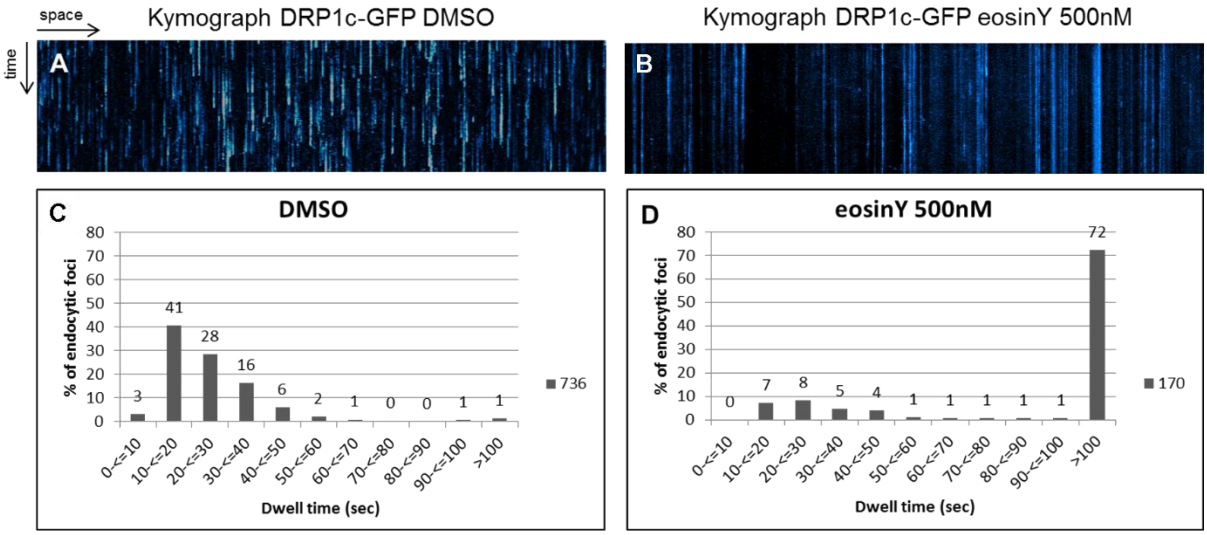

Figure 9: Eosin Y treatment arrests DYNAMIN-RELATED PROTEIN1c (DRP1c) at the plasma membrane. Kymographs of time-lapse recording (100 sec) of DRP1c1-GFP in elongated root epidermal cells treated for 90min with (A) DMSO or (B) 500nM Eosin Y. The length of the vertical lines is proportional to the life-time (dwell time) of a DRP1c-labelled endocytic spot at the plasma membrane. (C, D) Quantification of dwell time upon (C) DMSO and (D) 500nM Eosin Y treatment. Eosin Y treatment prolongs the life-time of the DRP1c-labelled endocytic spots supporting the inhibitory effect of elevated cytosolic Ca^{2+} on CME.

Ca^{2+}-dependent kinase activity inhibits PIN internalization

We thus established a model in which Ca^{2+} acts downstream of auxin to inhibit CME. Therefore, we aimed to explore the underlying molecular mechanism. The *Arabidopsis*

genome encodes many Ca^{2+}-sensing proteins, as illustrated by the observation that it encrypts more than 250 proteins that have at least one EF hand, a canonical Ca^{2+}-sensing domain. In many Ca^{2+}-dependent signaling cascades, phosphorylation plays an important role. Indeed, inhibition of PROTEIN PHOSPHATASE A activity with Cantharidin interfered with PIN internalization (Fig. 10, A, B), which could be partially overcome in CaMIN medium (Fig. 10, C). Conversely, treatment with the kinase inhibitor Staurosporin induced PIN internalization in the presence of NAA (Fig. 10, F).

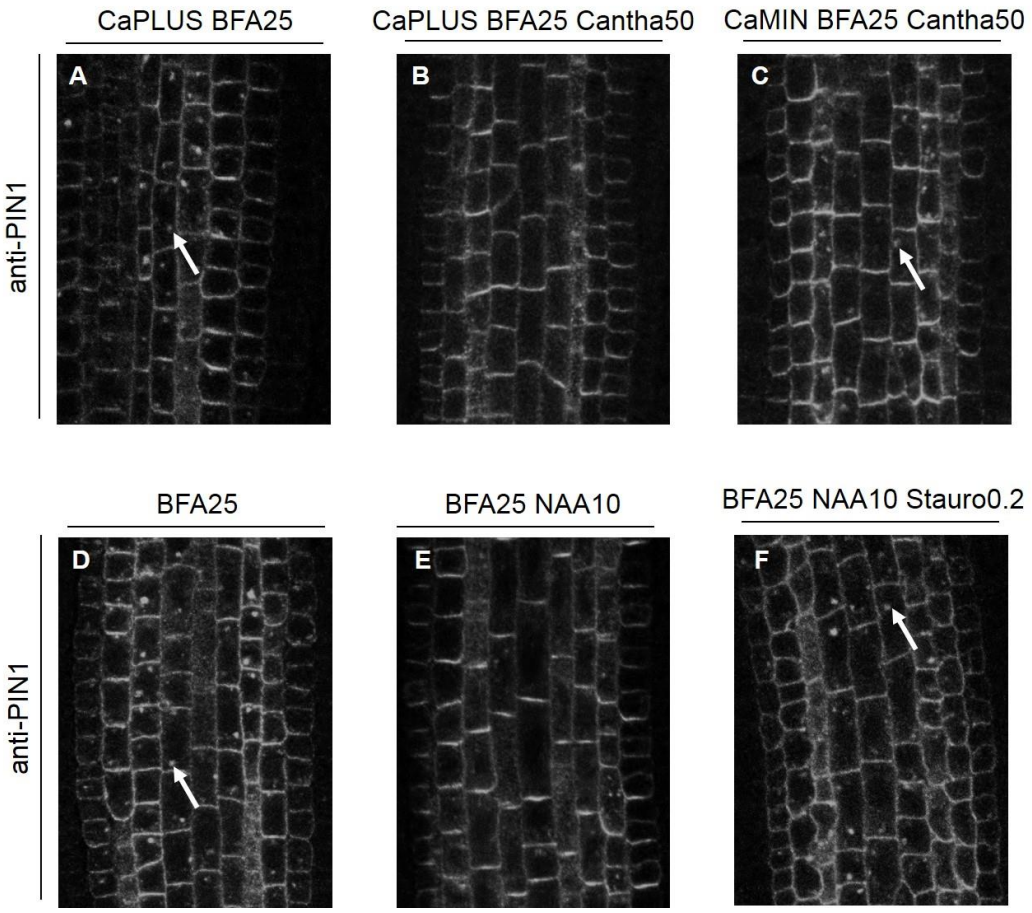

Figure 10: PIN1 localization upon pharmacological interference with kinase and phosphatase activity. (A-C) Pharmacological interference with phosphatase inhibitor Cantharidin. Upon 1h treatment with 25µM BFA in CaPLUS, PIN1-accumulating BFA bodies are formed (A). Upon cotreatment with 50µM Cantharidin (Cantha) PIN1 internalization is inhibited (B). However, this is partially overcome when BFA Cantharidin treatment is performed in CaMIN (C). (D-F) Pharmacological inhibition of kinase activity. In the BFA control, PIN1-accumulating BFA bodies can be observed (D), while cotreatment with 10µM NAA results in inhibition of PIN1 endocytosis and consequently lack of BFA bodies (E). Upon cotreatment with 200nM Staurosporine (Stauro) NAA-inhibited PIN endocytosis is overcome and BFA bodies can be observed (F). For inhibitor treatments seedlings were pretreated for 30min. White arrows indicate PIN1-accumulating BFA bodies.

Together, these observations suggest that an increased phosphorylation status is associated with inhibition of PIN internalization. Therefore, we explored a large set of published Ca^{2+}-sensing mutants for altered sensitivity of BFA-visualized PIN internalization to NAA. An important fraction of Ca^{2+} signaling in plants involves kinase activity via Ca^{2+}-DEPENDENT KINASEs (CPKs), and CALCINEURIN B-LIKE (CBL)-CBL-INTERACTING PROTEIN KINASE (CIPK) complexes. These include CPK single (*cpk1*, *cpk2*, *cpk3*, *cpk4*, *cpk5*, *cpk6*, *cpk7*, *cpk8*, *cpk10*, *cpk11*, *cpk13*, *cpk21*, *cpk28, cpk30*) and higher order mutants (*cpk5/6*, *cpk5/6*, *cpk1/2/5/6*, *cpk3/5/6/11*, *cpk7/8/32* and *cpk4/11*) (Boudsocq et al., 2010; Kanchiswamy et al., 2010; Franz et al., 2011; Hubbard et al., 2012; Matschi et al., 2013) and CBL higher order mutants (*cbl1/4/5/9*, *cbl2/3*, *cbl1/4/5/8/9*) (Eckert et al., 2014). However, none of these mutants showed PIN accumulation in BFA bodies upon co-treatment with NAA (data not shown), suggesting that the observed effects of CaMIN on PIN trafficking involve other Ca^{2+} sensors and/or combinations thereof.

In an alternative approach, we followed a gain-of-function screen for the CPK gene family, which displays strong functional redundancy. We generated a collection of estradiol-inducible overexpression lines of constitutive active (CA) variants for 13 out of 34 CPKs in *Arabidopsis* (Cheng et al., 2002). We obtained stable lines for CPK2, CPK3, CPK4, CPK7, CPK8, CPK11, CPK12, CPK13, CPK22, CPK27, CPK28, CPK29 and CPK30. We screened these lines for phenotypes that would reflect defects in auxin-dependent processes after transfer to estradiol medium. For CPK30 belonging to subgroup III (Fig. 11, A), we observed a partial loss of gravitropic root growth after transfer to inductive medium (Fig. 11, B; Fig. S5, C). Similarly, the related CPK13 showed agravitropic root growth upon induction (Fig. S5, B). However, none of the lines expressing slightly divergent subgroup III CPKs, CPK7 or CPK8, showed agravitropic root growth (Fig. S5, D, E). Immunolocalisation revealed reduced PIN2 levels in the root epidermis of induced CPK30 lines (Fig. 11, C, D), which could explain the gravitropic defect. In addition, the polarity of the remant PIN2 protein was reduced as indicated by apical and basal localisations of PIN2 (Fig. 11, C.i). Interestingly, we found that mainly PIN1 accumulation in BFA bodies was strongly reduced in these lines (Fig. 11, D, E). Both CPK13 and CPK30 have been reported to localize to the plasma membrane (Yuan et al., 2007; Ronzier et al., 2014). Reducing extracellular Ca^{2+} availability by pretreatment with CaMIN could not overcome the reduced PIN endocytosis (Fig. 11, G, H) which fits with the idea that CPK30 operates

downstream of Ca^{2+}. Interestingly, pretreatment with Bepridil, Nifedipine, and W-7 did induce PIN1 accumulation in BFA bodies and bypassed the PIN internalisation defect in the CPK30 line (Fig. S6). This suggest a difference in mode of action between CaMIN and these Ca^{2+} drug, as seen by their effects on late endosomal trafficking.

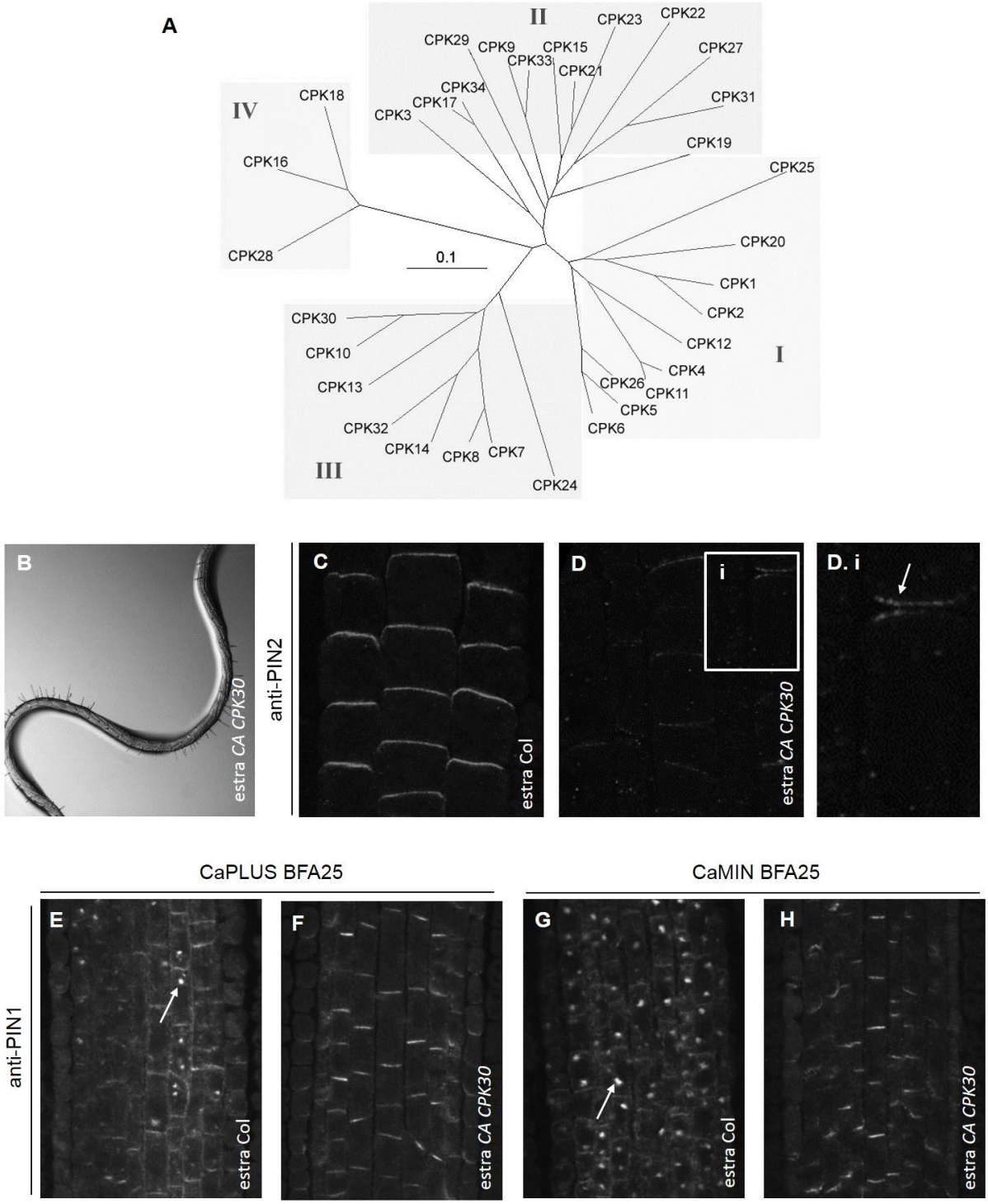

Figure 11: Agravitropic root growth and PIN1/PIN2 immunolocalization upon induction of constitutive active CPK30. (A) Unrooted distance tree based on protein sequence alignment of *Arabidopsis* CPKs (from Cheng et al., 2002). Roman numbers I-IV refer to the different CPK subgroups. The branch lengths are proportional to

divergence, with the scale of "0.1" representing 10% change. (B) Agravitropic root growth in estradiol (estra)-induced CA CPK30 seedling. (C, D) Immunolocalisation of PIN2 in roots. Estradiol-induced CA CPK30 seedlings (D) show a strong reduction in PIN2 abundance compared to wild type (C), and loss of PIN2 polarity (highlighted in D.i). The white arrow points on basal PIN2 which is normally restricted to the apical cell side. (E-H) Immunolocalisation of PIN1 in roots. (E, F) Upon 1h treatment with 25µM BFA in CaPLUS, BFA bodies (white arrow) are formed in estradiol-treated wild type seedlings (E), while the amount of PIN1-accummulating BFA bodies is strongly reduced in estradiol-induced CPK30 seedlings (F). (G, H) Upon pretreatment with CaMIN, BFA body formation is observed in estradiol-treated wild type (G, white arrow), but inhibited PIN endocytosis in the CA CPK30 line is not overcome (H).

Despite the clear effect of constitutive activation of CPK30 on PIN endocytosis, preliminary data showed that dynamics of the endocytic marker DRP1c did not seem to be affected in this line (Fig. S7). Observations from a single experiment showed a similar trend in DRP1c dynamics in both the induced CPK30 seedlings and wild type. Nevertheless, a subtle shift towards shorter dwell times could be observed for the *CA CPK30* line (Fig. S7, D) which might suggest a higher turn-over of DRP1c-labelled endocytic spots at the plasma membrane. However, the number of spots seemed to be strongly diminished (Fig. S7, B, D). Therefore, the defect in endocytosis in the *CA CPK30* line might be explained by a reduced abundance of DRP1c (and possibly other components of the CME machinery) rather than a difference in dynamics. Nevertheless, given the limited amount of seedlings available for this experiment, a biological repeat with a larger sample population is essential to draw reliable conclusions.

Together, these data show that, as for Eosin Y treatment, constitutive activation of CPK13 and CPK30 is sufficient to inhibit PIN internalization. This would suggest a model in which NAA-induced Ca^{2+} would activate CPK signaling leading to inhibition of PIN endocytosis. Identifying CPK13/30 phosphorylation targets could reveal how they regulate PIN endocytosis.

Physiological relevance of Ca^{2+}-regulated PIN trafficking

The question remains what the implications of our observations are for plant growth and development. We have collected preliminary data showing that growth on CaMIN results in shorter roots (Fig. 12, A) (Wang, Vanneste, Beeckman, unpublished results). Furthermore, gravitropic bending of the roots seemed to be delayed on CaMIN (Fig. 12, C), suggesting an underlying issue with auxin transport possibly caused by aberrant PIN localization. This would fit with our observations highlighting the importance of Ca^{2+} for proper regulation of PIN

endocytosis by NAA. To further clarify this hypothesis we should reconfirm these observations and look into DR5 expression marking auxin distribution during gravistimulation on CaMIN.

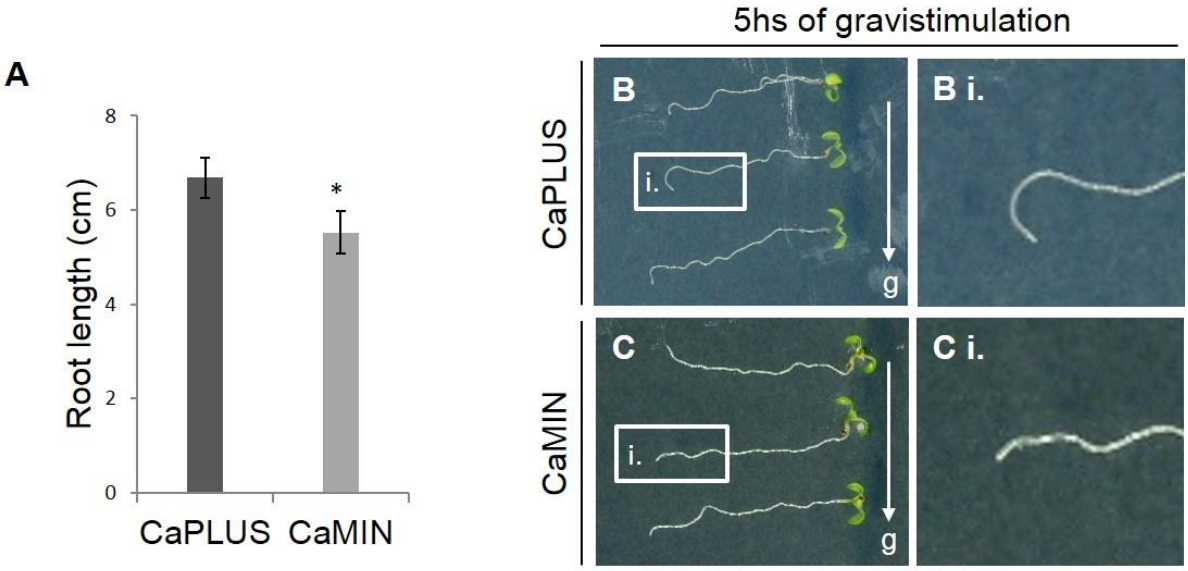

Figure 12: Phenotypic analysis of the root length and root gravitropic response on CaMIN. (A) Quantification of the root length of seedlings grown on CaPLUS and CaMIN. The root length is significantly shorter for roots grown on CaMIN. The asteriks represents a p-value<0,05 (*n* > 59). Four day-old seedlings were transferred to CaPLUS or CaMIN for 6,5 days prior to measurement of the root length. (B, C) Root gravitropic response of seedlings grown on CaPLUS (B) and CaMIN (C) after 5hs of gravistimulation. The arrows show the direction of the gravitropic vector (g). Note that gravitropic bending is delayed on CaMIN. (B i) and (C i) show a detail of a gravistimulated root tip on CaPLUS and CaMIN respectively. Four day-old plants were transferred to CaPLUS or CaMIN 24hs prior to gravistimulation. For gravistimulation the plates were rotated 90°.

Conclusions and perspectives

Based on Ca^{2+} pharmacology and manipulation of extracellular Ca^{2+} availability using 'Ca^{2+} -free medium' (CaMIN) (Fig. 13, Table 1), we have demonstrated that on the one hand Ca^{2+} is required for NAA-inhibited PIN endocytosis, and on the other hand that Ca^{2+} is sufficient for inhibition of PIN internalization.

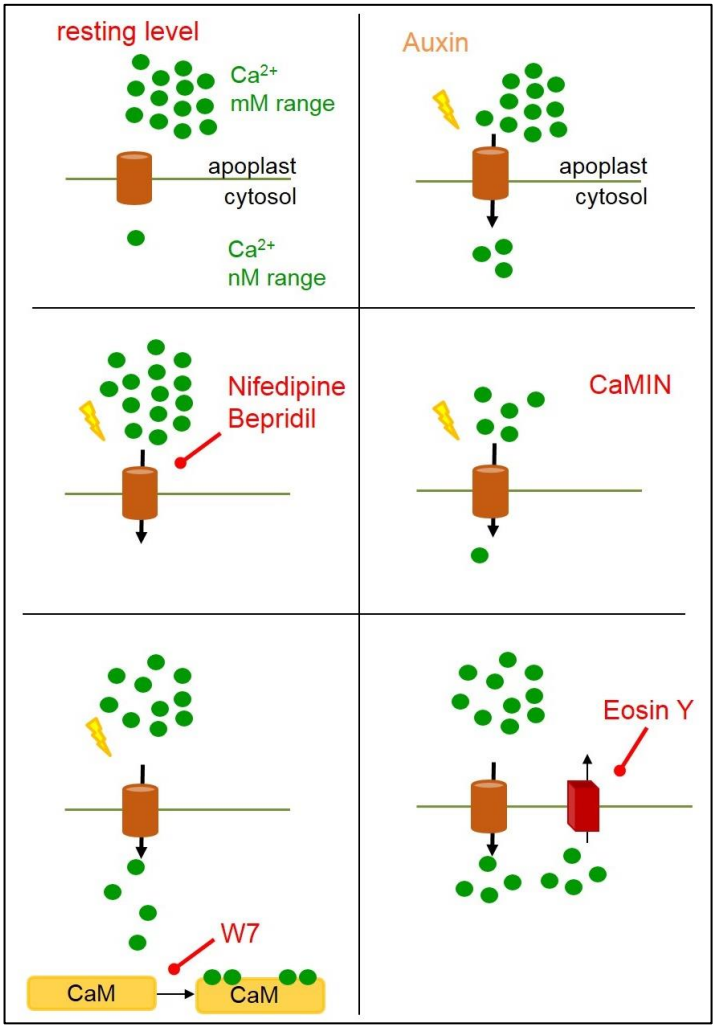

Figure 13: Schematic representation of the impact of Ca^{2+} drug and CaMIN treatment on Ca^{2+} distribution. Ca^{2+} ions, Ca^{2+} channels, and Ca^{2+} pumps are marked in green, brown, and red respectively. CaM: CALMODULIN.

Table 1. Overview of the Ca^{2+} drug used, their putative target and reported effects in plants. Flg22: flagellin peptide (22 amino acid fragment), CaM: calmodulin, ABA: abscisic acid, ACA: AUTO-INHIBITED Ca^{2+}-ATPASEs, ER: endoplasmic reticulum.

DRUG	PUTATIVE TARGET	EFFECTS IN PLANTS
Nifedipine	voltage gated Ca^{2+} channels (animals)	inhibits root hair tip growth (Schiefelbein et al., 1991); reduced blue light response (Łabuz et al., 2016); reduced auxin-induced Ca^{2+} influx (Shishova and Lindberg, 2004); reduced flg22-induced cytosolic Ca^{2+} oscillations (Thor & Peiter, 2014)
Bepridil hydrochloride	non-selective Ca^{2+} channels (animals)	inhibits protoplast division in *P. patens* (Bhatla et al., 2001)
W-7	CaM	inhibits the hypersensitive response to pathogens (Ma et al., 2008); interferes with ABA-induced anti-oxidant defense (Hu et al., 2006)
Eosin Y	ACA Ca^{2+}-ATPases	enhances Ca^{2+} increase in the cytosol and ER (Bonza et al., 2013)

Based on preliminary observations, it seems that Ca^{2+} is operating downstream of the auxin receptor ABP1 and ROP/RIC, two molecular players involved in NAA-inhibited PIN endocytosis. However, given the recent findings on the off-target effects in the ABP1 knock-down lines (see

Section I – Chapter 1) the auxin receptor function of ABP1 and its involvement in this pathway are questionable. Therefore, these data should be interpreted with caution. Meanwhile we are awaiting a molecular explanation that reconciles the observed inhibition of CME in the conditional ABP1 knock-down lines (Robert et al., 2010) and the auxin-resistance of PIN internalization in lines that overexpress a non-auxin-binding variant of ABP1 (Grones et al., 2015). To further consolidate the observation that Ca^{2+} would be operating downstream of ROP/RIC signaling, NAA-induced Ca^{2+} dynamics should be analyzed in the *scn1* background. Also in other signaling cascades, Ca^{2+} was shown to act downstream of ROP signaling (Venus and Oelmüller, 2013), however, this does not exclude the possible existence of another Ca^{2+}-dependent process that acts upstream of ROP signaling. Since *scn1* is defective in a negative regulator of ROP/RIC signaling, it is important to complement our observations with more direct evidence from analysis of overexpression and knock-out mutants of the ROPs and RICs.

The observation that Ca^{2+} is sufficient to inhibit PIN internalization is further corroborated by genetic evidence that constitutively active Ca^{2+} signaling by CPK13 and CPK30 was sufficient to prevent PIN endocytosis. More in depth analysis of the impact of CaMIN and Ca^{2+} drug treatment on endomembrane trafficking revealed that the Ca^{2+} drug not only affect endocytosis but also post-endocytic events such as vacuolar trafficking. Consistently, Ca^{2+} drug-induced PIN internalization was reduced in the early endocytic trafficking mutant *ben1-1 ben2*, but not in the *syp42 syp43* mutant, which is defective in secretion and vacuolar sorting. Furthermore, Bepridil and W-7 treatment resulted in aberrant MVB/LE morphology as shown by analysis of different marker lines and transmission electron microscopy. Interestingly, these effects could not be observed for CaMIN, implying that CaMIN and the Ca^{2+} drug might have distinct modes of action, or affect multiple steps in the endomembrane trafficking pathway.

Further study of the impact of CaMIN treatment revealed that Ca^{2+} operates downstream of NAA in the regulation of CME. Interestingly, we also observed that CaMIN-induced PIN internalization might partially occur via a clathrin-independent mechanism, or that CaMIN possibly affects additional levels in the endocytic trafficking pathway.

Together, these observations cumulate into a model in which NAA-induced Ca^{2+} would inhibit PIN endocytosis via CPK13 and/or CPK30 activity (Fig. 14). Additionally, Ca^{2+} could also operate at distinct levels in the endomembrane trafficking pathway. The Ca^{2+} channel mediating NAA-

induced Ca^{2+} influx and the target(s) of CPK13- and/or CPK30-dependent phosphorylation remain to be identified.

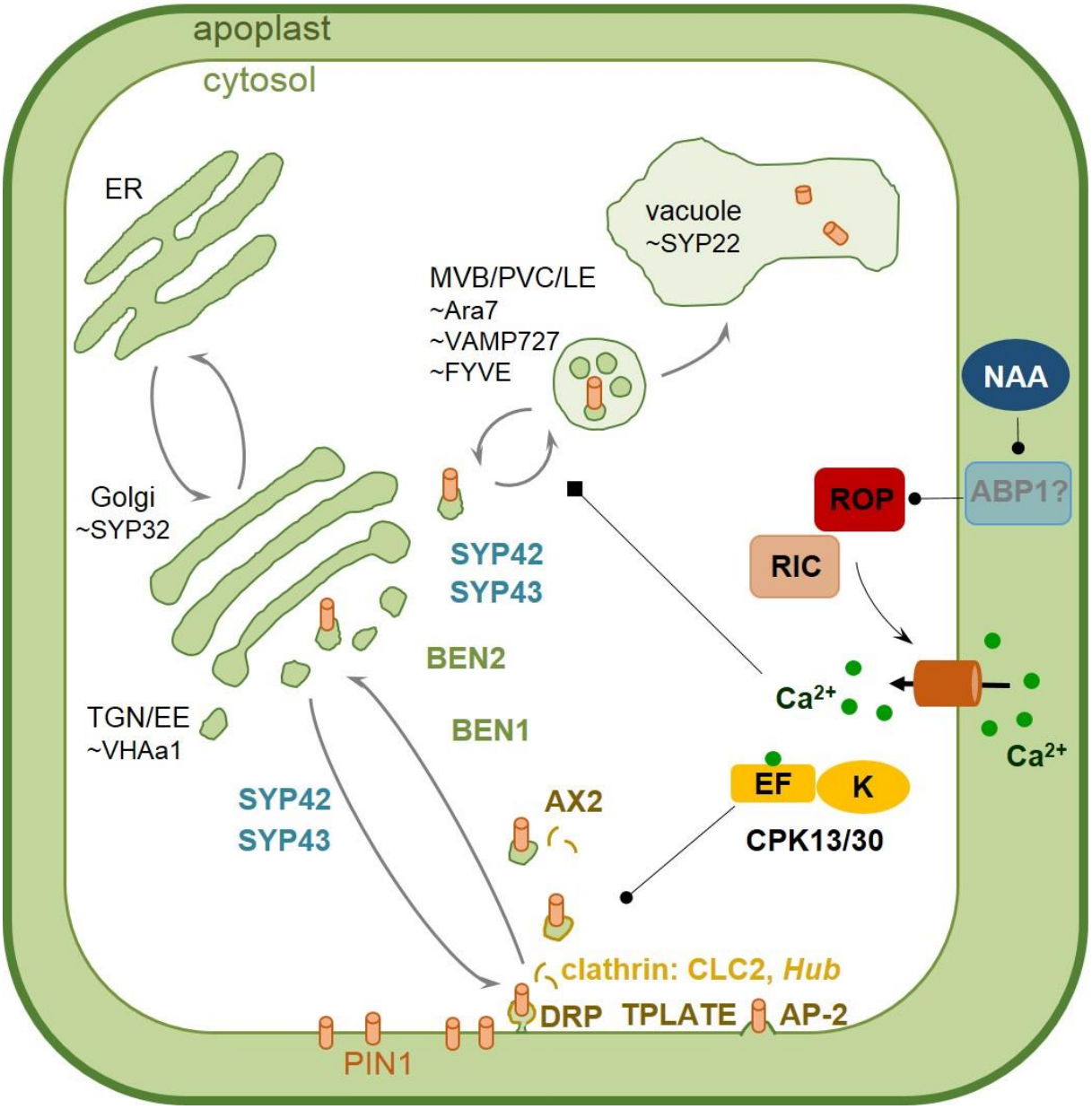

Figure 14: A schematic representation of the proposed model for Ca^{2+}-dependent inhibition of PIN endocytosis by auxin. We hypothesize that NAA-induced Ca^{2+} would activate CPK13/30-dependent signaling leading to inhibition of CME of PINs. Based on preliminary observations, we speculate that Ca^{2+} operates downstream of the auxin receptor ABP1 and ROP/RIC signaling. However, keep in mind that the function of ABP1 as an auxin receptor is currently under debate. Note that Ca^{2+} could possibly also regulate other steps in the endomembrane trafficking pathway e.g. late endosomal trafficking towards the vacuole. The different marker lines (VHAa1, SYP32, Ara7, VAMP727, 2xFYVE, SYP22, DRP1c, CLC2) and regulators (TPLATE complex subunit TML, AX2, BEN1, BEN2, SYP42, SYP43) of endosomal trafficking analyzed in this Chapter are indicated in the figure. Round arrow heads represent inhibition, diamond arrow heads are used where the type of interaction is not known. NAA: 1-

naphthaleneacetic acid; ABP1: AUXIN BINDING PROTEIN1, ROP: RHO-LIKE GTPASE FOR PLANTS, RIC: ROP INTERACTIVE CRIB MOTIF-CONTAINING PROTEINS, EF: EF hand domain, K: kinase domain, VHAa1: V-TYPE PROTON ATPASEa1; SYP: SYNTAXIN OF PLANT; DRP1c; DYNAMIN-RELATED PROTEIN1c; CLC2: CLATHRIN LIGHT CHAIN2; AX2: AUXILIN2; BEN: BFA-VISUALIZED ENDOCYTIC TRAFFIKING DEFECTIVE; CPK: Ca^{2+}-DEPENDENT PROTEIN KINASE.

It should be noted that previous research demonstrated that the *in vitro* activity of both CPK13 and CPK30 is Ca^{2+}-independent since phosphorylation levels of the synthetic peptide syntide-2 by CPK13 and CPK30 did not alter with increasing free Ca^{2+} concentration (Boudsocq et al., 2002). However, in the same assay it was shown that Ca^{2+} sensitivity of CPKs can vary depending on the substrate. Therefore, the absence of Ca^{2+}-dependent activation might be explained by the lack of an appropriate substrate. Furthermore, it is possible that Ca^{2+} binding is not sufficient for activation of these CPKs but forms a prerequisite for additional regulatory processes such as (auto)phosphorylation or phospholipid association (Klimecka and Muszyńska, 2007).

Our data suggest the involvement of CPK13 and CPK30 in inhibition of PIN endocytosis. However, to further consolidate this hypothesis, we should address auxin-inhibited PIN endocytosis in the corresponding knock-out mutants. As described earlier, screening single knock-out mutants did not yield any candidates, suggesting that there might be functional redundancy among related CPKs. CPK13 and CPK30 are part of the class III subgroup of CPKs in *Arabidopsis* containing 8 CKPs, and cluster together with CPK10 based on protein sequence similarity (Cheng et al., 2002). To exclude lack of phenotypes due to functional redundancy, we should assess PIN localization in the *cpk10 cpk13 cpk30* triple knock-out mutant. Secondly, analysis of CPK expression patterns in the root should be addressed, which would allow us to confirm the relevance of CPK13 and CPK30 in regulation of PIN endocytosis in roots, and might uncover additional CPKs as potential regulators. Thirdly, the CPK13 and CPK30 lines remain to be characterized in more detail. Preliminary data on DRP1c dynamics showed less DRP1c-labelled foci with a shorter life time, suggesting the defect in endocytosis might be attributed to a reduced abundance of DRP1c at the plasma membrane rather than aberrant dynamics. It is therefore crucial to reconfirm this observation and address dynamics and abundance of other endocytosis markers such as CLC or T-PLATE in these backgrounds to better understand the endocytic defect in the *CA CPK30* line. Given the agravitropic root growth of these CPK

lines, another interesting experiment would be to visualize auxin distribution in the roots. Finally, an important piece to the CPK-regulated PIN endocytosis puzzle is identification of the CPK target(s). A phosphoproteomics approach would allow to identify differentially phosphorylated proteins between wild type and the CA CPK lines that could represent potential CPK targets in the regulation of PIN endocytosis.

The observation that CaMIN treatment has an impact on CLC2-GFP localization, and that DRP1c-GFP dynamics is negatively regulated by increased cytosolic Ca^{2+} concentrations, suggests that the importance of Ca^{2+} for regulation of CME could not restricted to PINs but could also apply to other cargoes that are internalized in a clathrin-dependent manner. Furthermore, the observation that inhibition of CME in the TML KD and DN HUB1 line is bypassed upon CaMIN treatment could suggest the possible involvement of a clathrin-independent endocytic mechanism. The complete inhibition of (clathrin-dependent) PIN endocytosis by treatment with MβCD, an inhibitor of clathrin-independent lipid raft-mediated endocytosis, suggests MβCD might not be a reliable tool to assess the contribution of clathrin-independent endocytosis to PIN internalization in CaMIN, and alternative tools/markers would have to be used. Based on our observations it could be speculated that Ca^{2+} might have a more universal role in mediation of endocytosis in general. In order to address whether the importance of Ca^{2+} for regulation of endocytosis is specific for and restricted to PINs, we should verify the impact of our Ca^{2+} drug and CaMIN treatment on other (non-polar) transmembrane proteins such as the plasma membrane H^{+}-ATPase or the water channel PIP2, as it has been reported that endocytosis of these proteins is also inhibited by NAA (Paciorek et al., 2005). Since our read-out heavily relies on BFA treatment, most of our observations are obtained from (pharmacological) manipulation of an already perturbed system. Therefore, it is indispensable to also address PIN trafficking in a BFA-independent context. A possible strategy that could be used is measuring the turn-over of photoconverted PIN2-Dendra (Jásik et al., 2013). Dendra is a photoconvertible protein that can be converted from GFP to RFP by exposure to UV light. Photoconversion of PIN2-Dendra at the plasma membrane and subsequent follow-up of the decrease in RFP intensity at the plasma membrane over time can serve as a proxy for the rate of PIN2 endocytosis. Alternatively, we aimed to look at CME, not restricted to PINs, in a BFA-independent read-out by analyzing CLC2-GFP localization at the plasma membrane. To address the possible requirement of Ca^{2+} for regulation of endocytosis

in general we can monitor the uptake of the endocytic tracer Fei-Mao (FM; Malínská et al., 2014). FM is incorporated in the plasma membrane and thereby labels endosomes derived from the plasma membrane. The ratio of intracellular FM intensity over FM intensity at the plasma membrane reflects the rate of endocytosis. Altogether, these experiments will allow us to assess to what extent our observations are specific for PINs and CME, and address PIN trafficking in a BFA-independent set-up.

Our data strongly focus on cell biological events, but the question remains: what is the physiological relevance of our findings for plant growth and development? Preliminary experiments suggest a role for Ca^{2+}-regulated PIN trafficking and auxin transport during gravitropic bending of the root, however, this remains to be confirmed.

The biological function of both CPK13 and CPK30 has been addressed previously. CPK13 was shown to be expressed in guard cells where it reduces stomata aperture by inhibition of the K^+ TRANSPORTERS OF ARABIDOPSIS THALIANA 1 (KAT1) and KAT2 K^+ channels (Ronzier et al., 2014). Recently, the class III subfamily members CPK10, CPK30, and CPK32 have been shown to be important regulators of Ca^{2+}-dependent nitrate sensing (Liu et al., 2017). Nitrate-triggered Ca^{2+}-dependent activation of these CPKs results in phosphorylation of specific transcription factors and reprogramming of gene expression. As the *cpk10 cpk30* double knock-out is embryo-lethal, a chemically switchable rescue construct was integrated in the double knock-out and was used to generate a *cpk10 cpk30 cpk32* mutant, revealing defects in nitrate-regulated lateral root growth and root architecture. Given the importance of auxin in embryogenesis and root development, we postulate that the observed embryolethality and defects in root architecture could be explained by effects of the CPKs on auxin transport and distribution. In this model, auxin would activate CPK activity to inhibit PIN internalization and regulate PIN polarity, during auxin-regulated development, while providing an integration point for additional stimuli, such as nutrient availability.

References

Bonza, M.C., Loro, G., Behera, S., Wong, A., Kudla, J., and Costa, A. (2013). Analyses of Ca(2+) Accumulation and Dynamics in the Endoplasmic Reticulum of Arabidopsis Root Cells Using a Genetically Encoded Cameleon Sensor. Plant Physiology **163,** 1230-1241.

Boudsocq, M., Willmann, M.R., McCormack, M., Lee, H., Shan, L., He, P., Bush, J., Cheng, S.-H., and Sheen, J. (2010). Differential innate immune signalling via Ca2+ sensor protein kinases. Nature **464,** 418-422.

Braun, N., Wyrzykowska, J., Muller, P., Karine, D., Couch, D., Perrot-Rechenmann, C., and Fleming, A. (2008). Conditional Repression of AUXIN BINDING PROTEIN1 Reveals That It Coordinates Cell Division and Cell Expansion during Postembryonic Shoot Development in Arabidopsis and Tobacco. The Plant Cell **20**, 2746-2762.

Carol, R.J., Takeda, S., Linstead, P., Durrant, M.C., Kakesova, H., Derbyshire, P., Drea, S., Zarsky, V., and Dolan, L. (2005). A RhoGDP dissociation inhibitor spatially regulates growth in root hair cells. Nature **438**, 1013–1016.

Chen, X., Naramoto, S., Robert, S., Tejos, R., Löfke, C., Lin, D., Yang, Z., and Friml, J. (2012). ABP1 and ROP6 GTPase Signaling Regulate Clathrin-Mediated Endocytosis in Arabidopsis Roots. Current Biology **22,** 1326-1332.

Cheng, S.-H., Willmann, M.R., Chen, H.-C., and Sheen, J. (2002). Calcium Signaling through Protein Kinases. The Arabidopsis Calcium-Dependent Protein Kinase Gene Family. Plant Physiology **129,** 469-485.

Dettmer, J., Hong-Hermesdorf, A., Stierhof, Y.-D., and Schumacher, K. (2006). Vacuolar H(+)-ATPase Activity Is Required for Endocytic and Secretory Trafficking in Arabidopsis. The Plant Cell **18,** 715-730.

Dhonukshe, P., Aniento, F., Hwang, I., Robinson, D.G., Mravec, J., Stierhof, Y.-D., and Friml, J. (2007). Clathrin-Mediated Constitutive Endocytosis of PIN Auxin Efflux Carriers in Arabidopsis. Current Biology **17,** 520-527.

Dodd, A.N., Kudla, J., and Sanders, D. (2010). The Language of Calcium Signaling. Annual Review of Plant Biology **61,** 593-620.

Donaldson, J.G., and Jackson, C.L. (2000). Regulators and effectors of the ARF GTPases. Current Opinion in Cell Biology **12,** 475-482.

Ebine, K., Okatani, Y., Uemura, T., Goh, T., Shoda, K., Niihama, M., Morita, M.T., Spitzer, C., Otegui, M.S., Nakano, A., and Ueda, T. (2008). A SNARE Complex Unique to Seed Plants Is Required for Protein Storage Vacuole Biogenesis and Seed Development of Arabidopsis thaliana. The Plant Cell **20,** 3006-3021.

Eckert, C., Offenborn, J.N., Heinz, T., Armarego-Marriott, T., Schültke, S., Zhang, C., Hillmer, S., Heilmann, M., Schumacher, K., Bock, R., Heilmann, I., and Kudla, J. (2014). The vacuolar calcium sensors CBL2 and CBL3 affect seed size and embryonic development in Arabidopsis thaliana. The Plant Journal **78,** 146-156.

Felle, H. (1988). Auxin causes oscillations of cytosolic free calcium and pH inZea mays coleoptiles. Planta **174,** 495-499.

Franz, S., Ehlert, B., Liese, A., Kurth, J., Cazalé, A.-C., and Romeis, T. (2011). Calcium-Dependent Protein Kinase CPK21 Functions in Abiotic Stress Response in Arabidopsis thaliana. Molecular Plant **4,** 83-96.

Gadeyne, A., Sánchez-Rodríguez, C., Vanneste, S., Di Rubbo, S., Zauber, H., Vanneste, K., Van Leene, J., De Winne, N., Eeckhout, D., Persiau, G., Van De Slijke, E., Cannoot, B., Vercruysse, L., Mayers, Jonathan R., Adamowski, M., Kania, U., Ehrlich, M., Schweighofer, A., Ketelaar, T., Maere, S., Bednarek, Sebastian Y., Friml, J., Gevaert, K., Witters, E., Russinova, E., Persson, S., De Jaeger, G., and Van Damme, D. (2014). The TPLATE Adaptor Complex Drives Clathrin-Mediated Endocytosis in Plants. Cell **156,** 691-704.

Gehring, C.A., Irving, H.R., and Parish, R.W. (1990). Effects of auxin and abscisic acid on cytosolic calcium and pH in plant cells. Proceedings of the National Academy of Sciences of the United States of America **87,** 9645-9649.

Geldner, N., Friml, J., Stierhof, Y.-D., Jurgens, G., and Palme, K. (2001). Auxin transport inhibitors block PIN1 cycling and vesicle trafficking. Nature **413,** 425-428.

Geldner, N., Dénervaud-Tendon, V., Hyman, D.L., Mayer, U., Stierhof, Y.-D., and Chory, J. (2009). Rapid, combinatorial analysis of membrane compartments in intact plants with a multicolor marker set. The Plant journal : for cell and molecular biology **59,** 169-178.

Geldner, N., Anders, N., Wolters, H., Keicher, J., Kornberger, W., Muller, P., Delbarre, A., Ueda, T., Nakano, A., and Jürgens, G. (2003). The Arabidopsis GNOM ARF-GEF Mediates Endosomal Recycling, Auxin Transport, and Auxin-Dependent Plant Growth. Cell **112,** 219-230.

Gillooly, D.J., Simonsen, A., and Stenmark, H. (2001). Cellular functions of phosphatidylinositol 3-phosphate and FYVE domain proteins. Biochemical Journal **355,** 249-258.

Grebe, M., Friml, J., Swarup, R., Ljung, K., Sandberg, G., Terlou, M., Palme, K., Bennett, M.J., and Scheres, B. (2002). Cell Polarity Signaling in Arabidopsis Involves a BFA-Sensitive Auxin Influx Pathway. Current Biology **12,** 329-334.

Grones, P., Chen, X., Simon, S., Kaufmann, W.A., De Rycke, R., Nodzyński, T., Zažímalová, E., and Friml, J. (2015). Auxin-binding pocket of ABP1 is crucial for its gain-of-function cellular and developmental roles. Journal of Experimental Botany **66,** 5055-5065.

Himschoot, E., Beeckman, T., Friml, J., and Vanneste, S. (2015). Calcium is an organizer of cell polarity in plants. Biochimica et Biophysica Acta (BBA) - Molecular Cell Research **1853,** 2168-2172.

Himschoot E., P.R., Van Damme D., Vanneste S. (2017). The ins and outs of Ca2+ in plant endomembrane trafficking. . Current Opinion in Plant Biology **40**.

Hubbard, K.E., Siegel, R.S., Valerio, G., Brandt, B., and Schroeder, J.I. (2012). Abscisic acid and CO(2) signalling via calcium sensitivity priming in guard cells, new CDPK mutant phenotypes and a method for improved resolution of stomatal stimulus–response analyses. Annals of Botany **109,** 5-17.

Jásik, J., Boggetti, B., Baluška, F., Volkmann, D., Gensch, T., Rutten, T., Altmann, T., and Schmelzer, E. (2013). PIN2 Turnover in Arabidopsis Root Epidermal Cells Explored by the Photoconvertible Protein Dendra2. PLOS ONE **8,** e61403.

Kanchiswamy, C.N., Takahashi, H., Quadro, S., Maffei, M.E., Bossi, S., Bertea, C., Zebelo, S.A., Muroi, A., Ishihama, N., Yoshioka, H., Boland, W., Takabayashi, J., Endo, Y., Sawasaki, T., and Arimura, G.-i. (2010). Regulation of Arabidopsis defense responses against Spodoptera littoralisby CPK-mediated calcium signaling. BMC Plant Biology **10,** 97.

Ketchum, K.A., Poole, R.J. . (1990). FEBS **274,** 115-118.

Kitakura, S., Vanneste, S., Robert, S., Löfke, C., Teichmann, T., Tanaka, H., and Friml, J. (2011). Clathrin Mediates Endocytosis and Polar Distribution of PIN Auxin Transporters in Arabidopsis. The Plant Cell **23,** 1920-1931.

Kitakura, S., Adamowski, M., Matsuura, Y., Santuari, L., Kouno, H., Arima, K., Hardtke, C.S., Friml, J., Kakimoto, T., and Tanaka, H. (2017). BEN3/BIG2 ARF GEF is Involved in Brefeldin A-Sensitive Trafficking at the trans-Golgi Network/Early Endosome in Arabidopsis thaliana. Plant and Cell Physiology**,** pcx118-pcx118.

Kleine-Vehn, J., Wabnik, K., Martinière, A., Łangowski, Ł., Willig, K., Naramoto, S., Leitner, J., Tanaka, H., Jakobs, S., Robert, S., Luschnig, C., Govaerts, W., W Hell, S., Runions, J., and Friml, J. (2011). Recycling, clustering, and endocytosis jointly maintain PIN auxin carrier polarity at the plasma membrane. Molecular Systems Biology **7,** 540-540.

Klimecka, M., Muszynska, G. (2007). Structure and functions of plant calcium-dependent protein kinases. Acta Biochimica Polonica **54,** 219-233.

Kudla, J., Batistič, O., and Hashimoto, K. (2010). Calcium Signals: The Lead Currency of Plant Information Processing. The Plant Cell **22,** 541-563.

Łangowski, Ł., Wabnik, K., Li, H., Vanneste, S., Naramoto, S., Tanaka, H., and Friml, J. (2016). Cellular mechanisms for cargo delivery and polarity maintenance at different polar domains in plant cells **2,** 16018.

Lin, D., Nagawa, S., Chen, J., Cao, L., Chen, X., Xu, T., Li, H., Dhonukshe, P., Morita, C., Friml, J., Scheres, B., Fu, Y., and Yang, Z. (2012). A ROP GTPase-dependent auxin signaling pathway regulates the subcellular distribution of PIN2 in Arabidopsis roots. Current biology : CB **22,** 1319-1325.

Liu, K.-h., Niu, Y., Konishi, M., Wu, Y., Du, H., Sun Chung, H., Li, L., Boudsocq, M., McCormack, M., Maekawa, S., Ishida, T., Zhang, C., Shokat, K., Yanagisawa, S., and Sheen, J. (2017). Discovery of nitrate–CPK–NLP signalling in central nutrient–growth networks. Nature **545,** 311-316.

Ma, W., and Berkowitz, G.A. (2011). Ca2+ conduction by plant cyclic nucleotide gated channels and associated signaling components in pathogen defense signal transduction cascades. New Phytologist **190,** 566-572.

Malínská, K., Jelínková, A., and Petrášek, J. (2014). The Use of FM Dyes to Analyze Plant Endocytosis. In Plant Endosomes: Methods and Protocols, M.S. Otegui, ed (New York, NY: Springer New York), pp. 1-11.

Matschi, S., Werner, S., Schulze, W.X., Legen, J., Hilger, H.H., and Romeis, T. (2013). Function of calcium-dependent protein kinase CPK28 of Arabidopsis thaliana in plant stem elongation and vascular development. The Plant Journal **73,** 883-896.

Monshausen, G.B., Miller, N.D., Murphy, A.S., and Gilroy, S. (2011). Dynamics of auxin-dependent Ca2+ and pH signaling in root growth revealed by integrating high-resolution imaging with automated computer vision-based analysis. The Plant Journal **65,** 309-318.

Nebenfuhr, A., Ritzenthaler, C., and Robinson, D.G. (2002). Brefeldin A: Deciphering an Enigmatic Inhibitor of Secretion. Plant Physiology **130,** 1102-1108.

Ortiz-Morea, F.A., Savatin, D.V., Dejonghe, W., Kumar, R., Luo, Y., Adamowski, M., Van den Begin, J., Dressano, K., Pereira de Oliveira, G., Zhao, X., Lu, Q., Madder, A., Friml, J., Scherer de Moura, D., and Russinova, E. (2016). Danger-associated peptide signaling in Arabidopsis requires clathrin. Proceedings of the National Academy of Sciences **113,** 11028-11033.

Paciorek, T., Zazimalova, E., Ruthardt, N., Petrasek, J., Stierhof, Y.-D., Kleine-Vehn, J., Morris, D.A., Emans, N., Jurgens, G., Geldner, N., and Friml, J. (2005). Auxin inhibits endocytosis and promotes its own efflux from cells. Nature **435,** 1251-1256.

Peyroche, A., Paris, S., and Jackson, C.L. (1996). Nucleotide exchange on ARF mediated by yeast Geal protein. Nature **384,** 479.

Robert, S., Chary, S.N., Drakakaki, G., Li, S., Yang, Z., Raikhel, N.V., and Hicks, G.R. (2008). Endosidin1 defines a compartment involved in endocytosis of the brassinosteroid receptor BRI1 and the auxin transporters PIN2 and AUX1. Proceedings of the National Academy of Sciences of the United States of America **105,** 8464-8469.

Robert, S., Kleine-Vehn, J., Barbez, E., Sauer, M., Paciorek, T., Baster, P., Vanneste, S., Zhang, J., Simon, S., Čovanová, M., Hayashi, K., Dhonukshe, P., Yang, Z., Bednarek, S.Y., Jones, A.M., Luschnig, C., Aniento, F., Zažímalová, E., and Friml, J. (2010). ABP1 Mediates Auxin Inhibition of Clathrin-Dependent Endocytosis in Arabidopsis. Cell **143,** 111-121.

Ronzier, E., Corratgé-Faillie, C., Sanchez, F., Prado, K., Brière, C., Leonhardt, N., Thibaud, J.-B., and Xiong, T.C. (2014). CPK13, a Noncanonical Ca(2+)-Dependent Protein Kinase, Specifically Inhibits KAT2 and KAT1 Shaker K(+) Channels and Reduces Stomatal Opening. Plant Physiology **166,** 314-326

Shih, H.-W., DePew, Cody L., Miller, Nathan D., and Monshausen, Gabriele B. (2015). The Cyclic Nucleotide-Gated Channel CNGC14 Regulates Root Gravitropism in Arabidopsis thaliana. Current Biology **25,** 3119-3125.

Shishova, M., and Lindberg, S. (1999). Auxin-induced Cytosol Acidification in Wheat Leaf Protoplasts Depends on External Concentration of Ca2+. Journal of Plant Physiology **155,** 190-196.

Shishova, M., and Lindberg, S. (2004). Auxin induces an increase of Ca2+ concentration in the cytosol of wheat leaf protoplasts. Journal of Plant Physiology **161,** 937-945.

Shishova, M., Yemelyanov, V., Rudashevskaya, E., and Lindberg, S. (2007). A shift in sensitivity to auxin within development of maize seedlings. Journal of Plant Physiology **164,** 1323-1330.

Sieberer, T., Seifert, G.J., Hauser, M.-T., Grisafi, P., Fink, G.R., and Luschnig, C. (2000). Post-transcriptional control of the Arabidopsis auxin efflux carrier EIR1 requires AXR1. Current Biology **10,** 1595-1598.

Singh, Manoj K., Krüger, F., Beckmann, H., Brumm, S., Vermeer, Joop E.M., Munnik, T., Mayer, U., Stierhof, Y.-D., Grefen, C., Schumacher, K., and Jürgens, G. (2014). Protein Delivery to Vacuole Requires SAND Protein-Dependent Rab GTPase Conversion for MVB-Vacuole Fusion. Current Biology **24,** 1383-1389.

Tanaka, H., Kitakura, S., De Rycke, R., De Groodt, R., and Friml, J. (2009). Fluorescence Imaging-Based Screen Identifies ARF GEF Component of Early Endosomal Trafficking. Current Biology **19,** 391-397.

Tanaka, H., Kitakura, S., Rakusová, H., Uemura, T., Feraru, M.I., De Rycke, R., Robert, S., Kakimoto, T., and Friml, J. (2013). Cell Polarity and Patterning by PIN Trafficking through Early Endosomal Compartments in Arabidopsis thaliana. PLOS Genetics **9,** e1003540.

Ueda, T., Uemura, T., Sato, M.H., and Nakano, A. (2004). Functional differentiation of endosomes in Arabidopsis cells. The Plant Journal **40,** 783-789.

Uemura, T., Kim, H., Saito, C., Ebine, K., Ueda, T., Schulze-Lefert, P., and Nakano, A. (2012). Qa-SNAREs localized to the trans-Golgi network regulate multiple transport pathways and extracellular disease resistance in plants. Proceedings of the National Academy of Sciences of the United States of America **109,** 1784-1789.

Valitova, J., Sulkarnayeva, A., Kotlova, E., Ponomareva, A., Mukhitova, F.K., Murtazina, L., Ryzhkina, I., Beckett, R., and Minibayeva, F. (2014). Sterol binding by methyl-β-cyclodextrin and nystatin – comparative analysis of biochemical and physiological consequences for plants. FEBS Journal **281,** 2051-2060.

Venus, Y., and Oelmüller, R. (2013). Arabidopsis ROP1 and ROP6 Influence Germination Time, Root Morphology, the Formation of F-Actin Bundles, and Symbiotic Fungal Interactions. Molecular Plant **6,** 872-886.

Vermeer, J.E.M., van Leeuwen, W., Tobeña-Santamaria, R., Laxalt, A.M., Jones, D.R., Divecha, N., Gadella, T.W.J., and Munnik, T. (2006). Visualization of PtdIns3P dynamics in living plant cells. The Plant Journal **47,** 687-700.

Vieten, A., Vanneste, S., Wiśniewska, J., Benková, E., Benjamins, R., Beeckman, T., Luschnig, C., and Friml, J. (2005). Functional redundancy of PIN proteins is accompanied by auxin-dependent cross-regulation of PIN expression. Development **132,** 4521-4531.

Wabnik, K., Govaerts, W., Friml, J., and Kleine-Vehn, J. (2011). Feedback models for polarized auxin transport: an emerging trend. Molecular BioSystems **7,** 2352-2359.

Zažímalová, E., Křeček, P., Skůpa, P., Hoyerová, K., and Petrášek, J. (2007). Polar transport of the plant hormone auxin – the role of PIN-FORMED (PIN) proteins. Cellular and Molecular Life Sciences **64,** 1621-1637.

Zhang, J., Vanneste, S., Brewer, Philip B., Michniewicz, M., Grones, P., Kleine-Vehn, J., Löfke, C., Teichmann, T., Bielach, A., Cannoot, B., Hoyerová, K., Chen, X., Xue, H.-W., Benková, E., Zažímalová, E., and Friml, J. (2011). Inositol Trisphosphate-Induced Ca2+ Signaling Modulates Auxin Transport and PIN Polarity. Developmental Cell **20,** 855-866.

Zouhar, J., Rojo, E., and Bassham, D.C. (2009). AtVPS45 Is a Positive Regulator of the SYP41/SYP61/VTI12 SNARE Complex Involved in Trafficking of Vacuolar Cargo. Plant Physiology **149,** 1668-1678.

CONCLUSIONS and PERSPECTIVES

Previous work showed that auxin can feedback regulate its own distribution by inhibiting CME of the auxin efflux carriers PIN mediated by the auxin receptor ABP1 , intracellular activation of ROP/RIC signaling, and cytoskeletal rearrangements (Geldner et al., 2001; Paciorek et al., 2005b; Robert et al., 2010; Xu et al., 2010; Chen et al., 2012; Lin et al., 2012; Nagawa et al., 2012). It has been well established that auxin can induce a rapid cytosolic Ca^{2+} increase, and this auxin-induced Ca^{2+} increase has been linked to auxin-regulated root gravitropism. In my PhD dissertation entitled "The role of calcium in auxin-regulated PIN endomembrane trafficking", we wanted to bring together these two findings and address what could be the role of Ca^{2+} and auxin-induced Ca^{2+} as a second messenger mediating inhibition of PIN endocytosis by auxin.

The molecular mechanism behind the NAA-induced Ca^{2+} signature

As inhibition of PIN endocytosis was observed for the synthetic auxin NAA, one of our goals was to study NAA-induced Ca^{2+} dynamics in more detail. Our data revealed that NAA treatment rapidly generated a cytosolic biphasic Ca^{2+} signature that slowly recovered to the Ca^{2+} resting levels. Since the amplitude of the first Ca^{2+} peak was strongly diminished upon reduced availability of apoplastic Ca^{2+} by CaMIN pretreatment, we hypothesized that this initial Ca^{2+} peak is generated by influx of extracellular Ca^{2+}. Importantly, also the secondary Ca^{2+} release was reduced in CaMIN, suggestive of a Ca^{2+}-induced Ca^{2+} entry mechanism. The secondary Ca^{2+} peak can originate either from intracellular stores but also from the apoplast. We postulate that the secondary Ca^{2+} release would originate from intracellular stores rather than from the apoplast based on the observation that NAA treatment induces Ca^{2+} signaling throughout the cytoplasm, and not only in the periphery of the plasma membrane.

Major intracellular Ca^{2+} stores are the ER and vacuole. The mitochondria seem to be unlikely to release Ca^{2+} in response to NAA, as NAA treatment increases mitochondrial Ca^{2+} levels (Wagner et al., 2015). Thus, Ca^{2+} sensors that are targeted to specific subcellular compartments will be instrumental in revealing the origin of the secondary Ca^{2+} signal. In this case, apoplast-, ER-, and vacuole-targeted Ca^{2+} sensors might give us a better insight on which

Ca^{2+} sources contribute to shaping the NAA-induced Ca^{2+} signature. However, it is not highly straightforward to design appropriate GECI. The GECI should have a high sensitivity and a dynamic range that allows to capture semi-subtle Ca^{2+} changes in a high Ca^{2+} environment. Moreover, the lumen of the secretory pathway and the vacuole may interfere with the properties of the GECI, due to misfolding, oligomerisation, lysis or low pH (Zhao et al., 2011; Costantini et al., 2015). The palette of GECI designed for visualizing Ca^{2+} dynamics in intracellular compartments, such as ER and mitochondria, is rapidly expanding (Suzuki et al., 2014), but their implementation in plants lags behind.

Pinpointing the compartment(s) from which NAA-induced Ca^{2+} signals originate will allow narrowing down the number of Ca^{2+} signaling components involved, based on their subcellular localization. Analyzing NAA-regulated PIN trafficking in the corresponding mutants might provide evidence for Ca^{2+} signaling components linking the NAA-induced cytosolic Ca^{2+} increase to NAA its effect on PIN endocytosis. Shih and colleagues demonstrated that the IAA-induced cytosolic Ca^{2+} increase observed in roots is mediated by the Ca^{2+} channel CNGC14 (Shih et al., 2015). Evaluating Ca^{2+} dynamics upon NAA treatment in the *cngc14* background is a straightforward experiment to assess the contribution of CNGC14 to the NAA-induced Ca^{2+} influx.

Is NAA-induced Ca^{2+} involved in NAA-inhibited PIN endocytosis?

This has been one of our main questions that we wanted to address in this PhD project. We do have evidence that the NAA-induced Ca^{2+} signature is required for inhibition of PIN endocytosis by NAA. On the one hand, depleting the extracellular Ca^{2+} by CaMIN pretreatment reduced the first NAA-induced Ca^{2+} peak. On the other hand, CaMIN treatment resulted in PIN internalization and accumulation in BFA compartments in the presence of NAA. Similar observations were made for the Ca^{2+} channel inhibitor Nifedipine. Cotreatment with BFA, NAA and Nifedipine resulted in pronounced intracellular PIN accumulation, and preliminary data showed a reduced cytosolic Ca^{2+} increase upon treatment with NAA in seedlings pretreated with Nifedipine. We have demonstrated that Ca^{2+} most likely operates downstream of ROP/RIC signaling. Additional support for these observations and the hypothesis that the NAA-induced cytosolic Ca^{2+} increase is required for inhibition of PIN endocytosis could be found by

addressing NAA-induced Ca^{2+} dynamics upon interference with ROP/RIC function. Similar experiments could be performed for ABP1 using the proper mutant backgrounds, however, given that the role of ABP1 as an auxin receptor is currently under debate we should interpret these results with caution and await further clarification of the function of ABP1 in auxin signaling.

We have also made some observations which are not following the model in which NAA-induced Ca^{2+} inhibits PIN endocytosis. As mentioned in the previous paragraph, CNGC14 has been identified as the Ca^{2+} channel mediating Ca^{2+} dynamics in roots induced by 1 µM IAA and during auxin-regulated root gravitropism (Shih et al., 2015). However, our preliminary data showed that NAA-regulated PIN trafficking was not affected in the *cngc14* mutant (Fig. S8). Ideally, NAA treatment should be performed on a *cncg14* line expressing a Ca^{2+} sensor to see if *cngc14* would be unresponsive to the effects of 10µM NAA. If the NAA-induced response is abolished in *cngc14* this would suggest that the NAA-induced Ca^{2+} increase and inhibition of PIN endocytosis by NAA are not interconnected. In the case NAA-induced Ca^{2+} is not affected in *cngc14* an alternative explanation could be that, since IAA and NAA show subtle differences in their Ca^{2+} signatures, the Ca^{2+} influx might be mediated by distinct Ca^{2+} channels. Possibly CNGC14 is specific for IAA-induced Ca^{2+} influx and NAA might actuate other Ca^{2+} channels, or, perhaps NAA activates multiple Ca^{2+} channels, among which CNGC14, and a clear phenotype is masked by their functional redundancy.

A crucial experiment which still remains to be performed in order to link NAA-induced Ca^{2+} to NAA-inhibited PIN endocytosis is addressing the Ca^{2+} response to control treatments benzoic acid and 2-NAA. Benzoic acid is a weak acid like auxin, but does not inhibit PIN endocytosis (Paciorek et al., 2005). 2-NAA resembles auxin, yet it is inactive in the transcriptional auxin response and also does not inhibit PIN endocytosis (Paciorek et al., 2005). If these compounds yield Ca^{2+} responses that are obviously distinct from NAA-induced Ca^{2+} signatures, this would be in favor of our hypothesis. However, in the case that the Ca^{2+} signatures are highly overlapping, it remains possible that the observed Ca^{2+} response does not have enough subcellular resolution to capture differences between micro-domain Ca^{2+} signatures, which may be highly relevant for the downstream cellular read-out.

PIN endocytosis upon CaMIN treatment: clathrin-dependent or -independent?

It seems that CaMIN-induced PIN internalization is to some extent affected in CME mutants, suggesting that an alternative, clathrin-independent endocytic mechanism might be involved. In contrast to animals, clathrin-independent endocytosis (CIE) is poorly characterized in plants. Based on preliminary observations, we found that MβCD, an inhibitor of clathrin-independent lipid raft-mediated endocytosis, might not be a reliable tool to address this question due to possible secondary effects. Baral and coworkers suggested that glycosyl phosphatidyl inositol-anchored proteins such as SKU5 are internalized through a clathrin-independent endocytic mechanism that is restricted to the epidermal cell layer (Baral et al., 2015a). Furthermore, they showed that exposure to mM concentrations of NaCl induced CIE, albeit across all cell layers and not restricted to specific cargo. The latter mechanism is most likely mediated by membrane lipid rafts as lipid-raft-dependent endocytosis of the aquaporin PIP2;1 was shown to be increased by high NaCl (Li et al., 2011b). Flotillin1 (Flot1) localizes to such lipid rafts, also called detergent-resistant membranes (DRMs), and was shown to contribute to endocytic vesicle formation, independent of clathrin (Borner et al., 2005; Li et al., 2011b), making Flot1 a reliable marker for CIE. To test the contribution of CIE to CaMIN-induced PIN internalization we could verify how CaMIN affects SKU5 and Flot1 localization and make a quantitative comparison of CaMIN- and NaCl-induced PIN internalization in terms of number and size of BFA bodies formed.

CaMIN versus Ca^{2+} pharmacology

To assess the importance of Ca^{2+} for NAA-inhibited PIN localization we analyzed PIN localization when interfering with Ca^{2+} signaling by (1) Ca^{2+} depletion of the extracellular environment by pretreatment with Ca^{2+}-free medium (CaMIN) and (2) using a pharmacological approach. Although both CaMIN and the Ca^{2+} drug had similar impact on PIN localization in wild type seedlings, PINs were differentially affected in some mutant backgrounds (e.g. *syp42 syp43*, CA CPK30 line). Furthermore, different endomembrane markers showed distinct labeling and/or morphology after CaMIN versus Ca^{2+} drug treatment. Together, these observations suggest that the Ca^{2+} drugs operate via a different mechanism or that the Ca^{2+} drug might have multiple effects at different levels in the endocytic trafficking pathway. The

former explanation can be appreciated given the differential impact on extracellular free Ca^{2+} levels of CaMIN versus the Ca^{2+} drug, thereby also possibly differently affecting the luminal Ca^{2+} levels in the (early) endomembrane system. Treatment with Ca^{2+} channel inhibitor Nifedipine or Bepridil and CaM inhibitor W-7 is expected not to affect the free apoplastic Ca^{2+} concentration, while CaMIN would reduce the extracellular free Ca^{2+} levels. The latter could also affect the luminal Ca^{2+} concentrations in the (early) endomembrane system, as initially the lumen of endosomes is derived from the extracellular space. Since the luminal Ca^{2+} levels in the endosomes have not been established yet (see Section I - Chapter 3) it is difficult to assess how and to what extent changes in the extracellular Ca^{2+} levels by CaMIN, might affect luminal Ca^{2+} in the endosomes. Currently, constructs are being generated in our lab which would allow to target different Ca^{2+} sensors to the luminal side of distinct endomembrane compartments. Analysis of these lines would allow us to gain more insight into Ca^{2+} distribution throughout the endosomal trafficking pathway, and would allow us to assess possible differential effects of CaMIN versus Ca^{2+} drug treatment.

Importantly, the *bfa-visualized endocytic trafficking defective* double mutant (*ben1-1 ben2*) did not accumulate PINs in BFA bodies, both in CaPLUS and CaMIN. This demonstrates that the internalized PINs under CaMIN conditions follow an early endocytic trafficking pathway that is under control of the ARF-GEF BEN1/BIG5/MIN7 and BEN2/VPS45. Moreover, mutants in VPS45-regulated SYP4s (*syp42 syp43*) were also resistant to BFA-induced PIN internalization in CaMIN conditions. This double mutant was less sensitive to BFA-induced endosome aggregation and has defects in secretion and vacuolar trafficking (Uemura et al., 2012). This suggests that internalized PINs cannot be seen in BFA bodies simply due to a defect in endosome aggregation. The fact that we do see strong PIN-accumulation in BFA bodies in this mutant upon cotreatment with the Ca^{2+} drug could suggest that our drug affect endosome aggregation and/or membrane fusion. The latter is known to rely on Ca^{2+} (Section I – Chapter 3). Therefore, it will be of interest to see how Ca^{2+} affects endosomal mobility, and to which extent this could explain our observations.

Ca^{2+} and PIN recycling

Besides affecting PIN endocytosis, we have observations that CaMIN also affects PIN recycling to the plasma membrane (Fig. S9). In BFA wash-out experiments, seedlings are initially treated with BFA resulting in formation of PIN-accumulating BFA compartments (Fig. S9, A), followed by BFA removal from the medium and wash-out from the cells, so that exocytosis can be resumed and BFA bodies disappear in time. In case the wash-out step is performed in CaMIN, we observed a slower dissociation of BFA bodies (Fig. S9, C). This resembles BFA wash-out phenotypes of mutants defective in protein recycling/exocytosis such as mutants in exocyst complex subunits (Drdová et al., 2013) and *bex5* (Feraru et al., 2012). The fact that CaMIN affects exocytosis besides endocytosis, might explain why enlarged BFA bodies can be observed when BFA treatment is performed in CaMIN compared to CaPLUS. The controlled regulation of PIN endo- and exocytosis is crucial for proper PIN distribution, suggesting that Ca^{2+} might indirectly be a key regulator of auxin transport.

Final conclusion

Based on the Ca^{2+} pharmacology and CaMIN experiments we have clear evidence for a role of Ca^{2+} in inhibition of CME of PINs by NAA. We speculated that the cytosolic Ca^{2+} increase which is triggered by NAA treatment could initiate inhibition of PIN internalization. The NAA-induced Ca^{2+} signature is generated immediately and rapidly and shows two Ca^{2+} peaks pointing on extracellular Ca^{2+} influx and secondary intracellular Ca^{2+} release. However, the Ca^{2+} channel(s) involved remains to be identified. Part of the results supports our hypothesis that NAA-induced Ca^{2+} blocks PIN endocytosis, however, the lack of genetic data has made it difficult to resolve the link between NAA-induced Ca^{2+} and NAA-inhibited PIN endocytosis. Given that we found the involvement of CPKs (such as CPK30 and CPK13), it will be of interest to dissect the dynamic auxin-regulated phosphoproteome, and define an overlap with the direct targets of these CPKs. The proposed experiments should allow us to unambiguously clarify this.

References

Baral, A., Irani, N.G., Fujimoto, M., Nakano, A., Mayor, S., and Mathew, M.K. (2015). Salt-Induced Remodeling of Spatially Restricted Clathrin-Independent Endocytic Pathways in Arabidopsis Root. The Plant Cell **27,** 1297-1315.

Borner, G.H.H., Sherrier, D.J., Weimar, T., Michaelson, L.V., Hawkins, N.D., MacAskill, A., Napier, J.A., Beale, M.H., Lilley, K.S., and Dupree, P. (2005). Analysis of Detergent-Resistant Membranes in Arabidopsis. Evidence for Plasma Membrane Lipid Rafts. Plant Physiology **137,** 104-116.

Carol, R.J., Takeda, S., Linstead, P., Durrant, M.C., Kakesova, H., Derbyshire, P., Drea, S., Zarsky, V., and Dolan, L. (2005). A RhoGDP dissociation inhibitor spatially regulates growth in root hair cells. Nature **438,** 1013-1016.

Costantini, L., Baloban, M., L Markwardt, M., Rizzo, M., Guo, F., V Verkhusha, V., and Snapp, E. (2015). A palette of fluorescent proteins optimized for diverse cellular environments.

Chen, X., Naramoto, S., Robert, S., Tejos, R., Löfke, C., Lin, D., Yang, Z., and Friml, J. (2012). ABP1 and ROP6 GTPase Signaling Regulate Clathrin-Mediated Endocytosis in Arabidopsis Roots. Current Biology **22,** 1326-1332.

Drdová, E.J., Synek, L., Pečenková, T., Hála, M., Kulich, I., Fowler, J.E., Murphy, A.S., and Žárský, V. (2013). The exocyst complex contributes to PIN auxin efflux carrier recycling and polar auxin transport in Arabidopsis. The Plant Journal **73,** 709-719.

Feraru, E., Feraru, M.I., Asaoka, R., Paciorek, T., De Rycke, R., Tanaka, H., Nakano, A., and Friml, J. (2012). BEX5/RabA1b Regulates trans-Golgi Network-to-Plasma Membrane Protein Trafficking in Arabidopsis. The Plant Cell **24,** 3074-3086.

Geldner, N., Friml, J., Stierhof, Y.-D., Jurgens, G., and Palme, K. (2001). Auxin transport inhibitors block PIN1 cycling and vesicle trafficking. Nature **413,** 425-428.

Kim, M., Kim, Y., Kim, J., Lee, H.-S., Sung Lee, W., Kim, S.-K., Wang, Z.-Y., and Kim, S.-H. (2013). Identification of Arabidopsis BAK1-Associating Receptor-Like Kinase 1 (BARK1) and Characterization of its Gene Expression and Brassinosteroid-Regulated Root Phenotypes.

Kitakura, S., Vanneste, S., Robert, S., Löfke, C., Teichmann, T., Tanaka, H., and Friml, J. (2011). Clathrin Mediates Endocytosis and Polar Distribution of PIN Auxin Transporters in Arabidopsis. The Plant Cell **23,** 1920-1931.

Li, X., Wang, X., Yang, Y., Li, R., He, Q., Fang, X., Luu, D.-T., Maurel, C., and Lin, J. (2011). Single-Molecule Analysis of PIP2;1 Dynamics and Partitioning Reveals Multiple Modes of Arabidopsis Plasma Membrane Aquaporin Regulation. The Plant Cell **23,** 3780-3797.

Lin, D., Nagawa, S., Chen, J., Cao, L., Chen, X., Xu, T., Li, H., Dhonukshe, P., Yamamuro, C., Friml, J., Scheres, B., Fu, Y., and Yang, Z. (2012). A ROP GTPase-Dependent Auxin Signaling Pathway Regulates the Subcellular Distribution of PIN2 in Arabidopsis Roots. Current Biology **22,** 1319-1325.

Nagawa, S., Xu, T., Lin, D., Dhonukshe, P., Zhang, X., Friml, J., Scheres, B., Fu, Y., and Yang, Z. (2012). ROP GTPase-Dependent Actin Microfilaments Promote PIN1 Polarization by Localized Inhibition of Clathrin-Dependent Endocytosis. PLOS Biology **10,** e1001299.

Paciorek, T., Zazimalova, E., Ruthardt, N., Petrasek, J., Stierhof, Y.-D., Kleine-Vehn, J., Morris, D.A., Emans, N., Jurgens, G., Geldner, N., and Friml, J. (2005). Auxin inhibits endocytosis and promotes its own efflux from cells. Nature **435,** 1251-1256.

Robert, S., Kleine-Vehn, J., Barbez, E., Sauer, M., Paciorek, T., Baster, P., Vanneste, S., Zhang, J., Simon, S., Čovanová, M., Hayashi, K., Dhonukshe, P., Yang, Z., Bednarek, S.Y., Jones, A.M., Luschnig, C., Aniento, F., Zažímalová, E., and Friml, J. (2010). ABP1 Mediates Auxin Inhibition of Clathrin-Dependent Endocytosis in Arabidopsis. Cell **143,** 111-121.

Shih, H.-W., DePew, Cody L., Miller, Nathan D., and Monshausen, Gabriele B. (2015). The Cyclic Nucleotide-Gated Channel CNGC14 Regulates Root Gravitropism in Arabidopsis thaliana. Current Biology **25,** 3119-3125.

Suzuki, J., Kanemaru, K., Ishii, K., Ohkura, M., Okubo, Y., and Iino, M. (2014). Imaging intraorganellar Ca at subcellular resolution using CEPIA.

Valitova, J., Sulkarnayeva, A., Kotlova, E., Ponomareva, A., Mukhitova, F.K., Murtazina, L., Ryzhkina, I., Beckett, R., and Minibayeva, F. (2014). Sterol binding by methyl-β-cyclodextrin and nystatin – comparative analysis of biochemical and physiological consequences for plants. FEBS Journal **281,** 2051-2060.

Wagner, S., Behera, S., De Bortoli, S., Logan, D.C., Fuchs, P., Carraretto, L., Teardo, E., Cendron, L., Nietzel, T., Füßl, M., Doccula, F.G., Navazio, L., Fricker, M.D., Van Aken, O., Finkemeier, I., Meyer, A.J., Szabò, I.,

Costa, A., and Schwarzländer, M. (2015). The EF-Hand Ca²⁺ Binding Protein MICU Choreographs Mitochondrial Ca²⁺ Dynamics in Arabidopsis. The Plant Cell.

Xu, T., Wen, M., Nagawa, S., Fu, Y., Chen, J.-G., Wu, M.-J., Perrot-Rechenmann, C., Friml, J., Jones, A.M., and Yang, Z. (2010). Cell surface- and Rho GTPase-based auxin signaling controls cellular interdigitation in Arabidopsis. Cell **143,** 99-110.

Xu, T., Dai, N., Chen, J., Nagawa, S., Cao, M., Li, H., Zhou, Z., Chen, X., De Rycke, R., Rakusová, H., Wang, W., Jones, A.M., Friml, J., Patterson, S.E., Bleecker, A.B., and Yang, Z. (2014). Cell Surface ABP1-TMK Auxin-Sensing Complex Activates ROP GTPase Signaling. Science (New York, N.Y.) **343,** 1025-1028.

Zhao, Y., Araki, S., Wu, J., Teramoto, T., Chang, Y.-F., Nakano, M., Abdelfattah, A.S., Fujiwara, M., Ishihara, T., Nagai, T., and Campbell, R.E. (2011). An Expanded Palette of Genetically Encoded Ca(2+) Indicators. Science (New York, N.Y.) **333,** 1888-1891.

OTHER SCIENTIFIC CONTRIBUTIONS

Salicylic acid interferes with clathrin-mediated endocytic protein trafficking

Author contribution:
E.H. performed an immunolocalization experiment using anti-PIN1 and anti-PIN2 antibodies on wild type seedlings treated with BFA and seedlings cotreated with BFA and salicylic acid (Figure 5).

Salicylic acid interferes with clathrin-mediated endocytic protein trafficking

Yunlong Du[a,b], Ricardo Tejos[a], Martina Beck[c], Ellie Himschoot[a], Hongjiang Li[a], Silke Robatzek[c], Steffen Vanneste[a], and Jiří Friml[a,d,1]

[a]Department of Plant Systems Biology, VIB and Department of Plant Biotechnology and Bioinformatics, Ghent University, 9052 Ghent, Belgium; [b]Key Laboratory of Agro-Biodiversity and Pest Management of Education Ministry of China, Yunnan Agricultural University, Kunming 650201, China; [c]The Sainsbury Laboratory, Norwich Research Park, Norwich NR4 7UH, United Kingdom; and [d]Institute of Science and Technology Austria, 3400 Klosterneuburg, Austria

Edited* by Natasha V. Raikhel, University of California, Riverside, CA, and approved April 1, 2013 (received for review November 21, 2012)

Removal of cargos from the cell surface via endocytosis is an efficient mechanism to regulate activities of plasma membrane (PM)-resident proteins, such as receptors or transporters. Salicylic acid (SA) is an important plant hormone that is traditionally associated with pathogen defense. Here, we describe an unanticipated effect of SA on subcellular endocytic cycling of proteins. Both exogenous treatments and endogenously enhanced SA levels repressed endocytosis of different PM proteins. The SA effect on endocytosis did not involve transcription or known components of the SA signaling pathway for transcriptional regulation. SA likely targets an endocytic mechanism that involves the coat protein clathrin, because SA interfered with the clathrin incidence at the PM and clathrin-deficient mutants were less sensitive to the impact of SA on the auxin distribution and root bending during the gravitropic response. By contrast, SA did not affect the ligand-induced endocytosis of the FLAGELLIN SENSING2 (FLS2) receptor during pathogen responses. Our data suggest that the established SA impact on transcription in plant immunity and the nontranscriptional effect of SA on clathrin-mediated endocytosis are independent mechanisms by which SA regulates distinct aspects of plant physiology.

Salicylic acid (SA) is an important plant signaling molecule involved in a broad range of biotic and abiotic stress responses, including immunity, defense-related cell death, systemic acquired resistance (1), drought (2), salt stress (3), ozone (4), and chilling (5). Moreover, SA action converges with signaling of several growth regulating hormones, such as jasmonic acid, ethylene, gibberellins, abscisic acid, and auxin, by which SA can impact on plant growth and development (6). A current notion of SA signaling suggests that SA mediates this broad range of physiological processes by regulation of gene transcription in the nucleus (1).

A growing number of studies demonstrate the importance of endocytosis in different physiological processes in plants, including immunity (7, 8). Endocytosis is the mechanism by which plasma membrane (PM) materials (including lipids and proteins) and cargos from the extracellular space are internalized and redirected toward different subcellular destinations. In plants, the most prominent endocytic mechanism is endocytosis that depends on the vesicle coat protein clathrin or clathrin-mediated endocytosis (CME) (9, 10). Besides its involvement in plant immune responses (8), CME also plays an essential role in nutrient uptake (11) and intercellular transport of the plant hormone auxin, specifically in internalization of auxin transporters from the PIN-FORMED (PIN) family (12). Interestingly, multiple endogenous signals, such as auxin (13), cytokinin (14), and GOLVEN peptides (15), have been shown to converge on the regulation of endocytosis via signal transduction pathways that might not require regulation of transcription.

Here, we found that SA acts as an endogenous signal that impairs CME. Whereas SA was found to potentiate secretion by transcriptional up-regulation of secretory pathway genes (16), we found that this CME inhibition by SA neither involves SA-induced transcriptional changes nor known components of the SA-regulated transcriptional signaling. This result opens unsuspected possibilities by which SA regulates different aspects of plant physiology.

Results

SA Interferes with the Endocytic Cycling of PM Proteins. To identify possible mechanism(s) by which SA can affect the cellular behavior, we tested its effect on the endocytic cycling of PM proteins. We visualized the auxin transporters PIN1 and PIN2 or the aquaporin PLASMA MEMBRANE INTRINSIC PROTEIN2 (PIP2) that constitutively undergo cycles of endocytosis and recycling back to the PM (17). This recycling (18) and, to a lesser extent, endocytosis (19) are inhibited by the trafficking inhibitor brefeldin A (BFA). The imbalance in recycling and endocytosis caused by the BFA treatment results in intracellular accumulation of internalized PM proteins, which end up in BFA-induced aggregations of endosomes, called BFA bodies (20). Therefore, we used the relative amount of PM proteins in BFA bodies as a proxy for internalization rate.

Previous studies had established that concentrations of SA from 0.1 to 1 mM were effective in plant defense (21, 22). When *Arabidopsis thaliana* seedlings were treated with a range of SA concentrations in combination with BFA, the BFA-induced PIN2 internalization was partially inhibited in root epidermal cells at concentrations as low as 15 μM. At this concentration, the PIN2-positive BFA bodies were smaller than those in the controls (Fig. 1 *A*, *B*, and *D*), whereas at 50 μM, the PIN2-GFP internalization was nearly completely abolished, as reflected by the strongly reduced PIN2-GFP signal in BFA bodies and the reduced number of BFA bodies per cell (Fig. 1 *A*, *C*, and *D*). Similar effects were visible for PIN1 (detected by anti-PIN1 antibodies) (Fig. S1) and PIP2-GFP (Fig. 1 *E*–*G*). Because SA is a weak acid, it lowers the pH of the medium from 5.8 to 5.4 when added at a final concentration of 200 μM (Fig. S2*N*). However, using 0.5× Murashige and Skoog (MS) medium at pH 5.4 did not reduce the BFA body size for PIN1 and PIN2 (Fig. S2 *B*, *D*, *F*, and *H*). Moreover, the more neutral sodium salicylate also reduced the BFA body size from 50 μM onward (Fig. S2 *I*–*M*). These results show that physiological concentrations of exogenous SA interfere with the accumulation of diverse PM proteins in intracellular BFA bodies.

To test whether endogenously increased SA levels had an impact, we examined the mutants *cpr1* (an allele of *constitutive expressor of PR gene 1*) and *cpr5*, which are known for their higher endogenous SA levels (23, 24). In roots of these mutants, the BFA-induced PIN2 and PIN1 intracellular accumulations were significantly lower than

Author contributions: Y.D., M.B., S.R., S.V., and J.F. designed research; Y.D., R.T., M.B., E.H., and H.L. performed research; Y.D., R.T., and M.B. analyzed data; and Y.D., M.B., S.R., S.V., and J.F. wrote the paper.

The authors declare no conflict of interest.

*This Direct Submission article had a prearranged editor.

[1]To whom correspondence should be addressed. E-mail: jiri.friml@ist.ac.at.

This article contains supporting information online at www.pnas.org/lookup/suppl/doi:10.1073/pnas.1220205110/-/DCSupplemental.

RBOH-mediated ROS production facilitates lateral root emergence in *Arabidopsis*

Author contribution:
E.H. provided seeds for the *rboh* single mutants and made crosses to generate double and triple *rboh* mutants used in the paper.

© 2016. Published by The Company of Biologists Ltd | Development (2016) 143, 3328-3339 doi:10.1242/dev.136465

RESEARCH ARTICLE

RBOH-mediated ROS production facilitates lateral root emergence in *Arabidopsis*

Beata Orman-Ligeza[1,2,3,*], Boris Parizot[2,3], Riet de Rycke[2,3], Ana Fernandez[2,3], Ellie Himschoot[2,3], Frank Van Breusegem[2,3], Malcolm J. Bennett[4], Claire Périlleux[5], Tom Beeckman[2,3,‡,§] and Xavier Draye[1,‡]

ABSTRACT

Lateral root (LR) emergence represents a highly coordinated process in which the plant hormone auxin plays a central role. Reactive oxygen species (ROS) have been proposed to function as important signals during auxin-regulated LR formation; however, their mode of action is poorly understood. Here, we report that *Arabidopsis* roots exposed to ROS show increased LR numbers due to the activation of LR pre-branch sites and LR primordia (LRP). Strikingly, ROS treatment can also restore LR formation in *pCASP1:shy2-2* and *aux1 lax3* mutant lines in which auxin-mediated cell wall accommodation and remodeling in cells overlying the sites of LR formation is disrupted. Specifically, ROS are deposited in the apoplast of these cells during LR emergence, following a spatiotemporal pattern that overlaps the combined expression domains of extracellular ROS donors of the RESPIRATORY BURST OXIDASE HOMOLOGS (RBOH). We also show that disrupting (or enhancing) expression of RBOH in LRP and/or overlying root tissues decelerates (or accelerates) the development and emergence of LRs. We conclude that RBOH-mediated ROS production facilitates LR outgrowth by promoting cell wall remodeling of overlying parental tissues.

KEY WORDS: Lateral root emergence, Reactive oxygen species, Auxin, Respiratory burst oxidase homologs, Auxin-mediated cell wall remodeling

INTRODUCTION

Root branching plays a crucial role enhancing the ability of the root system to explore and take up water and nutrients from the soil environment. In the model plant *Arabidopsis*, lateral roots (LRs) are derived from pairs of xylem pole pericycle cells located deep within the primary root (Dubrovsky et al., 2006; Himanen et al., 2002; Jansen et al., 2013; Malamy and Benfey, 1997). The hormone auxin plays a key role during early developmental stages of LRP (Casimiro et al., 2001). Increased auxin levels mediated by auxin influx and efflux transporters (Benkova et al., 2003; Marchant et al., 2002; Marhavy et al., 2013) are perceived by TIR1 and AFB receptors and trigger degradation of different AUX/IAA repressors of auxin response transcription factors (ARFs), releasing the expression of auxin-responsive genes (De Smet, 2011; Lavenus et al., 2013).

Early auxin-response modules controlling LRP formation, namely *ARF7* and *ARF19* (Okushima et al., 2007), *SLR* (also known as *IAA14*) (Fukaki et al., 2002), *IAA28* (Rogg et al., 2001) and *SHY2* (*IAA3*) (Goh et al., 2012; Hosmani et al., 2013; Tian and Reed, 1999; Vermeer et al., 2014), operate within the LRP and in the tissues of the parental root that overlie the LRP to coordinate its initiation and emergence (Swarup et al., 2008). It is now clear that auxin-mediated modifications of cell wall properties represent an essential step during LR development. In the endodermis, the *SHY2* signaling module triggers changes in cell volume and wall properties termed 'spatial accommodation', thereby facilitating the passage of LRP (Vermeer et al., 2014). In the cortex and the epidermal cells overlying the expanding LRP, cell wall remodeling enzymes are induced to facilitate LRP emergence (Gonzalez-Carranza et al., 2007; Lewis et al., 2013; Neuteboom et al., 1999; Swarup et al., 2008). The activity of the auxin influx carrier LIKE AUX1 3 (LAX3) localizes the auxin-induced expression of these cell wall remodeling genes that degrade the pectin-rich middle lamellae. In agreement with this, LRP emergence through the cortex and epidermis is hampered in *lax3* mutants (Swarup et al., 2008) and defects in genes involved in cell wall formation increase the rate of LRP emergence, as shown recently with mutants with impaired cell wall biosynthesis (Roycewicz and Malamy, 2014) and abscission (Kumpf et al., 2013).

In addition to hormones like auxin, there is compelling evidence that ROS also function as signaling molecules during plant development, as shown for several signal transduction pathways (D'Haeze et al., 2003; Ishibashi et al., 2012; Joo et al., 2001; Mori et al., 2001) and developmental events such as xylem differentiation (Ros Barcelo, 2005), root gravitropism (Joo et al., 2001), adventitious root formation (Liao et al., 2012) and root-to-shoot coordination (Passaia et al., 2013). Recent evidence also suggests that ROS act during LR formation (Correa-Aragunde et al., 2013; Li and Jia, 2013; Manzano et al., 2014) in relation to auxin response (Correa-Aragunde et al., 2013; Ma et al., 2014), but the mechanistic basis of this crosstalk remains unclear. Among ROS, O_2^- and H_2O_2 were shown to be involved in cell wall modifications during several plant developmental processes (Carol et al., 2005; Foreman et al., 2003; Monshausen et al., 2007; Ros Barcelo, 2005). The production of ROS in extracellular spaces depends on several classes of enzymes, including respiratory burst oxidase homologs (RBOH) and class III peroxidases (Sagi and Fluhr, 2006; Shapiguzov et al.,

[1]Université Catholique de Louvain, Earth and Life Institute, Louvain-la-Neuve B-1348, Belgium. [2]Department of Plant Biotechnology and Bioinformatics, Ghent University, Ghent B-9052, Belgium. [3]Department of Plant Systems Biology, VIB, Ghent B-9052, Belgium. [4]Centre for Plant Integrative Biology, School of Biosciences, University of Nottingham, Sutton Bonington LE12 5RD, UK. [5]PhytoSYSTEMS, Laboratory of Plant Physiology, University of Liège, Sart Tilman Campus, 4 Chemin de la Vallée, Liège B-4000, Belgium.
*Present address: PhytoSYSTEMS, Laboratory of Plant Physiology, University of Liège, Sart Tilman Campus, 4 Chemin de la Vallée, Liège B-4000, Belgium.
‡These authors contributed equally to this work

§Author for correspondence (Tom.Beeckman@psb.ugent.be)

B.O., 0000-0002-7171-2473; B.P., 0000-0003-1445-6925; M.J.B., 0000-0003-0475-390X; T.B., 0000-0001-8656-2060; X.D., 0000-0002-3637-3330

Received 15 February 2016; Accepted 4 July 2016

ACKNOWLEDGEMENTS

I would like to thank the members of the Examination Board **Geert De Jaeger**, **Lieven De Veylder**, **Jiří Friml**, **Alex Costa**, and **Simon Stael** for taking the time to evaluate my PhD thesis and for your valuable comments and feedback.

I would like to thank my promotor **Tom Beeckman** for his supervision and for letting me be part of the Root Development group after the Auxin lab moved to Vienna, allowing me to proceed with my PhD project at PSB.

Thank you to my promotor **Steffen Vanneste** for the guidance and help with practical work and writing over the past 7 years I think, including my master project and master thesis. I would also like to thank you for creating the opportunity for me to gain some experience abroad by arranging scientific visits to our collaborators, and giving me the freedom to attend some courses at UGent during my PhD. I wish you all the best with the calcium (and other) projects, and your future (scientific) plans!

I would like to thank **UGent** and **FWO** for funding my PhD project, and enabling me to travel to different collaborating research groups.

Thank you to **Jiří Friml** and **Eva Benková** for hosting my visit at IST Austria and your guidance, remotely and during my stay. It was a fantastic experience for me to spend some time in a great institute abroad; I had an amazing time and have learned a lot.

I would also like to thank the members of the former **Auxin lab** at PSB. I was part of this group for only a short period of time, but everyone was very helpful to find my way around in the lab/institute and share their experience when starting my PhD project.

During the last years I have really enjoyed working in the **Root/Vascular Development lab.** Thank you **Tom, Steffen, Kjell, Jian, Ren, Maria, Kun, Ana, Gieljan, Hugues, Hanne, Davy, Chouke, Hans, Franky, Agnieszka, Nick, Joris, Long, Andrzej, Vera, Dominique, Wilson, Rudy, Barbara, Pierre-Mathieu, Alexa, Boris, Fabian, Brecht, Wouter, Eliana, Jos, and Bert** for the nice working atmosphere and your help. A special thanks to **Franky** and **Chouke** for

transferring many of my plates to the growth room :). Thank you to **Hanne and Davy** for the nice company and BBQs. I hope there will be many more to come, without car trouble next time. I also really enjoyed your visit to Vienna. And in case the 3D-printed shoe will break, you know where to find me! Thank you **Hugues** for the tasty waffles, giving me so much desk space (even though it was not your free choice to draw the borders of Wallonia so close to each other) and standing me when I was sighing the whole time. Last, but not least, a special thank you to **Gieljan**. Thank you for bringing a lot of entertainment and moral support, never letting me get bored by keeping your secretary busy, sharing your grapes, cherries, haricots, pumpkins, eggs, and other goodies, giving a weekly update on the highlights of GOT (still didn't see season 7), and much more. I had a lot of fun in our corner! The best of luck with finishing your PhD, and I am looking forward to your defense.

A big thank you to the **PSB support teams and administration** for making our lives at PSB so much easier by taking care of our plants, media, plant transformation, product stock, IT, administrative issues, and so on.

Thank you to **Matthais (Madur)** for being so helpful over the past years inside and outside the department, and playing Soul Calibur with Kamil (which I truly suck at). Thank you **Jan (Jamer)** for your help with my many PhD thesis-related questions and giving me the opportunity to work with *Medicago* roots :). Thank you **Francis**, **Eline**, and **Lore** for the entertaining time during our Biology studies, and the fun 'reunions' over the past years. There were not so many of them at which I could join, but I had a lot of fun every time. Thank you **Marieke (Malip)** for always being so concerned about my well-being, and sharing your straightforward opinion. A big thank you to **Silke (Lenaerts)** for the amusing meetings ever since secondary school, and your supportive text messages.

De volgende 'dank u' zou ik graag ook vermelden tijdens de publieke verdediging, maar voor het geval ik het begeef onder de zenuwen wil ik toch zeker zijn dat jullie het weten. Dank u **mama, papa, zus, en broer**! Tijdens mijn studies was ik meestal bezig met leren (en af en toe kaastaart eten en apple crumble maken), en jullie zorgden voor al de rest. Ik heb soms spijt dat ik niet wat meer betrokken was en zo opging in mijn eigen dingen, maar het is dankzij jullie steun dat ik mijn studies goed heb kunnen afronden en een beurs voor mijn doctoraat heb kunnen binnenhalen. Ik ben heel blij dat jullie er vandaag bij kunnen zijn!! Ook een grote dank u en dikke knuffel voor mijn lief petekindje **Emma**! Je tekeningen, briefjes, verjaardagsvideos,

en facebook berichtjes hebben mémé veel doen lachen :) En natuurlijk ook dank u lieve **Lennert**, **Mercedes**, **Vincent, en Monique** om de toffe bende compleet te maken.

And last, but most importantly, I want to thank my second half **Kamil Błaszkiewicz aka my kochanie**. We met shortly before this PhD adventure started and I am very happy and proud to call you my fiancé on this day. Many things have happened/improved over the past years, and I owe so much to you. You have made me a better and happier person, and helped me put things in perspective which otherwise would have overwhelmed me. Even though you had a lot of work on your plate, I would just have to ask and you would be there right away to help and support me. You may have not noticed, but I have always admired your spirit to work hard and determination to succeed. I am happy and a bit proud to finalize this PhD chapter today, and I am looking forward to start the next challenge with you at my side.

CURRICULUM VITAE

PERSONAL DETAILS

Name:	Himschoot
First Name:	Ellie
Address:	Martelaarslaan 264 G B9000 Gent Belgium
Date and place of birth:	October 17th 1988, Wilrijk (Belgium)
Identification number National register:	88.10.17-416.22
Bank account number:	IBAN BE57 7775 9747 7135
Mobile phone number:	+32 494720993
E-mail:	ellie.himschoot@gmail.com
Nationality:	Belgian

EDUCATION

2012-present **PhD in Plant Biotechnology**, Plant Systems Biology department, Vlaams Instituut voor Biotechnologie, Belgium

2010-2012 **Master in Biochemistry and Biotechnology**, Universiteit Gent, Belgium
Master thesis: 'Auxin-mediated Ca^{2+} signaling and polar auxin transport', Plant Systems Biology department, Vlaams Instituut voor Biotechnologie, Belgium

2009-2010 Preparatory year for Master in Biochemistry and Biotechnology, Universiteit Gent, Belgium

2006-2009 **Bachelor in Biology**, Universiteit Gent, Belgium

PROFESSIONAL EXPERIENCE

2012-present **PhD in Plant Biotechnology**, Plant Systems Biology department, Vlaams Instituut voor Biotechnologie, Belgium

- Bio-imaging: *Arabidopsis thaliana* seedlings, BY-2 cell cultures, fluorescence microscopy, immunolocalization, live cell imaging.

- Image processing: Fiji, Matlab, CellProfiler
- Programming: Python
- 3D printing: FDM printers, Slicer software
- 04.2014-05.2014: Visiting scientist in Alex Costa lab, Università Degli Studi Di Milano, Italy
- 01.2016-07.2016: Visiting scientist in Eva Benková lab, IST Austria, Austria

COURSES AND TRAININGS

Image analysis for biologists summer school, University of Nottingham, UK
Statistical Thinking & Smart Experimental Design, VIB, Belgium
Image processing course, University of Gent, Belgium
Introduction to Python, VIB, Belgium
Programming course (Python), University of Gent, Belgium

PUBLICATIONS

A1 publications

1. Himschoot E., Pleskot R., Van Damme D., Vanneste S. (2017) The ins and outs of Ca^{2+} in plant endomembrane trafficking. Current Opinion in Plant Biology 40. Current Opinion in Plant Biology 40(C): 131-137
2. Himschoot E., Costa A., Krebs M., Vanneste S. (2017) Calcium ion dynamics in roots: imaging and analysis. Methods in Molecular Biology. Accepted publication
3. Orman-Ligeza B., Parizot B., de Rycke R., Fernandez A., Himschoot E., Van Breusegem F., J. Bennett M., Périlleux C., Beeckman T., Draye X. (2016) RBOH-mediated ROS production facilitates lateral root emergence in *Arabidopsis*. Development 143(18): 3328–3339
4. Himschoot E., Beeckman T., Friml, J., Vanneste S. (2015) Calcium is an organizer of cell polarity in plants. Biochim Biophys Acta. 1853(9):2168-2172
5. Du Y., Tejos R., Beck M., Himschoot E., Li H., Robatzek S., Vanneste S., Friml J. (2013) Salicylic acid interferes with clathrin-mediated endocytic protein trafficking. Proc Natl Acad Sci U S A. 110(19):7946-51

C3 publications

1. Himschoot, E., Costa, A., Bonza, C., De Vriese, K., Krebs, M., Schumacher, K., Kudla, J., Sheen, J., Boudsocq, M., Robatzek, S., Yoshioka, K., Beeckman, T., Friml, J., Vanneste,

S. (2016) Calcium controls endomembrane trafficking at various levels. Calcium Signaling Meeting 2016, Freising, Germany. (POSTER)

2. Himschoot, E., Costa, A., Bonza, C., De Vriese, K., Krebs, M., Schumacher, K., Kudla, J., Sheen, J., Boudsocq, M., Robatzek, S., Yoshioka, K., Beeckman, T., Friml, J., Vanneste, S. (2014) The involvement of calcium in auxin-regulated PIN endocytosis. 13th European Calcium Society meeting 2014, Aix-en-Provence, France. (POSTER)
3. Himschoot, E., Vanneste, S., Friml, J., Beeckman, T. (2013) Role of calcium signaling in auxin-dependent inhibition of PIN endocytosis. Society for Experimental Biology Annual Main Meeting Valencia 2013, Valencia, Spain. (POSTER)
4. Himschoot, E., Vanneste, S., Friml, J. (2013) Auxin-induced calcium inhibits endocytosis. European Network for Plant Endomembrane Research 2013, Gent, Belgium. (TALK)

AWARDS and FUNDING

2012 Bayer CropScience Master Price 2012 Biochemistry and Biotechnology
2012 Bijzonder Onderzoeks Fonds (BOF) Doctoral research grant
2014 Fonds Wetenschappelijk onderzoek (FWO) Travel grant for short stay abroad
2014 Poster price at the 13th European Calcium Society meeting, Aix-en-Provence, France
2015 Fonds Wetenschappelijk onderzoek (FWO) Travel grant for long stay abroad
2017 PSB Science Fund

STUDENT SUPERVISION

Supervisor for a Bachelor thesis (students Robin Colpaert, Eline De Rore, and Eva Seghers)
Supervisor for two Master projects (students Sofie Aesaert and Julie Veryser)

LANGUAGES

Dutch: native
English: fluent
French: basic

INTEREST

Music, microscopy, 3D printing.

SUPPLEMENTARY DATA

Supplementary material and methods

Supplementary figures Section II – Chapter 1: Figure S1

Supplementary figures Section II – Chapter 2: Figure S2 - S7

Supplementary figures Conclusions and perspectives: Figure S8, S9

Supplemental experimental procedures

Plant material

The AtSS12S (Braun et al., 2008), AtABP1AS (Braun et al., 2008), Yellow Cameleon 3.6 (Krebs et al., 2011), *scn1* (Carol et al., 2005), *cngc14-1* (Shih et al., 2015; SALK_206460), *cngc14-2* (Shih et al., 2015; WisDsLox437E09) lines have been described previously. Seeds of the CA CPK lines have been provided by Prof. Dr. Steffen Vanneste. The crosses used in the experiments were obtained by controlled cross pollination, and homozygous lines were generated for the YC3.6 crosses.

Drugs and treatments

Alfa-(phenyl ethyl-2-one)-indole-3-acetic acid (PEO-IAA, 10µM) was kindly provided by Prof. Dr. Jiří Friml. Methyl-β-cyclodextrin (MβCD, 5mM) was purchased from Sigma Aldrich and dissolved in DMSO. Seedlings were pretreated with the drugs and hormones for 30min in CaPLUS or CaMIN, followed by 60min coincubation with 25µM BFA or 25µM BFA 10µM NAA in CaPLUS or CaMIN. For the BFA wash-out experiments, seedlings were treated with 25µM BFA for 90min in CaPLUS and subsequently transferred to CaPLUS or CaMIN for 60min.

Induction of mutant lines

For induction of the mutant lines AtSS12S and AtABP1AS, plates with 3 day-old seedlings were used. An 0,5mL Eppendorf tube with 5% EtOH was attached to the inside of the lid of the plate for 2 days. The Eppendorf tube remained opened so the vapors could reach the seedlings.

Phenotypic analysis of CA CPK lines

For phenotypic screening of the CA CPK lines, seeds were plated on 0.5x MS with agar, vernalized in the cold room (4°C, dark) for 1 day, and then transferred to the growth room (21°C, continuous light) for 3 days. The 3 day-old seedlings were transferred to solid 0.5x MS

with 10µM estradiol for induction for 7 days and subsequently screened for aberrant phenotypes.

Microscopy and image analysis

For imaging the FRET-based ratiometric Ca^{2+} sensor Yellow Cameleon 3.6 (YC3.6), an Ultra View Vox spinning disc microscope (Perkin Elmer) was used equipped with a 20x air objective (NA 0.45) and a top and rear electron microscopy charge-coupled device camera (Hamamatsu Phototonics). The samples were prepared in the customized imaging chamber as described in Section II – Chapter 1 (Himschoot et al., 2017). The donor fluorophore CFP was excited using 440 nm and emission was detected from 420nm to 460nm. FRET was detected between 520nm and 570nm. Images were acquired every 3 sec, and were analyzed using Fiji (Schindelin et al., 2012). The fluorescence intensity was measured in our region of interest (meristematic zone) for both the CFP and FRET channel over time. For every time frame and channel, background fluorescence intensities were measured as well. After background subtraction, the FRET/CFP emission ratio (R) was calculated for every timepoint and normalized to R at the reference timepoint prior to NAA treatment. The average normalized ratios R of all the seedlings were plotted over time.

Supplemental figures Section II – Chapter 1

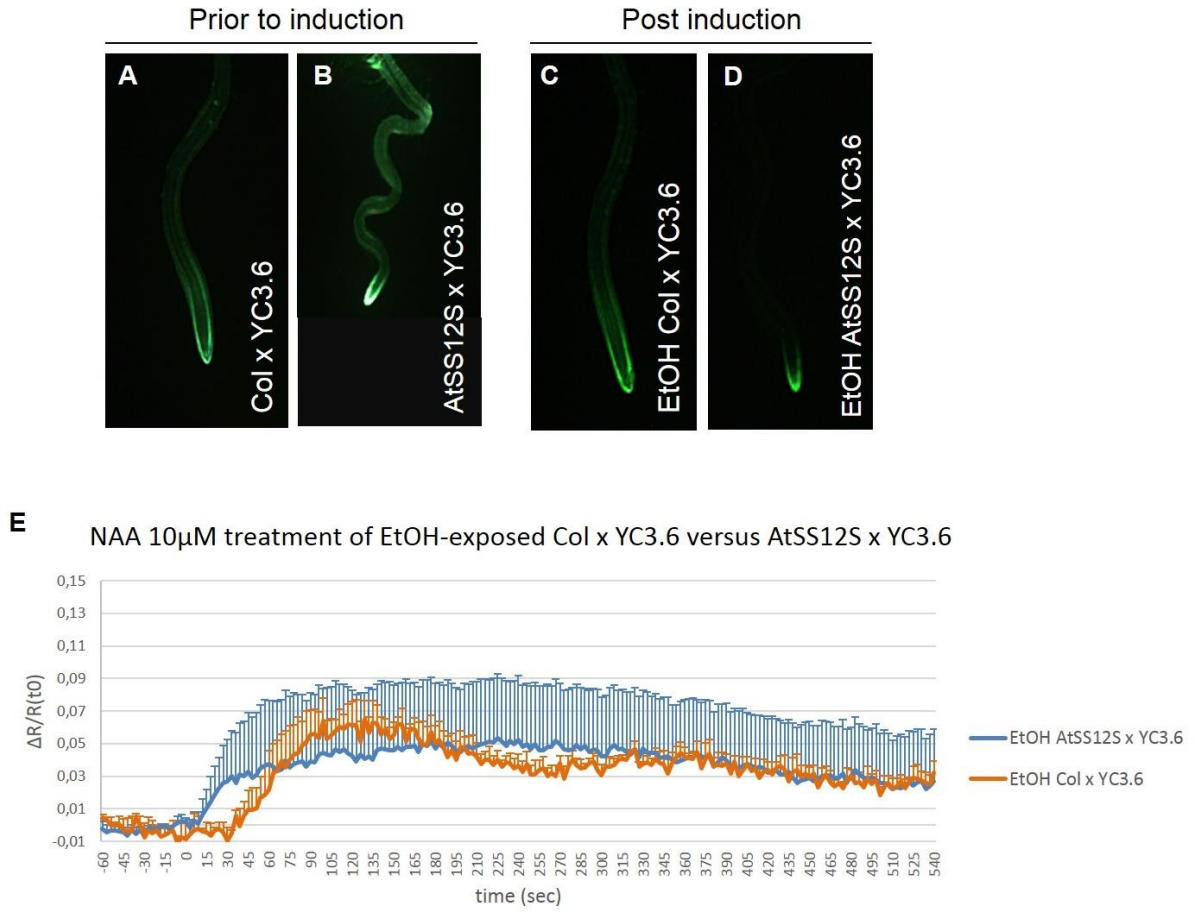

Figure S1: Ca^{2+} imaging using Yellow Cameleon 3.6 (YC3.6) upon inactivation of apoplastic ABP1. (A-D) Silencing of YC3.6 upon induction of ABP1 inactivation in the majority of the seedlings. (A, B) YC3.6 fluorescence prior to induction in the wild type (A) and the AtSS12S line (B). (C, D) YC3.6 expression seems to be silenced upon EtOH exposure of the AtSS12S seedlings (D), but not in the wild type seedlings (C). The AtSS12S line expresses an apoplast-targeted antibody upon exposure to EtOH vapors that binds and inactivates apoplastic ABP1 (Braun et al., 2008). Reporter silencing occurred in the majority of the seedlings. Due to lack of YC3.6 expression in our region of interest measurement of NAA-induced Ca^{2+} dynamics upon apoplastic ABP1 inactivation became strongly impeded. (E) NAA-induced Ca^{2+} dynamics upon inactivation of apoplastic ABP1. For a few seedlings in which the Ca^{2+} reporter did not become silenced after EtOH exposure, NAA-induced Ca^{2+} dynamics could be assessed. In contrast to the other Ca^{2+} imaging experiments, these experiments have been performed with the FRET-based ratiometric Ca^{2+} sensor Yellow Cameleon 3.6 (YC3.6). The Y-axis depicts the average normalized FRET/donor emission ratios (R) which increase with increasing Ca^{2+} levels in the cytosol. The error bars represent the SE. 10µM NAA was added at timepoint 0. Note the large error bars for the AtSS12S line reflecting the variability in response among different seedlings. (n > 3).

Supplemental figures Section II – Chapter 2

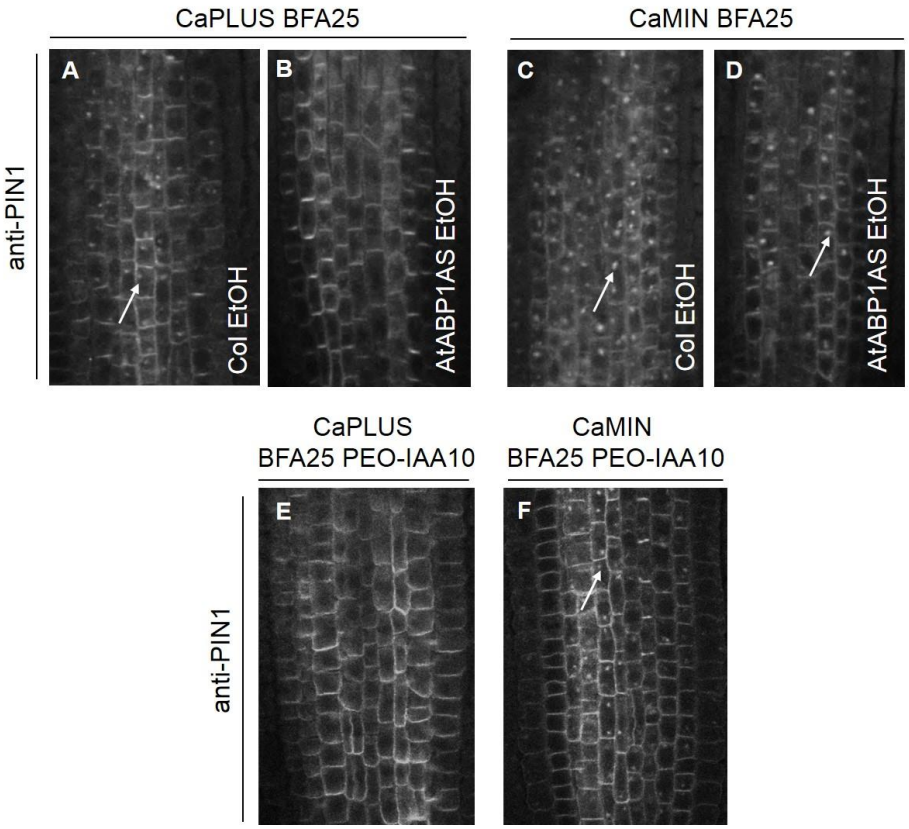

Figure S2: PIN1 internalization in CaMIN upon interference with ABP1 signaling and PEO-IAA cotreatment. Analysis of PIN1 internalization through whole-mount immunolocalization in 4 day-old seedling root meristems. (A-D) PIN1 internalization in the EtOH-inducible ABP1 antisense line (AtABP1AS) in CaPLUS versus CaMIN. 25µM BFA in CaPLUS caused PIN1 accumulation in BFA bodies in EtOH-exposed wild type seedlings (A), while in EtOH-exposed AtABP1AS seedlings PIN1 internalization was inhibited (B). Treatment with 25µM BFA in CaMIN resulted in PIN1 accumulation in BFA bodies in both EtOH-treated wild type (C) and AtABP1AS (D) seedlings. (E, F) PIN1 internalization upon treatment with α-(phenyl ethyl-2-one)-indole-3-acetic acid (PEO-IAA). PEO-IAA is an auxin derivative that specifically activates non-transcriptional auxin signaling and inhibits PIN endocytosis (Robert et al., 2010). Cotreatment of 25µM BFA and 10µM PEO-IAA results in inhibition of PIN1 internalization in CaPLUS (E), but not in CaMIN (F). White arrows highlight PIN1 in BFA bodies.

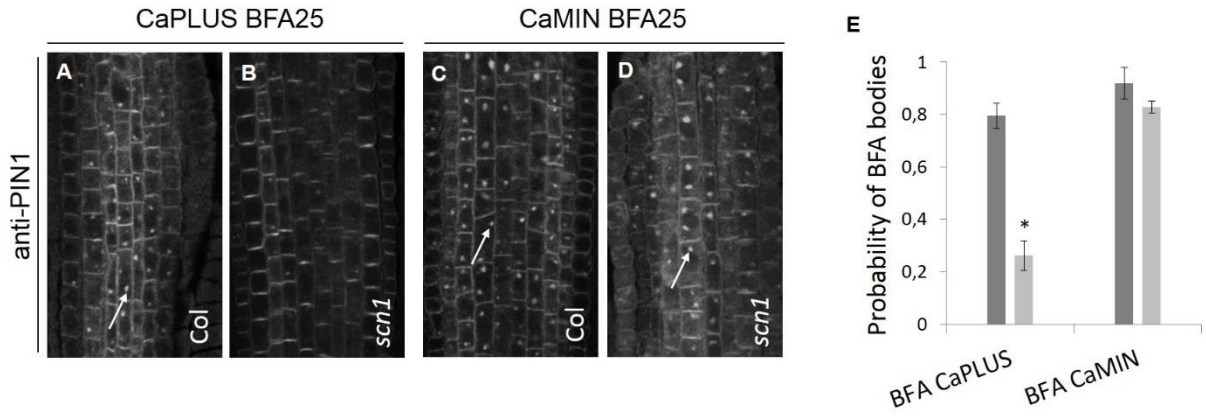

Figure S3: PIN1 internalization in CaMIN upon interfering with ROP/RIC signaling. Analysis of PIN1 internalization through whole-mount immunolocalization in 4 day-old seedling root meristems. (A-D) PIN1 internalization in the *supercentipede1* (*scn1)* mutant in CaPLUS versus CaMIN. *scn1* is defective in a RHO-GDI resulting in constitutive activation of ROP/RIC signaling (Carol et al., 2005). 25µM BFA in CaPLUS caused PIN1 accumulation in BFA bodies in wild type seedlings (A), while in *scn1* seedlings PIN internalization was inhibited (B). Treatment with 25µM BFA in CaMIN resulted in PIN1 accumulation in BFA bodies in both wild type (C) and *scn1* (D) seedlings. (E) Quantification of the probability that BFA bodies will be present in root cells. The asteriks represents a p-value <0.05. The error bars represent the 95% confidence interval ($n > 5$).

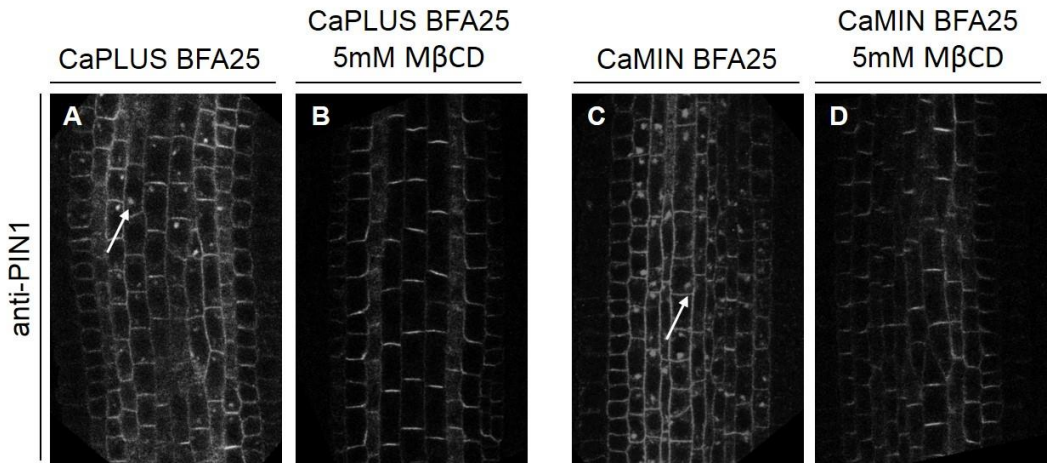

Figure S4: PIN1 internalization in CaMIN upon inhibition of clathrin-independent lipid raft-mediated endocytosis by methyl-β-cyclodextrin (MβCD). Analysis of PIN1 internalization through whole-mount immunolocalization in 3 day-old seedling root meristems. (A) 25µM BFA in CaPLUS caused PIN1 accumulation in BFA bodies. (B) Treatment with 25µM BFA and 5mM MβCD in CaPLUS interfered with PIN1 internalization, reflected by a lack of BFA bodies. (C) As for CaPLUS, treatment with 25µM BFA in CaMIN resulted in formation of PIN1-accumulating BFA bodies. (D) Upon cotreatment with 25µM BFA and 5mM MβCD in CaMIN no BFA bodies could be observed. White arrows highlight PIN1 in BFA bodies. For cotreatments with inhibitors, seedlings were pretreated for 30min.

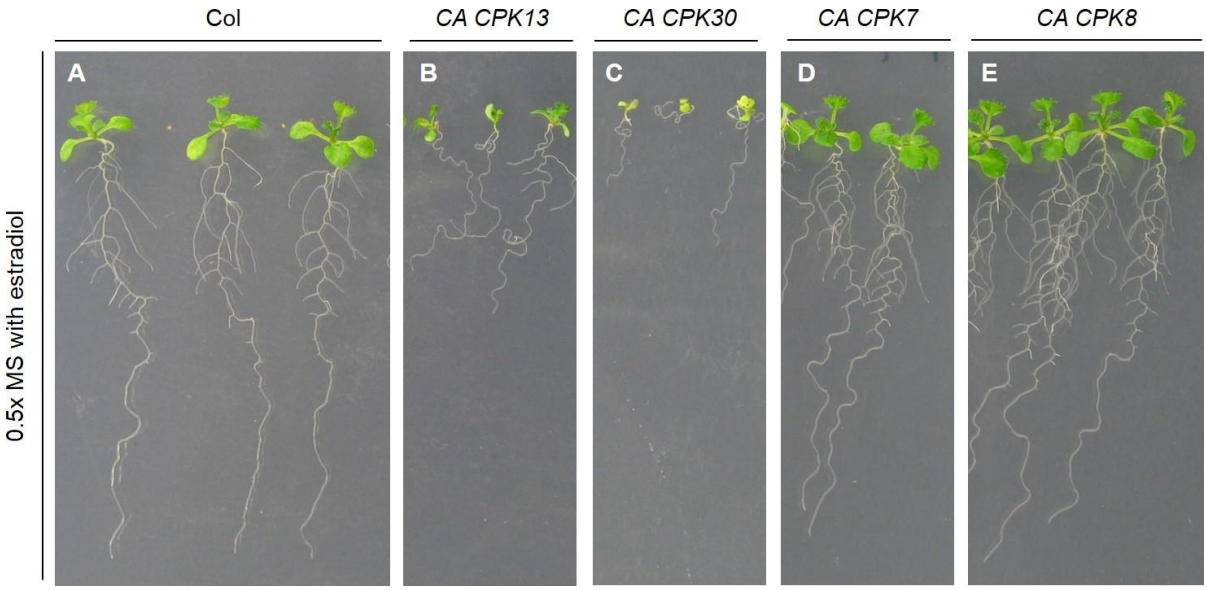

Figure S5: Root gravitropism upon overexpression of constitutive active CPK7, 8, 13, and 30 (CA CPK). (A) Wild type seedlings grown on estradiol show gravitropic root growth. (B, C) The *CA CPK13* (B) and *CA CPK30* (C) line however grow agravitropically. (D, E) For the related CPKs, CPK7 (D) and CPK8 (E), overexpression of their constitutive active form did not affect root gravitropism. Seeds were germinated on 0.5x MS and 3 day-old seedlings were transferred to 0.5x MS with estradiol for induction for 7 days.

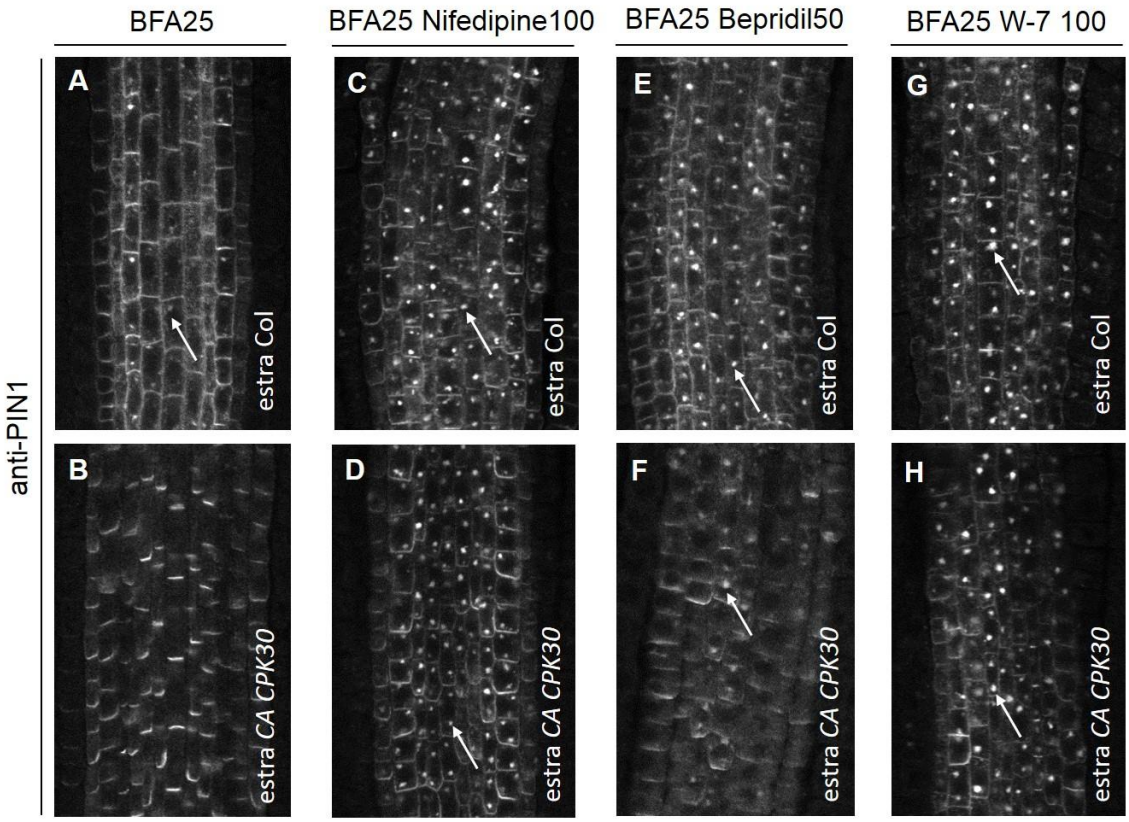

Figure S6: The effect of Ca^{2+} drug on PIN1 trafficking in the constitutively active CPK30 (*CA CPK30*) line. (A, C, E, G) Immunolocalization of PIN1 in estradiol-treated wild type upon (A) 25µM BFA treatment and 25µM BFA

cotreatment with (C) 100µM Nifedipine, (E) 50µM Bepridil, and (G) 100µM W-7. In all cases PIN1-accumulating BFA bodies can be observed (white arrows). (B, D, F, H) Immunolocalization of PIN1 in the estradiol-treated constitutively active CPK30 (*CA CPK30*) line upon (B) 25µM BFA treatment and 25µM BFA cotreatment with (D) 100µM Nifedipine, (F) 50µM Bepridil, and (H) 100µM W-7. Seedlings were pretreated with the Ca^{2+} drug for 30min prior to 1h co-incubation with BFA.

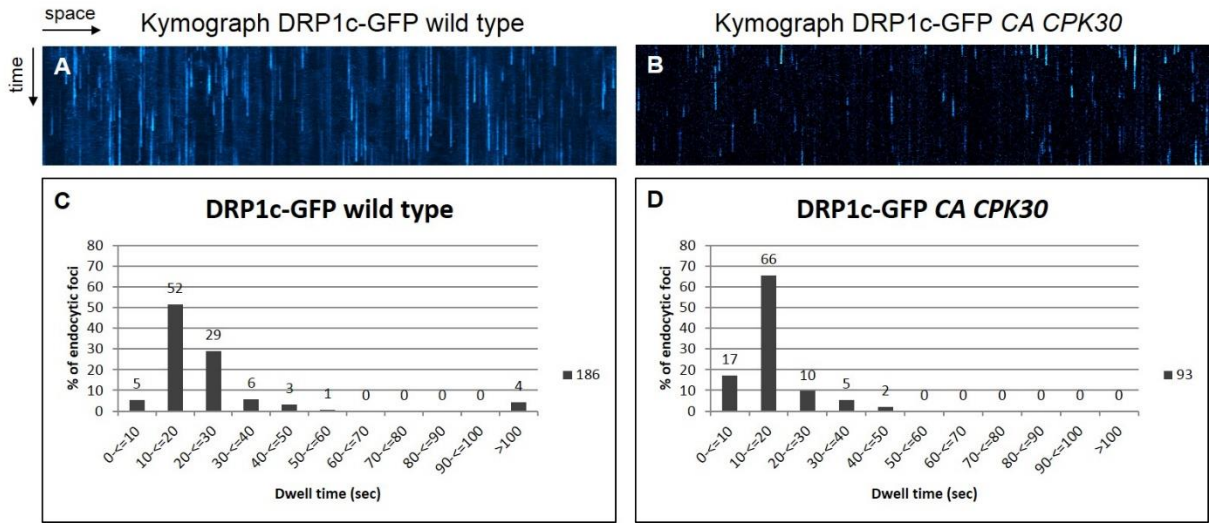

Figure S7: DYNAMIN-RELATED PROTEIN1c (DRP1c) dynamics in estradiol-induced *CA CPK30*. (A, B) Kymographs of time-lapse recording (100 sec) of DRP1c1-GFP in elongated root epidermal cells in estradiol-treated wild type (A) and *CA CPK30* seedlings (B). The length of the vertical lines is proportional to the life-time (dwell time) of DRP1c-labelled endocytic spots at the plasma membrane. Note that there are less lines in the kymograph of *CA CPK30* (B) reflecting less DRP1c-labelled endocytic spots at the plasma membrane. (C, D) Quantification of the dwell time of DRP1c-labelled endocytic foci in estradiol-treated wild type (C, 3 seedlings) and *CA CPK30* seedlings (D, 4 seedlings). Note that, even though more CA CPK seedlings were analyzed compared to wild type, the number of spots that could be counted is much lower for CA CPK (93) compared to the wild type (186).

Supplemental figures Conclusions and perspectives

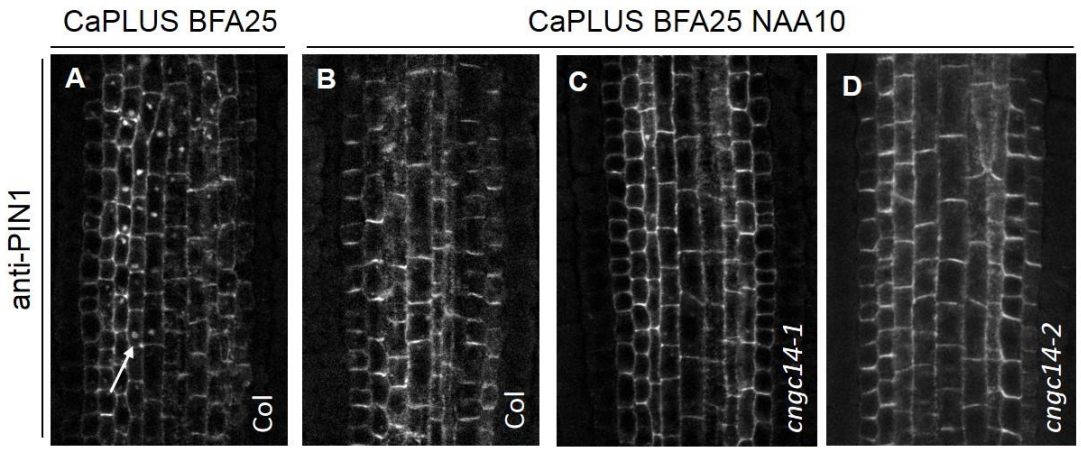

Figure S8: NAA-inhibited PIN1 endocytosis in *cngc14* mutants. Analysis of PIN1 internalization through whole-mount immunolocalization in 3 day-old seedling root meristems. (A) 25µM BFA caused PIN1 accumulation in BFA bodies (white arrow). (B-D) Cotreatment with 25µM BFA and 10µM NAA interfered with PIN1 internalization in the wild type (B), and the *cngc14-1* (C) and *cngc14-2* (D) mutants.

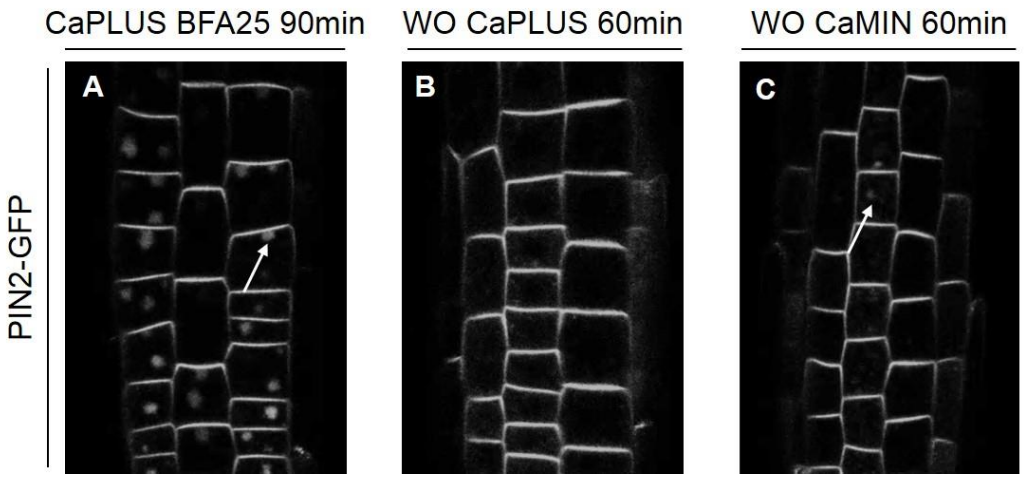

Figure S9: BFA wash-out in CaPLUS versus CaMIN. (A) PIN2-GFP expressing seedlings were treated with 25µM BFA in CaPLUS for 90min resulting in formation of PIN2-accumulating BFA bodies. (B, C) Seedlings were subsequently transferred to CaPLUS (B) or CaMIN (C) for 60min to wash out BFA. In CaPLUS (B), no BFA bodies remained after 60min of wash-out, while a few BFA bodies could be observed after 60min of wash-out in CaMIN (C). The latter reflects a delay in recycling/secretion of PIN2 to the plasma membrane in CaMIN. White arrows highlight PIN2 in BFA bodies.

Supplemental references

Braun, N., Wyrzykowska, J., Muller, P., Karine, D., Couch, D., Perrot-Rechenmann, C., and Fleming, A. (2008). Conditional Repression of AUXIN BINDING PROTEIN1 Reveals That It Coordinates Cell Division and Cell Expansion during Postembryonic Shoot Development in Arabidopsis and Tobacco. The Plant Cell **20**, 2746-2762.

Carol, R.J., Takeda, S., Linstead, P., Durrant, M.C., Kakesova, H., Derbyshire, P., Drea, S., Zarsky, V., and Dolan, L. (2005). A RhoGDP dissociation inhibitor spatially regulates growth in root hair cells. Nature **438**, 1013–1016.

Krebs, M., Held, K., Binder, A., Hashimoto, K., Den Herder, G., Parniske, M., Kudla, J. and Schumacher, K. (2012). FRET-based genetically encoded sensors allow high-resolution live cell imaging of Ca2+ dynamics. The Plant Journal, **69**: 181–192.

Shih, H.-W., DePew, Cody L., Miller, Nathan D., and Monshausen, Gabriele B. (2015). The Cyclic Nucleotide-Gated Channel CNGC14 Regulates Root Gravitropism in Arabidopsis thaliana. Current Biology **25,** 3119-3125.